



UNIL | Université de Lausanne

Faculté de biologie
et de médecine

Département de Microbiologie Fondamentale

**ON THE USE OF REPORTER BACTERIA FOR
MEASURING AVAILABILITY OF ORGANIC
CONTAMINANTS**

Thèse de doctorat ès sciences de la vie (PhD)

présentée à la Faculté de biologie et de médecine
de l'Université de Lausanne par

Robin Tecon

Biologiste diplômé de l'Université de Lausanne

Jury

Prof. Christian Fankhauser, Président
Prof. Jan Roelof van der Meer, Directeur de thèse
Prof. Dieter Haas, Co-directeur de thèse
Prof. Rik Eggen, Expert
Prof. Hauke Harms, Expert

Lausanne 2009

Imprimatur

Vu le rapport présenté par le jury d'examen, composé de

Président	Monsieur Prof.	Christian Fankhauser
Directeur de thèse	Monsieur Prof.	Jan Roelof Van der Meer
Co-directeur de thèse	Monsieur Prof.	Dieter Haas
Experts	Monsieur Prof.	Hauke Harms
	Monsieur Prof.	Rik Eggen

le Conseil de Faculté autorise l'impression de la thèse de

Monsieur Robin Tecon

Biologiste diplômé de l'Université de Lausanne

intitulée

**ON THE USE OF REPORTER BACTERIA FOR MEASURING
AVAILABILITY OF ORGANIC CONTAMINANTS**

Lausanne, le 24 avril 2009

pour Le Doyen
de la Faculté de Biologie et de Médecine


Prof. Christian Fankhauser

TABLE OF CONTENTS

SUMMARY	V
RÉSUMÉ	XI
GOALS	XVII
OUTLINE	XIX
CHAPTER 1 General Introduction	1
CHAPTER 2 A new GFP-based bacterial biosensor for analyzing phenanthrene fluxes	19
CHAPTER 3 Influence of dissolved organic matter on NAH and PHE availability to the bacterial biosensor <i>Burkholderia sartisoli</i> RP037	45
CHAPTER 4 Co-cultivation of the bacterial biosensor <i>Burkholderia sartisoli</i> strain RP037 with a biosurfactant-producing <i>Pseudomonas putida</i> strain and effect of two types of biosurfactants on PAH availability	63
CHAPTER 5 Double-tagged fluorescent bacterial biosensor for the study of PAH diffusion and bioavailability	79
CHAPTER 6 Development of a multiwell bacterial biosensor platform for the monitoring of hydrocarbon contaminants in aqueous environments	103
CHAPTER 7 Development of new bacterial biosensors for the detection of alkanes based on the transcriptional activator AlkS from the marine bacterium <i>Alcanivorax borkumensis</i> strain SK2	123
CHAPTER 8 General discussion	135
REFERENCES	143
CURRICULUM VITAE	155
LIST OF PUBLICATIONS	157

SUMMARY

Natural ecosystems are constantly exposed to a variety of hydrophobic organic contaminants (HOCs) of industrial, agricultural or even natural origin. HOCs threaten the environment, animal and plant well-being and human health, but they can be degraded by micro-organisms such as bacteria and fungi, which may be able to transform them into harmless products such as CO₂ and water. The biodegradation of HOCs, however, is often limited by their low availability to degraders. Hence, although biodegradation partially occurs, HOCs tend to persist in the environment at low concentrations, which potentially still can cause chronic toxic effects. Since most HOCs can be metabolized in the environment by microbial activity, their persistence generally stems from physico-chemical rather than biological constraints. For instance, their poor water solubility reduces their uptake by potential degraders. In addition, sorption to organic matter and sequestration in soil micropores participate to reducing the availability to microbes. The *bioavailability processes*, i.e., the processes that govern dissolution and uptake of pollutants by biota, are generally viewed as a key parameter for the natural and stimulated clean-up (bioremediation) of contaminated sites.

Polyaromatic hydrocarbons (PAHs) are model HOC produced by natural as well as human activities and are listed as chronic contaminants of air, soils and sediments. They can be degraded by a vast number of bacterial species but their biodegradation rates are often limited by the constraints mentioned above. In order to understand bioavailability processes for bacterial cells, we decided to use the bacterial cells themselves to sense and report relevant HOC fluxes. This was done by application of a design strategy to produce so-called biosensor-reporter bacteria, which literally ‘light up’ when detecting the target compound to which they are designed for. In first instance, we focused on *Burkholderia sartisoli* strain RP007, a PAH degrader isolated from soil. This strain served as a basis for the construction of a genetic circuitry that would allow formation of the autofluorescent protein GFP as soon as the cells would detect naphthalene or phenanthrene, two low molecular mass PAHs. Indeed we could show that the resulting bacterium, which was called *B. sartisoli* strain RP037, produced increasing GFP fluorescence when exposed in liquid culture to phenanthrene in the form of crystals (0.5 mg per ml of culture medium). We discovered that for optimal induction it was necessary to provide the cells with additional carbon in the form of acetate, or else very

few cells would become induced. Still, however phenanthrene induced a very heterogeneous response over the whole population of cells, with some cells being very poorly induced and others very strongly. The reason for this extreme heterogeneity even in mixed liquid cultures is currently not very clear. More importantly, we could indeed show that the magnitude of GFP induction was dependent on physical parameters affecting the phenanthrene flux to the cells: such as, the contact surface area between solid phenanthrene and the aqueous phase; the addition of surfactant; the embedding of phenanthrene inside Model Polymer Release System beads; or the dissolution of phenanthrene in a water-immiscible oil. We concluded that strain RP037 was properly sensing phenanthrene fluxes and we proposed a relationship between the overall phenanthrene mass transfer and GFP production.

We then used the strain to examine the effect of a number of chemical parameters, which are known from literature to influence PAH bioavailability. First of all, this consisted of humic acids. A few reports state that PAH availability might increase in the presence of dissolved organic matter. We measured GFP induction as a function of phenanthrene or naphthalene exposure to the RP037 cells in the presence or absence of humic acids in the culture. We tested humic acids at concentrations of 0.1 and 10 mg/L, while adding phenanthrene via the non aqueous phase-liquid heptamethylnonane (HMN), which we previously showed to produce the highest constant phenanthrene flux to the cells. In addition, we used gas phase assays with humic acid concentrations of 0.1, 10 and 1000 mg/L but with naphthalene. Contrary to literature, our results indicated that under these conditions the GFP expression as a function of phenanthrene exposure in growing cultures of strain RP037 was not modified by the presence of humic acids. On the other hand, the gas phase assay with naphthalene showed that 1000 mg/L humic acids slightly but significantly lowered the GFP production in RP037 cells. We concluded that there is no general effect of humic acids changing PAH availability to bacterial cells.

We then asked the question as to whether biosurfactants would change availability of phenanthrene to bacterial cells. Surfactants are often described in literature as ways to enhance HOC bioavailability. Surfactants are tensio-active agents that increase the apparent solubility of HOC by dissolving them into micelles. We thus tested whether biosurfactants (surfactants produced by living organisms) could be used to increase the phenanthrene bioavailability to *B. sartisoli* strain RP037. First, we attempted to have biosurfactants produced by another bacterium living in coculture with the sensor cells. Secondly, we used purified biosurfactants. Co-cultivation with the lipopeptide-producing bacterium *Pseudomonas putida* strain PCL1445 enhanced phenanthrene-induced GFP expression in *B.*

sartisoli compared to single culture, but this effect was not significantly different when strain RP037 was co-cultivated with a non-lipopeptide producing mutant of *P. putida*. The addition of partially purified lipopeptides to a RP037 culture did result in surface tension reduction, but failed to trigger any changes in GFP expression. On the other hand, the addition of a commercial solution of rhamnolipids (another type of biosurfactants produced by *Pseudomonas* spp.) facilitated phenanthrene degradation by strain RP037 and induced a high GFP expression in a larger proportion of cells. We therefore concluded that biosurfactant effects are measurable with the biosensor strain, but are dependent on the type of surfactant used in conjunction to phenanthrene.

The next question we addressed was whether biosensor assays could be improved as such that direct fluxes from PAH contaminated material could be detected. Liquid assays with soils do not result in easy measurements, and given that PAH concentrations in the water phase are usually extremely low, we designed diffusion assays in which we could study PAH induction as a function of distance to the cells. The bacterial biosensor *B. sartisoli* strain RP037 was hereto tagged with a second fluorescent protein (mCherry), which was constitutively expressed in the cells and conferred them a red/pink fluorescence. The resulting strain RP037-mChe showed constitutive red fluorescence, but induced green fluorescence only in the presence of naphthalene or phenanthrene. The presence of a constitutive fluorescent tag permitted us to visualize the bacterial biosensor cells more easily among soil particles. A diffusion assay was designed by preparing a gel consisting of a biosensor cell suspension mixed with 0.5 % agarose. Gel patches with dimensions of 0.5 x 2 cm x 1 mm were mounted in incubation chambers and exposed to PAH sources either dissolved in HMN or as solid material, and applied to one extremity of the gel patch. Using this experimental set-up, both naphthalene and phenanthrene (dissolved in HMN at a concentration of 2.5 $\mu\text{g}/\mu\text{l}$) induced a gradient of GFP fluorescence intensity after 24 hours of incubation, while mCherry fluorescence remained comparable. A PAH-contaminated soil (from a former gas manufacturing site) appeared to induce the GFP production at a level comparable to naphthalene. Individual bacterial biosensors also detected a phenanthrene flux in a gel containing soil particles spiked with 1 and 10 mg/g phenanthrene. This showed that the diffusion assay can be used to measure PAH fluxes from contaminated material. On the other hand, the sensitivity with a number of contaminated soils was still too low, and autofluorescence with some materials made it difficult to discern the GFP response from the cells.

Finally, one of the major focuses of this work was the production and testing of a multiwell bacterial biosensor platform, which would permit the simultaneous use of a number of different biosensor strains for the detection of major oil components. For this we chose linear alkanes, monoaromatics, biphenyls and polyaromatics. In addition, we used a genotoxicity sensor to detect ‘overall toxicity’ in aqueous samples. A number of engineering efforts were initiated to complete this set. First of all, all strains were equipped with either *gfp* or *luxAB* as a reporter signal. Secondly, since no biosensor strains were available for PAH or for long-chain alkanes, we specifically constructed two new biosensors.

One of these was again based on *B. sartisoli* RP007, which we equipped with the plasmid pPROBE-phn-luxAB, for the detection of naphthalene and phenanthrene but with bacterial luciferase as output. Another was a new bacterial biosensor for alkanes. Although we had an *Escherichia coli* strain DH5 α (pGEc74, pJAMA7), which satisfyingly detected short alkanes, this strain failed to report the presence of long-chain alkanes. We cloned the gene for the transcriptional activator AlkS and the operator/promoter region of the operon *alkSB₁GHJ* from the alkane-degrader bacterium *Alcanivorax borkumensis* strain SK2 in order to construct a new bacterial biosensor with higher sensitivity towards long-chain alkanes. However, the resulting strain *E. coli* DH5 α (pAlk3) showed no increased light emission in presence of tetradecane (C₁₄), while still efficiently reporting low concentrations of octane (C₈). Surprisingly, the use of *A. borkumensis* as a host-strain for the new GFP-based reporter plasmid totally abolished the sensitivity towards octane, whereas the detection of tetradecane was not enhanced. This aspect will have to be resolved in further work.

To calibrate the multiwell biosensor platform, we mimicked an oil spill at sea in a 5 L open glass bottle with 2 L of clean sea water contaminated with 20 ml (1 %) of crude oil. The aqueous phase was sampled at regular time intervals after the spill for a period of up to one week while biosensing the key oil contaminants. The emission of bioluminescence was measured in order to determine the biosensor response and an integrated calibration with typical inducers served to calculate equivalent inducer concentrations in the sample. *E. coli* was used as a host strain for most of the sensor specificities, except naphthalene and phenanthrene, in which case we used *B. sartisoli*. This strain, however, would be used more or less under the same assay procedures. Interestingly, the oil spill produced a sequential appearance of dissolved compounds in the water phase, which were detectable with the sensors. This profile contained first short-chain alkanes and BTEX (i.e., benzene, toluene, ethylbenzene and xylenes), appearing within minutes to hours after the oil spillage. Their aqueous concentrations then strongly decreased in water sampled after 24 hours, due to

volatilization or biodegradation. After a few days of incubation, these compounds had become undetectable. PAHs, on the other hand, appeared later than alkanes and BTEX, and their concentration increased with prolonged incubation time. No significant signals were picked with either the biphenyl sensor or the genotoxicity sensor. This conclusively demonstrated the usefulness of the biosensors specifically for petroleum oil compounds, including short chain alkanes, BTEX and light PAHs.

RÉSUMÉ

Les écosystèmes naturels sont constamment exposés à nombre de contaminants organiques hydrophobes (COHs) d'origine industrielle, agricole ou même naturelle. Les COHs menacent à la fois l'environnement, le bien-être des espèces animales et végétales et la santé humaine, mais ils peuvent être dégradés par des micro-organismes tels que les bactéries et les champignons, qui peuvent être capables des les transformer en produits inoffensifs comme le gaz carbonique et l'eau. La biodégradation des COHs est cependant fréquemment limitée par leur pauvre disponibilité envers les organismes qui les dégradent. Ainsi, bien que la biodégradation opère partiellement, les COHs persistent dans l'environnement à de faibles concentrations qui potentiellement peuvent encore causer des effets toxiques chroniques. Puisque la plupart des COHs peuvent être métabolisés par l'activité microbienne, leur persistance a généralement pour origine des contraintes physico-chimiques plutôt que biologiques. Par exemple, leur solubilité dans l'eau très limitée réduit leur prise par des consommateurs potentiels. De plus, l'adsorption à la matière organique et la séquestration dans les micropores du sol participent à réduire leur disponibilité envers les microbes. Les *processus de biodisponibilité*, c'est-à-dire les processus qui gouvernent la dissolution et la prise de polluants par les organismes vivants, sont généralement perçus comme des paramètres clés pour la dépollution (bioremédiation) naturelle et stimulée des sites contaminés.

Les hydrocarbures aromatiques polycycliques (HAPs) sont un modèle de COH produits par les activités aussi bien humaines que naturelles, et listés comme des contaminants chroniques de l'air, des sols et des sédiments. Ils peuvent être dégradés par un vaste nombre d'espèces bactériennes mais leur taux de biodégradation est souvent limité par les contraintes mentionnées ci-dessus. Afin de comprendre les processus de biodisponibilité pour les cellules bactériennes, nous avons décidé d'utiliser les bactéries elles-mêmes pour détecter et rapporter les flux de COH. Ceci a été réalisé par l'application d'une stratégie de conception visant à produire des bactéries 'biocapteurs-rapporteurs', qui littéralement s'allument lorsqu'elles détectent un composé cible pour lequel elles ont été conçues. En premier lieu, nous nous sommes concentrés sur *Burkholderia sartisoli* (souche RP007), une bactérie isolée du sol et consommatrice de HAP. Cette souche a servi de base à la construction d'un circuit génétique permettant la formation de la protéine autofluorescente GFP dès que les cellules détectent le

naphtalène ou le phénanthrène, deux HAP de faible masse moléculaire. En effet, nous avons pu montrer que la bactérie obtenue, la souche RP037 de *B. sartisoli*, produit une fluorescence GFP grandissante lors d'une exposition en culture liquide à du phénanthrène sous forme cristalline (0.5 mg par ml de milieu de culture). Nous avons découvert que pour une induction optimale il était nécessaire de fournir aux cellules une source additionnelle de carbone sous la forme d'acétate, ou sinon seul un nombre limité de cellules deviennent induites. Malgré cela, le phénanthrène a induit une réponse très hétérogène au sein de la population de cellules, avec quelques cellules pauvrement induites tandis que d'autres l'étaient très fortement. La raison de cette hétérogénéité extrême, même dans des cultures liquides mélangées, reste pour le moment incertaine. Plus important, nous avons pu montrer que l'amplitude de l'induction de GFP dépendait de paramètres physiques affectant le flux de phénanthrène aux cellules, tels que : la surface de contact entre le phénanthrène solide et la phase aqueuse ; l'ajout de surfactant ; le scellement de phénanthrène à l'intérieur de billes de polymères (Model Polymer Release System) ; la dissolution du phénanthrène dans un fluide gras immiscible à l'eau. Nous en avons conclu que la souche RP037 détecte convenablement des flux de phénanthrène et nous avons proposé une relation entre le transfert de masse de phénanthrène et la production de GFP.

Nous avons par la suite utilisé la souche afin d'examiner l'effet de plusieurs paramètres chimiques connus dans la littérature pour influencer la biodisponibilité des HAP. Premièrement, les acides humiques. Quelques rapports font état que la disponibilité des HAP pourrait être augmentée par la présence de matière organique dissoute. Nous avons mesuré l'induction de GFP comme fonction de l'exposition des cellules RP037 au phénanthrène ou au naphtalène en présence ou absence d'acides humiques dans la culture. Nous avons testé des concentrations d'acides humiques de 0.1 et 10 mg/L, tandis que le phénanthrène était ajouté via l'heptamethylnonane (HMN), un liquide non aqueux, ce qui au préalable avait produit le plus haut flux constant de phénanthrène aux cellules. De plus, nous avons utilisé des tests en phase gazeuse avec des concentrations d'acides humiques de 0.1, 10 et 1000 mg/L mais avec du naphtalène. Contrairement à ce que décrit la littérature, nos résultats ont indiqué que dans ces conditions l'expression de GFP en fonction de l'exposition au phénanthrène dans des cultures en croissance de la souche RP037 n'était pas modifiée par la présence d'acides humiques. D'un autre côté, le test en phase gazeuse avec du naphtalène a montré que 1000 mg/L d'acides humiques abaissent légèrement mais significativement la production de GFP dans les cellules de RP037. Nous avons conclu qu'il n'y a pas d'effet général des acides humiques sur la disponibilité des HAP pour les bactéries.

Par la suite, nous nous sommes demandés si des biosurfactants modifieraient la disponibilité du phénanthrène pour les bactéries. Les surfactants sont souvent décrits dans la littérature comme des moyens d'accroître la biodisponibilité des COHs. Les surfactants sont des agents tensio-actifs qui augmentent la solubilité apparente de COH en les dissolvant à l'intérieur de micelles. Nous avons ainsi testé si des biosurfactants (des surfactants produits par des organismes vivants) peuvent être utilisés pour augmenter la biodisponibilité du phénanthrène pour la souche *B. sartisoli* RP037. Premièrement, nous avons tenté d'obtenir des biosurfactants produits par une autre bactérie vivante en co-culture avec les biocapteurs bactériens. Deuxièmement, nous avons utilisé des biosurfactants purifiés. La co-cultivation en présence de la bactérie productrice de lipopeptide *Pseudomonas putida* souche PCL1445 a augmenté l'expression de GFP induite par le phénanthrène chez *B. sartisoli* en comparaison des cultures simples, mais cet effet n'était pas significativement différent lorsque la souche RP037 était co-cultivée avec un mutant de *P. putida* ne produisant pas de lipopeptides. L'ajout de lipopeptides partiellement purifiés dans la culture de RP037 a résulté en une réduction de la tension de surface, mais n'a pas provoqué de changement dans l'expression de GFP. D'un autre côté, l'ajout d'une solution commerciale de rhamnolipides (un autre type de biosurfactants produits par *Pseudomonas* spp.) a facilité la dégradation du phénanthrène par la souche RP037 et induit une expression de GFP élevée dans une plus grande proportion de cellules. Nous avons ainsi conclu que les effets des biosurfactants sont mesurables à l'aide de la souche biocapteur, mais que ceux-ci sont dépendants du type de surfactant utilisé conjointement avec le phénanthrène.

La question suivante que nous avons abordée était si les tests utilisant des biocapteurs peuvent être améliorés de manière à ce que les flux de HAP provenant de matériel contaminé soient détectés. Les tests en milieu liquide avec des échantillons de sol ne fournissant pas de mesures, et sachant que les concentrations de HAP dans l'eau sont en général extrêmement basses, nous avons conçu des tests de diffusion dans lesquels nous pouvons étudier l'induction par les HAPs en fonction de la distance aux cellules. Le biocapteur bactérien *B. sartisoli* souche RP037 a été marqué avec une seconde protéine fluorescente (mCherry), qui est constitutivement exprimée dans les cellules et leur confère une fluorescence rouge/rose. La souche résultante RP037-mChe témoigne d'une fluorescence rouge constitutive mais n'induit la fluorescence verte qu'en présence de naphthalène ou de phénanthrène. La présence d'un marqueur fluorescent constitutif nous permet de visualiser les biocapteurs bactériens plus facilement parmi des particules de sol. Un test de diffusion a été conçu en préparant un gel fait d'une suspension de cellules mélangées à 0.5 % d'agarose. Des bandes de gel de

dimensions 0.5 x 2 cm x 1 mm ont été montées dans des chambres d'incubation et exposées à des sources de HAP (soit dissouts dans du HMN ou en tant que matériel solide, puis appliqués à une extrémité de la bande). En utilisant ce montage expérimental, le naphtalène ou le phénanthrène (dissouts dans du HMN à une concentration de 2.5 µg/µl) ont induit un gradient d'intensité de fluorescence GFP après 24 heures d'incubation, tandis que la fluorescence mCherry demeurait comparable. Un sol contaminé par des HAPs (provenant d'un ancien site de production de gaz) a induit la production de GFP à un niveau comparable à celui du naphtalène. Des biocapteurs bactériens individuels ont également détecté un flux de phénanthrène dans un gel contenant des particules de sol amendées avec 1 et 10 mg/g de phénanthrène. Ceci a montré que le test de diffusion peut être utilisé pour mesurer des flux de HAP provenant de matériel contaminé. D'un autre côté, la sensibilité est encore très basse pour plusieurs sols contaminés, et l'autofluorescence de certains échantillons rend difficile l'identification de la réponse de la GFP chez les cellules.

Pour terminer, un des points majeurs de ce travail a été la production et la validation d'une plateforme multi-puits de biocapteurs bactériens, qui a permis l'emploi simultané de plusieurs souches différentes de biocapteurs pour la détection des constituants principaux du pétrole. Pour cela nous avons choisi les alcanes linéaires, les composés mono-aromatiques, les biphényles et les composés poly-aromatiques. De plus, nous avons utilisé un capteur pour la génotoxicité afin de détecter la 'toxicité globale' dans des échantillons aqueux. Plusieurs efforts d'ingénierie ont été investis de manière à compléter ce set. En premier lieu, chaque souche a été équipée avec soit *gfp*, soit *luxAB* en tant que signal rapporteur. Deuxièmement, puisqu'aucune souche de biocapteur n'était disponible pour les HAP ou pour les alcanes à longues chaînes, nous avons spécifiquement construit deux nouveaux biocapteurs.

L'un d'eux est également basé sur *B. sartisoli* RP007, que nous avons équipé avec le plasmide pPROBE-phn-luxAB pour la détection du naphtalène et du phénanthrène mais avec production de luciférase bactérienne. Un autre est un nouveau biocapteur bactérien pour les alcanes. Bien que nous possédions une souche *Escherichia coli* DH5α (pGEC74, pJAMA7) détectant les alcanes courts de manière satisfaisante, la présence des alcanes à longues chaînes n'était pas rapportée efficacement. Nous avons cloné le gène de l'activateur transcriptionnel AlkS ainsi que la région opérateur/promoteur de l'opéron *alkSB₁GHJ* chez la bactérie dégradant les alcanes *Alcanivorax borkumensis* souche SK2, afin de construire un nouveau biocapteur bactérien bénéficiant d'une sensibilité accrue envers les alcanes à longues chaînes. Cependant, la souche résultante *E. coli* DH5α (pAlk3) n'a pas montré d'émission de lumière

augmentée en présence de tétradécane (C₁₄), tandis qu'elle rapportait toujours efficacement de basses concentrations d'octane (C₈). De manière surprenante, l'utilisation de *A. borkumensis* en tant que souche hôte pour le nouveau plasmide rapporteur basé sur la GFP a totalement supprimé la sensibilité pour l'octane, tandis que la détection de tétradécane n'était pas accrue. Cet aspect devra être résolu dans de futurs travaux.

Pour calibrer la plateforme de biocapteurs, nous avons simulé une fuite de pétrole en mer dans une bouteille en verre ouverte de 5 L contenant 2 L d'eau de mer contaminée avec 20 ml (1 %) de pétrole brut. La phase aqueuse a été échantillonnée à intervalles réguliers après la fuite durant une période allant jusqu'à une semaine tandis que les principaux contaminants pétroliers étaient mesurés via les biocapteurs. L'émission de bioluminescence a été mesurée de manière à déterminer la réponse des biocapteurs et une calibration intégrée faite avec des inducteurs types a servi à calculer des concentrations d'équivalents inducteurs dans l'échantillon. *E. coli* a été utilisée en tant que souche hôte pour la plupart des spécificités des biocapteurs, à l'exception de la détection du naphtalène et du phénanthrène pour lesquels nous avons utilisé *B. sartisoli*. Cette souche, cependant, peut être employée plus ou moins selon la même procédure. Il est intéressant de noter que le pétrole répandu a produit une apparition séquentielle de composés dissouts dans la phase aqueuse, ceux-ci étant détectables par les biocapteurs. Ce profil contenait d'abord les alcanes à courtes chaînes et les BTEX (c'est-à-dire benzène, toluène, éthylbenzène et xylènes), apparaissant entre des minutes et des heures après que le pétrole a été versé. Leur concentrations aqueuses ont par la suite fortement décliné dans l'eau échantillonnée après 24 heures, à cause de la volatilisation ou de la biodégradation. Après quelques jours d'incubation, ces composés sont devenus indétectables. Les HAPs, en revanche, sont apparus plus tard que les alcanes et les BTEX, et leur concentration a augmenté de pair avec un temps d'incubation prolongé. Aucun signal significatif n'a été mis en évidence avec le biocapteur pour le biphenyl ou pour la génotoxicité. Ceci démontre l'utilité de ces biocapteurs, spécifiquement pour la détection des composés pétroliers, comprenant les alcanes à courtes chaînes, les BTEX et les HAPs légers.

GOALS

This study specifically aimed at:

- 1. Developing a bacterial bioreporter for measuring bioavailable phenanthrene**
- 2. Studying the influence of dissolved organic matter and biosurfactants on the PAH bioavailability to bacteria**
- 3. Measuring PAH diffusion with bacterial bioreporters**
- 4. Developing a biosensor platform for the simultaneous monitoring of relevant crude oil components**

When this work was initiated, the bacterial biosensors for PAH that were described in the literature were restricted to the detection of naphthalene [1-3]. (Although one had been developed to detect fluorene [4], its utilization had remained marginal.) A bacterial biosensor expressing GFP as a reporter protein and based on the phenanthrene-degrading bacterium *Burkholderia sartisoli* strain RP007 [5] had been designed in the lab, producing the new biosensor strain RP037. Hence, the thesis first focused on validating the reliability of *B. sartisoli* strain RP037 as sensor for the detection of phenanthrene in liquid assays. Due to the hydrophobic properties of phenanthrene (its solubility in water is about 25 times lower than that of naphthalene), we specifically focused our attention to the study of phenanthrene mass transfer to the bacterial cells and how this was affected by physico-chemical conditions. The PAH flux (or mass transfer) to the aqueous phase is often considered as a limiting factor of bioavailability, and consequently of high importance for PAH biodegradation [6]. Since strain RP037 was genuinely reporting the phenanthrene flux in liquid cultures, our goal with these studies was to understand how different physicochemical factors would influence phenanthrene bioavailability, as seen directly by the bacterial cells. We therefore investigated the effect of substances that were i) acknowledged to modify the availability of organic contaminants and ii) that were environmentally relevant. Firstly, humic acids were employed in the culture medium in order to mimic the influence of dissolved organic matter on the PAH flux to the cells. Secondly, we tried to determine what effects several biosurfactants had on the phenanthrene availability and degradation by *B. sartisoli* strain RP037. Initiated early in this work, the tagging of the strain RP037 with another autofluorescent protein was achieved

with the insertion of a transposon encoding mCherry. The resulting strain, RP037-mChe, was tested with a new experimental set-up developed for the study of PAH diffusion on the millimetre to centimetre scale. We also investigated the capacity of individual RP037-mChe cells to report for the presence of phenanthrene.

In parallel, we wanted to achieve a more complete set of biosensors to cover the full spectrum of compounds released from petroleum oil. Hereto we constructed a set of new bacterial biosensors for the measurement of alkanes based on the AlkS transcriptional activator of the marine bacterium *Alcanivorax borkumensis*. We hypothesized that these new constructs, unlike existing alkane biosensors, might detect long-chain alkanes. In addition, we designed a bacterial biosensor platform that allowed us to rapidly screen aquatic samples for the presence of typical crude oil components, such as alkanes, BTEX (benzene, toluene, ethylbenzene and xylenes) and PAH, and used this extensively to analyze the bioavailable fractions of dissolved compounds released directly after oil spillage.

OUTLINE

CHAPTER 1

General Introduction: bacterial biosensors for measuring availability of organic pollutants

This chapter describes the concept of bacterial biosensors, the construction of the genetic circuitry and the choice of a reporter protein. It highlights the advantages or disadvantages for using living cells as sensors and reporters. The concept of bioavailable and bioaccessible fractions of an environmental pollutant are described. It focuses on biological and chemical assays for measuring availability and accessibility. We give examples from the literature on existing bacterial biosensors used for the detection of BTEX, for the detection of PAHs, for the detection of phenolic compounds and for the detection of PCBs and oils.

CHAPTER 2

A new GFP-based bacterial biosensor for analyzing phenanthrene fluxes

In this study, we begin by introducing the concept of PAHs in the environment and their microbial degradation, with a focus on the low bioavailability of PAHs. We describe the construction of *B. sartisoli* strain RP037, a GFP-based bacterial biosensor for the detection of phenanthrene. It is shown how the growth on phenanthrene crystals can trigger GFP expression from strain RP037. A comparison is made between the GFP expression and the metabolic state of the cells. We show how the bacterial biosensor RP037 detects variations in the flux of phenanthrene to the aqueous phase, and that exposure to a historically PAH-contaminated soil induces GFP expression in RP037 at a high level.

CHAPTER 3

Influence of dissolved organic matter on NAH and PHE availability to the bacterial biosensor *Burkholderia sartisoli* RP037.

Here are evoked the interactions of dissolved organic matter (DOM) with hydrophobic contaminants in natural environments. Using humic acids as a model DOM, we ask whether humic acids have an effect on PAH availability to *B. sartisoli* strain RP037. We show that a

vapour phase delivery assay of naphthalene can be influenced by the presence of humic acids. On the other hand, we conclude that the degradation of phenanthrene by strain RP037 grown in liquid culture is not influenced by humic acids, neither is its GFP expression.

CHAPTER 4

Co-cultivation of the bacterial biosensor *Burkholderia sartisoli* strain RP037 with a biosurfactant-producing *Pseudomonas putida* strain and effect of two types of biosurfactants on PAH availability.

We give a definition of biosurfactants, and we present *Pseudomonas putida* strain PCL1445, a rhizosphere inhabitant that produces lipopeptides. We show that the co-cultivation of strain RP037 with strain PCL1445 enhances GFP expression compared to a single culture, but that the same effect is observed with a non-lipopeptide producing mutant of *P. putida*. In addition, the addition of semi-purified lipopeptides to cultures of strain RP037 does not enhance phenanthrene bioavailability to the bacterial biosensor. However, the addition of a commercial solution of rhamnolipids increases the growth rate on phenanthrene of strain RP037 and slightly induces its GFP expression.

CHAPTER 5

Double-tagged fluorescent bacterial biosensor for the study of PAH diffusion and bioavailability

In this chapter, we present the construction of the double-tagged GFP/mCherry biosensor *B. sartisoli* RP037-mChe. We demonstrate the constitutive mCherry expression and the inducible GFP expression in RP037 in presence of naphthalene or phenanthrene. A new experimental set-up with RP037-mChe biosensor cells embedded in a gel patch is proposed, in which naphthalene and phenanthrene diffusion from a point source trigger a gradient of GFP fluorescence. We finally show that the exposure to historically PAH-contaminated soil induces high GFP expression and that non-contaminated soil samples spiked with phenanthrene are also able to induce GFP expression in individual RP037-mChe cells.

CHAPTER 6

Development of a multiwell bacterial biosensor platform for the monitoring of hydrocarbon contaminants in aqueous environments

We describe here a biosensor platform for the measurement of typical oil components in water samples. We mimic an oil spill in a glass bottle and analyse the oil-spilled sea water with a multiwell bacterial biosensor platform over time. We also report the construction of a new bacterial biosensor for the detection of PAH and its implementation in the platform.

CHAPTER 7

Development of new bacterial biosensors for the detection of alkanes based on the transcriptional activator AlkS from the marine bacterium *Alcanivorax borkumensis* strain SK2

We present *Alcanivorax borkumensis*, a marine bacterium that feeds preferentially on alkanes. We describe a series of reporter fusions based on the alkane degradation operon of *A. borkumensis*, in order to construct a new bacterial biosensor for long-chain alkanes. A comparison is made between *E. coli*-based and *A. borkumensis*-based biosensors. A calibration of the new *E. coli*-based biosensor towards octane and tetradecane is provided.

CHAPTER 1

GENERAL INTRODUCTION:

BACTERIAL BIOSENSORS FOR MEASURING AVAILABILITY OF ORGANIC POLLUTANTS

Traditionally, pollution risk assessment is based on the measurement of a pollutant's total concentration in a sample. The toxicity of a given pollutant in the environment, however, is tightly linked to its bioavailability, which may differ significantly from the total amount. Physico-chemical and biological parameters strongly influence pollutant fate in terms of leaching, sequestration and biodegradation. Bacterial sensor-reporters, which consist of living micro-organisms genetically engineered to produce specific output in response to target chemicals, offer an interesting alternative to monitoring approaches. Bacterial sensor-reporters detect bioavailable and/or bioaccessible compound fractions in samples. Currently, a variety of environmental pollutants can be targeted by specific biosensor-reporters. Although most of such strains are still confined to the lab, several recent reports have demonstrated utility of bacterial sensing-reporting in the field, with method detection limits in the nanomolar range. This review illustrates the general design principles for bacterial sensor-reporters, presents an overview of the existing biosensor-reporter strains with emphasis on organic compound detection. A specific focus throughout is on the concepts of bioavailability and bioaccessibility, and how bacteria-based sensing-reporting systems can help to improve our basic understanding of the different processes at work.

This chapter was previously published as a review in the open access journal *Sensors* (2008), issue 8, pp. 4062-4080, by Robin Tecon and Jan Roelof van der Meer.

INTRODUCTION

Sensing techniques form an integrated part of our modern life. We like to be accurately and constantly informed about the quality, security and composition of products that we consume or encounter in our daily life. Medical tests need to provide instantaneous answers on health parameters, blood values or presence of potential pathogenic organisms. Industrial processes rely on constant physical and chemical sensing of process parameters, system inflow or outflow. Sensors come in thousand and more forms and shapes, principles and output. Future demand calls for further miniaturization, continuous sensing, rapidity, increased sensitivity or flexibility.

One of the emerging domains in sensing technology is the use of living (microbial) cells or organisms. Whereas this principle is arguable very old (for example, mine canaries were used in Roman times to sense carbon monoxide), it is only since the last twenty years that living cell-based sensing assays have gained impetus and developed into a scientific and technological area by itself. The question we would like to discuss here is why one would use living cells and organisms for sensing? What are the specific purposes for basing sensing methods on living cells and what are the advantages that cellular-based sensing can have over other sensing techniques? In this overview we will concentrate specifically on bacteria-(microbe-) based sensor (MBS) methods. We will shortly rehearse the major design principles in MBS and give some examples of potentially useful applications that have been achieved up to now. Furthermore, we will focus our attention on the concepts *bioavailability* and *bioaccessibility*, which are useful to explain the central conceptual differences between sensing based on living cells and other sensing methods.

MICROBE-BASED SENSORS (MBS)

Initiated almost twenty years ago [7], the engineering of microbial cells with the purpose of chemical detection has enormously expanded since [8-10]. The major driving force for this development has been the advance in genetic engineering techniques; the relative ease to redesign (certain) hardware components in microbial cells and to assemble synthetic genetic circuitry for sensing and producing robust output signals. Although in principle any constituent, product or reaction of living cells can form the basis for a 'sensing device', most research has concentrated on non-cognate so-called reporter proteins that are to be produced

by the cell after specific contact or interaction with a target analyte or condition [11, 12]. The use of non-cognate proteins as reporters ensures a low background in the absence of the trigger, and, ideally, a highly specific output signal [9, 13, 14]. In addition, the conditional synthesis of the reporter protein is an important prerequisite for a high signal-to-noise ratio.

The choice of a suitable reporter protein is dependent on the targeted application form. For example, MBS used for *in-situ* single-cell measurements often apply autofluorescent proteins as reporters [15, 16]. A large variety of autofluorescent proteins with different spectral properties, maturation kinetics, photobleaching or temperature stability is now available, mostly but not exclusively based on mutants of green fluorescent protein (GFP) or DsRed [17, 18]. Recently, a new type of fluorescent protein based on the YtvA protein of *Bacillus subtilis* and *Pseudomonas putida* was developed that can produce fluorescence even in the absence of oxygen, a characteristic which GFP does not have [19]. Bulk measurements of MBS have been carried out with several different types of reporter proteins [9], of which bacterial and eukaryotic luciferases have been particularly popular [20, 21]. Mostly because of their relatively high quantum yields, luciferases have been the optimal choice for highly sensitive applications. Different spectral variants have been developed by mutagenesis strategies [22, 23]. On the other hand, eukaryotic luciferases require substrate addition and cell membrane permeabilization in bacteria, which somewhat limits their practicality for MBS assay configurations. Bacterial luciferases have been the most applied reporters in MBS. Two different configurations have been used, one (LuxCDABE), in which the cells synthesize the substrate for the luciferase, and another (LuxAB), in which external substrate addition is needed [20, 21]. Although external substrate addition is somewhat more cumbersome, it avoids false-positive stimulation of luciferase activity by membrane regeneration [24] and is less energy demanding for the cell. Other reporter proteins can be used for colorimetric or electrochemical detection [9]. Of these, beta-galactosidase is currently probably the most versatile, because a large variety of substrates is available for different detection purposes.

In most of the current designs, the *de novo* synthesis of reporter protein is under control of a transcription factor, which directs the repression or induction of reporter gene expression from a dedicated site on the DNA (e.g., promoter). The sensory function can be provided by the transcription factor itself via, for instance, an internal effector binding domain that transmits target perception to forming productive interactions with RNA polymerase [13], or via a sensory protein, which subsequently transmits the perception event via a signalling cascade (e.g., phosphorylation) to the ultimate transcription regulator [25] (Fig. 1). Sensing events are thus translated and amplified in the form of reporter protein synthesis, the activity

of which is generally measured in the assay (resulting in further signal amplification). The specificity of target detection is determined by the recognition specificity of the primary sensor protein or transcription factor, and by any other condition influencing the signaling cascade or acting on the same promoter [26]. The construction of the genetic circuitry for the sensor-reporter conditional switch is accomplished by established recombinant DNA technology or, more and more, by direct DNA synthesis. Dedicated resources have become available that list available biological parts and their specifications needed for the circuitry, much like catalogues of electronic parts (http://partsregistry.org/Main_Page, Fig. 1). Due to the ease of manipulation, bacteria such as *Escherichia coli* are very often used as host cells for the sensor-reporter constructs, but likewise have yeast [27] or human cell lines [28] been employed. Many different instruments can be used for the measurement of the reporter signal, and both populations of sensor-reporter cells (i.e., bulk measurements) or individual cells can serve as basis for reporter analysis (Fig. 2).

BIOAVAILABILITY

Are there specific advantages for exploiting living cells for sensory purposes rather than e.g., physico-chemical detectors, or even purified proteins and antibodies? Obviously, in order for the sensor-reporter construct to operate, the MBS need to be maintained alive and in some sort of active state and optimal environment to produce the required response. This requirement in practise puts serious constraints on the shelf-life of MBS. On the other hand, MBS are self-propagating entities and therefore relatively easy and cheap to produce. The fact that different MBS can be engineered, which solely differ in target recognition but otherwise have the same reporter output signal, may pave the way for sensing arrays while maintaining relatively simple detectors and devices [10] (box 1). The main important advantage for using MBS, however, that (for the time being) only cells themselves can provide is the integration of biological processes relevant to the target one would like to address. Cellular toxicity, for instance, is conceptually most easily determined by the cell in question itself, if we succeed in interrogating the appropriate biochemical elements in the cell. Bacterial pollutant degradation activity (another domain where MBS are used) is most accurately measured by the bacterial cells themselves, which we can translate into a useful reporter signal when directing the dedicated genetic sensor-reporter circuit to the appropriate key elements in the cell.

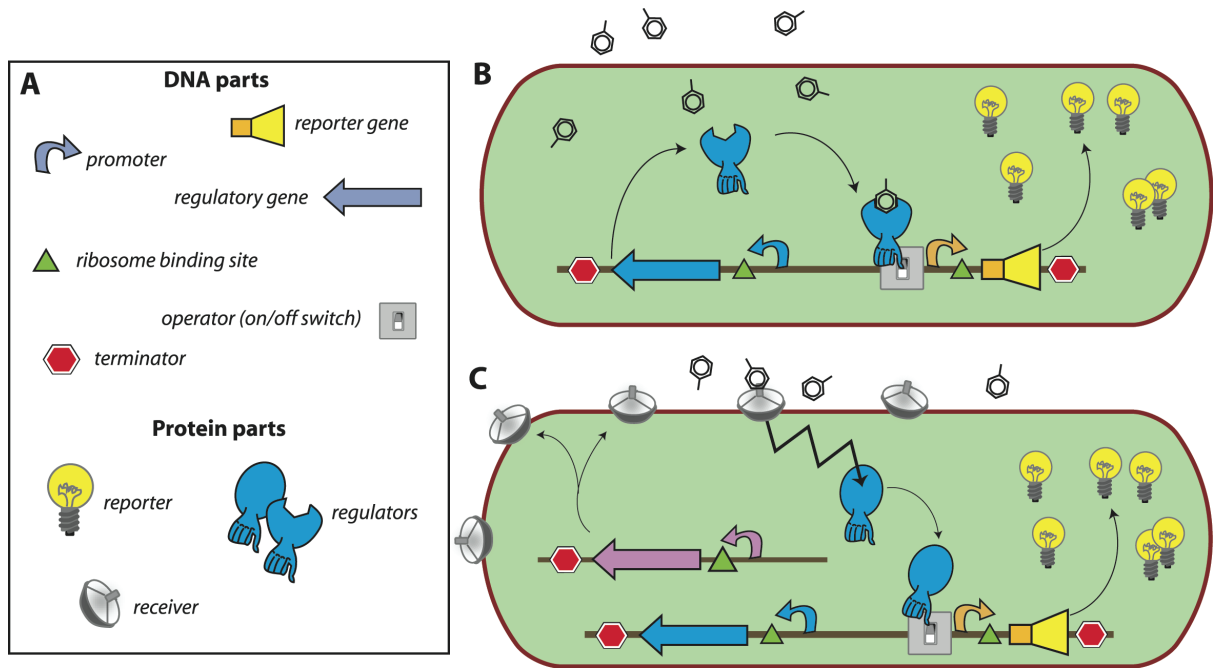


Fig. 1. Concept of a bacterial sensor-reporter cell. (A) DNA parts necessary for constructing an inducible sensor-reporter circuit. Parts can be combined and assembled by genetic engineering techniques. Regulatory and reporter genes are necessary for the sensing function and system output, respectively. Promoter, operator(s), terminators, ribosome binding sites, etc. are DNA sequences needed for control of the gene expression. (B) Set-up in which the sensor function is provided by a single regulatory protein. In this example, the regulator protein binds the target compound and induces the transcription of the reporter gene, leading to the production of reporter proteins (signal amplification). (C) Set-up for separated sensor and regulator functions. In this configuration, the target compound is sensed by a periplasmic receiver protein that transmits the detection event via a signalling (e.g. phosphorylation) cascade to the regulatory protein (zigzag arrow). The activated regulator then induces reporter gene expression as before.

In the following, we will thus argue that the key advance made by MBS is to analyze biologically relevant processes while providing at the same time a certain analogue (the bioavailability or bioaccessibility fraction) to classical chemically derived compound concentrations (or chemical ‘activities’). This is most easily explained in the form of the example of pollutant remediation and environmental risk assessment.

BIOREMEDIATION AND RISK ASSESSMENT

Environmental risk assessment is an essential tool in the investigation of polluted sites and the subsequent decision making process on the eventuality of active site remediation. In Switzerland alone, some 50’000 polluted sites have been entered in inventory – among which 4’000 may represent a danger for environment and will have to be treated in the next 15 years [29]. Obviously, there is insufficient public funding available for an extensive treatment of every site, and thus priorities have to be set on the basis of pollution exposure and risks. Current regulations most often base on total pollutant concentrations at a site for predicting risks. However, most likely only a fraction of the total amount of hazardous substance will actually have an impact on living organisms (by definition, the fraction which is available or accessible to the organisms). Therefore, the use of the total amount is likely to overestimate the risk [30]. The discrepancy between the total and the bioavailable or bioaccessible fractions is particularly significant in the case of contaminants with poor aqueous solubility (e.g., PCBs, PAHs) or very low dissociation constants (e.g., certain heavy metal precipitates). Nowadays, increasing attention is thus given to *bioavailability* assays that better predict the real exposure of specific organisms to pollutants [31].

Although the term *bioavailability* is frequently used in scientific papers, it does not always have the same definition. For this reason, other authors preferred to speak of *bioavailability processes*, to reflect the fact that various biological, chemical or physical steps influence the final outcome [31]. In this review, we will use Semple’s definition of bioavailability as the fraction of a chemical in a system “which is freely available to cross an organisms’s (cellular) membrane from the medium the organism inhabits at a given point in time” [32, 33]. The authors further suggested using the term *bioaccessibility* to distinguish the fraction that could *potentially* cross the cellular membrane if the organism had access to it. A bioaccessible fraction can become bioavailable over time or in space if physical barriers that restrict access to the organism are relieved.

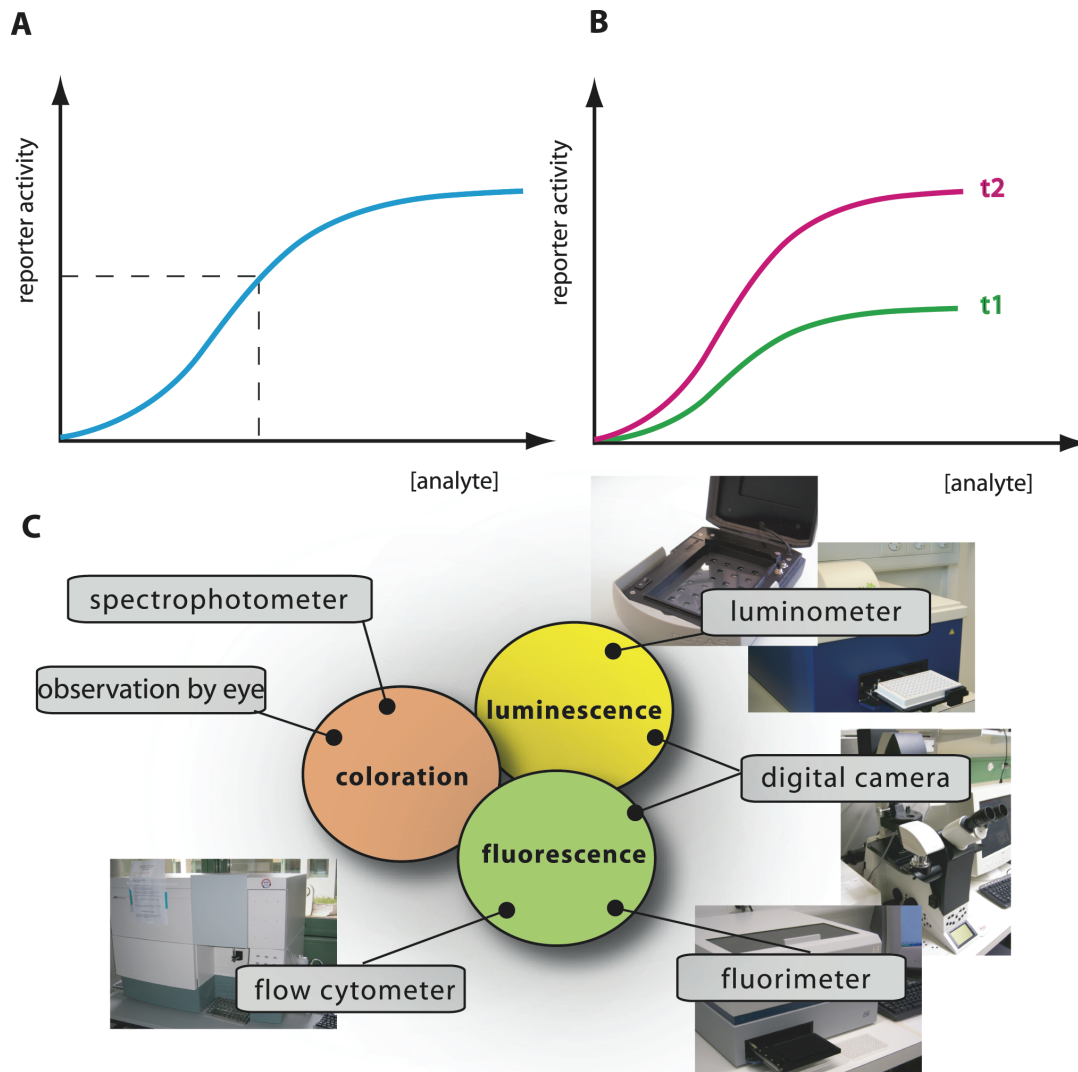


Fig. 2. Schematic analysis of an MBS-assay. (A) Typical calibration curve with reporter output as a function of analyte concentration, produced from incubations with a set of known analyte concentrations. Output from an unknown sample is interpolated on the calibration curve (dotted lines), analyzed at the same time and under the same conditions, to derive a value of 'equivalent target compound concentration'. Additional spiking assays can be performed (i.e., adding known target amounts to unknown samples) to correct for possible sample interferences or presence of toxic compounds. (B) Time-dependent signal calibration. MBS-assays are usually carried out in such a manner that output values are relative: dependent on incubation time and amount of cells in the assay. Here as an example curves t2 and t1 for longer and shorter incubations, respectively. For this reason, simultaneous calibration curves must accompany analysis of unknowns. (C) Various instruments for measuring reporter output, here shown as an example for three currently used reporter activities: fluorescence, bio- or chemiluminescence, and colorimetry.

Organisms themselves can influence the bioaccessible fraction by changing the compound mass-transfer rate to the cells [6]. For example, a bacterium metabolizing a poorly water-soluble carbon compound will deplete this from solution, which can drive further dissolution from a solid phase. Semple *et al.* argued that it would be useful to differentiate chemically active compound (bioavailable) from chemically inactive but potentially exploitable (bioaccessible), and that for risk assessment the bioaccessible fraction would be the more relevant determinant. Bioaccessibility is inherently organism-dependent [31], but its actual (numeric) value may be the same among various organisms. Therefore, model organisms such as MBSs may be useful to assay bioaccessibility.

BIOAVAILABILITY AND BIOACCESSIBILITY ASSAYS WITH MBS

We could thus envision different types of bioassays targeting compound bioavailability and bioaccessibility. A typical MBS assay consists of incubating the cells in an aqueous sample for a particular pre-defined reaction period, after which the reporter signal is determined (Fig. 2). Because in this case the sensor-reporter cells can be assumed not to have been limited by the access of the compound in solution (i.e., no mass transfer limitation existed), they must have detected the fraction which was bioavailable to them during the assay period. We will see that this is essentially the case, although metabolic decisions in cells can still influence the behaviour of the sensor-reporter [26, 34]. Bioaccessibility assays are trickier to perform, because in essence they have to somehow overcome the time or spatial barrier that prevents further compound transfer to the cells. Chemically, bioaccessibility can be tested by using so called non-exhaustive extraction techniques (NEETs). NEETs employ, for instance, Tenax or cyclodextrins to rapidly retrieve a compound fraction from the sample that is similar to the fraction metabolized by (micro-) organisms during a much longer incubation period [32, 35]. For example, Dick *et al.* added [^{14}C]-labeled phenanthrene or pyrene to soils, and showed that the total fraction of PAHs metabolized by bacteria in the soil during thirty days as derived from [^{14}C]- CO_2 evolution was almost the same as the PAH-amount extracted by hydroxypropyl-beta-cyclodextrin [35]. In a MBS assay, this might be imitated by using sensor-reporter cells which not only detect, but also metabolize the target compound. These cells will create a mass transfer flux during the assay and may thus more faithfully detect the bioaccessible fraction (Fig. 3). For the remainder we will discuss a

number of MBS assays specifically in the light of bioavailability – bioaccessibility detection of organic chemicals.

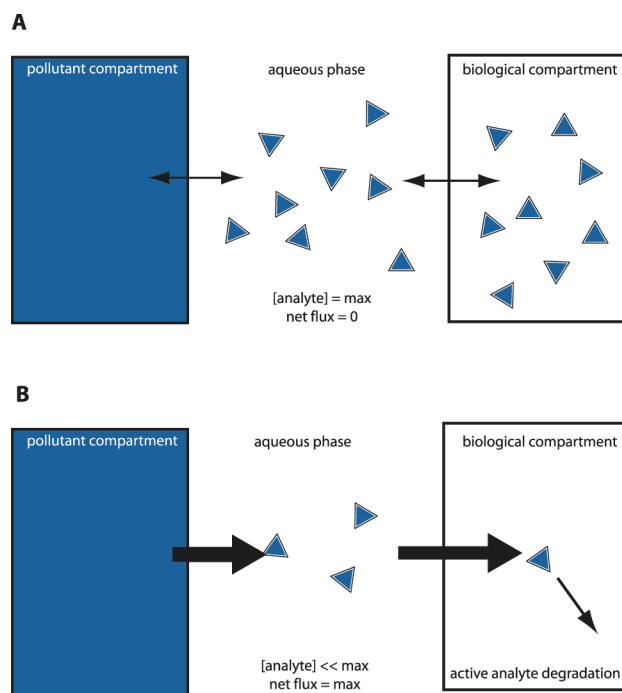


Fig. 3 'Equilibrium' versus 'sink' sensor-reporter cells to differentiate between bioavailable and bioaccessible fractions. (A) Microbe-based sensors (MBS) which do not degrade the analyte rely on the aqueous phase concentration or chemical activity. An equilibrium will arise between bulk aqueous phase concentration, lipid fraction and intracellular compound concentration (the latter more or less equalling the aqueous phase concentration). The MBS can only sense the immediate or bioavailable fraction. (B) MBS that can degrade the analyte. By degrading the analyte, a flux is created from the pollutant compartment to the biological compartment. The MBS thus acts as a 'sink' and can detect part of the bioaccessible fraction. Thickness of the arrow points to the pollutant flux from one compartment to the other. The MBS cell here is depicted as a square box.

MBS DETECTION OF BENZENE, TOLUENE, ETHYLBENZENE AND XYLENES

In a number of MBS-assays so-called BTEX compounds were addressed. BTEX stands for benzene, toluene, ethylbenzene and xylene; four volatile aromatic compounds that are found in crude oil, gasoline and natural gas. BTEX are also massively produced by industry as solvent and starting materials for chemical synthesis, and are considered as one of the major environmental pollutant classes [36-38]. The four compounds have various toxic effects, including blood disorder, impact on the central nervous, reproductive and respiratory systems, whereas benzene is also a known carcinogen [39]. Because BTEX compounds are rather water soluble (e.g., up to 1.8 g/L for benzene [40]), they represent a risk for drinking water pollution [39]. On the other hand, their volatility and hydrophobicity make it hard to predict their bioavailability and bioaccessibility.

The first MBSs for the detection of BTEX and related compounds were created more than ten years ago using the regulatory protein XylR and the P_u promoter from the xylene degradation pathway on the TOL plasmid of the bacterium *Pseudomonas putida* mt-2 as a conditional switch [41, 42]. One of these consisted of an *Escherichia coli* strain carrying the plasmid pGLUTR, which expresses firefly luciferase (*luc* gene) from the XylR- P_u system [43]. Other MBSs for BTEX used the TodST sensor-regulatory proteins and the P_{todX} promoter from the toluene degradation pathway of *Pseudomonas putida* F1, coupled to expression of bacterial luciferase [44-46]. Also the regulatory protein TbuT and the P_{tbuA1} promoter from the toluene degradation pathway in *Ralstonia pickettii* PKO1 have been used as a basis for a BTEX-MBS, this time exploiting *Pseudomonas fluorescens* A506 (pTS) as a host strain expressing the green fluorescent protein (GFP) as reporter [47]. Both *E. coli* DH5alpha (pGLUTR) and *P. fluorescens* A506 (pTS) were not able to degrade BTEX compounds, whereas the MBSs employing the TodST- P_{todX} constructions was. Interestingly, the presence of other carbon substrates diminished the reporter output from *P. putida* F1- P_{todX} -*luxAB* [46]. The authors explained this behaviour by assuming that multiple usable carbon substrates diluted the metabolic flux through the toluene pathway [46]. Although this can be considered as a hindrance for successful use of the MBS for bioaccessibility measurements, the system does present a faithful reaction of the cells. This implies that in this case toluene bioaccessibility is diminished because of simultaneous presence of other compounds. Even the non-degrading MBS for BTEX did not in all cases respond to the available fraction in aqueous solution, because of metabolic interference at the P_u -promoter. This promoter is especially prone to secondary control, such as via the phenomenon of

‘exponential phase silencing’ [48]. The result of this interference is that the promoter is not induced even though sufficient toluene is present for the cell.

As outlined above, in most assays the MBS were calibrated in aqueous solution with known BTEX concentrations. The reporter signal produced from unknown aqueous sample incubations is interpolated on the calibration curve, from which a so-called BTEX-equivalent concentration can be derived (box 1). In order to appropriately estimate BTEX availability and accessibility in contaminated soils, samples have been extracted and the extract incubated in the MBS assay. Willardson *et al.* attempted to extract soils with ethanol and add the ethanol extract in the MBS-assay. A dilution of almost twenty times had to be used, at which ethanol concentration still \approx 40% inhibition of the cells occurred. This resulted in a BTEX detection limit of 30 mg/L [43]. Other groups used soil-water extracts [49, 50], and showed that toluene-equivalent concentrations determined in the MBS-assay were similar as the total concentration of ethylbenzene plus benzene in the soil-pore aqueous phase by GC-MS [50]. Dawson further compared BTEX degradation in soil over a 30-days time period and measured toluene-equivalent concentrations in the soil-water extract by their BTEX-biosensor. They showed that the MBS detected less-and-less over time as biodegradation proceeded, but no correlation was made to the total BTEX load in the soil determined by methanol extraction and GC [49]. From these studies we can thus conclude that MBS detect bioavailable fractions in soil-water extracts which are similar as the dissolved chemical concentration (except in the case of metabolic interference as discussed above). Organic extractions on the other hand, retrieve higher BTEX fractions from soil, and, therefore, MBS-assays on the organic solvent extracts provide an idea about the bioaccessible fraction. Disadvantage of use of organic phases is that they easily inhibit the cells in the assay. For this reason, the extracts have to be used in highly diluted form.

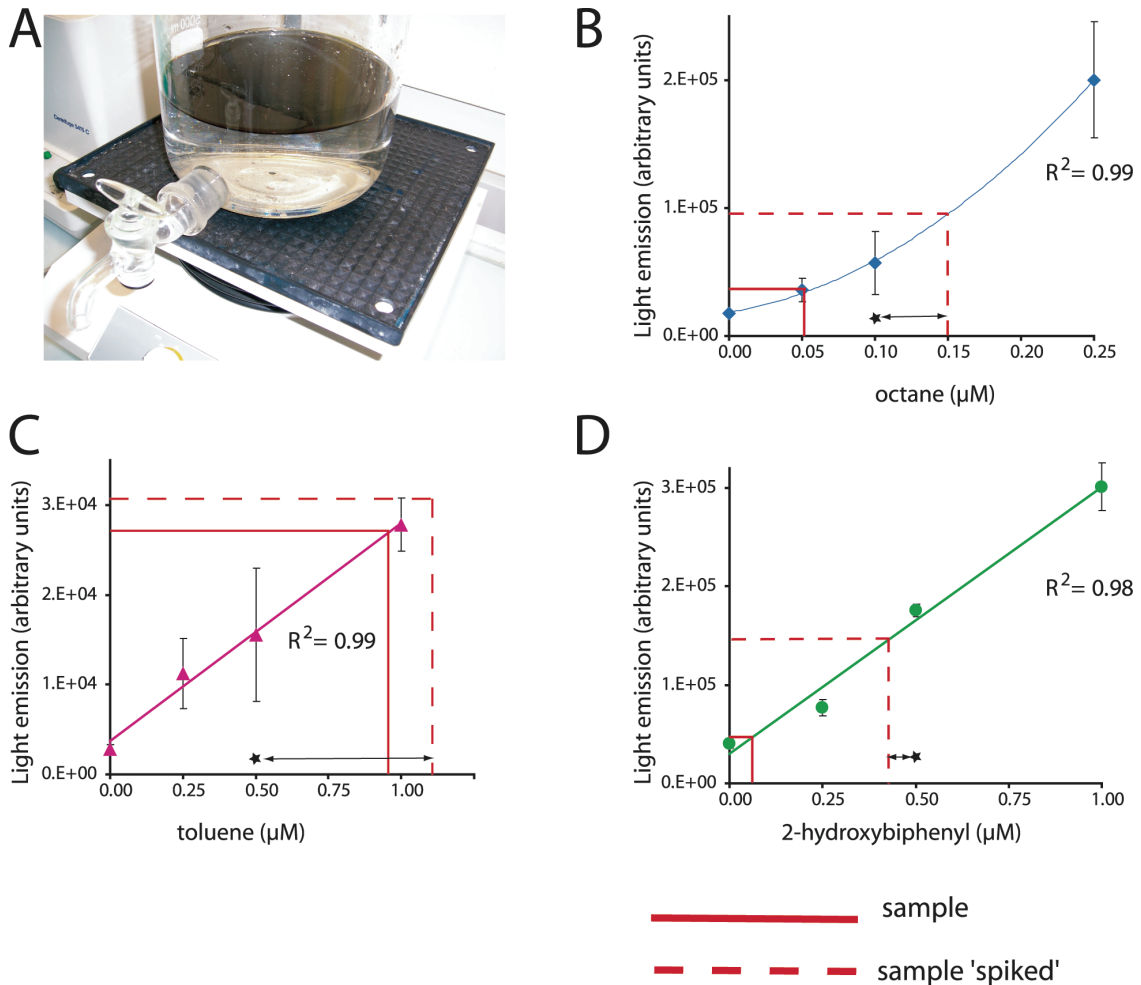
Very few studies actually investigated BTEX availability and accessibility fractions in soil without the introduction of an extraction step. In principle, an incubation of MBS cells with the sample and subsequent retrieval and measurement of the MBS reporter signal at different incubation time periods would show the immediate response (i.e., bioavailable fraction) and the slow released fraction (bioaccessible). An excellent example of this principle was provided by Leveau *et al.* [51], who analyzed fructose bioaccessibility on plant leaves. Casavant and colleagues [52] developed a similar idea for monitoring toluene availability *in planta*. However, their sensor-reporter system did not show a dosage effect, but only produced a yes-or-no signal. From the number of individual MBS cells expressing GFP isolated from the exposed plant root they could infer the past exposure to toluene. These

biosensor cells did not degrade the target compound and, therefore, only detected the bioavailable fraction of toluene in the system above the threshold needed to trigger the response. Also in this study, the authors observed that the MBS was influenced by indigenous chemicals such as isoprene, which led to GFP induction.

THE BIOAVAILABILITY PROBLEM OF VERY POORLY WATER SOLUBLE COMPOUNDS

The distinction between bioavailability and bioaccessibility becomes even more pronounced for polycyclic aromatic hydrocarbons (PAHs) than for BTEX. PAHs comprise a large group of compounds (>100 chemicals studied), most of which have no direct commercial use. They consist of two or more fused aromatic rings, have an elevated melting point and poor water solubility, and are typically formed during incomplete burning of organic material [53]. Combustion of coal, oil, gas and garbage are common sources of PAH production, but they can be found in cigarette smoke or grilled meat as well. PAHs in the environment mostly occur in sorbed form to organic matter or soil particles [53]. Apart from their acute toxicity, some PAHs are known or suspected carcinogens and they accumulate in animal tissue [40]. PAH biodegradation rates are strongly dependent on the chemical nature and number of aromatic rings, and are generally strongly limited by poor aqueous solubility [54]. For all these reasons, it is extremely important to have accurate measurements of PAH bioavailability and bioaccessibility, and in a variety of environments.

Bacterial MBS have mostly been designed for naphthalene(s) – a two-ring PAH of low molecular weight and moderate solubility in water – because of the known genetic details on naphthalene degradation [3, 55, 56]. Naphthalene-sensing MBS have typically applied the NahR regulatory protein in conjunction with the P_{sal} or P_{nah} promoters from the NAH7 plasmid of *P. putida* pPG7 [7, 57]. Interestingly, use of this genetic circuit automatically leads to the detection of a metabolic ‘flux’ rather than of equilibrium concentration, since the chemical effector for NahR is not naphthalene but its metabolite salicylate [56]. Naphthalene needs to be metabolized by the MBS in order to generate internal salicylate, which then triggers reporter protein synthesis. Once in fully ‘activated’ state, the flux through the naphthalene pathway is high and internal salicylate concentrations will be low.



Box 1. Multi-target biosensor analysis. Because a single bacterial host strain can be implemented with a wide diversity of genetic reporter circuits, multi-target arrays can be designed. The bacterium *Escherichia coli* is a long known laboratory ‘pet’ organism, whose growth and maintenance are easy and well controllable. For this reason, this bacterium has often been used as a host strain for sensor-reporter constructions and various reporter strains of *E. coli* are now available for a diversity of target chemicals. Since only small volumes of aqueous sample are required for an MBS-assay, a single sample can be tested against a battery of sensors with different target specificities. (A) Two liters of sea water were contaminated with 1% (v/v) of crude oil in a glass flask. Two hours after the addition of oil, water was sampled via the tap and analyzed for three compound classes in parallel, alkanes, BTEX and 2-hydroxybiphenyl. (B, C and D) Typical calibration curves with pure compounds in uncontaminated sea water. Output values obtained from the contaminated sample and from a spiked sample are indicated. Spiking consists of adding a known concentration of inducer (indicated by a star) that allows us to verify if the MBS is reporting satisfactorily. Data: R. Tecon and S. Beggah (unpublished).

Cells thus act as a sink for naphthalene and drive naphthalene diffusion toward them, a prerequisite for bioaccessibility assays [3]. A fluorene-targeting MBS was developed on the basis of randomly introducing a *luxAB* transposon into *Sphingomonas* sp. strain L-132 [4]. Although these cells could no longer completely metabolize fluorene as a consequence of the transposon insertion, they still partially transformed the compound and thus continue to act as sink. The strain detected fluorene concentrations as low as 200 µg/L (1.2 µM) in aqueous phase with a response time of between 30 min and 4 h. A phenanthrene-detecting MBS was constructed using *Burkholderia sartisoli* strain RP037. This strain produced GFP after contact with phenanthrene and naphthalene under control of the regulatory protein PhnR and its activated promoter P_{phnS} [58]. PAHs have also been assessed with the help of a sensor-reporter strain induced by a toxicity-response invoked by PAHs [42, 54].

MBS-assays for PAHs demonstrated that the cells are very sensitive to mass-transfer processes and are easily limited by the aqueous phase concentration. For example, the detection limit for naphthalene was lowered from 0.5 µM to 50 nM by using an MBS-assay in the gas-phase rather than in aqueous suspension [3, 59]. This is due to the high volatility of naphthalene and the ~10'000 times faster diffusion rates in air than in liquid [3]. Kohlmeier and colleagues then could further show that biosensor-reporter cells exposed to saturated naphthalene concentrations in aqueous solution without or with further naphthalene crystals produced the same maximum GFP reporter output after 4 h incubation time. However, cells in the assay with crystalline naphthalene continued to grow, leading to a dilution of the amount of GFP in the cells at incubations longer than 4 h as a consequence of the activated state of the naphthalene metabolic pathway (as explained above) [59]. This demonstrated that such cells can be used to differentiate naphthalene bioavailability (4 h measurement) and bioaccessibility (20 h measurement).

For PAHs with higher molecular weight, volatility is strongly reduced and the advantage for measuring with MBS in the gas phase is abolished. For this class of compounds the aqueous solubility strongly limits their bioavailability to the cells. Simple 'calibration' of the MBS-assay by incubating with different aqueous concentrations of the target compound no longer produces sufficiently different reporter activities in the cell. In that case, it becomes an option to calibrate the MBS on the basis of metabolic flux instead of equilibrium concentration (Fig. 3). We illustrated this possibility by using the *B. sartisoli* strain RP037 phenanthrene-sensing MBS [58]. *B. sartisoli* cells produce a stable GFP in response to phenanthrene metabolism. Probably because growth rates on phenanthrene are slower than the GFP synthesis rates, cells experiencing differences in phenanthrene flux produce more GFP

over time. Four days-exposure times were required in order to obtain optimal signal-to-noise ratio, but this allowed us to calculate bioaccessible fractions for phenanthrene loadings in different materials, or from different surface areas [58].

MBS FOR TOXIC ORGANIC COMPOUNDS

Phenol and derivatives are widespread contaminants whose sources are both natural and industrial. Phenol is massively produced and used as a starting material for synthetic polymers and fibers. Phenol is a strong irritant and long time exposure can cause a wide variety of health damages, including effects on the immune system [60]. Various phenol derivatives are known for their toxic action. Examples include 2-hydroxybiphenyl, a common disinfectant and fungicide, and 2,4-dichlorophenoxyacetic acid (2,4-D), a widely used herbicide that can cause nervous system damage in humans. One of the main metabolites of 2,4-D is 2,4-dichlorophenol (DCP), a proton shuttle and dissipator of membrane potential [61]. Various MBS have been developed to target phenolics, and have usually been based on bacteria degrading them.

Some of the earliest MBS for phenols were based on the regulatory protein DmpR and the P_o promoter from the plasmid pVI150 of *Pseudomonas* sp. strain CF600. One MBS of this type, the strain *P. putida* KT2440::DmpR (pVI360), could be activated by phenol, cresols and some dimethylphenols, but did not respond to dichlorophenols or BTEX [62]. Similar MBS were constructed using the CapR-system from *P. putida* KCTC1453 [63] or the MopR-circuit from *Acinetobacter* sp. DF4 [64]. Modifying the sensor domain of DmpR by random mutations resulted in strains with an increased sensitivity to phenols and a broader range of detection [65].

Leedjarv *et al.* reconstructed an MBS based on the DmpR system (*P. fluorescens* OS8 [pDNdmpRlux]) and determined the bioavailable fractions of phenols in dump leachates and contaminated groundwater samples [66]. Since phenols are sufficiently water soluble, the MBS was calibrated in the classical ‘equilibrium’ mode (Fig. 3). The MBS-assay detected phenols in almost all samples, but the bioavailable fractions varied enormously, ranging from 0 to almost 100% of the total chemically-determined phenol amount in the sample. This demonstrated the great importance of taking compound bioavailability in samples into consideration for risk and bioremediation assessments. Sandhu and colleagues addressed the question of phenol bioavailability in the air nearby plant-leaves. Airborne phenol was

detected using an MBS-assay directly on the plant leaves with *P. fluorescens* strain A506, expressing GFP under control of a mutated DmpR [65, 67]. Their results showed that the sensors-reporter cells were able to detect phenol on plant leaves exposed to phenols in the vapour phase. Interestingly, the phenol concentration reported by the cells was more than tenfold higher than the chemically-determined phenol concentration in the air, which the authors interpreted as an accumulation of phenol on leaves.

Jaspers *et al.* developed an MBS-assay for the detection of 2-hydroxybiphenyl, a disinfectant and fungicide, based on the HbpR transcription activator of *Pseudomonas azelaica* [68]. Classical incubation assays in aqueous solution resulted in method detection limits of 0.5 μM , but this could be lowered some twentyfold by using a hypersensitive mutant of HbpR [69]. A hybrid assay was then developed which would detect bio-accumulation of 2-hydroxybiphenyl via crab urine, and this showed that the crabs concentrated 2-hydroxybiphenyl up to 100-fold after being exposed in contaminated seawater for one week (Lewis *et al.*, unpublished).

Using a bacterium degrading 2,4-D and producing luciferase under control of the regulatory protein TfdR and P_{DII} promoter from *Cupriavidus necator* JMP134 [61], Toba and Hay developed a solid-phase MBS-assay for the detection of 2,4-D in soil [70]. In this assay the sensor-reporter cells were spotted onto filter discs that were brought in direct contact for ≈ 60 min with the contaminated soil sample, after which the cells were retrieved and luciferase expression was analysed. Under appropriate moisture conditions, the MBS-assay detected 2,4-D at amounts between 1 and 50 mg/kg soil. Because these MBS cells degrade 2,4-D it would be conceivable to replace the luciferase reporter for GFP, expose for longer times and obtain a 2,4-D bioaccessibility assay – similar as outlined above for phenanthrene [58].

MBS ASSAYS FOR POLYCHLORINATED BIPHENYLS (PCBs) AND OILS

It is particularly challenging to obtain MBSs for PCBs, since no bacterial systems are known that can sense PCBs and trigger gene expression. PCBs are ubiquitous in the environment at low concentrations, are toxic and poorly degraded. PCBs have been shown to cause a large variety of health effects, which is more severe for the higher chlorinated congeners [71]. Because of the lack of appropriate sensory proteins in bacteria, most developments have relied on using co-induction involving further uncharacterized activator proteins. For example, a PCB-degrading *Ralstonia eutropha* served as a host strain for the

construction of a MBS (*R. eutropha* ENV307 [pUTK60]). The strain expresses bacterial luciferase from the P_{bphA1} promoter under control of an unidentified regulatory protein [72]. Although it is not clear whether this sensor-reporter bacterium directly senses chlorinated biphenyls or one of their metabolites, the MBS-assay enabled detection of biphenyl, monochlorinated biphenyls and Aroclor 1242 (a PCB mixture) in aqueous solution down to 1 mg/L. More recently, biosensor-reporter strains were used for PCB detection via its metabolites 3-chlorobenzoate [73] or chloromuconic acids [74]. Furthermore, the aforementioned HbpR system in *E. coli* was used in an assay to detect hydroxylated PCBs in aqueous solution and in human serum, with the idea of detecting metabolites in animals and human exposed to PCBs [75]. Interestingly, some hydroxylated PCBs were detectable at concentrations as low as 10 nM and serum as assay medium was found to result in higher reporter output in the assay [75]. Finally, most recently we ourselves showed that mutants of the HbpR regulatory protein can be obtained which enable direct detection of 2-chlorobiphenyl and triclosan [69]. None of those MBS-assays so far really addressed the issue of PCB bioavailability or bioaccessibility, except indirectly the one using human serum [75].

Another compound class for which bioavailability and bioaccessibility are important issues, are alkanes. Alkanes are common constituents of crude oil, natural gas and oil products, but come in a large variety of different chain lengths, branchings or cyclic forms (e.g., cyclohexane). Their environmental fate strongly depends on the number of carbon atoms, their solubility in water being inversely proportional to this number [40]. Although their acute and chronic toxicity are not extremely high, they form good indicators for oil pollution in the environment. Very few bacterial biosensor-reporter cells were constructed for alkane detection. The first described strain produced bacterial luciferase under control of the AlkS regulatory protein and P_{alkB} promoter from *Pseudomonas oleovorans* [76]. Assays with the AlkS-MBS efficiently detected linear alkanes with chain lengths from C₆ to C₁₀ at nominal concentrations as low as 10 nM [76, 77]. Poor reporter signals were obtained with linear alkanes with longer chain lengths, with branched alkanes or cycloalkanes [76]. Because short-chain alkanes are very volatile, gas-phase based MBS-assays can be used like described for naphthalene detection. Consequently, decreasing the volume of gas phase in the assay helps to lower the apparent method detection limit with sensor-reporter cells in aqueous suspension [77]. An example of the functioning and calibration of this MBS is presented in Box 1. The detection of long-chain alkanes by MBS has proven to be very difficult, probably because of extremely low aqueous solubility (≈ 10 nM [78]), and thus very low bioavailability fraction. As a proof of principle, however, we previously studied the octane mass-transfer

from a point source through the aqueous phase by using an *E. coli* strain with octane-inducible GFP formation [77]. This strain could not degrade but only detect octane and, therefore, could not form a sink driving further diffusion from the source. Octane diffusion gradients could be detected over a length of 2.5 cm in as short as 30 minutes [77].

CONCLUSIONS

We illustrated here that microbial sensors, and in particular bacterial sensors, can easily be designed for a wide variety of purposes. For the sake of shortness, we have omitted any further examples of MBS for heavy metals or toxicity, which have been recently reviewed elsewhere [10, 20]. Leaning on the tools of genetic engineering, today's huge genomic resources and the natural diversity within the microbial world, there is little limitation to our imagination for designing MBSs. In addition, we have shown that a plethora of assay forms can be easily conceived. Cultivation of bacterial cells – the heart of the MBS-assay – is easy, and production costs are very low. Method detection limits of MBS-assays, as we have demonstrated, are often in the nanomolar range, thereby competing effectively with existing chemical analytics. Despite these aspects, MBS-assays are still rarely applied outside research laboratories [14]. Convincing data have been produced which demonstrate field robustness, good measurement precision and accuracy of MBS-assays in comparison to chemical analytics, as in the case of arsenic in groundwater [79] or rice [80]. It is high time that regulatory authorities accept MBS as realistic alternative for a variety of analytical procedures, which would certainly help their implementation. In addition, MBS could offer excellent possibilities for assaying the complex nature of bioavailable and bioaccessible fractions in thousands of cases of severe and toxic pollution, which currently cannot be easily addressed. We are confident that MBS sensing-reporting technology will contribute to fill this gap in the near future.

CHAPTER 2

A NEW GFP-BASED BACTERIAL BIOSENSOR FOR ANALYZING PHENANTHRENE FLUXES

The PAH-degrading strain *Burkholderia sartisoli* RP007 served as host strain for the design of a bacterial biosensor for the detection of phenanthrene. RP007 was transformed with a reporter plasmid containing a transcriptional fusion between the *phnS* putative promoter/operator region and the gene encoding the enhanced Green Fluorescent Protein (GFP). The resulting bacterial biosensor – *Burkholderia sartisoli* strain RP037 – produced significant amounts of GFP after batch incubation in presence of phenanthrene crystals. Coincubation with acetate did not disturb the phenanthrene-specific response but resulted in a homogenously-responding population of cells. Active metabolism was required for induction with phenanthrene. The magnitude of GFP induction was influenced by physical parameters affecting the phenanthrene flux to the cells, such as the contact surface area between solid phenanthrene and the aqueous phase, addition of surfactant, and slow phenanthrene release from Model Polymer Release System beads or from a water-immiscible oil. These results strongly suggest that the bacterial biosensor can sense different phenanthrene fluxes while maintaining phenanthrene metabolism, thus acting as a genuine sensor for phenanthrene bioavailability. A relationship between GFP production and phenanthrene mass transfer is proposed.

This chapter was previously published as a research article in the journal *Environmental Microbiology* (2006), issue 4, volume 8, pp. 697-708, by Robin Tecon, Mona Wells and Jan Roelof van der Meer.

INTRODUCTION

Polycyclic aromatic hydrocarbons (PAHs) belong to a class of widespread organic pollutants whose sources are both natural and industrial – being produced during incomplete combustion of organic matter. Besides their ubiquitous distribution in the environment (in air, soils and sediments), PAHs possess toxic and, for several of them, carcinogenic properties. For this reason there is a substantial interest to remediate PAH-contaminated sites or to stimulate spontaneous natural microbial degradation. Actually, quite a large number of bacterial species are able to degrade PAHs – including genera such as *Pseudomonas*, *Mycobacterium*, *Sphingomonas*, *Burkholderia* and *Ralstonia* [81]. Yet, biodegradation of PAHs in the environment is often limited, e.g. by their low aqueous solubility and their strong tendency to sorb to organic matter, processes which reduce bioavailability [82, 83].

Although the term *bioavailability* is not defined unequivocally [84], we, in this study, shall use a definition similar to that of Semple et al. [83] of bioavailability as “the fraction of a chemical (in a system) that can be taken up or transformed by living organisms” (during the time frame of the experiment). This fraction (and thus bioavailability) can vary under the influence of mass transfer parameters, which include physicochemical processes governing dissolution, desorption and diffusion, hydrological processes like mixing and, finally, biological processes, such as uptake and metabolism [82, 83, 85]. For example, bioavailability is maximal in aqueous phase for completely dissolved compounds harboring suspended cells that may completely degrade the compound. On the contrary, for strongly adsorbing and poorly water soluble compounds, bioavailability is low. The consequence of low bioavailability may be that the compound’s dissolution and transport rates limit its biodegradation kinetics [82, 86]. This is the situation encountered for PAHs with higher molecular mass, leading to the somewhat paradoxical situation that the compound itself may be intrinsically biodegradable, but effectively is not degraded by microorganisms, because they cannot acquire sufficient of it to remain metabolically active. For this reason is bioavailability a key concept to assess the potential for microbial degradation in contaminated soils. Several chemical approaches have been developed to estimate the bioavailability of organic contaminants in soil (e.g., [87-90], which, however, do not satisfactorily mimic uptake and degradation by active microbial populations [83]. Biological approaches include

biomineralization tests with radioisotopes [87, 91], or the use of molecular methods for the detection of specific degradation genes and or their transcription (e.g., [92-94]).

Particularly promising for the concept of bioavailability are so-called bacterial biosensors (or whole-cell living bioreporters) [21]. Bacterial biosensors are micro-organisms engineered to detect target chemical compounds or changes in physico-chemical conditions through inducible expression of reporter proteins [21]. Hence, a bacterial biosensor in principle responds to exactly the fraction of target compound that passes through its cell during the time of the experiment [21]. If this fraction translates into a proportional signal of the reporter protein, theoretically one would have a perfect bioavailability measurement (i.e., for that type of cell). Traditionally, bacterial biosensors have been exploited to detect ‘presence/absence’ of a target compound or to quantify the concentration of target compound in an aqueous phase environment according to a pre-established calibration curve. Measuring aqueous phase concentrations with bacterial biosensors makes sense under conditions where bioavailability is adequate (as described above). However, for most PAHs, the bioavailability for microbial degradation is in most realistic cases not appreciable thus presenting an interesting test-case to apply a bacterial biosensor. For PAHs, bacterial biosensors have only been constructed for naphthalene [1-3], and for fluorene [4], though toxicity-responsive bacterial biosensors have been used for the (unspecific) detection of PAHs with higher molecular weight and lower solubility, such as phenanthrene and anthracene [95].

Here we present the construction and testing of a new bacterial biosensor for the specific detection of phenanthrene, a three-ring PAH which is a good model to study the factors influencing poorly bioavailable compounds. The solubility of phenanthrene in water is lower than that of naphthalene (at 1.2 and 31.7 mg/l at 25°C, respectively). As a basis for designing the phenanthrene biosensor, we applied the phenanthrene-degrading strain *Burkholderia sartisoli* strain RP007 [5, 96]. The *phn* operon involved in phenanthrene catabolism in this strain has previously been characterized by Laurie and Lloyd-Jones [5]. Inducibility of the *phn* genes in the presence of phenanthrene had been demonstrated by reverse-transcriptase PCR [5] and transcription was inferred to be driven from an inducible promoter in front of the *phnS* gene (Fig. 1).

Here we created a transcriptional fusion between the *phnS* promoter region and the gene coding for the enhanced green fluorescent protein (GFP) (Fig. 1). The fusion was introduced on a broad-host range plasmid which was transferred into *Burkholderia sartisoli* strain RP007. The resulting strain, RP037, remained able to degrade phenanthrene and was tested for its ability to produce GFP during exposure to phenanthrene either via phenanthrene or its

metabolites as actual effectors for PhnR. GFP production in the bacterial biosensor RP037 was studied as a function of the surface area of crystalline phenanthrene that was provided to the system (i.e., in varying amounts), which would primarily change the phenanthrene dissolution rate, or as a function of a constant amount of phenanthrene provided in different forms known to influence the mass transfer release. Finally, the ‘phenanthrene-equivalent’ bioavailable fraction during the same experimental time was estimated in contaminated lampblack soil by applying the new biosensor. Interestingly, the phenanthrene biosensor seemed to sense variations in phenanthrene mass transfer (‘flux’) rather than different aqueous phase concentrations.

RESULTS

Growth of *Burkholderia sartisoli* strain RP037 on phenanthrene

Suspended batch growth of *Burkholderia sartisoli* strain RP037 with various amounts of phenanthrene crystals as the sole source of carbon and energy showed a comparable duration of the lag phase, irrespective of the amount of crystals (Fig. 2). Growth curves of cultures with 0.50 and 0.25 mg (solid) phenanthrene per ml showed a brief exponential phase followed by linear growth. No exponential growth was observed with 0.10 or 0.05 mg phenanthrene per ml. Eventually, after the linear growth phase, the cultures stopped growing as indicated by no further turbidity increase of the culture (OD_{600}), even though phenanthrene crystals were still present in the medium. This might indicate that, after ~120-140 h of cultivation, the rate of phenanthrene dissolution diminished to a level sufficient only for metabolic maintenance of the cells, or that the cells started to form biofilms on the crystal surface. The turbidity after 160 h of cultivation was linearly proportional to the amount of solid phenanthrene added to the culture (as determined by linear regression, with a R^2 of 0.99). In the presence of phenanthrene crystals (0.50 mg/ml) plus 10 mM acetate, cultures grew exponentially until an OD_{600} of ~0.45, after which growth became linear again as in cultures with phenanthrene only (data not shown). Cells cultured on 10 mM acetate but without phenanthrene reached a final turbidity of ~0.45 as well, indicating that this turbidity represented the cell density at which all acetate had been consumed.

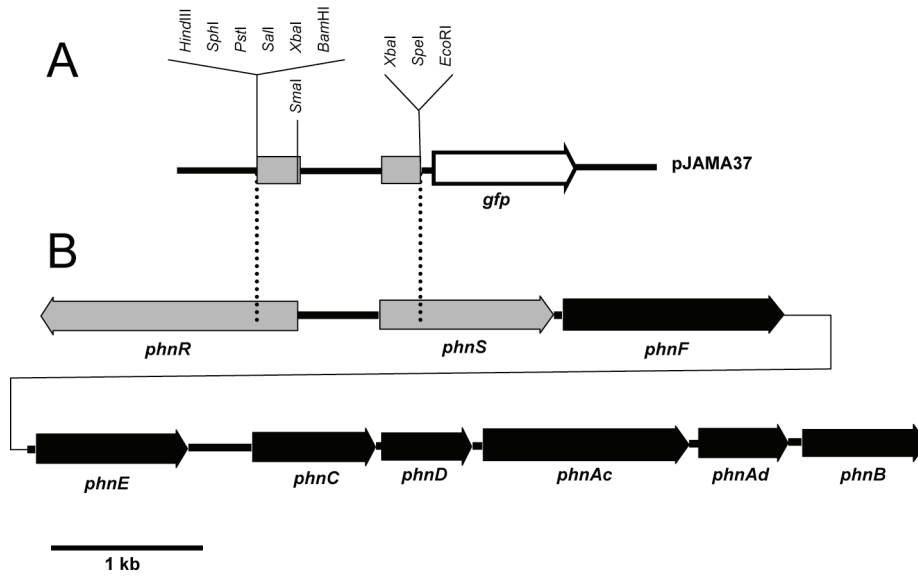


Fig. 1. Genetic construct for phenanthrene detection in *Burkholderia sartisoli* strain RP037 (A) and phn operon from the same species (B) [5]. A 1.1 kb-fragment containing the phnS operator/promoter region and 5' extremity of both phnR and phnS was inserted upstream of the gfp reporter gene in plasmid pPROBE-gfp[tagless] to make plasmid pJAMA37.

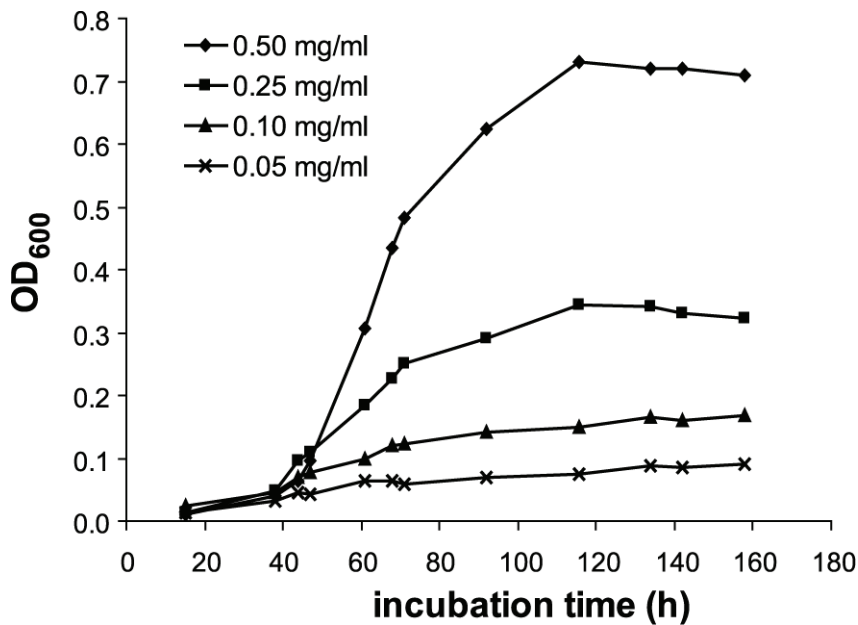


Fig. 2. Batch growth of *Burkholderia sartisoli* strain RP037 in minimal medium with various amounts of phenanthrene crystals (0.05, 0.10, 0.25 and 0.50 mg/ml), measured via turbidity at 600 nm (OD₆₀₀).

Exposure to phenanthrene triggers GFP expression from *Burkholderia sartisoli* strain RP037

We first verified the inducibility of the GFP reporter system constructed on the basis of the *phnR-S* intergenic region in *Burkholderia sartisoli* strain RP037 (Fig. 1) and assessed its potential for quantifying different phenanthrene aqueous phase concentrations. Preliminary tests showed that when growing cultures of RP037 cells were exposed to crystalline phenanthrene, almost no GFP production was observable during the first eight hours (data not shown), although phenanthrene seemed at least partially metabolized by the cells (as indicated by the appearance of a yellow colour in the medium, indicative for *meta* cleavage of phenanthrene metabolites). Since exposure times of up to 8 h apparently did not trigger any measurable GFP induction, we followed GFP formation and accumulation in RP037 cells during the complete growth phase in minimal medium, with phenanthrene only or with phenanthrene plus additional 10 mM of acetate. Supplementary carbon was used in order to obtain faster and more homogeneously growing cultures of RP037. In both cases, prolonged incubation times resulted in GFP production measurable by epifluorescence microscopy (EFM), albeit with a right-skewed distribution (Fig. 3A). GFP in cells grown with acetate and phenanthrene started to become measurable by EFM after one day of incubation and reached a maximum after two days. Between day 2 and day 3 the fluorescence values in the population did not further increase (Fig. 3A). The maximal responses obtained with cultures grown on phenanthrene only or phenanthrene plus acetate were similar. However, the incubation time required for optimal induction was longer and more irregular in the absence of an additional carbon source. In addition, very often only a small part of the population in cultures grown on phenanthrene alone responded strongly, leading to a less homogenous distribution (Fig. 3A). No GFP induction was observed when cells were incubated with acetate alone. Strangely, RP037 cells grown in the presence of acetate in a medium nominally saturated with phenanthrene (~1.2 mg/L) but devoid of crystals did not measurably induce GFP either (data not shown).

The distribution of the fluorescence among the population of RP037 cells indicated that some cells showed very bright fluorescence whereas others remained almost totally dark (Fig. 3A). Conventional statistical treatment, such as taking the mean fluorescence intensity of the whole population proved to be a poor descriptor of the induction effect triggered by phenanthrene, due to the rather large proportion of cells with low fluorescence.

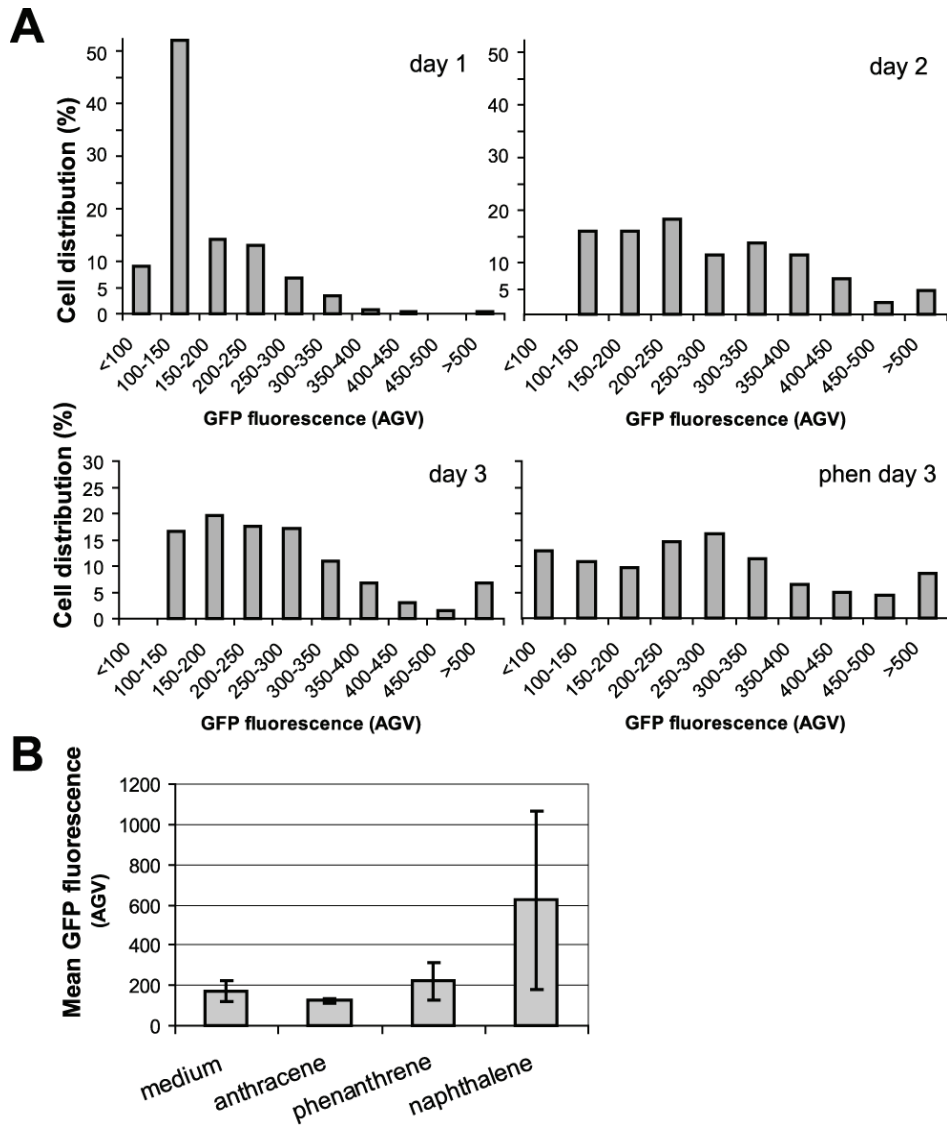


Fig. 3. (A) Distribution of GFP fluorescence, expressed as average gray value (AGV) per individual cell, within a population of individual RP037 cells at different incubation times in cultures with phenanthrene plus acetate (day 1, 2 and 3) or with phenanthrene only (phen day 3). (B) Relative response of RP037 to anthracene, phenanthrene and naphthalene expressed as the mean GFP fluorescence over the whole population. Bars indicated standard deviations from the arithmetic mean.

To compare effects of different conditions on GFP induction, we employed the 75% percentile – the level at which 75% of all the cells in the population has responded and a distribution-free statistical descriptor – to characterize the response of the bacterial biosensor. The choice of the 75% percentile was motivated by its good discrimination between control and induced cultures and by its strong sturdiness against outliers (i.e. extremely fluorescent cells). The 75% percentile values calculated for the populations represented in Fig. 3A are shown in Table 1.

From these experiments we concluded that the GFP reporter system present in *Burkholderia sartisoli* strain RP037 was operational, i.e., the region containing the putative promoter of the *phnSFECDAcAdB* operon was able to induce the transcription of the *gfp* reporter gene when cells were grown in the presence of phenanthrene. However, it was not possible to quantify differences in GFP production in response to different defined aqueous phase concentrations of phenanthrene (between 0 and maximally 1.2 mg/L or 6.7 μ M), either because the total amount of phenanthrene per cell in this case was not sufficient to induce the *phnS* promoter, or because the effective GFP expression was below the EFM detection limit.

Response of the bacterial biosensor to various substrates and effect of surfactant

We tested the specificity of the induction of *Burkholderia sartisoli* strain RP037 towards two other PAHs. After one day of incubation, no induction was observed in the presence of anthracene, another three-ring PAH whose solubility in water is even lower than phenanthrene (0.076 mg/L). On the contrary, cells incubated under the same conditions but with naphthalene, gave significantly higher GFP fluorescence than cells exposed to phenanthrene (Fig. 3B), although the cells did not grow on naphthalene in our experiment (data not shown). Salicylate (at 0.5 mM) also resulted in GFP induction in strain RP037 to a similar level as with acetate plus phenanthrene crystals (not shown). Instead of acetate, pyruvate also supported coinduction with phenanthrene, although 10 mM pyruvate itself resulted in measurable GFP production as well (not shown).

Tween 80 is a surfactant which can increase the apparent solubility of poorly soluble compounds, and is not used as carbon source for RP037. We tested the effect of the addition of Tween 80 to RP037 cultures supplemented with phenanthrene crystals. Interestingly, cells which were exposed to both phenanthrene and Tween 80 showed higher GFP fluorescence than the cells exposed only to phenanthrene or Tween 80 alone (Table 2).

Culture	Incubation time (day)	75% percentile (AGV)	95% confidence interval (AGV)
phenanthrene + acetate	1	200	185-217
	2	349	304-395
	3	315	291-337
	4	281	257-306
phenanthrene	3	345	310-372

Table 1. 75% percentile values for GFP fluorescence (expressed as average gray value, or AGV) among individual cells in cultures of *Burkholderia sartisoli* strain RP037 exposed to phenanthrene in the presence or absence of acetate at different incubation times. Results calculated using data from Fig. 3A.

Culture	75% percentile (AGV)	95% confidence interval (AGV)
Tween	29.6	28.5-30.7
Phenanthrene (1)	34.2	33.4-34.9
Phenanthrene (2)	34.2	33.8-34.7
Phenanthrene (3)	36.0	35.5-36.6
Phe + tween (1)	42.3	40.2-43.9
Phe + tween (2)	42.6	40.7-44.4
Phe + tween (3)	43.3	41.8-45.1

Table 2. 75% percentile values for GFP fluorescence (expressed as average gray value, or AGV) among individual cells in cultures of *Burkholderia sartisoli* strain RP037 exposed to phenanthrene in the presence or absence of Tween 80 (triplicates, labeled 1-3). Data were collected with a different EFM-system (see material and methods) and thus are not directly quantitatively comparable to the others.

GFP expression and metabolic state of the cells

In order to determine under which physiological conditions the biosensor cells were predominantly inducing the *gfp* reporter, we inferred the cells' metabolic state from their ribosome content and measured GFP production during the growth phase. Cells were grown in medium supplemented with acetate in the presence or absence of phenanthrene as described above. The ribosome content of each single cell was determined by fluorescence in-situ hybridisation (FISH) with a 16S rRNA-directed oligonucleotide (i.e., CY3-stained EUB338) [97]. Four hours after inoculation, almost no GFP fluorescence was observed and FISH intensity was low, which was consistent with the fact that the cells were still in lag phase and contained relatively low numbers of ribosomes (Fig. 4A). Nineteen hours after inoculation the cells had entered the exponential phase (Fig. 4E). At this moment the fluorescence intensity of the CY3-marker had increased three- to fourfold, indicating rapidly dividing cells, both in cultures with or without phenanthrene (Fig. 4B). Cells growing in the presence of phenanthrene also had increased fluorescence due to GFP formation compared to the cells growing with acetate only (Fig. 4B). Twenty-seven hours after inoculation the CY3 fluorescence intensity of cells incubated with acetate only had again decreased and after 44 h had returned to similar values as during lag phase. This correlated with the end of the exponential growth phase and the entrance into stationary phase, during which all acetate must have been consumed (Figs. 4C-E). In contrast, cells growing with acetate plus phenanthrene continued to be metabolically active at 27 h, which is probably due to the presence of a supplementary carbon source (phenanthrene) available for the cells. Forty-four hours after inoculation, also more or less all phenanthrene-induced cells had returned to a ribosome content of the lag/stationary phase (Figs. 4D and E), however, the fluorescence due to GFP was maximum at this moment (Fig. 4D).

Sensitivity of the bacterial biosensor towards different fluxes of phenanthrene

Since no EFM-detectable GFP was formed in *Burkholderia sartisoli* strain RP037 cells incubated with different aqueous concentrations of phenanthrene, we hypothesized that the reporter system might be more sensitive to variations in the phenanthrene flux rather than of the dissolved concentration – in other words, to the amount of phenanthrene that each cell experienced per unit of time during the time course of the experiment (usually two days).

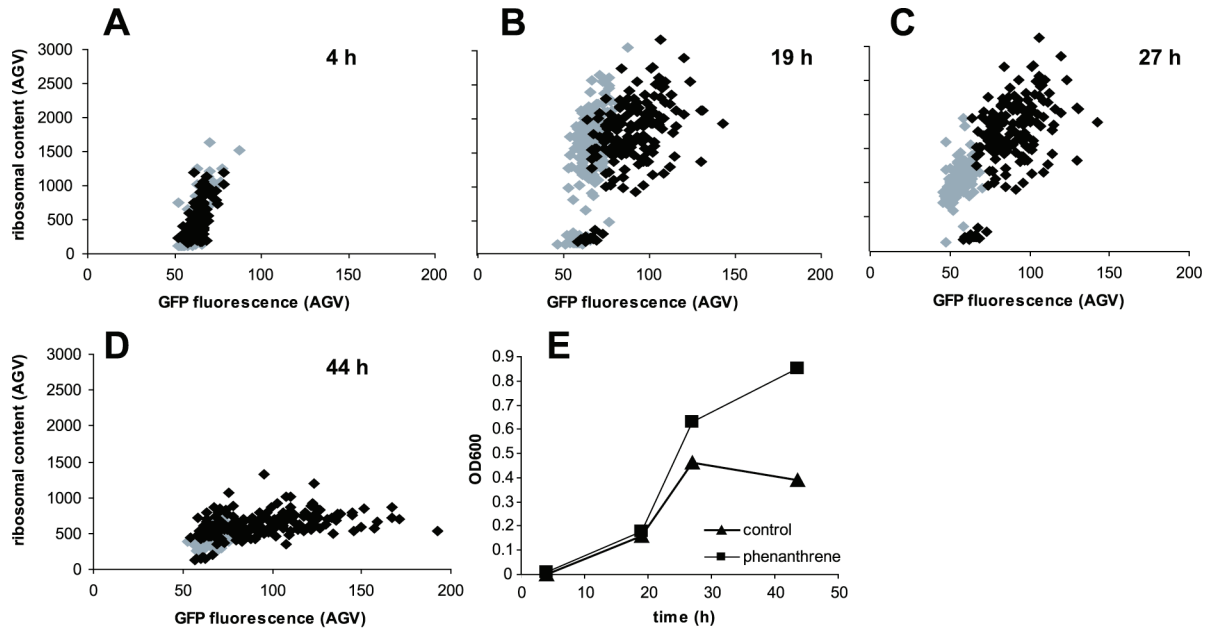
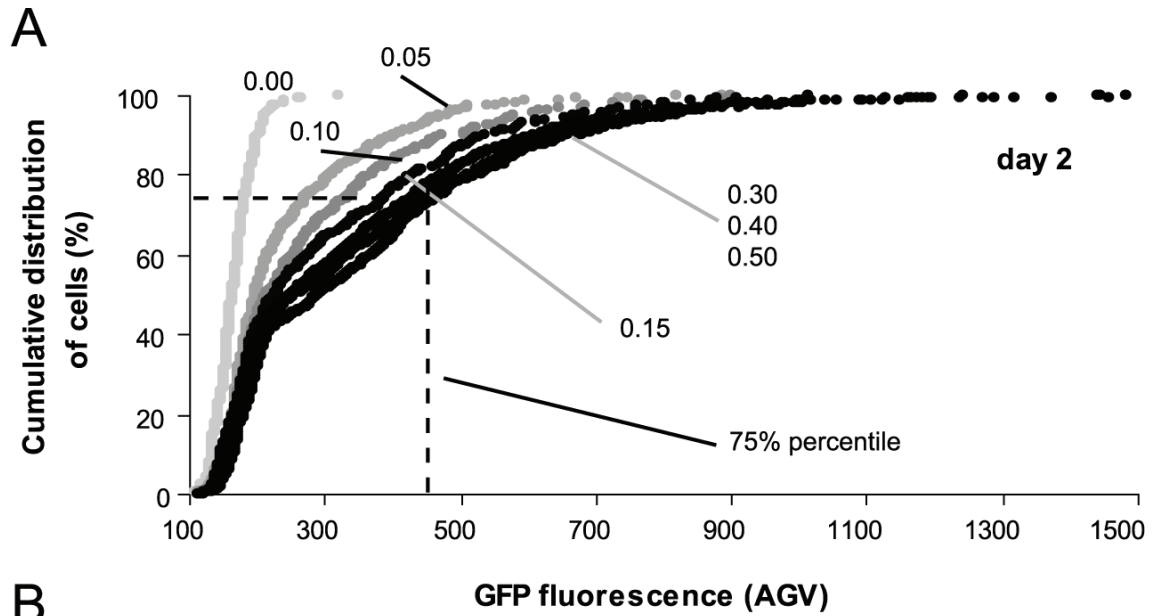


Fig. 4. GFP fluorescence and relative ribosomal content in *Burkholderia sartisoli* strain RP037 grown in the presence of 10 mM acetate only (control, grey diamonds) or acetate plus 0.5 mg/ml of phenanthrene crystals (phenanthrene, black diamonds). Relative ribosomal content was assessed as intensity of fluorescence from the CY3-labelled 16S rRNA targeted probe (EUB338). (A), (B), (C), (D) culture after 4 h, 19 h, 27 h and 44 h of incubation time, respectively. (E) Growth curves of both cultures used for FISH and GFP analysis.

If this were so, then increasing the total surface area from which phenanthrene would dissolve would lead to an increase in phenanthrene dissolution rate and, thus, to an augmentation of the phenanthrene flux toward the cells and increased GFP formation. We tested this hypothesis on acetate-growing cultures of *Burkholderia sartisoli* strain RP037, in the absence or presence of final amounts of phenanthrene (solid/liquid) between 0.05 and 0.50 mg/ml (Fig. 5). The cumulative distribution curve of individual cellular fluorescence intensities showed that even the smallest amount of phenanthrene (0.05 mg/ml) triggered a GFP induction distinct from the culture with only acetate. More importantly, the cumulative distribution curve of GFP fluorescence in individual cells shifted to higher fluorescence values at higher amounts of phenanthrene (Fig. 5A). GFP formation expressed as 75% percentile values (Fig. 5B) increased as a function of phenanthrene amount between 0.00 and 0.30 mg/ml, and levelled off for higher amounts (0.40 and 0.50), suggesting a saturation at the promoter or of the phenanthrene flux.

To further test our hypothesis, we exposed cells to equal amounts of phenanthrene but with different delivery rates. Phenanthrene was provided hereto: (i) as small crystals, (ii) as large crystals, (iii) dissolved into heptamethylnonane and (iv) captured in Model Polymer Release System (MPRS) beads. In this case, small crystals resulted in higher values of GFP fluorescence than one single or two large crystals with the same amount of phenanthrene (Fig. 6). Phenanthrene in MPRS beads resulted in an intermediate level of GFP formation. The effect of small crystals could be mimicked by dissolving phenanthrene in a secondary immiscible organic phase (heptamethylnonane), to which the cells reacted with the same GFP formation after 2 days incubation. Only small crystals and heptamethylnonane resulted in a continued turbidity increase above the ~0.45 reached with 10 mM of acetate, indicating that the higher flux in this case could be productively used for cellular growth. With lower amounts of phenanthrene (0.15 mg/ml) in the system (either as small crystals or dissolved in organic phase), both GFP fluorescence distributions in cultures with small crystals and with heptamethylnonane were again similar (Figure 6B). This suggests that small crystals and phenanthrene dissolved in heptamethylnonane result in the same phenanthrene flux to the cells.



phenanthrene (mg/ml)	0.00	0.05	0.10	0.15	0.30	0.40	0.50
75% percentile	183	274	336	390	455	432	469
(95% confidence interval)	(177-189)	(247-297)	(307-371)	(359-422)	(427-479)	(411-455)	(446-496)

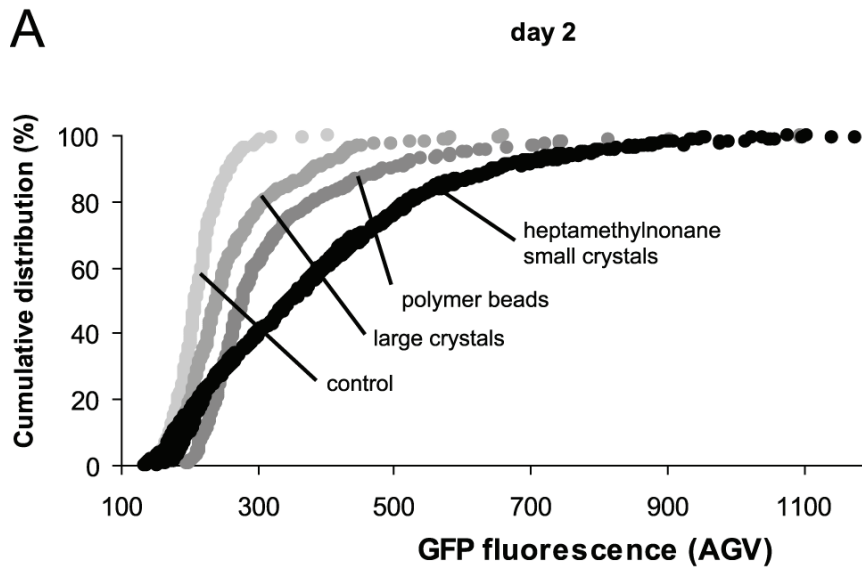
Fig. 5. GFP fluorescence of *Burkholderia sartisoli* strain RP037 cells in response to different amounts of phenanthrene crystals. (A) Cumulative distributions of individual cellular fluorescence in cultures induced with various amounts of crystals (in mg/ml). As on illustration, the 75% percentile is indicated for the culture that received 0.50 mg phenanthrene/ml. (B) Summary table of the 75% percentile AGV and the corresponding 95% confidence intervals (in brackets) calculated by bootstrapping in the program R.

Induction of the bacterial biosensor with samples of PAH-contaminated soil

To determine whether the RP037 cells could detect phenanthrene in environmental contaminated samples, soil containing PAHs was incubated with acetate-growing cells. The cells in contact with the contaminated soil showed even higher GFP fluorescence than cells induced by pure phenanthrene crystals (Fig. 7), which was likely the result of a high amount of naphthalene in the sample. Strangely, 40-60% of the bacterial population showed little or no GFP fluorescence, whereas the remaining cells showed a distribution profile comparable to what had been obtained before with cells induced with pure phenanthrene. Assessment of propidium iodide incorporation in combination with GFP fluorescence revealed two distinct subpopulations. The cells which showed low or no GFP fluorescence incorporated a high level of propidium iodide, and vice versa, those with high GFP fluorescence levels did not (data not shown). Therefore, it is likely that the non-responding subpopulation consisted of dead or damaged cells, while the subpopulation of cells which produced GFP fluorescence contained metabolically active, healthy cells. This strongly indicates that although the biosensor cells detected a (very high) 'phenanthrene-equivalent' flux from the contaminated soil, they were intoxicated by some other compound from the contamination.

DISCUSSION

In the present study we have described the construction and characterization of a GFP-based bacterial biosensor for monitoring bioavailability of phenanthrene. *Burkholderia sartisoli* strain RP037, unlike most bacterial biosensors described in the literature, failed to report EFM-measurable and proportional GFP signals when exposed to different phenanthrene aqueous concentrations. On the other hand, the biosensor distinguished and reported different phenanthrene fluxes while degrading phenanthrene (Figs. 5 and 6), acting in this respect as a genuine sensor for phenanthrene bioavailability. Our observations indicated that active phenanthrene metabolism was needed for good response of the sensor cells. This may suggest that not phenanthrene itself but a metabolite would be the true effector for activating PhnR and the *phnS* promoter, but can also be an effect of poor phenanthrene availability or limited phenanthrene intake by the cells. Current information is not sufficient to conclude on the nature of the PhnR effector compound.



B

		75% percentile	95% confidence interval
control	1	230	221-238
	2	218	214-221
	3	227	220-234
small crystals	1 (0.5 mg/ml)	490	465-517
	2 (0.5 mg/ml)	470	426-502
large crystals	1 (0.5 mg/ml)*	292	278-308
	2 (0.75 mg/ml)**	270	254-283
polymer beads	1 (0.4 mg/ml)	346	314-370
	2 (0.4 mg/ml)	404	436-452
HMN	1 (0.5 mg/ml)	494	472-516
	2 (0.5 mg/ml)	486	463-505
small crystals	1 (0.15 mg/ml)	362	319-399
	2 (0.15 mg/ml)	324	273-365
HMN	1 (0.15 mg/ml)	359	333-384
	2 (0.15 mg/ml)	368	346-397

* as 2 crystals, **as 1 crystal

Fig. 6. GFP fluorescence of *Burkholderia sartisoli* strain RP037 cells in response to different fluxes of phenanthrene. (A) Cumulative distributions of individual cellular fluorescence intensities after two days of cultivation in absence or presence of 10 mg phenanthrene, dosed in the form of small crystals, large crystals, MPRS beads or dissolved in heptamethylnonane. For clarity, only one each of the duplicate cultures is plotted. (B) Summary table of the 75% percentile AGV and the corresponding 95% confidence intervals calculated by bootstrapping in the program R.

Both phenanthrene and naphthalene induced GFP formation in RP037, which is in agreement with RT-PCR results of Laurie and Lloyd-Jones [5] on the original strain RP007, but so did salicylate (at 0.5 mM, not shown) and even pyruvate (at 10 mM). However, neither *E. coli* nor *Pseudomonas fluorescens* equipped with the *phnS* promoter-*gfp* fusion and with an intact *phnR* produced GFP in the presence of phenanthrene, naphthalene or salicylate, suggesting that either *phnR* is not correctly expressed in those host strains or they are not the true PhnR effectors. An active metabolic state, achievable by growth on acetate, was also favourable for a consistent response to phenanthrene of all cells in a population, which could be concluded from measuring the relative ribosome content in growing cultures by 16S rRNA-directed FISH and simultaneous GFP formation. In contrast, growth of the sensor cells on crystalline phenanthrene alone resulted in non-optimal GFP responses, both with respect to the proportion of reacting cells and the time needed for induction (between 2 and 7 days). This, however, we think may be a consequence of the genuine bioavailability of phenanthrene in such a suspended batch system; it might be that the concentration of phenanthrene is too low to trigger effective degradation in the whole population of cells (from the same *phnS* promoter of the native *phn* operon still present in the cells), whereas only those cells actively metabolizing phenanthrene will be able to lower the aqueous phase concentration and thus ‘drive’ further phenanthrene dissolution.

The reasons for the absence of a detectable GFP signal in EFM even at nominally-saturated aqueous phenanthrene concentrations are not immediately clear. In comparison, naphthalene biosensors based on *Pseudomonas putida* and the *nahG* promoter have a lower detection limit for naphthalene of $\approx 0.5 \mu\text{M}$ [1, 3], although these were equipped with the *luxAB* bacterial luciferase as reporter protein and the detection limit was derived from a global response of a larger population of cells simultaneously. Actually most whole-cell living bioreporters responsive to organic compounds start giving off measurable reporter signals above 100 nM target compound concentration, but then again this is usually based on a ‘global’ measurement of cells in aqueous suspension, i.e., for a large population of cells and not per single cell [21]. EFM measurements of GFP are less sensitive than luciferase, which can be concluded from those biosensor types where both luciferase and GFP were compared for the same promoter [98, 99]. Hence, EFM measurements of GFP as the reporter protein would already increase the ‘apparent’ detection limit of the cells.

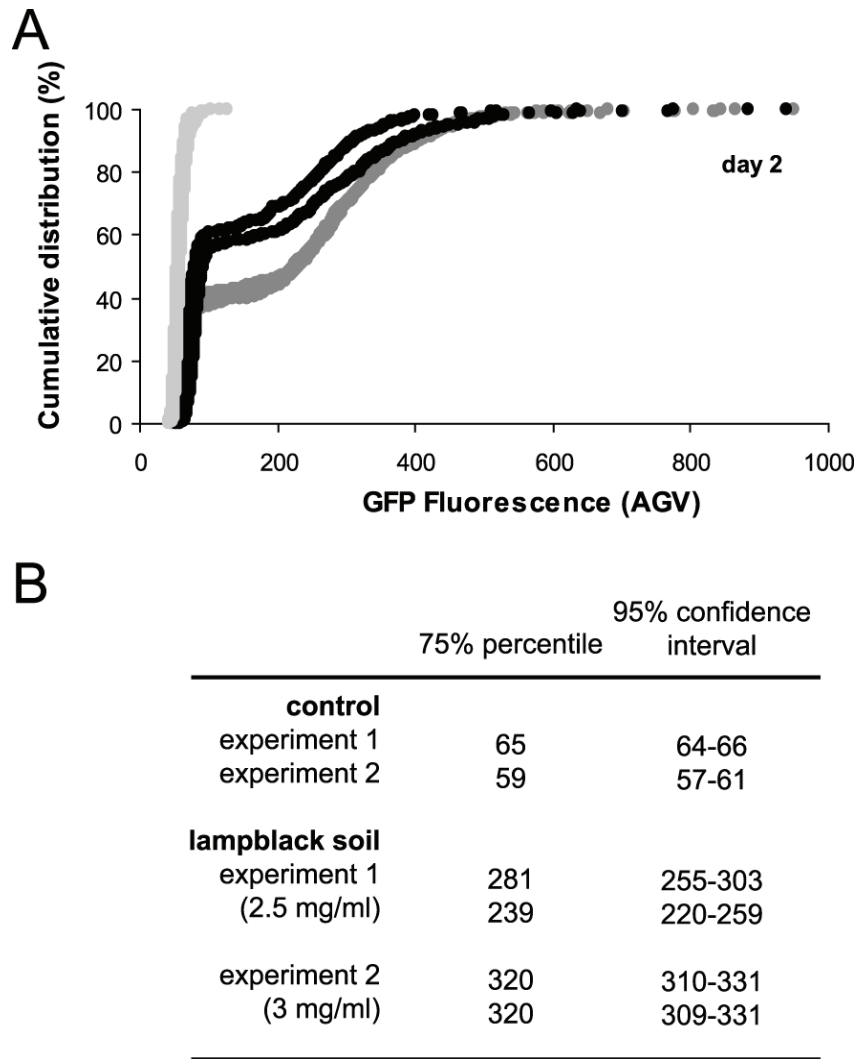


Fig. 7. GFP fluorescence of *Burkholderia sartisoli* strain RP037 cells in response to lampblack soil contaminated with various PAHs. (A) Cumulative distributions of the individual cellular fluorescence intensities from two distinct experiments (exp. 1, black dots; exp. 2, dark grey dots) and the controls carried out simultaneously (cells in medium without soil, light grey dots). (B) Summary table of the 75% percentile AGV and the corresponding 95% confidence intervals calculated by bootstrapping in the program R. Experiments with contaminated soil were performed in duplicate.

Another factor in the *Burkholderia* assays contributing to the relatively high detection limit was the relatively high amount of cells used in the assays. For practical reasons of detecting sufficient cells in the microscope we could not lower the amount of cells in our assays (which would have increased the relative amount of phenanthrene per cell) and had to maintain an active population by including acetate in the assay. Calculated on a per cell basis, a measurable (luciferase) response for the mentioned *P. putida* naphthalene biosensors occurred at around 0.02 fmol of naphthalene per cell (0.5 μ M means adding 0.5 nmol naphthalene to $2.2 \cdot 10^7$ cells; [3]). We will argue below that this value is actually not very different than the per cell availability of phenanthrene for the *Burkholderia* sensor.

By keeping cellular metabolism ‘constant’ and homogenous (via simultaneous growth on acetate) and by changing the physico-chemical mass transfer parameters for phenanthrene bioavailability (dissolution rate, partitioning), we could achieve different cellular GFP levels, representative for differential induction from the *phnS* promoter. GFP fluorescence increased with increasing total amounts of phenanthrene in the system, up to a certain ‘saturation’ level (≈ 0.30 mg of crystals per millilitre) (Fig. 5). Since even for the smallest amount of crystals no complete dissolution was observed during the incubation time of the experiment, and since the maximal soluble phenanthrene concentration cannot have been exceeded, the main differences concerned the interfacial area between the crystals and the aqueous phase. The dissolution rate is known to be proportional to the interfacial area [82, 86]. Consequently, also the phenanthrene flux towards the cells was proportional to the interfacial area and the different GFP levels must have been the result of phenanthrene flux differences (i.e., more crystals, higher dissolution flux). To verify this hypothesis further we changed the interfacial area between phenanthrene and the aqueous phase while keeping the total phenanthrene amount constant. In this case lower GFP fluorescence was produced in the culture exposed to larger crystals, and higher GFP in the presence of smaller crystals (Fig. 6), which is consistent with the idea that a smaller surface area (i.e., large crystal) will sustain a smaller flux than a larger surface area (i.e., many small crystals). Three further modifications were made to demonstrate the effect of changing phenanthrene mass transfer on biosensor output. Previous work documented how the release of phenanthrene from MPRS beads mimicks the slow release kinetics of PAHs from sediments and soil [100], which indeed the cells faithfully detected in the present work (Fig. 6). Adding Tween 80, a surfactant increasing the apparent aqueous solubility, resulted in higher GFP response from the cells than with phenanthrene only (Table 2). Phenanthrene mass transfer to the cells (as inferred from GFP response) from a secondary non-aqueous phase, at the same total amount as in crystalline form, resembled the

GFP production in cells exposed to small crystals, thus, those experiencing the highest phenanthrene flux.

From these mass transfer variations, we then tried to calculate a different sort of 'calibration' curve of the cellular GFP response as a function of phenanthrene flux. Such a calibration curve may further be used to quantify phenanthrene fluxes in unknown systems, such as contaminated soils. In order to calculate this, we first adopted a mathematical model which considered one single crystal as a pure particle of perfect spherical shape [101]. For large crystals, a theoretical radius was calculated from the mass of the particle and the volumetric mass of phenanthrene. For small crystals, an average diameter (0.10 mm) was calculated from observations of the various crystals at 25-fold magnification, and the total number of particles was calculated from the total mass of phenanthrene added to the experimental system. To simplify flux calculations, the phenanthrene dissolved aqueous concentration was set to zero, which means that every molecule released from the particle was instantaneously taken up by a bacterial cell. Such an assumption is supported by observations of rapid and preferential partitioning of hydrophobic pollutants in cellular lipid bilayers of the cytoplasmic membrane [102]. From this model, the calculated average amount of phenanthrene per single cell during a two day course amounted to between 10 and 70 fg (0.06-0.4 fmol) for the small crystals, depending on the quantity of phenanthrene in the system (Fig. 8). For the large crystals, however, the calculated available phenanthrene fractions were less than 1 fg per cell during two days. The relationship between phenanthrene mass transfer and GFP production (as 75% percentile) as drawn in Fig. 8 could further be verified by calculating the average phenanthrene flux for the MPRS beads. In order to calculate this, another model was used [99, 100] which predicted values of 20-25 fg phenanthrene per cell. These values fitted reasonably well to the rest of the curve (Fig. 8). The experiments where phenanthrene was dissolved in heptamethylnonane were not represented, because no satisfying expression was found to calculate the flux of phenanthrene in this particular condition. However, we can predict that the phenanthrene flux from such a heptamethylnonane mixture (0.15 mg phenanthrene per ml) must have been around 30 fg per cell.

It is clear that the *Burkholderia* RP037 cellular assay does not provide a rapid (e.g., few hours) test for phenanthrene bioavailability. However, because the cells metabolize phenanthrene, they add the biological component of the bioavailability complexity. A 2-3 day incubation assay with the material seems necessary to us to investigate the combined process of instantaneously present concentration in the aqueous phase and the release kinetics.

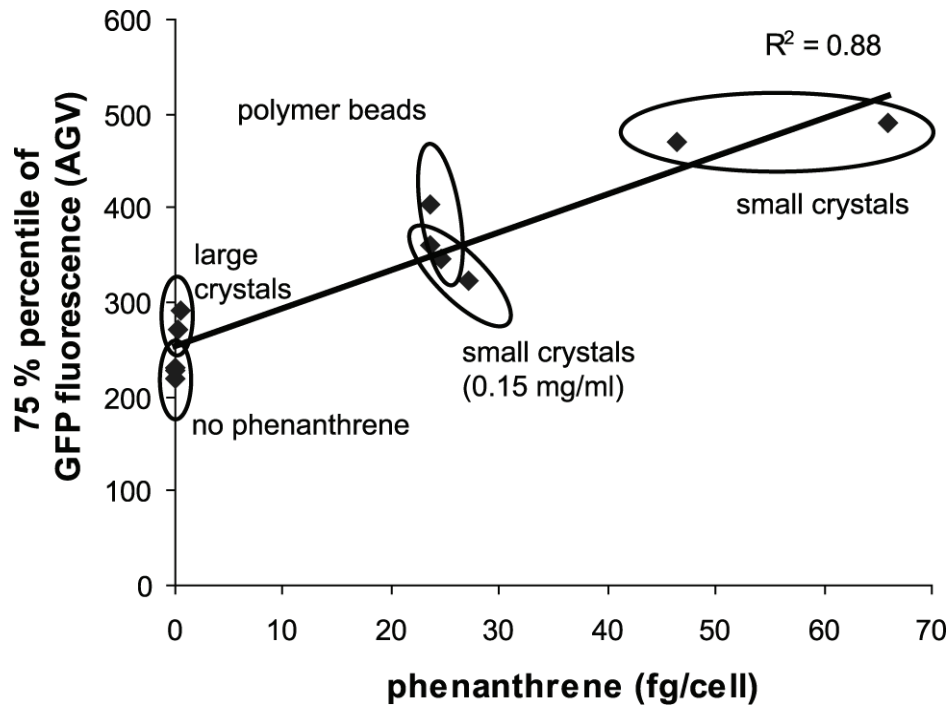


Fig. 8. The 75% percentile values of GFP fluorescence in cultures exposed to different phenanthrene fluxes (data from Fig. 6), plotted as function of the calculated amount of phenanthrene experienced per single cell after two days of incubation. The linear regression curve showed an R^2 coefficient of 0.88.

In a first trial, the RP037 cells did detect large quantities of available ‘phenanthrene’-equivalent material in the lampblack soil we tested. With the help of the quantitative calibration of the relation between phenanthrene mass transfer per cell and the average GFP output (Fig. 8) more and other contaminated sites may be analyzed for bioavailable ‘phenanthrene-equivalents’ (naphthalene plus phenanthrene). The GFP-based sensor may have another important property which we could not employ fully until now, namely to allow direct microscopic detection of submillimeter zones with higher PAH fluxes than others. This phenomenon of particle-type dependent PAH desorption in soils has been recognized before [103] and would be an interesting challenge for the GFP sensor cells.

ACKNOWLEDGMENTS

The authors greatly thank Alexandra Baehler for her initial help in this project. Furthermore, we thank the Department of Microbiology at the University of Leiden for the opportunity given to JRM to use the Biorad EFM-laser scanning system applied in one experiment here.

MATERIAL AND METHODS

Chemicals and soil samples

Phenanthrene crystals (97% purity) were purchased from Fluka (Buchs, Switzerland). The crystals were of various sizes, ranging from a diameter of 0.05 to 0.50 mm, with an approximative average of 0.10 mm. To produce larger crystals of phenanthrene, ~10 mg of phenanthrene crystals were deposited on a metal spoon and heated on gas until melting. Molten phenanthrene was allowed to cool down in the spoon at ambient temperature, forming one or two large crystals which could be detached from the spoon surface. Synthesis of MPRS beads, which mimic the slow desorption of contaminants, is described elsewhere [100]. The MPRS beads had an average radius of 1.6 mm (to within a maximum uncertainty of 1.9%, relative standard deviation in repeated experiments) and contained an average phenanthrene load of 1.4 mg [99]. The physical characterization of MPRS beads, experimental quantitation of their release behaviour, and their suitability for studies of bioavailability of contaminations in soils and sediments has been discussed in extensive detail elsewhere; the interested reader is referred to the above citations. Lampblack soil, from a PAH contaminated oil-gas manufacturing site, is referenced as soil CA-18 in an article by Hong *et al.* [104].

Strains and growth conditions

Burkholderia sartisoli strain RP007 is the wild type strain isolated and described by Laurie and Lloyd-Jones [5] and grows on phenanthrene as sole carbon and energy source. Strain RP007-rif is a spontaneous mutant resistant to rifampycin (50 µg/ml). RP037 is a derivative of RP007-rif containing the plasmid pJAMA37 (see below). *Burkholderia* strains RP007 and RP037 were routinely grown at 30°C on Tryptone Yeast (TY, contains 3 g/l of yeast extract and 5 g/l of Bacto tryptone) agar plates or liquid cultures with 50 mM NaCl. (For unknown reasons, growth and survival was optimal in the presence of 50 mM NaCl.) Fifty µg/ml of kanamycin was added to the culture of RP037 to select for the presence of the reporter plasmid pJAMA37. As defined minimal medium (MM) we used type 21C mineral medium [105] supplemented with 10 mM sodium acetate as a carbon source.

Genetic constructions

A 1087 bp-fragment containing the complete presumed operator/promoter region of the operon *phnSFECDAcAdB* flanked with the 5' extremities of *phnR* and *phnS* genes (Fig. 1) was amplified by PCR from total DNA of strain RP007 using the primers *phnF1* (5'-CCCTTCGAGCATGCA-3') and *phnR1* (5'-GCCTGCTCTAGAAGCCGCTC-3') (engineered to contain internal *SphI* and *XbaI* restriction sites, indicated in bold, respectively). This fragment was cloned into pGEM-T Easy (Promega, Catalys AG, Wallisellen, Switzerland) and subsequently reisolated by cutting with *SphI* and *XbaI*, after which it was ligated with the vector pPROBE-gfp[tagless] treated with the same enzymes. The result was the plasmid pJAMA37 (Fig. 1), in which the presumed *phnS*-promoter drives expression of a promoterless *gfp* gene, encoding the enhanced Green Fluorescent Protein (with F64L and S65T mutations) [106]. The gene coding for neomycine phosphotransferase (*nptII*) on pPROBE-gfp[tagless] allowed selection of the plasmid via resistance to kanamycin. Heat shock was used to transform *Escherichia coli* DH5α with the new vector (Sambrook and Russell, 2001). A mating was performed with *E. coli* DH5α (pJAMA37) as donor strain, *E. coli* HB101 (pRK2013) as helper strain and *Burkholderia sartisoli* strain RP007-rif as recipient strain, to conjugate pJAMA37 into RP007. Transconjugants were selected on TY agar plates with kanamycin and rifampycin to counter select against donor and wild type recipient strains. Potential transconjugants were purified and the plasmid was reisolated to verify its integrity. One of such transconjugants was named *Burkholderia sartisoli* strain RP037. 5% and 20% of colonies plated from 4 d stationary phase cultures of RP037 grown on

MM without kanamycin with 10 mM pyruvate or 10 mM acetate, respectively, had lost kanamycin resistance.

Induction assays

A preculture of *Burkholderia sartisoli* strain RP037 was grown in TY medium until an OD₆₀₀ of ~ 1.0 was reached, and then centrifuged at 1,200 g for 5 min. The supernatant was discarded and the cells were resuspended in an appropriate volume of MM to obtain an OD₆₀₀ of 0.4. At this point both the presence of the *phnB* gene and the *phnS* promoter-*gfp* construct were verified by PCR. A 50 ml-flask containing 20 ml of minimal medium with 10 mM acetate and 50 µg/ml of kanamycin was inoculated with 2% (400 µl) of resuspended preculture. The flasks were supplemented with the desired amount of phenanthrene in various forms: (i) small crystals directly in the medium, (ii) large crystals directly in the medium, (iii) MPRS beads [100] placed directly into the medium, or (iv) phenanthrene dissolved in 4 ml of 2,2',4,4',6,8,8'-heptamethylnonane (Sigma Chemical CO., St-Louis, USA) which formed a non-aqueous phase layer on top of the culture medium. To test induction with PAH contaminated soil, 50 to 60 mg of CA-18 lampblack soil [104] were added directly into the liquid culture. Among other PAHs, CA-18 soil contained naphthalene and phenanthrene (respectively, 6974 and 255 µg per liter of water phase equilibrated with the soil) ([104] and Upal Gosh, personal communication). Samples were taken at different incubation times either for GFP observations with EFM or for fixation and FISH analysis (see below). Viability of the cells was established with the LIVE/DEAD BacLight bacterial viability kit (Molecular Probes, USA), using only the propidium iodide component of the kit. To test induction with naphthalene, 0.1 g of crystals was added in a glass tube inside the Erlenmeyer flask, in order to provide naphthalene through the gas phase, and flasks were closed with teflon lined screw caps. Induction with anthracene was tested by adding 0.1 g crystals directly into 25 ml of liquid culture. Tween 80 (Fluka) was added to the cultures at a concentration of 0.2 mg/ml. Cultures were incubated at 30°C with 180 rpm shaking.

Biosensor immobilization on glass slides

Round glass cover slips of 42 mm diameter and 0.17 mm thickness (H. Saur, Reutlingen, Germany) were soaked in a solution of ethanol with 5% potassium hydroxide (w/v) for 10 min, rinsed with bidistilled water and then soaked in a solution of 0.01% poly L-lysine (v/v) in water (Sigma Diagnostics Inc.) for 5 min. The glass slides were rinsed again with bidistilled water and allowed to dry under the hood. One coated glass slide was mounted into

an *ad hoc* base chamber (POC chamber, H. Saur), and drops (1-2 μl) of sampled cell culture were placed upon the surface of the slide. A Teflon ring of 0.5 mm thickness and a second glass slide were successively placed on top of the first glass slide. The system was closed with a metal ring and could be incubated for several days without loss of moisture (for a schematic view of the chamber, see [77]). Cells were allowed to settle for 15-20 min on the lower glass surface, after which the chamber was turned upside down and the fluorescence intensity of the attached cells was determined by epifluorescence microscopy.

Epifluorescence microscopy and image analysis

GFP fluorescence of individual cells was measured with an Axioskop2 epifluorescence microscope (Zeiss, Germany), using a 100x objective (Plan-NEOFLUAR 100x/1.30 oil, Zeiss). Images of at least one hundred cells per field were recorded with a SPOT RT-KE monochrome camera (Diagnostic Instruments, USA) with various exposure times and utilizing the following GFP filter cube (exciter: HQ470/40; emitter: HQ525/50; beamsplitter Q495lp) (AF Analysentechnik, Tübingen, Germany). For the experiment with Tween 80 (Table 2) we used a Zeiss Axioplan epifluorescence microscope equipped with a Biorad MRC1024 ES laser detection system (Biorad). Images were treated and intensities of individual cells were calculated with the program Metaview (version 6.1r5, Visitron Systems, Germany). An automated macro of the program Metaview was created to quantify the intensity of fluorescence of each individual cell [77]. Individual fluorescence intensity data were then further analysed using the statistical program R [107] (<http://cran.r-project.org>), and the 95% confidence interval for the 75% percentile value was calculated based on 500 bootstrapping cycles (using the R algorithms *quantiles* and *boot.ci*).

FISH procedure and analysis

Two hundred μl of cell culture were mixed with 600 μl of fixation buffer consisting of 4% (w/v) paraformaldehyde in phosphate buffered saline (PBS : 137 mM NaCl, 2.7 mM KCl, 10 mM Na_2HPO_4 , 2 mM KH_2PO_4 , pH 7.4), and incubated for 3 h at room temperature. The cells were centrifuged at 1,200 g for 5 min, then the supernatant was discarded and the pellet was washed twice with PBS. The cells were resuspended in order to have the approximate same cell density in a solution containing ethanol and PBS in 1:1 proportion (v/v). Five μl of fixed cells were pipetted on a gelatine-coated glass slide [108] and dried at room temperature. The samples were dehydrated by soaking the glass slide in ethanol-water solutions with increasing concentration of ethanol: 50, 70 and 100 % (v/v), 3 min each. Ten μl of hybridization buffer

(0.9 M NaCl, 20 mM Tris-HCl, 0.01% sodium dodecyl sulfate at pH 8.0) preheated at 48°C with 50 ng of the CY3 labelled oligonucleotide probe EUB338 [108] was then added to each dehydrated sample. The glass slide was placed in a closed chamber moisturized with hybridization buffer and incubated for 1.5 h at 45°C. The slide was washed in buffer (containing 0.9 M NaCl, 20 mM Tris-HCl at pH 8.0) at 48°C for 15 min. The glass slide was rinsed with bidistilled water and dried at room temperature. One drop of antifading reagent (FluoroGuard, Biorad) was added to each well. The fixed cells were observed with EFM and images recorded as described above. The same microscopic field was imaged three times: once in phase contrast, again in epifluorescence mode with the GFP filter set, and finally with the CY3 filter. The exposure time for the images using the GFP or CY3 filters was 500 ms. Images were subsequently analyzed for fluorescence intensities of individual cells in Metaview as described above.

Modeling

Modeling of phenanthrene release from differently sized crystals was performed according to Mulder *et al.* [101], who also provide background regarding the applicability of this model to contaminated sites. Phenanthrene release from MPRS beads was calculated according to formulae given in Wells *et al.* [99, 100]. In both of these cases, we note that a spherical geometry is employed in modelling, in accord with the geometry of the release matrix used in experiments. The choice of this geometry was largely to suit logistical convenience – it is an easy geometry from which to estimate release fluxes, and hence to demonstrate relations between sensor response and flux; we also note however, that it is a common assumption in environmental contaminant transport models, viz. the seminal paper by Wu and Gschwend [109], and more recently work from Shor *et al.* [110].

CHAPTER 3

INFLUENCE OF DISSOLVED ORGANIC MATTER ON NAH AND PHE AVAILABILITY TO THE BACTERIAL BIOSENSOR *BURKHOLDERIA SARTISOLI* RP037

Robin Tecon, Kilian Smith

Dissolved and particulate organic matter, which are mostly composed of humic substances, are an essential component of both aquatic and terrestrial environments. These undefined organic complexes can interact with hydrophobic pollutants, which may influence their bioavailability to biota in different ways. Here we study the question as to whether humic acids change availability of naphthalene (NAH) and phenanthrene (PHE) to the bacterium *Burkholderia sartisoli* strain RP037. This strain is a bacterial biosensor that produces GFP when metabolizing NAH and PHE, and GFP fluorescence intensity can serve as a measure for the history of NAH and PHE flux to the cells. We thus tested the effect of humic acids on NAH- and PHE-induced GFP formation by strain RP037 in two different assays. One deployed a vapour phase delivery of NAH to the cells and the other an aqueous solution delivery of PHE. A slight but significant decrease of GFP formation was detected in the vapour phase delivery assay at 1 μ M NAH and 1 g per L humic acids. No effect of humic acids was discernable on PHE-induced GFP formation in growing cultures of strain RP037 in aqueous solution. Our results thus showed that the biosensor can be used to trace humic acid induced bioavailability changes of NAH and PHE, but that its influence for RP037 is minimal.

INTRODUCTION

We demonstrated previously (Chapter 2) that transport rates of phenanthrene (PHE) in aqueous solution could be adequately measured by a genetically modified PHE-degrading bacterium *Burkholderia sartisoli* strain RP037 [58]. This strain carries a second copy of the *phnS* promoter fused to the gene for green fluorescent protein (GFP), which is activated when the cells sense and metabolize phenanthrene (PHE) or naphthalene (NAH). The accumulation of GFP in single cells then serves as a history of exposure to PHE, and, as a consequence, can be used to describe differences in PHE fluxes to the cells. For flux (i.e., transport) assays, we previously deployed a defined liquid culture medium at pH 7 containing acetate as single external carbon source other than PHE, and a restricted number of inorganic salts in water. These compounds *per se* did not have any known effect on the dissolution of PHE from a solid (crystal) or oily source (PHE dissolved in heptamethylnonane), and the subsequent transport of PHE to the cells. In natural aquatic and terrestrial habitats, however, a variety of compounds may interact with compounds such as PHE (in general: hydrophobic organic contaminants or HOCs). This interaction may change the HOC's availability to the bacterial cells. For instance, HOCs may form covalent bonds or hydrogen bridges with dissolved organic matter (DOM), or they can sorb to the DOM matrix via hydrophobic chemical interactions [111, 112]. DOM consists of a wide range of constituents, varying widely in size (e.g., small soluble molecules or complexes as large as colloidal particles), that mostly originate from dead organisms and are further modified in the environment via partial degradation and chemical rearrangements [40]. Through molecular interactions outlined above, DOM may increase the apparent water solubility of HOCs but reduce their freely dissolved fraction. As a consequence, the rates of their volatilization from aqueous solution may also be reduced. HOC-DOM interactions are generally thought to result in a decrease of the HOC-bioavailability for bacteria in aqueous solution, presumably because of the larger molecular size of the HOC-DOM complex that prevents them from crossing the cell membrane [40]. In certain cases, however, the presence of DOM resulted in increased bioaccumulation of HOCs in aquatic organisms (e.g. in mussels, water fleas, fish, and daphnia) [111, 113]. This suggests, therefore, that HOC-DOM complexes may under certain circumstances actually provide additional mass transfer of HOC to biota.

In aquatic and terrestrial environments the most abundant form of DOM is humic substances, which comprise polyaromatic compounds with a large compositional variety and molecular mass. Humic substances are subdivided into humic acids and fulvic acids, based on their solubility under acid conditions. Approximately 50% of the molecular mass of humic substances is carbon. Humic acids (HA) are often used to substitute DOM and they are commercially available. Previous experiments have shown that the addition of soil-derived humic acids increased the PHE biodegradation rate by a *Pseudomonas fluorescens* species in batch cultivation [114]. More recently, the same research group could show that PHE-degrading bacteria of the genera *Burkholderia*, *Delftia* and *Sphingomonas* could be enriched more efficiently by using humic acid-sorbed PHE, suggesting that this dosing makes PHE more available to the cells [115].

In this work, we wanted to test the hypothesis that DOM (here: humic acids) can alter the bioavailability for bacterial cells of two polycyclic aromatic hydrocarbons (PAHs), NAH and PHE. Since the previously constructed *B. sartisoli* RP037 biosensor strain had worked adequately in detecting PHE fluxes and NAH bioavailability, we asked the question whether humic acids would change PHE and NAH-induced GFP expression in the biosensor compared to non humic-acid additions. Two experimental set-ups were chosen. First, we investigated whether humic acids would change NAH-inducible GFP formation measured by biosensor cells in the vapour phase. Secondly, we tested humic acid effects on PHE-induced GFP formation with biosensor cells in aqueous solution. In the gas-phase set-up we ensured that the number of biosensor bacteria was sufficiently low that no significant depletion of NAH by biodegradation or sorption to biota would occur within the duration of the experiment. Our hypothesis was that if humic acids would lower the steady-state NAH concentration in the aqueous and, consequently, in the gas phase, this would be detected by the biosensor cells and result in lower GFP fluorescence. In the aqueous phase biosensor tests the cell density was high enough to cause measurable PHE degradation and prevent the formation of a steady state aqueous phase concentration. The cells would thus measure a PHE flux. If humic acids would change the PHE flux, this would result in a different GFP fluorescence of cells compared to conditions without humic acids.

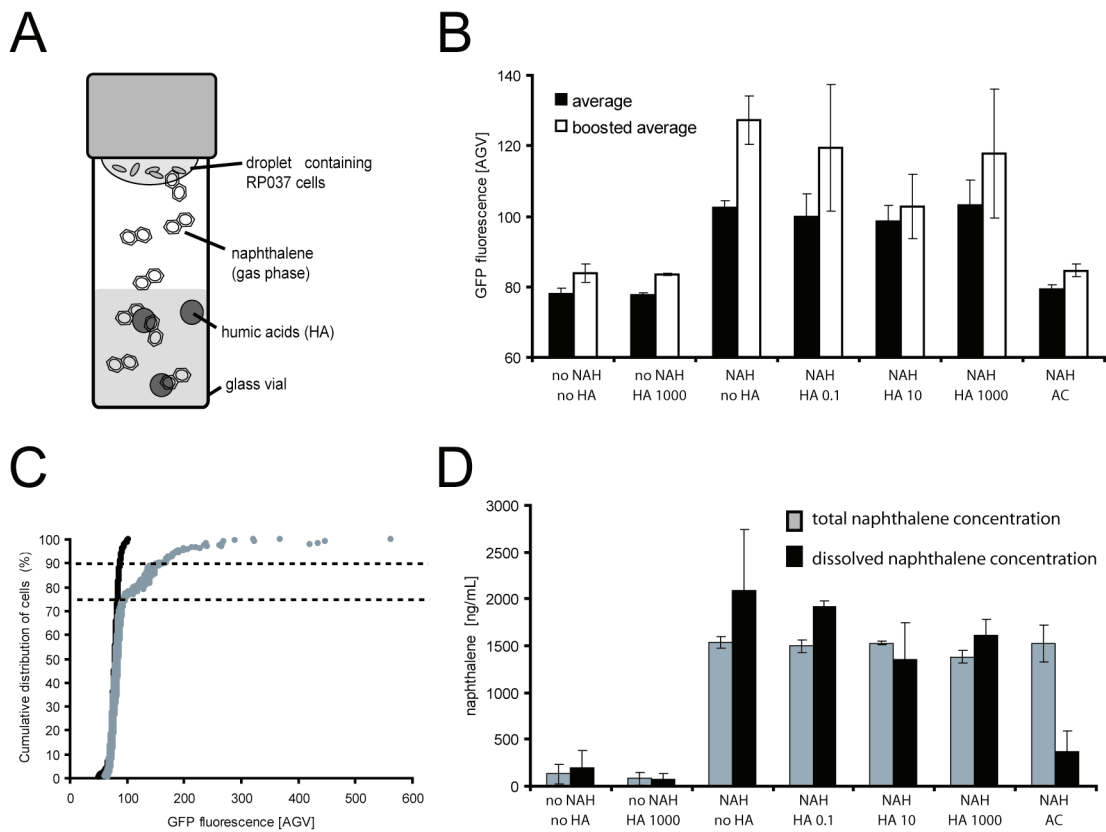


Fig. 1. Effect of DOM on *B. sartisoli* RP037 induction by gaseous NAH. (A) Schematic view of the experimental set-up. In a glass vial, a droplet of *B. sartisoli* RP037 cells was exposed to the vapour of a solution with a nominal NAH concentration of 10 μM ('NAH'). Humic acids (HA) or activated charcoal (AC) were added to the solution. (B) GFP fluorescence intensity in individual RP037 cells after 4 hours of incubation, expressed as average gray value (AGV). Results indicate the average fluorescence intensity over the whole sample population, or the average fluorescence intensity of the cells comprised between the 75th and 90th percentile (boosted average). Concentration of HA in the solution is presented as mg per liter. (C) Exemplary cumulative distribution plots of GFP fluorescence intensity in a population of RP037 cells exposed to NAH (grey dots) or not (black dots). The dashed lines delimit the data used to calculate the boosted average. (D) Solid phase micro extraction (SPME) measurements of total NAH in the system and freely aqueous dissolved NAH at the end of the experiment. All error bars indicate standard deviations calculated from triplicate measurements.

RESULTS

Influence of humic acids on NAH-inducible GFP formation via the gas phase in *B. sartisoli* RP037

A five microliter droplet of bacterial biosensor suspension (*B. sartisoli* strain RP037) containing approximately 3×10^6 cells was introduced in a hermetic glass vial and exposed to NAH evaporating from aqueous solution in the presence or absence of humic acids (Fig. 1A). We knew from preliminary experiments that NAH evaporating from aqueous solution efficiently induced GFP production by strain RP037 at a distance (data not shown). Various concentrations of humic acids (0.1, 10 and 1000 mg/L) were tested in aqueous solutions containing a nominal NAH concentration of 10 μ M (1.3 mg/L). After 4 hours incubation time, the hanging droplet of biosensor cells was removed and the individual cellular fluorescence intensities were measured by epifluorescence microscopy and digital imaging. The control incubation with 10 μ M NAH but without HA showed inducible GFP formation in the biosensor cells, which was completely absent when activated charcoal was added to the aqueous phase (Fig. 1B). The charcoal-dependent complete reduction of GFP induction by NAH had been deployed before [116] and served as a control for sorptive effects. Incubations with humic acids alone or without NAH did not result in GFP induction (Fig. 1B). Irrespective of the humic acid concentration in the assays, the mean NAH-inducible GFP fluorescence intensity in the biosensor cells was the same (Fig. 1B). Because of extreme heterogeneity of GFP fluorescence intensities in individual cells in the hanging droplets (i.e., with only 15 to 25% of the cells having fluorescence intensities higher than background (Fig. 1C)), we applied two different descriptors for the biosensor response: (i) the mean fluorescence over all cells and (ii) the boosted average fluorescence, which considers fluorescence of cells comprised between the 75th and 90th percentile. In case of boosted average GFP values, there was a significant decrease with 10 mg/L HA versus no HA addition, but surprisingly not with 1000 mg/L HA.

Total and freely dissolved NAH concentrations in the aqueous medium were measured at the end of the experiment by solid phase micro extraction (SPME) followed by a toluene extraction and analysis with GC-MS (Fig. 1D). The total measured NAH concentration in the assays was similar to the nominal added concentration (≈ 1.3 mg/L), which indicated that indeed no measurable disappearance had taken place during the time course of the experiment. In contrast, the freely dissolved NAH concentration calculated from SPME

somewhat confirmed the trend seen with the biosensor cells, because a slight but significant diminution had taken place in the presence of 1000 mg/L HA versus 0.1 mg/L HA. As obvious, and again confirming the biosensor results, the addition of activated charcoal strongly reduced the dissolved NAH concentration in the aqueous phase.

In a next experiment two nominal concentrations of NAH were applied (1 and 10 μM), whereas the fluorescence intensities of individual biosensor cells were assessed by flow cytometry. The fluorescence values of RP037 cells grown similarly but in the absence of NAH were analysed to set the threshold fluorescent value, above which statistically speaking cells would appear as 'induced'. For every assay three data descriptors were then recorded: (i) the mean GFP fluorescence of the total biosensor cell population, (ii) the proportion of cells with GFP values higher than the threshold (% of active cells), and (iii) the mean GFP fluorescence of the active subpopulation (Fig. 2). These descriptors were not independent, because the total mean GFP fluorescence encompasses that of the active subpopulation. Data from the experiment with 10 μM NAH showed that GFP fluorescence of the biosensors cells was the same irrespective of humic acids being present or not (Fig. 2A, B). On the other hand, with 1 μM NAH (0.13 mg/L) a significant decrease of GFP fluorescence was observed that was proportional to the amount of humic acids in solution. This was obvious both from the proportion of active cells with a GFP fluorescence intensity higher than the threshold and from their mean fluorescence (Fig. 2A, B). This therefore suggested that HA indeed had a slight but detectable effect on the availability of NAH to the cells.

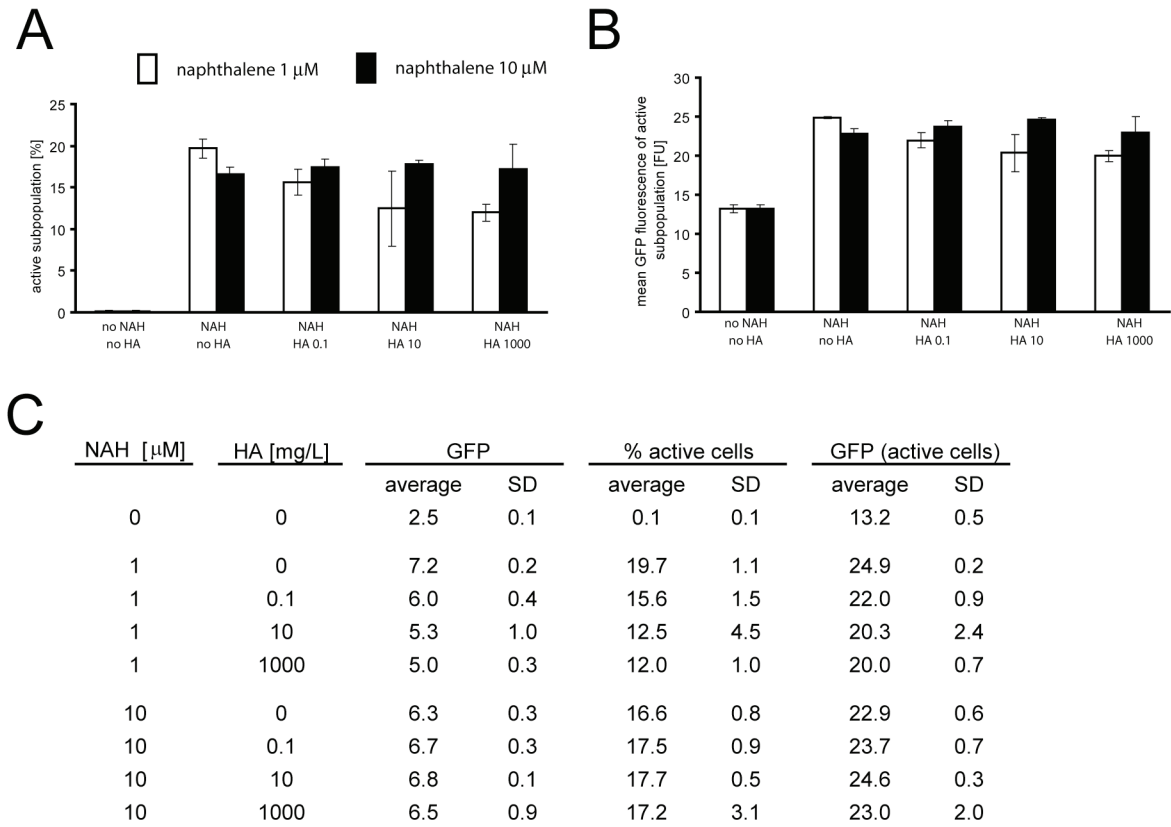


Fig. 2. Effect of DOM on *B. sartisoli* RP037 induction by two concentrations of NAH (1 and 10 μM). Cells were exposed in gas phase (Fig. 1) in the presence or absence of various amounts of humic acids (HA). After 4 hours of incubation, the cells were removed and the individual cellular fluorescence intensities were analysed by flow cytometry. (A) The percentage of cells that showed fluorescence intensity above background. (B) Mean individual cellular fluorescence intensities in the subpopulation of (A), expressed in fluorescence units (FU). Error bars indicate standard deviations calculated from triplicate measurements. (C) Data summary of the total population mean fluorescence ('GFP'), the percentage of active cells ('% active cells') and the mean fluorescence of the active cells ('GFP (active cells)').

Influence of humic acids on the availability of PHE to *B. sartisoli* RP037 in the aqueous phase

In the following experiment, we tested whether the availability of PHE for strain RP037 would change in the presence of dissolved HA. In order to provide the same PHE flux in all assays, we dosed PHE in heptamethylnonane (HMN) to the system, forming a non-aqueous phase layer. Acetate was added to the assay to permit exponential growth, which was followed by linear growth on PHE or stationary phase entrance in the absence of PHE (Fig. 3A). As observed before, the intensity of GFP fluorescence in biosensor cells (expressed as the 75th percentile of GFP fluorescence intensity in individual cells) increased in the presence of PHE between 24 and 64 hours after incubation, after which it decreased somewhat by 168 h. After 21 h, the GFP fluorescence intensity was similar in the cells exposed or not to PHE, but became significantly higher in the exposed cells after 41 h. Since the growth of the non exposed cells stopped after ~40 h, we excluded them from the further GFP fluorescence analyses. There was a slight but insignificant tendency that increasing amounts of dissolved HA resulted in higher 75th percentile values (Fig. 3B). Chemical measurements confirmed that the PHE concentration in HMN decreased over time because of degradation by the biosensor bacteria. In contrast, PHE concentrations in the HMN layer after different incubation times were not significantly different in the presence or absence of humic acids (Fig. 3C).

We repeated the experiment in the absence of acetate, with PHE as the sole source of carbon and energy for growth. All cultures showed the same growth pattern with the same decrease in PHE concentration in the HMN phase at every measured time point, irrespective of HA addition (Fig. 4A and B). GFP expression in the biosensor cells was not significantly different among the various assays, but increased slowly upon prolonged incubation time (Fig. 4C). These results suggested that HA had no influence on PHE availability to strain RP037 cells in aqueous solution.

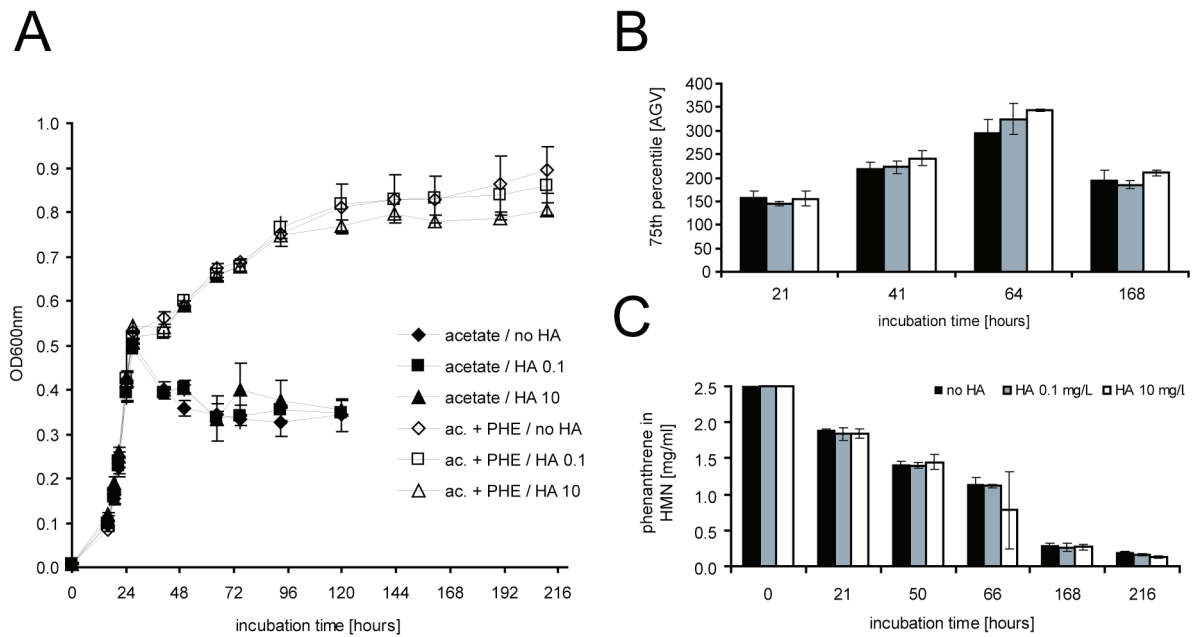


Fig. 3. Response of *B. sartisoli* RP037 to PHE in liquid culture with acetate, with or without increasing amounts of humic acids (HA). (A) Batch growth of *B. sartisoli* RP037 in minimal medium containing 10 mM of acetate and supplemented with the non-aqueous phase liquid heptamethylnonane (HMN), in the presence or absence of 2.5 mg per ml phenanthrene ('PHE'). Cell growth is measured as culture turbidity at 600 nm (OD600nm). Humic acid concentrations (0.1, 10) indicated as mg per L. (B) 75th percentile of the individual cellular fluorescence intensities in populations induced by PHE, expressed as average gray value (AGV). (C) Measured PHE concentration in HMN during the time course of the experiment. All error bars are calculated standard deviations from triplicate measurements.

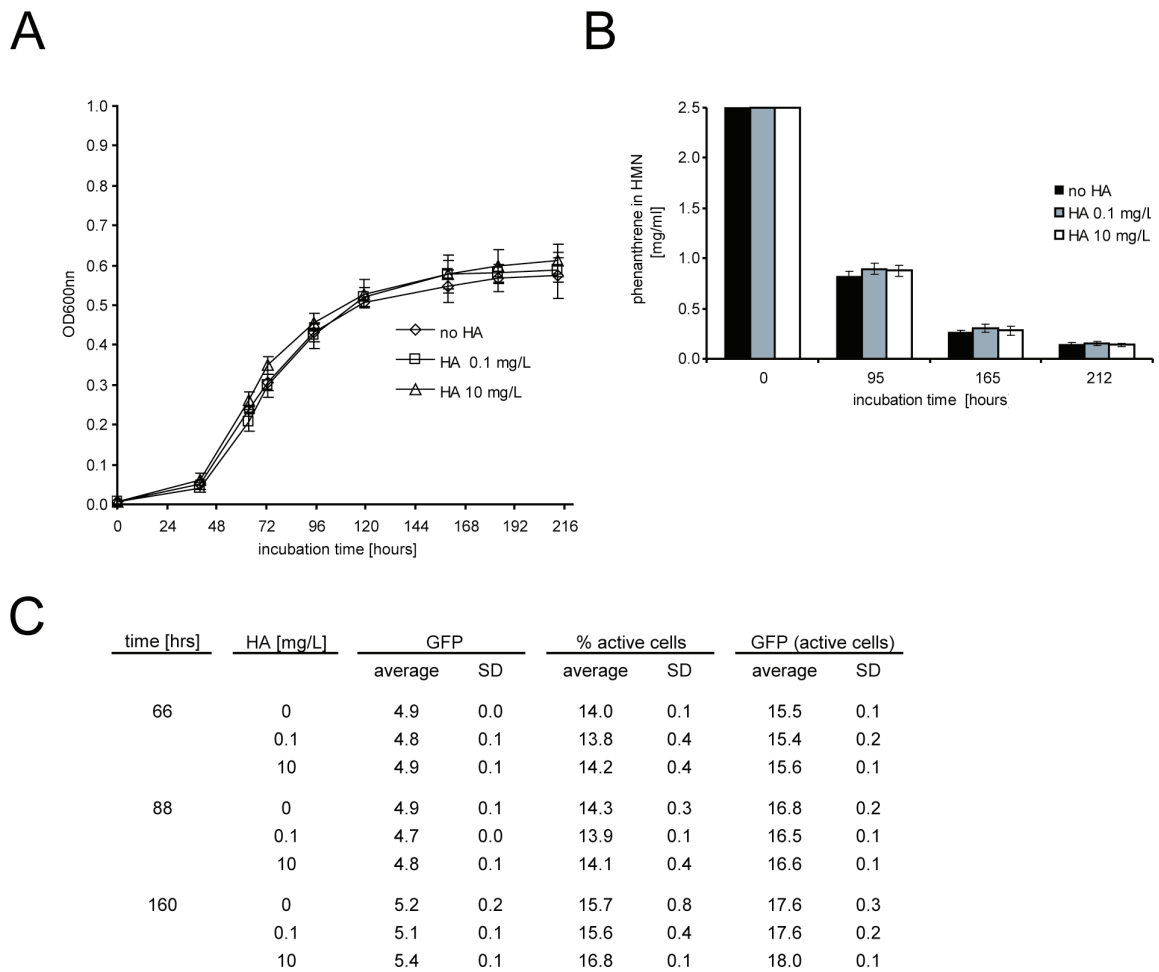


Fig. 4. Response of *B. sartisoli* RP037 to PHE as sole carbon source in liquid culture with various amounts of humic acids (HA). (A) Batch growth of *B. sartisoli* RP037 in minimal medium supplemented with PHE via heptamethylnonane (HMN, 2.5 mg PHE per ml HMN). (B) Measured PHE concentrations in HMN during the time course of the experiment. Error bars are calculated standard deviations from triplicate measurements. (C) Flow cytometry results of the GFP fluorescence intensity in strain RP037. Three indicators are shown: the mean individual cellular fluorescence intensity in the sample ('GFP'), the percentage of cells that showed higher fluorescence intensity than a defined fluorescence background ('% active cells') and the mean individual cellular fluorescence intensity in this cell subpopulation ('GFP (active cells)').

DISCUSSION

In this study, we asked the question whether DOM could change NAH or PHE availability to *B. sartisoli* RP037. In a NAH gas phase assay, DOM in the form of humic acids (HA) slightly decreased the reporter formation in the bacteria, but in one of two experiments requiring high HA concentrations (1 g/L). In addition, the effect was more pronounced when at 1 μ M than at 10 μ M dosed NAH to the system (Fig. 1, 2). RP037 cells in the droplet were only in contact with the volatile fraction of NAH, which is a function of the freely dissolved NAH concentration. This point is illustrated by the fact that when adding activated charcoal to the aqueous phase all NAH was rendered unavailable and the reporter signal from cells exposed via the gas phase was abolished. We therefore conclude that there was a slight but measurable decrease of NAH availability to the cells upon dosage of HA to the aqueous phase. Interestingly, we observed a high heterogeneity in the response of individual cells both in case of 1 and 10 μ M NAH (Fig. 1C, 2C), with only a 15 to 20 % of the cells being actively induced for GFP formation. There might be two explanations for this heterogeneity. First, there might be local availability differences for cells at micro-positions within the droplet. For instance, cells located at the water/air interface might sense more incoming NAH than cells deeper in solution. Secondly, cells in the population used for sensing may have been in different physiological states, because their cellular cycle is not synchronized during batch growth. Sensor cells that were not actively metabolizing NAH thus will not have generated the metabolite, which is necessary to induce the *phnS* promoter and GFP formation.

What might be the reason that only a small effect could be seen of HA addition to NAH availability to cells, whereas from literature one had expected a much more obvious effect? Under the righteous assumption that NAH biodegradation by RP037 cells in the assay was negligible, we modelled the equilibrium distribution of NAH in each phase: aqueous, vapour, and DOM (while ignoring the lipid phase taken up by the few bacterial cells), as a function of HA concentration (Fig. 5). In absence of HA, partitioning predicts that 98% of NAH remains in the aqueous phase. Interestingly, the 2% fraction in the vapour phase is sufficient for good induction of the cells, the main reason for this being that diffusion kinetics in the gas phase is much higher than in liquid phase, as demonstrated earlier [3]. In the presence of 1 g/L HA, the NAH fraction in the aqueous phase decreases to 64%, while 34% is bound to HA. Under these conditions, the NAH mass fraction in the gas phase decreases from 2% in absence of HA to 1.3% at 1 g/L HA. According to the partitioning model, 10 mg/L HA would diminish aqueous and gaseous NAH fractions with less than 1%.

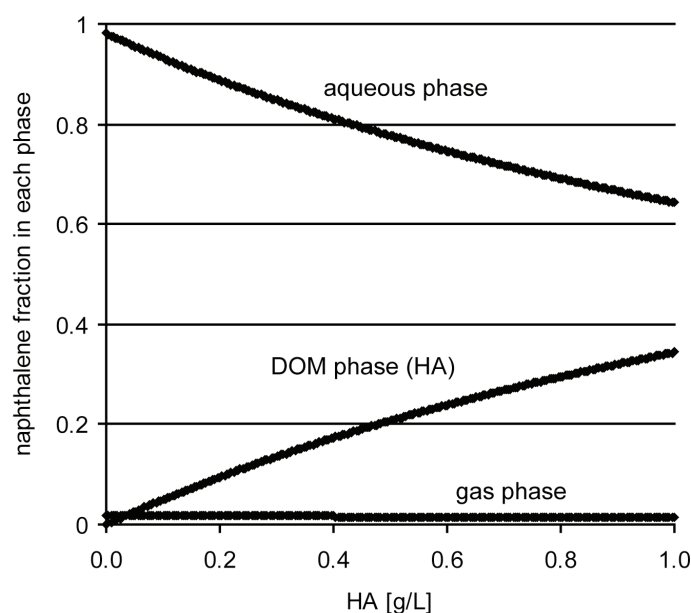


Fig. 5. Prediction of the NAH mass fraction distribution over the aqueous, gaseous and DOM phases as a function of the aqueous concentration of humic acids (HA). Calculations were done under the assumption of a gaseous assay in a 4 ml-glass vial containing 2 ml of aqueous phase and 10 μ M NAH (Fig.1). See material and methods for a description of the model.

Interestingly, our results showed a slightly weaker induction response of the sensor cells even at 10 mg HA per L and NAH concentrations of both 10 and 1 μ M (Fig. 1, 2), with the diminishment being stronger at 1 μ M NAH. We propose that this might be due to a saturation of the reporter system at high NAH fluxes to the cells. Saturation would occur at the maximum number of productive initiations of RNA polymerase at the *phnS* promoter per unit of time. Previous studies of such events at the *tfdC* promoter in *Cupriavidus necator* suggested that this saturation occurs when the intracellular metabolite that is the actual effector for activation of RNA polymerase is temporarily overproduced [117]. In this case, the inductive response is prolonged but cannot be higher per time. Since the intracellular inducer concentration is a function of the NAH flux through the cells and the maximal rate-limiting step in NAH transformation rate by the cells, increases in NAH flux above this maximum may lead to higher metabolite concentrations but not to a further induction from the *phnS* promoter. Since exposure to 10 and 1 μ M NAH elicits the same GFP response by the cells, we can conclude that any reduction in the effective NAH concentration to the cells will not immediately translate into a lower GFP response. Therefore, the effect of HA may be more pronounced at 1 μ M NAH exposure than at 10 μ M. Biosensor observations were essentially confirmed by SPME measurements of NAH in aqueous solution (Fig. 1). SPME also

validated that the total amount of NAH in the system did not significantly change during the time of the experiment (3 μg measured at the end, compared to 2.5 μg added), and that no biodegradation of NAH was occurring, which would have influenced NAH partitioning in the system. Surprisingly, the freely dissolved NAH concentrations calculated with SPME were systematically higher than the measured total NAH concentrations. This may be explained, however, by the utilization of a SPME/water partition coefficient taken from the literature rather than experimentally determined in our assay conditions.

In contrast to NAH in the gas phase, addition of HA to RP037 liquid cultures with PHE dissolved in heptamethylnonane (HMN), had no effect on the GFP expression by strain RP037 (Fig. 3, 4). This was confirmed by the measurements of total PHE concentrations, which showed comparable PHE disappearance rates in presence and absence of HA (Fig. 3 and 4), and by SPME analysis, which showed no significant variation of the dissolved PHE concentration in presence or absence of HA (data not shown). It has to be noted, however, that the maximum HA concentration used in the PHE assays was 10 mg per L, or else the assay turned completely brown, which complicated fluorescence measurements of individual cells. PHE has an octanol-water partition coefficient one order of magnitude higher than NAH ($\log K_{ow}$ of 4.57 and 3.33, respectively [40]), which would suggest that PHE is more susceptible to sorption to HA. However, the consequence of PHE sorption to HA in liquid culture is not obvious. Although sorption to HA can reduce the freely dissolved PAH concentration, it has been shown to induce faster PAH biodegradation rate in some experiments, apparently by functioning as a carrier to the cells [114]. Whether the ‘sorbent’ or the ‘carrier’ behaviour of HA dominates in natural environments remains unclear. In addition, strain-specific factors may play a role, which are presently not well understood. For instance, 100 mg/L and 1 g/L HA enhanced the PHE degradation rate of *Sphingomonas* sp. LH162 in batch cultures by factors of 3.1 and 4.8, respectively (Kilian Smith, personal communication). We used at least ten times lower HA concentrations, that were nevertheless comparable to what is found in lake water environments [118]. In addition, we applied relatively high amounts of PHE (500 mg/L), but dosed via HMN, so as to achieve a constant flux [58]. The experimental conditions (high PHE amount dissolved in HMN, shaking) produced a high flux of PHE to the cells, which maybe was too high to be changed by the presence of 10 mg/L HA. In addition, since we allowed growth of the sensor cells in the assay, the fraction represented by their total quantity of lipid membranes does become a competing fourth ‘phase’ in the system. For example, after 24 h incubation time with 10 mM acetate, the total bacteria cell mass equalled approximately 3 mg, of which the lipid fraction takes up ~8% [e.g., $(6 \times 10^9$

cells) \times 0.5 pg per cell, membrane thickness 16 nm)], compared to 0.2 mg HA in the system at a concentration of 10 mg/L. In conclusion, however, our results do not immediately confirm data from other groups that HA may increase PHE bioavailability, which to us suggests that HA effects at this point should not be generalized.

MATERIAL AND METHODS

Chemicals

Phenanthrene (97% purity) and naphthalene (99% purity) were purchased from Fluka (Buchs, Switzerland). Humic acids sodium salt was purchased from Sigma-Aldrich (Steinheim, Germany).

Strains and growth conditions

Burkholderia sartisoli sp. strain RP037 is a GFP-based biosensor described previously. The strain carries a plasmid with the *phnS* promoter fused to the *egfp* gene [58]. RP037 was routinely grown at 30°C in Tryptone Yeast (TY, contains 3 g/l of yeast extract and 5 g/l of Bacto tryptone) agar plates or liquid cultures with 50 mM NaCl. The strain was grown with the presence of 50 μ g/ml of kanamycin to maintain the reporter plasmid pJAMA37. Minimal medium (MM) was used in defined growth conditions (type 21C mineral medium, [105]). If not specified, 10 mM sodium acetate was added as a carbon source.

Gas phase NAH induction assays in vials

RP037 was cultivated in TY into early exponential growth phase. Cells were centrifuged at 1000 \times g for 10 min. The supernatant was removed and the cells were resuspended in minimal medium without any carbon source in order to obtain a culture turbidity of 0.4 at 600 nm (OD600). In 4 ml sterile glass vials, we mixed 1.8 ml of minimal medium without carbon source with 0.2 ml of an aqueous solution containing various amounts of humic acids. Twenty microliters of a solution of 1 mM or 100 μ M NAH in dimethylsulfoxide were added, in order to obtain a final nominal concentration of 10 μ M or 1 μ M, respectively. Five μ l of washed cell suspension were pipetted on the surface of a disposable Teflon liner (Supelco, USA) that was inserted inside the vial cap. The cap was rapidly turned upside down to ensure that the droplet remained at the same position, and used to hermetically seal the glass vial. Different conditions were tested in triplicate vials. The cells were incubated at room temperature

without shaking for 4 hours, thereafter removed and GFP fluorescence per individual cell was directly analysed using epifluorescence microscopy or flow cytometry.

PHE induction assays in liquid batch cultures

Burkholderia sartisoli RP037 was pre-cultivated overnight in TY medium, then centrifuged at $300 \times g$ for 10 min. The supernatant was discarded and the cells were resuspended in an appropriate volume of minimal medium so as to obtain an OD600 of 0.4. A 50 ml Erlenmeyer flask containing 20 ml of minimal medium with 10 mM acetate and 50 $\mu\text{g/ml}$ of kanamycin was inoculated with 0.4 ml of washed cell suspension. The flasks were supplemented with 4 ml of 2,2',4,4',6,8,8'-heptamethylnonane (Sigma-Aldrich Chemie, Steinheim, Germany) into which PHE was pre-dissolved at a concentration of 2.5 mg/ml HMN (nominal equivalent to 0.5 mg PHE per ml of aqueous phase). Cultures were incubated at 30°C with shaking at 180 rpm, sampled at different times for GFP expression using epifluorescence microscopy or flow cytometry. Small subsamples of HMN phase (10 μl) were retrieved at different incubation times in order to measure the remaining PHE concentration.

SPME and chemical analyses

PHE in HMN was measured by mixing 10 μl of HMN phase with 990 μl toluene. Ten μl of a deuterated PHE solution in toluene (100 ng PHE per μl) was added as internal standard after which the samples were directly injected on GC-MS (HP 6890 Series GC, Palo Alto, USA). SPME was performed by adding a 0.5 cm PDMS coated-fiber to 6 ml of solution (in the case of PHE measurements), or a 1.0 cm fiber in 2 ml aqueous sample (in case of NAH measurements). Mercury chloride was added to a concentration of 50 μg per mL to aqueous samples containing RP037 cells in order to inhibit further PHE degradation during the period of SPM extraction. Deuterated NAH or PHE standards were added at final concentration of 1000 ng per ml. For extraction, the solution containing the fiber was shaken vigorously overnight. The fiber was subsequently removed and placed in a GC vial with 200 μl toluene. One thousand ng of deuterated acenaphthylene was added to the solution as injection standard, after which a subsample of the toluene solution was injected on GC-MS. Standards were run before and after the measurement of samples in order to calculate a correlation curve of the GC-MS peak area ratio against the amount ratio between PAH and deuterated PAH. The correlation factors were used to calculate the total amount of PAH in the sample and the total amount of PAH sorbed to the PDMS fiber. From this we derived the total PAH concentration in the sample and the PAH concentration in the fiber. The latter served to calculate the freely

dissolved PAH concentration from the PAH partition coefficient between PDMS and water. The following correlation was used: $\log K_{\text{PDMS/water}} = \log K_{\text{OW}} - 0.91$ ($\log K_{\text{OW}}$ for NAH taken as 3.37).

Fluorescence microscopy and image analysis

Burkholderia sartisoli RP037 cells were examined on glass slides and the GFP intensity in individual cells was measured as described previously [58].

Flow cytometry analyses

For GFP expression analysis via flow cytometry, one ml of sample was centrifuged at $1'200 \times g$ for 15 min to recover the cells. The supernatant was discarded and the cells were resuspended in 50 μl of phosphate buffered saline (PBS). Two μl of cell suspension were diluted in 500 μl of PBS in a 5 ml polystyrene tube (Becton Dickinson, USA), then analysed with a FACS Calibur system (Becton Dickinson). In case of cells exposed to NAH in the vapour phase, the 5 μl droplet was removed from the Teflon surface and immediately diluted in 500 μl of PBS prior to analysis. Cultures not exposed to NAH or PHE served to define a fluorescence threshold above which cells were assumed to have been induced. Forward and side scatter settings were optimized for the detection of RP037 cells and a gate was defined in order to exclude background events from the analysis. Each analysis consisted of the measurement of $10'000$ cells. The 488 nm laser intensity was adjusted so that uninduced RP037 cells would not produce fluorescent signals above 10 units (arbitrary units).

Modelling

We calculated the mass fraction partitioning of NAH in a 4-ml glass vial filled with 2 ml of aqueous suspension containing a fixed nominal concentration of NAH (10 μM) and a variable concentration of humic acids. We assumed a partitioning of NAH over the aqueous phase, the gas phase and the dissolved organic phase (humic acids). The bacterial lipid phase was neglected at this low and constant amount of cells. The following mass fraction equation describes equilibrium conditions:

$$M_{\text{tot}} = M_{\text{aq}} + M_{\text{gas}} + M_{\text{DOM}} \quad (1)$$

with M_{tot} being the total mass of NAH in the system, and M_{aq} , M_{gas} and M_{DOM} the masses in the aqueous, gaseous and DOM phases, respectively. Assuming that the volume of

dissolved HA is negligible compared to the volume of the aqueous phase, the equation can be written as follows:

$$C_{aq}^i \times V_{aq} = (C_{aq} \times V_{aq}) + (C_{gas} \times V_{gas}) + (C_{DOM} \times M_{HA}) \quad (2)$$

where C is the NAH concentration in mg/ml (C^{aq} and C^{gas}) or in mg/g (C^{DOM}), V the volume (in ml), and M_{HA} the mass of HA dissolved in the system. From equation (2), we obtain:

$$C_{aq}^i \times V_{aq} = (C_{aq} \times V_{aq}) + (H \times C_{aq} \times V_{gas}) + (K_{DOM} \times C_{aq} \times M_{HA}) \quad (3)$$

where H is the Henry's law constant of NAH (dimensionless) and K_{DOM} is the partition coefficient for NAH between dissolved organic matter (in this case, HA) and the aqueous phase (in ml/g). From this, we calculate that C_{aq} at equilibrium would be equivalent to:

$$C_{aq} = \{C_{aq}^i \times V_{aq}\} / \{V_{aq} + (H \times V_{gas}) + (K_{DOM} \times M_{HA})\} \quad (4)$$

We can now calculate C_{gas} and C_{DOM}

$$C_{gas} = C_{aq} \times H$$

$$C_{DOM} = C_{aq} \times K_{DOM}$$

and the respective NAH mass in each phase:

$$M_{aq} = C_{aq} \times V_{aq}$$

$$M_{gas} = C_{gas} \times V_{gas}$$

$$M_{DOM} = C_{DOM} \times M_{HA}$$

We also assume that NAH degradation by the bacteria is negligible, and that the amount of NAH remained constant in the system over the time period of the experiment:

$$M_{aq} + M_{gas} + M_{DOM} = M_{tot} = c$$

The mass fraction in each phase is then given by

$$M_{aq} / M_{tot}$$

$$M_{gas} / M_{tot}$$

$$M_{DOM} / M_{tot}$$

The following values for the Henry and partitioning coefficients were used: $H = 0.02$ and $K_{DOM} = 534$ ($0.25K_{ow}$ [119]).

CHAPTER 4

CO-CULTIVATION OF THE BACTERIAL BIOSENSOR *BURKHOLDERIA SARTISOLI* STRAIN RP037 WITH A BIOSURFACTANT-PRODUCING *PSEUDOMONAS PUTIDA* STRAIN AND EFFECT OF TWO TYPES OF BIOSURFACTANTS ON PAH AVAILABILITY

Robin Tecon, Fatimatou Baldé

Biosurfactants are tensio-active agents that are often acknowledged as a means to enhance the aqueous solubility of recalcitrant organic contaminants, such as polycyclic aromatic hydrocarbons (PAH). Biosurfactant-producing bacteria such as belonging to the genus *Pseudomonas* might therefore enhance PAH availability to PAH-degraders. We tested the effects of two types of biosurfactants produced by *Pseudomonas* sp., cyclic lipopeptides and rhamnolipids, on phenanthrene bioavailability. Bioavailability was judged from growth rates on phenanthrene or specific phenanthrene induction of a GFP-reporter in *Burkholderia sartisoli* strain RP037. Coculturing of strain RP037 with the lipopeptide-producing bacterium *Pseudomonas putida* strain PCL1445 enhanced GFP expression compared to a single culture, but this effect was not significantly different when strain RP037 was co-cultivated with a non-lipopeptide producing mutant of *P. putida*. The addition of partially purified supernatant extracts from the *P. putida* lipopeptide producer equally did not unequivocally enhance phenanthrene bioavailability to strain RP037 compared to controls. In contrast, a 0.1% rhamnolipid solution strongly augmented RP037 growth rates on phenanthrene and led to a significantly larger proportion of cells in culture with high GFP expression. Our data suggest that biosurfactant effects may be strongly strain- and biosurfactant-type specific.

INTRODUCTION

Biosurfactants, i.e., surface-active molecules that are produced by living organisms, are frequently presented in the scientific literature as a means to increase the apparent solubility and/or bioavailability of hydrophobic organic contaminants (HOCs) [120-126]. They are produced by a variety of microbes and can be of various chemical types, including glycolipids, lipopeptides, phospholipids and fatty acids [123, 125]. Rhamnolipids, a major class of glycolipids produced by certain *Pseudomonas* species, represent common biosurfactants which are commercially exploited as emulsifiers and dispersants [125, 127]. Common features of biosurfactants are their amphiphilic properties, their ability to reduce the surface tension of water and their enhancement of hydrocarbon emulsification. Compared to synthetic surfactants, biosurfactants are in general non-toxic and biodegradable. Most of them increase the apparent solubility of HOCs by dissolving them into micelles, and for this reason their potential for improving the biodegradation rate of HOCs was extensively investigated. Biosurfactant production was shown a key characteristic of alkane-degrading bacteria, for which this serves to augment alkane bioavailability and thus degradation rate [121, 128-130]. A similar strategy has been proposed for the degradation of polycyclic aromatic hydrocarbons (PAHs) by bacteria, but it appears that biosurfactant production is not an essential trait of PAH degraders [85]. The external addition of biosurfactants, however, was shown to increase the solubilization of PAHs from non-aqueous phase liquids (NAPLs) and solid particles [124, 131]. Yet, an augmentation of PAH solubilization is not necessarily associated with an equivalent increase of its bioavailability to microorganisms [132], and the nature of biosurfactants effects on PAH degradation rate are complex and still debated [133]. In fact, one might consider that molecules dissolved in micelles are actually less available to certain bacteria than freely dissolved molecules, when they are incapable of releasing the molecules from the micelles. Alternatively, biosurfactants themselves might be used as a preferential substrate by microorganisms, which would lead to a reduction of the degradation rate of the pollutant [133].

Pseudomonas putida strain PCL1445 is a rhizosphere inhabitant that produces two lipopeptides (referred to as putisolvin I and II) consisting of a 12 amino acid cyclic peptide with a hexanoic acid chain at the N-terminus [134]. Due to their biosurfactant properties, putisolvin I and II inhibited biofilm formation of *Pseudomonas* on hydrophobic surfaces.

Both compounds were able to lower the surface tension of culture medium and increase its emulsifying activity [134]. The biosynthesis of lipopeptides in strain PCL1445 was shown to be influenced by nutritional and environmental conditions, controlled by quorum sensing and dependent of the two-component regulatory system GacA/GacS [135-137].

Here we tested the impact of lipopeptides on the bioavailability of phenanthrene (PHE) to the bacterial biosensor *Burkholderia sartisoli* strain RP037, a model degrader for low molecular weight PAHs. Two assays were hereto developed. In the first, semi-purified lipopeptide extract from PCL1445 was added directly to RP037 cultures growing on PHE to examine the effects on PHE growth rate and induction of the green fluorescent reporter (GFP) protein. In the second, we tested coculturing of the lipopeptide producing strain PCL1445 or one of the mutants impaired in lipopetide biosynthesis (PCL1436), with RP037. Although a multitude of publications investigated the effect of pure biosurfactants, very few addressed co-inoculation of a biosurfactant-producing and a HOC-degrading bacterium [138, 139]. The use of a bioagent producing surfactants *in situ* may have promising applications in bioremediation strategies. Finally, we compared the results obtained with lipopeptides with a different biosurfactant type, rhamnolipid.

RESULTS

Co-cultivation of *B. sartisoli* strain RP037 with *P. putida* strain PCL1445 or PCL1436

First we tested whether wild type lipopeptide producing strain *P. putida* PCL1445 (1445) and its derivative mutant PCL1436 (1436, with a Tn5-insertion in the genes for lipopeptide biosynthesis [134]) were able to grow in the minimal medium used to cultivate *B. sartisoli* with acetate or glycerol as sole carbon source. Growth on glycerol promoted higher production of lipopeptides than on acetate, which was evident from a lower surface tension in the culture medium measured by a drop-collapsing assay (data not shown). Single cultures of *P. putida* strains 1445 and 1436 grew similarly on minimal medium with glycerol (Fig. 1A). *P. putida* and *Burkholderia* were then co-cultured in minimal medium with glycerol, in the presence or absence of PHE as crystals. Precultures of RP037 and *P. putida* strains (1445 or 1436) were washed and mixed in an inoculum so as to have approximately ten times more colony forming unit (CFU) per ml for *Burkholderia* than for *Pseudomonas*. Co-cultures of RP037 and 1445 on glycerol and PHE grew slight faster and to a slightly higher density than a coculture of RP037 plus 1436 (Fig. 1B), but on glycerol alone this effect was opposite.

Growth of RP037 alone on PHE was obvious after 65 h, but the strain essentially did not grow with glycerol only, which suggested that in the co-cultures most of the glycerol was used by *P. putida*. After 44 and 68 hours of incubation, we sampled the cultures in order (i) to determine the GFP production in the bacterial biosensor RP037 and (ii) to estimate the proportion of *Burkholderia* and *Pseudomonas* cells by plating (Fig. 1C and D). *P. putida* strains were not fluorescent and thus were automatically excluded from epifluorescence microscope GFP measurements on individual cells. After 44 hours, the GFP intensities in the population of RP037 – expressed here as the 75th percentile of individual cellular fluorescence intensities in the bacterial culture – were slightly higher in cocultures with PHE or with PCL1436 in the absence of PHE. Because of triplicate variability none of the differences were significant. The single cultures of strain RP037 exposed to glycerol alone without PHE did not grow sufficiently for a proper GFP analysis. The proportion of colony forming units of RP037 in all cultures (except on glycerol alone) was approximately similar, but that of *Pseudomonas* varied considerably. In particular strain 1445 produced far fewer CFU per ml than strain 1436, and much less than was expected from the culture turbidity (Fig. 1C). Microscopic observations of independent cultures revealed that *P. putida* had the tendency to form aggregates of 10 to 100 cells, and that this tendency was much more pronounced for the wild-type strain 1445 than for the mutant 1436. After 68 hours of incubation, bacterial biosensors exposed to PHE expressed increased GFP amounts compared to glycerol only, irrespective of the presence or nature of the co-inoculum. The number of CFU per ml of strain RP037 was highest in single culture, about twice as low in coculture with 1445 and four times as low with 1436, suggesting partial inhibition.

Cultivation of *B. sartisoli* strain RP037 in presence of culture extracts from *P. putida*

We employed a simple procedure to extract and concentrate the lipopeptides from the supernatant of *P. putida* 1445 cultures grown on minimal medium with glycerol. The addition of the concentrated extract from a culture of 1445 to water lowered its surface tension, as indicated by the flattening of a small droplet on parafilm. Such effect was not observed with an extract from a culture of mutant 1436, impaired for the synthesis of lipopeptides. We cultivated RP037 in minimal medium with acetate and with 1% (v/v) of lipopeptide extract from either 1445 or 1436 cultures, in presence or absence of PHE crystals in the medium.

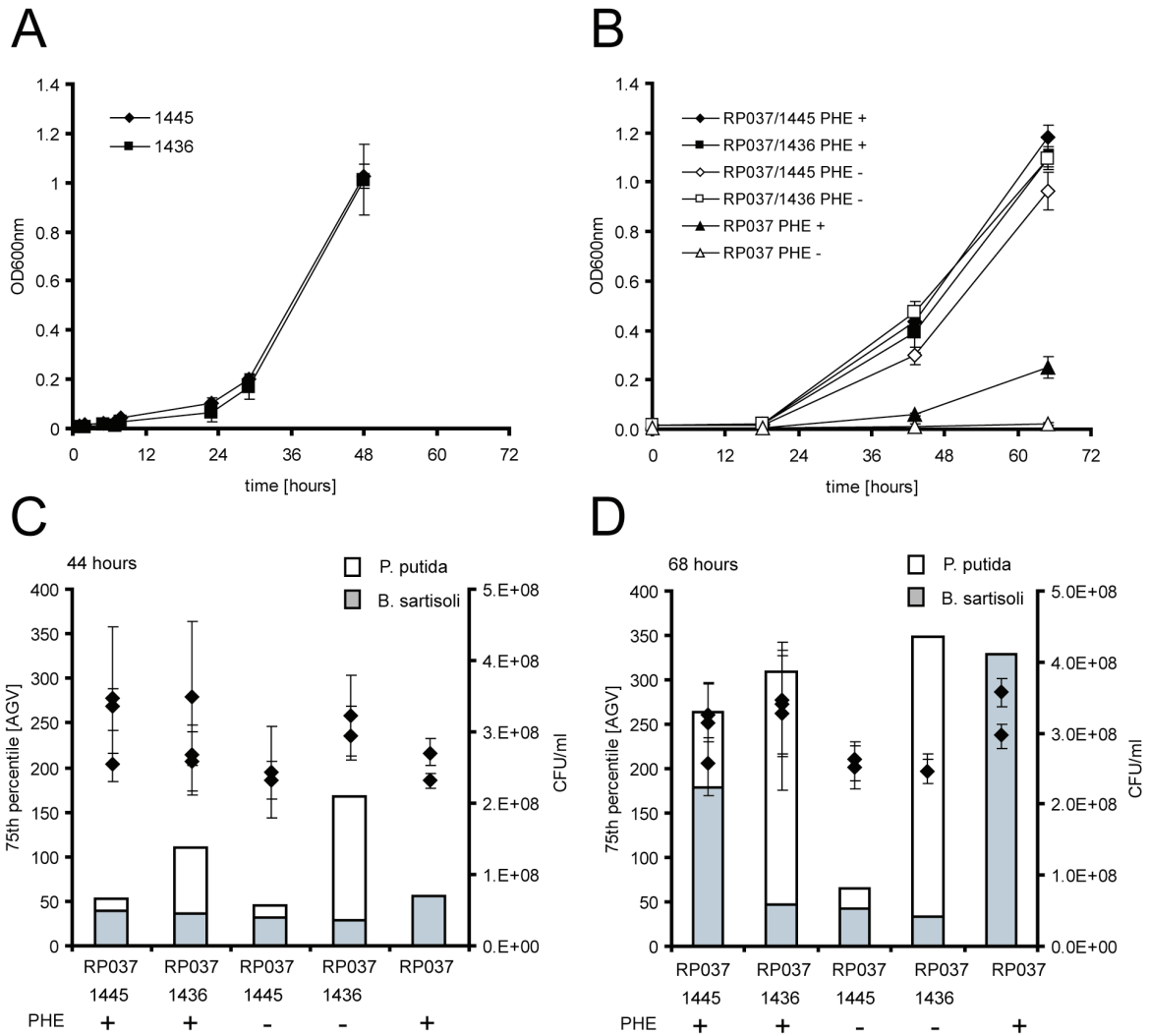


Fig. 1. Co-cultivation of *B. sartisoli* strain RP037 with *P. putida* strain PCL1445 or PCL1436, compared to RP037 alone. Development of culture turbidity in minimal medium with 10 mM glycerol, for *P. putida* single cultures (A) or *P. putida*/*B. sartisoli* co-cultures and *B. sartisoli* single cultures (B), without (PHE -) or with phenanthrene (PHE +, 0.25 mg per ml), measured at 600nm (OD600nm). Error bars indicate standard deviations from triplicate (co-cultures) or duplicate (single cultures) measurements. (C) GFP fluorescence intensity of RP037 cells after 44 hours. (D) Similar after 68 hours of cultivation. Black diamonds present the 75th percentile of the individual cellular fluorescence intensities in a bacterial sample, expressed as average gray value produced by the microscope and imaging program (AGV). Error bars indicate the 95% confidence interval for the percentile, calculated by bootstrapping in the program R [58]. Histogram bars show the number of CFU per ml of culture for *B. sartisoli* and *P. putida*.

Cultures grew similarly on acetate and reached an optical density at 600 nm of ~ 0.45 after 24 hours (Fig. 2A). Once all acetate was used, the cells cultivated in absence of extract stopped to grow, whereas the presence of extract supported extra growth of strain RP037. PHE addition prevented the decrease of turbidity that was observed with control cells, sustaining a flux of carbon sufficient to maintain the cells but not to allow extra growth. At selected time intervals, the cultures were sampled and their surface tension were assessed using a simple drop-collapsing assay (Fig. 2B). The cultures supplemented with 1445 but not 1436 extract showed a reduction of the surface tension of the medium, which could be attributed to the presence of lipopeptides. This difference persisted at least after five days of cultivation, although it appeared to fade with time (Fig. 2B). After 22 and 42 hours of cultivation, the RP037 population was sampled and the GFP fluorescence intensity in individual cells was measured by epifluorescence microscopy. Figure 2C indicates the 75th percentiles of GFP fluorescence intensities in independent RP037 cultures. After 22 hours of incubation, cultures without extract and PHE expressed the lowest percentile values, followed by the cultures without extract, but with PHE. Interestingly, RP037 cultures supplemented with *P. putida* 1445 extract showed the highest GFP expression. After 42 hours, RP037 cells incubated with PHE and with *P. putida* extract, but irrespective of 1445 or 1436 displayed higher GFP expression than cultures without extract.

In a similar experiment, we cultivated RP037 in minimal medium in presence or absence of *P. putida* extract, with PHE but without acetate. In addition to 1445 and 1436 extracts, we tested the influence of an extract from a culture of *P. putida* strain PCL1438 (1438), another transposon mutant that was impaired in the production of lipopolysaccharides (LPS) but still capable to produce lipopeptide (Irene Kuiper, pers. communication). All extracts promoted faster bacterial growth as well as a higher final culture density than the culture with PHE only (Fig. 3A). After 64 and 90 hours of incubation, cultures were sampled and the GFP fluorescence intensity in individual RP037 cells was measured by flow cytometry (Fig. 3B). Surprisingly, after 64 hours of incubation the mean GFP fluorescence intensity of the whole population was significantly higher in the cells that were not exposed to *Pseudomonas* extract ($p < 0.05$ with a unilateral Student t-test). After 90 hours of incubation, the percentage of active cells (i.e., those above a predefined threshold gate) was also significantly higher ($p < 0.05$). Among the different supernatant extracts, the 1438 extract produced the lowest values for GFP expression.

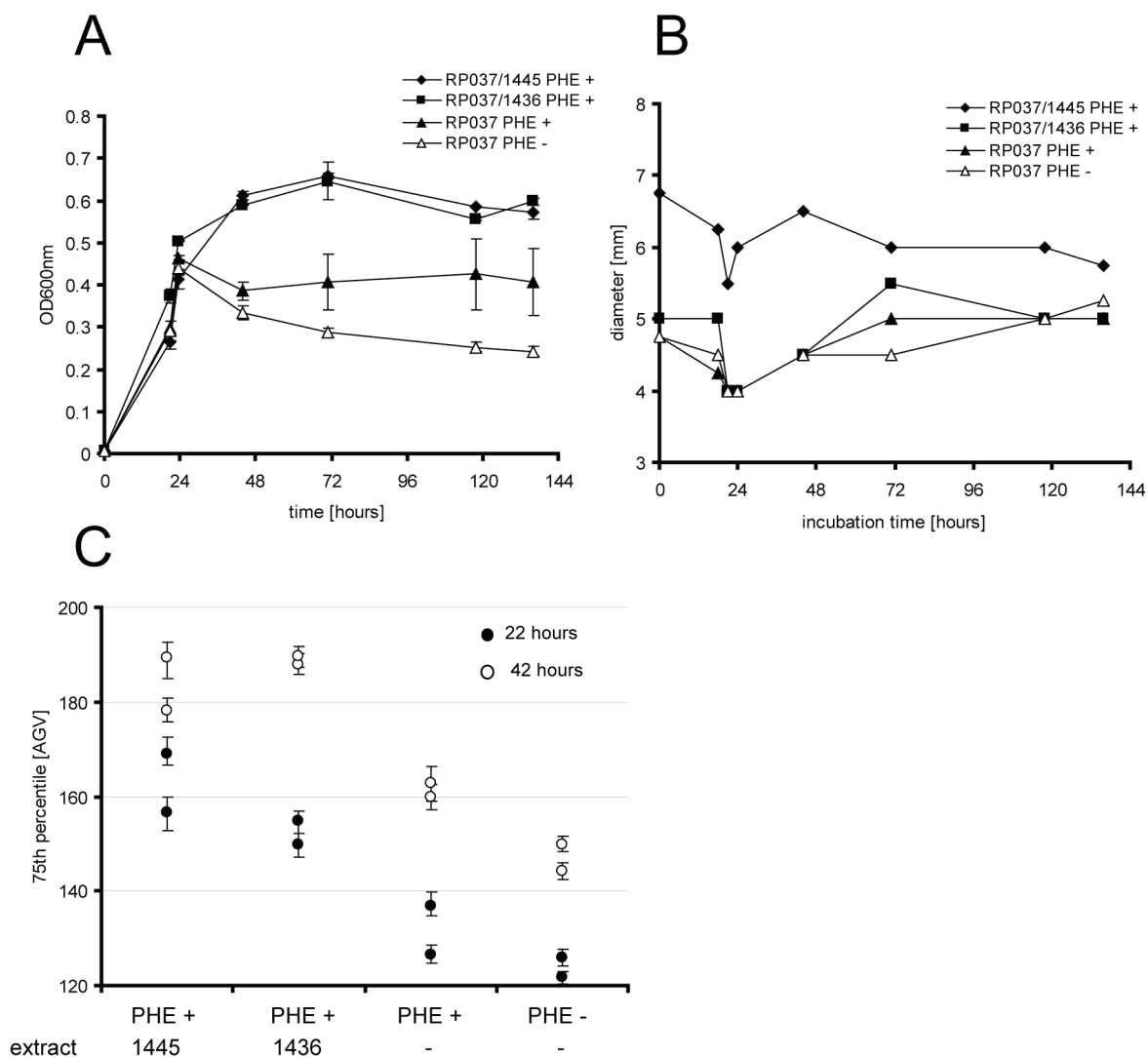
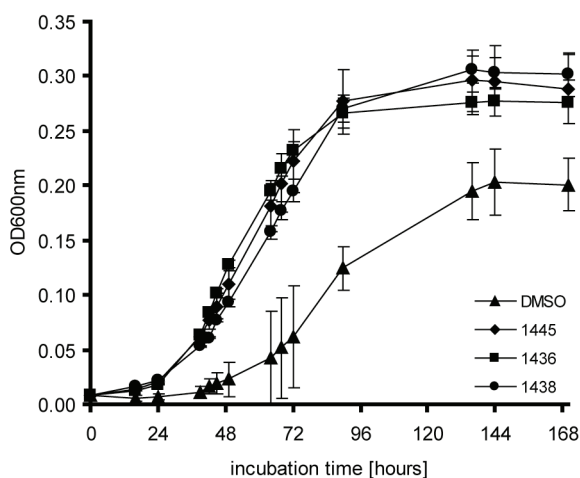


Fig. 2. Cultivation of *B. sartisoli* strain RP037 in presence of supernatant extract from *P. putida* strain PCL1445 or PCL1436. (A) Culture turbidity at 600 nm of RP037 in minimal medium with 10 mM acetate, 1% supernatant extract in DMSO (1445 or 1436), and without (PHE -) or with phenanthrene crystals (PHE +, 0.10 mg/ml). Error bars indicate standard deviations from duplicate measurements. (B) Culture droplet (25 μ l) diameters on parafilm. An increase of the droplet diameter indicates a decrease of surface tension. Measurement accuracy is \pm 0.5 mm. (C) GFP fluorescence intensity in RP037 cells after 22 and 42 hours of incubation. Circles represent the 75th percentile of the individual cellular fluorescence intensities in the culture sample. Error bars indicate the 95% confidence intervals for the percentile, calculated by bootstrapping.

Cultivation of *B. sartisoli* strain RP037 in presence of the biosurfactant JBR215

Finally, we utilized the commercial biosurfactant JBR215, which consisted of a mixture of mono- and di-rhamnolipids from *Pseudomonas aeruginosa*, in combination with RP037 cells cultivated in minimal medium with a thin layer of solid PHE on the surface of the glass flask. We added the biosurfactant solution at a concentration of 0.1 %. At this concentration, the surface tension of the medium was strongly reduced, as indicated by a droplet-collapsing assay, and this effect persisted at least after two days of incubation (data not shown). The bacteria cultivated in presence of JBR215 and exposed to PHE grew very rapidly until they stabilized at a certain cell density, whereas those exposed to PHE only showed a long lag phase followed by linear growth phase (Fig. 4A). Bacteria exposed to biosurfactant solution only showed limited but significant growth, indicating that strain RP037 was able to degrade the rhamnolipids, or that the biosurfactant solution contained other available carbon sources. This supplementary growth corresponded approximately to the differences in final culture densities between PHE only, biosurfactant only, and PHE plus biosurfactant. Growth on the biosurfactant product was not sufficient to explain the more rapid growth rate observed in cultures on PHE plus biosurfactant (Fig. 4A). We observed that the addition of the JBR215 product partly disrupted the PHE layer, producing many small and insoluble PHE crystals. This may have modified PHE mass transfer rates to the bacteria by increasing the contact surface between PHE and the aqueous phase. GFP expression in individual cells not exposed to PHE bacterial biosensors was measured by flow cytometry (Fig. 4B). Cells grown with acetate in the presence or absence of JBR215 were not inducing GFP ($p < 0.01$). RP037 cells grown with acetate, PHE and JBR215, or with PHE plus JBR215, or with PHE alone, all expressed GFP higher than in the absence of PHE (Fig. 4B). In addition, cultures with PHE to which biosurfactant was added expressed significantly more GFP than in the absence of biosurfactants ($p < 0.01$). In particular, biosurfactant addition seemed to increase the proportion of 'active' cells in culture (i.e., those expressing GFP, Fig. 4B). A delayed addition of JBR215 to the culture produced intermediate results. Results with rhamnolipids thus suggest that a temporary increase of the number of active cells may allow faster growth of RP037 on PHE.

A



B

time	treatment	GFP		% active cells		GFP (active cells)	
		average	SD	average	SD	average	SD
64 hours	DMSO	4.6	0.4	9.8	2.5	14.2	0.3
	1445 extract	3.3	0.1	4.2	0.3	13.8	0.1
	1438 extract	3.0	0.0	3.3	0.3	14.1	0.1
	1436 extract	3.5	0.1	5.1	0.4	13.5	0.1
90 hours	DMSO	4.1	0.2	9.2	0.8	14.5	0.2
	1445 extract	3.3	0.4	4.3	1.6	13.8	0.2
	1438 extract	2.6	0.0	1.9	0.1	13.7	0.4
	1436 extract	3.2	0.1	4.1	0.5	13.8	0.1

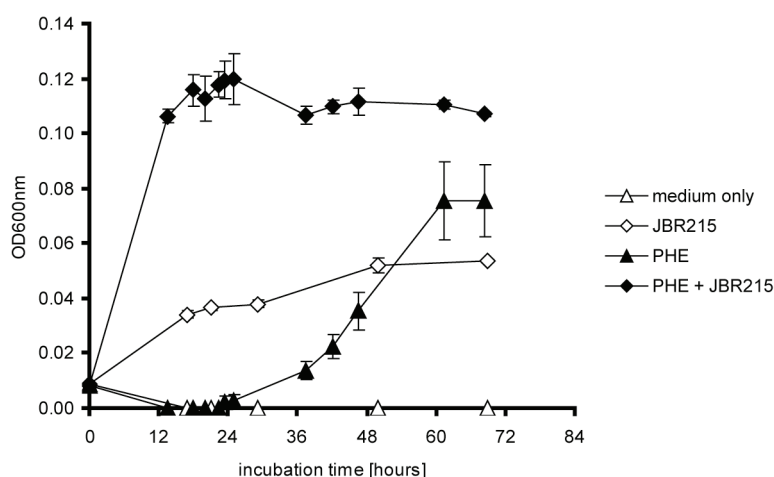
Fig. 3. Effect of supernatant extract from *P. putida* strains PCL1445, PCL1438 or PCL1436 on growth of RP037 with PHE. (A) Culture turbidity development at 600 nm of RP037 in minimal medium with PHE (0.15 mg per ml), plus 0.75% (v/v) of culture extract of strain 1445, 1436 or 1438. Error bars indicate standard deviations from triplicate measurements. (B) GFP fluorescence intensity of RP037 cells measured by flow cytometry. Three indicators are shown: the mean individual cellular fluorescence intensity in the sample ('GFP'), the percentage of cells with higher fluorescence intensity than a defined fluorescence background ('% active cells') and the mean individual cellular fluorescence intensity in this cell subpopulation ('GFP (active cells)'). Data show averages and standard deviations calculated from three independent cultures.

DISCUSSION

We used the bacterial biosensor *B. sartisoli* strain RP037 as a model bacterium to test the hypothesis as to whether biosurfactants can enhance the bioavailability of PHE to cells in liquid culture. Two assays were deployed to test our hypothesis. One in which RP037 was cocultured with a biosurfactant producer simultaneously. The other in which purified biosurfactant was added from the start of cultivation on PHE. Two biosurfactant types were tested, lipopeptides and rhamnolipids. In general, *Pseudomonas* lipopeptides did not seem to enhance PHE bioavailability to RP037. This was concluded from the absence of more rapid growth of RP037 on PHE in cocultures with a lipopeptide producing strain (PCL 1445) compared to a non-lipopeptide isogenic strain (PCL 1436), from the absence of more rapid growth on PHE with purified lipopeptide extract from a producer culture compared to a non-producer culture, and from the absence of augmented GFP induction in RP037 cells compared to non-supplemented cultures of RP037 on PHE. Some effects were seen, which will be discussed in more detail below, but which could not be attributed to lipopeptides. In contrast, the rhamnolipid JBR215 induced both more rapid growth of RP037 on PHE and a higher proportion of GFP-producing cells compared to a non-amended RP037 culture on PHE. Although we ignore the exact mechanism of this effect, as discussed below, we can conclude that rhamnolipids can enhance PHE bioavailability to RP037.

We realized that co-cultivation of two bacterial species, although in principle the simplest bacterial ‘community’ that can be produced in the laboratory, show a much more complex and unpredictable behaviour than pure cultures [140]. Two bacterial species can interact in a variety of direct (e.g., contact, aggregation) and indirect ways (e.g., competition for nutrients, use of non-self metabolites, production of bacteriocides). Whereas our initial hypothesis was that lipopeptide production by PCL1445 could enhance the utilization rate of PHE by RP037, our results demonstrate that possibly metabolites other than lipopeptides can (slightly) enhance RP037 growth on PHE. The optimized growth media conditions (i.e., glycerol as carbon source) we employed for co-culturing *B. sartisoli* and *P. putida* essentially sustained *P. putida* growth only while allowing lipopeptide production. Growth of RP037 in coculture thus had to come from PHE utilization exclusively, and any enhancement of PHE utilization rates might have originated in lipopeptide production or other secondary metabolites excreted by *P. putida*. Acetate, in contrast, could be utilized by both bacteria, but proved to be less favourable for biosurfactant production.

A



B

	acetate	phenanthrene	JBR215	GFP		% active cells		GFP (active cells)	
				average	SD	average	SD	average	SD
(a)	10 mM	-	-	2.9	0.0	0.8	0.1	11.9	0.2
	10 mM	+	-	3.7	0.0	6.0	0.3	15.4	0.0
	10 mM	+	0.1%	4.1	0.1	8.6	0.3	15.6	0.1
	10 mM	+	0.1% (d)	3.9	0.1	7.3	0.5	15.6	0.4
(b)	10 mM	-	-	2.8	0.0	0.8	0.1	12.0	0.3
	10 mM	-	0.1%	3.0	0.0	0.9	0.1	11.6	0.1
	-	+	-	5.2	0.2	13.1	1.5	14.7	0.3
	-	+	0.1%	5.6	0.0	16.5	0.0	15.5	0.1

Fig. 4. Effect of biosurfactant JBR215 on growth and GFP expression in *B. sartisoli* strain RP037 on PHE. (A) Culture turbidity development at 600 nm of RP037 in minimal medium without acetate but with 0.1% of JBR215 in the presence or absence of a PHE crystalline layer (0.05 mg per ml). Error bars indicate standard deviations from triplicate (PHE +) or duplicate (PHE -) measurements. The graph results from the combination of two separate experiments (black and white symbols). (B) GFP expression in RP037 cultures with or without 10 mM acetate, absence or presence of JBR215, and with or without crystalline PHE (0.05 mg/ml). JBR215 was added directly at time 0 or after 24 hours of incubation (*d*). GFP expression was recorded by flow cytometry after 44 hours (a) or 38 hours (b), and is represented by the mean individual cellular fluorescence intensity in the sample ('GFP'), the percentage of cells that showed higher fluorescence intensity than a defined fluorescence background ('% active cells') and the mean individual cellular fluorescence intensity in this cell subpopulation ('GFP (active cells)'). Averages and standard deviations were calculated from three independent cultures.

Culture droplet-collapsing measurements indicated that PCL1445 indeed lowered the surface tension of the medium, but this was more pronounced at the end of the growth phase (\approx three days). Since the production of lipopeptides by PCL1445 is known to take place at late exponential phase [134], it might thus be that the lipopeptide production was not high enough during the most critical time of PHE utilization by RP037. In contrast, GFP production in RP037 was slightly stimulated in cocultures with both PCL1445 and PCL1436 at early growth stage (44 hours), suggesting that some compounds other than lipopeptides influenced the biosensor activity of RP037. This tendency disappeared after three days (68 hours) of incubation.

The proportion of the two bacterial types in the community is known as another important variable [141]. We ensured RP037 sustenance by using an inoculum approximately ten times higher than that of *P. putida*. Our results indicated that *P. putida* rapidly colonized the suspended community at the expense of its exclusive carbon source glycerol, which RP037 was unable to productively utilize. Interestingly, we also observed that the RP037 population doubled twice or thrice even in the absence of PHE in the culture medium, which suggested that RP037 utilized some carbon source released by *P. putida* during growth on glycerol. Compared to the control on PHE only, RP037 after three days had multiplied less rapidly in the presence of *P. putida*, with the non-lipopeptide producer having a stronger effect than PCL1445. It is unclear if this inhibition was due to competition for nutrients or other factors.

To rule out the possibility that lipopeptide production by PCL1445 had not occurred at the right moment for RP037 to enhance its utilization rate of PHE, we employed partially purified lipopeptides and demonstrated that a 1% extract from strain PCL1445 indeed lowered the surface tension of the medium (Fig. 2B). Furthermore, we ensured that surfactant effects would act only on the apparent aqueous solubility of PHE by using PHE crystals, and not on dispersion of PHE dissolved in non-aqueous phase liquid such as heptamethylnonane employed before [58]. However, also in this case we could not demonstrate a direct effect of lipopeptides on PHE availability. Interestingly, *P. putida* culture extracts, both from PCL1445 or PCL1436 increased RP037 growth rates (Fig. 2A, 3A), which reinforces the conclusion drawn from coculture experiments that some other compound(s) produced by *P. putida* serve as a carbon source for RP037. Both extracts were even able to increase GFP expression in RP037 cells compared to non-amended cultures with PHE, which may be due to an overall higher metabolic activity of the cells rather than to increased PHE bioavailability. This stimulatory result on GFP expression could not be confirmed when the experiment was repeated in cultures with PHE (with or without extract) but without acetate (Fig. 3B).

Contrary to the lipopeptides, a 0.1% commercial solution of rhamnolipids, produced by *P. aeruginosa* species, had a spectacular effect on RP037 growth on PHE. Rhamnolipids has before been shown to enhance PAH biodegradation rates by a *Pseudomonas* species [132, 142]. Addition of rhamnolipids also increased the proportion of active GFP expressing RP037 cells in culture, which suggests that the PHE availability in solution increased importantly compared to a non-amended control. Despite this strong effect, we cannot firmly conclude the mechanism of rhamnolipid action on PHE availability. We observed that a 0.1% concentration of rhamnolipids ‘disrupted’ the layer of crystalline PHE deposited at the bottom of the culture flask. Instead of increasing the apparent PHE solubility in the aqueous phase, the rhamnolipids may have caused a break-up of the confluent PHE layer into numerous very small crystals. This may have produced an enormous increase in the contact surface between PHE and aqueous phase, and, therefore, a higher dissolution flux. The higher PHE flux could then have sustained a larger proportion of cells degrading PHE. To discriminate between these interpretations, it would be necessary to repeat the experiment with a fixed amount of crystals rather than a layer, in order to exclude the effect of dispersion.

Obviously, the utilization of biosurfactants holds great promise for bioremediation technologies, because it might increase the bioavailability of HOCs for bacterial degradation. HOC biodegradation rates, which otherwise and often are limited in the environment by mass transfer processes, may thus be enhanced by biosurfactant application. Despite its promise and successful applications [139], there is no general rule for the most optimal type of biosurfactant or for the best application method. For example, Mulligan et al., considered *in situ* biosurfactant production easier and more cost efficient than external addition [125], but we show here that *in situ* production may lead to numerous secondary effects that have nothing to do with increasing HOC availability. For this reason, there is an interest in better understanding the interactions between surfactant producers and pollutant degraders, in particular because it was demonstrated that the observed effects can be strain-dependent [138]. This was corroborated by our results here, which showed no effects for lipopeptides but strong effects for rhamnolipids on PHE availability by RP037. Given that numerous secondary effects can play a role, a detailed understanding of biosurfactant mechanisms on HOC bioavailability is necessary. For instance, biosurfactants have been proposed not only to increase the apparent aqueous phase solubility of a HOC, but also to modify the bacterial cell membrane. This could render the membrane more hydrophobic and lead to increased HOC concentrations in the cell [127]. Increased cell wall hydrophobicity could also promote better attachment to HOC phases or particles, which can reduce mass transport distances and

thereby increase HOC degradation rates. We think that simple pathway induction assays like the ones with bioreporters deployed here, can provide an effective means for screening other biosurfactants and perhaps, obtain more generalized knowledge on the different bioavailability mechanisms.

ACKNOWLEDGMENTS

We thank Terry McGenity from the University of Essex (UK) for the gift of the commercial rhamnolipid solution JBR215.

MATERIAL AND METHODS

Chemicals and biosurfactant

Phenanthrene (97% purity) was purchased from Fluka (Buchs, Switzerland). PHE crystals were of various sizes with an approximate diameter average of 0.10 mm. The rhamnolipid solution JBR215 was obtained from Jeneil Biosurfactant Company (Saukville, USA), and was provided as a 15% aqueous solution. It was produced from sterilized and centrifuged fermentation broth. The two major components in the solution, a mono- and a di-rhamnolipid, had molecular weights of 504 and 650, respectively, with an approximate ratio of 1:1. The critical micellar concentration (CMC) of the biosurfactant is 37 μM , or ~ 20 mg/L [143]. In our experiments, we used the rhamnolipid solution at a concentration of 0.1%, which corresponded to 150 mg/L, or ~ 270 μM , i.e. ~ 7 times above the CMC.

Strains and growth conditions

B. sartisoli strain RP037 is a GFP-based biosensor described previously [58]. *P. putida* PCL1445 is a wild type strain that colonizes grass roots and produces two lipopeptides (putisolvin I and II) which possess biosurfactant activity [134]. *P. putida* PCL1436 is a transposon mutant derived from PCL1445 which has lost the ability to synthesize the two lipopeptides [134]. *P. putida* PCL1438 is another transposon mutant which still produces biosurfactants but not lipopolysaccharides (LPS). All *P. putida* strains were routinely grown in Luria-Bertani medium or in type 21C minimal medium with 2 % (w/v) glycerol, at 30°C without antibiotics. For co-cultivation experiments, strains of *P. putida* were cultivated under the conditions for RP037 alone [58].

Co-cultivation of *B. sartisoli* and *P. putida*

RP037 and *P. putida* strains were pre-cultivated in single culture overnight in TY and LB medium, respectively. The cells were centrifuged at $1'200 \times g$ for 10 min and the supernatant was removed. The cells were then resuspended in minimal medium in order to obtain a culture turbidity at 600 nm of ~ 0.4 . Twenty ml of minimal medium containing 10 mM glycerol but no antibiotics were inoculated with 2 % of each preculture (RP037 plus one of the *P. putida* strains). The cultures were incubated at 30°C with shaking at 180 rpm in presence or absence of PHE crystals (0.25 mg/ml of medium). The number of colony forming units in culture was determined from serially diluted samples plated on TY with 50 mM NaCl agar plates for RP037, or LB agar for *Pseudomonas*. GFP fluorescence was assessed in individual RP037 cells using epifluorescence microscopy or flow cytometry, as described previously [58].

Lipopeptide extraction from *P. putida* cultures.

P. putida strains were grown for two days in minimal medium with 2% (w/v) glycerol. Cells were removed by centrifugation and the supernatant was further filtered through 0.45 μm . In a glass beaker, 50 ml of supernatant were mixed with 50 ml of ethyl acetate and agitated at room temperature for one hour with a magnetic stirrer. The organic phase was recovered and evaporated using a Rotavap system. Subsequently the extract was resuspended in 5 ml of ethyl acetate, transferred to a glass vial, and evaporated using a stream of N_2 . Finally, the dried extract was resuspended in 500 μl of dimethylsulfoxide (DMSO).

Droplet-collapsing assay

Twenty-five μl of bacterial culture or culture supernatant to which lipopeptide or rhamnolipid was added, were pipetted on a hydrophobic surface (parafilm). After 5 min incubation at room temperature, the diameter of the droplet was measured using graduated paper.

Flow cytometry analysis

One ml of cell culture was centrifuged at $1'200 \times g$ for 15 min. The supernatant was discarded and the cells were resuspended in 50 μl of phosphate buffered saline (PBS). Two μl of this cell suspension were further diluted in 500 μl of PBS in a 5 ml polystyrene tube (Becton Dickinson, USA), then analysed with a FACS Calibur system (Becton Dickinson).

Specific settings were optimized for the detection of RP037 cells based on the forward and side scattered light channels, and a gate was defined in order to detect bacterial biosensor cells and exclude background events from the analysis. Each analysis consisted of the measurement of the green fluorescence intensity on the FL1-H channel in 10^7 000 cells. The 488 nm laser intensity was set in order that uninduced RP037 cells (i.e., grown on acetate alone) would not produce fluorescent signals above 10 units (arbitrary units).

CHAPTER 5

DOUBLE-TAGGED FLUORESCENT BACTERIAL BIOSENSOR FOR THE STUDY OF PAH DIFFUSION AND BIOAVAILABILITY

Robin Tecon, Olivier Binggeli

Polycyclic Aromatic Hydrocarbons (PAHs), ubiquitous contaminants from oil and coal, can be entirely degraded by a large number of bacteria. In practise, PAH biodegradation rates may be strongly reduced, which is often due to limited accessibility of the contaminant to the bacteria. In order to measure PAH availability in complex systems, we developed a double-tagged bacterial reporter strain *Burkholderia sartisoli* RP037-mChe. The reporter strain induces the enhanced green fluorescent protein (eGFP) as a function of the PAH flux to the cell, and produces a second autofluorescent protein (mCherry) in constitutive manner. Single cell quantitative epifluorescence imaging was deployed in order to record reporter signals as a function of PAH availability. The reporter strain expressed eGFP proportionally to dosages of naphthalene or phenanthrene in batch liquid cultures. No detectable fluorescence cross-talk occurred between eGFP and mCherry. To detect PAH diffusion from solid materials the reporter cells were embedded in 0.5 % agarose and 2 cm long gel patches, and fluorescence was recorded over time and distance for both markers. eGFP fluorescence gradients were detected after 4, 8 and 24 h from naphthalene or phenanthrene provided as point sources in a glass capillary contacting one extremity of the gel, demonstrating that the PAH diffusion and degradation kinetics could be followed by the reporter cells. A PAH-contaminated lampblack soil from a former gas manufacturing site induced even higher GFP expression than 10 μg equivalent naphthalene. To detect reporter gene expression at even smaller diffusion distances we mixed and immobilized cells with contaminated soils in an agarose gel. mCherry visualization helped to localize individual cells amidst soil particles. eGFP fluorescence measurements confirmed gel patch diffusion results that exposure to 2-3 mg lampblack soil gave four times higher expression than to material contaminated with 10 or 1 mg PHE per g.

INTRODUCTION

Industry, agriculture and household activities lead to a continuous release of a variety of chemicals into natural environments. Even though some of the most toxic and persistent chemicals have been banned by international regulations [144], they can still be detected in the environment and even in biota. Many of the utilized chemicals pose potential threats to organisms and ecosystems, and, consequently, it is of utmost importance to properly predict their short- and long-term toxic effects. From the perspective of clean-up operations, it is also important to judge the availability of polluting chemicals for biodegradation. Biodegradation of pollutants by bacteria is a major process aiding the clean-up of contaminated sites, and in many cases society will have to rely on spontaneous (non-stimulated) biodegradation in the environment, a process called natural attenuation [145]. Biodegradation rates will be optimal when the microorganisms responsible for the transformation process have unlimited access to the pollutant. Interestingly, ‘access’ to a pollutant is determined by both biological and physicochemical processes [6, 82]. Physical chemistry governs pollutant dissolution, desorption and diffusive or dispersive transport to bacterial cells, but by taking up and transforming a compound cells influence the kinetics of the overall transport. Such processes have been described as *bioavailability processes* [33], and it has been realized more and more that a proper description of bioavailability is essential to comprehend and predict the fate of contaminants in a given environment. However, investigations of contaminated sites are still essentially based on measurements of total pollutant amounts rather than their bioavailable (or potentially biodegradable) fractions. Making better links between total compound analysis, bioavailability analysis and biodegradation activity would permit a better understanding of the fates of environmental pollution.

A distinction between total and bioavailable fractions is particularly significant for chemical compounds with poor aqueous solubility or very low dissociation constants, such as hydrophobic organic contaminants and heavy metal precipitates. Polyaromatic hydrocarbons (PAHs) are a good example of widespread and hydrophobic pollutants: they represent a major component of crude oil and are produced during all combustion processes. Several PAHs can be degraded by microorganisms, but in particular the high molecular mass PAHs tend to persist in the environment due to their extremely low aqueous phase solubility and bioavailability [81, 85].

Chemical approaches have indeed been developed to assess the bioavailable fraction of a pollutant in a sample, most of which are based on partial extraction methods or on specific sorptive materials. More recently so-called non-exhaustive extraction techniques (NEETs) have been developed, which extract a fraction of the chemical from a sample similar to that degraded by bacteria over a much longer period of time [32, 35]. NEET has also been combined with bacterial bioreporter technology (see below). Biological techniques for bioavailability include isotope fractionation methods, biomineralization of added light or heavy isotopes, as well as molecular methods which measure bacterial catabolic gene expression in the form of specific mRNA [146-148]. Bacterial bioreporter technology (the use of genetically engineered living bacteria for the detection of specific chemicals) would be an interesting alternative that might permit a rapid investigation of bioavailability in environmental samples (see Chapter 1).

In a previous study we showed that enhanced green fluorescent protein (eGFP) formation in *Burkholderia sartisoli* strain RP037 was a good measure for the flux of phenanthrene (PHE, a low molecular mass PAH) in standard batch cultivation and from sorbed materials [58]. Strain RP037 metabolizes PHE and induces the eGFP reporter at the same time, meaning that it can influence PHE transport kinetics in the system it is in. Therefore, it can potentially act as an appropriate ‘sensor’ for PHE bioavailability. Here we ask the questions of how bioavailability assays for PAHs in complex samples can be designed and whether reporter cells can detect differential PAH availability from samples and over time.

In order to increase the microscopic visibility of the reporter cells even in absence of an inducing signal in complex samples such as soils, we tagged strain RP037 with a second fluorescent protein (mCherry) that would be constitutively expressed in the cell. Among the variety of monomeric fluorescent proteins that have been developed in the past decade, mCherry possesses excellent complementary excitation and emission characteristics to eGFP. In addition, mCherry is well tolerated by bacterial cells and combines excellent fluorescence properties with high photostability [18, 149]. The new dual reporter strains were tested for co-expression of mCherry and eGFP under non-inducing standard conditions, and after exposure to naphthalene (NAH) or PHE. Various new experimental assays were developed to calibrate and measure PAH-inducible eGFP expression, from controlled source material to a few contaminated environmental samples. One of such assays consisted of a diffusion gel matrix, in which PAHs or contaminated material were placed as a point source and bacterial reporter cells were embedded in a gel matrix, detecting the compound flux over time.

RESULTS

Constitutive and inducible fluorescence expression from *Burkholderia sartisoli* strain RP037-mChe exposed to naphthalene and phenanthrene

The bacterial biosensor *B. sartisoli* RP037-mChe was tagged with a mini-Tn7 transposon gene cassette containing the gene for mCherry under control of the P_{tac} promoter. In addition, this strain carries a plasmid with *egfp* under control of the NAH/PHE-metabolism inducible P_{phnS} promoter by the transcription activator PhnR (Fig. 1). Expression of mCherry was constitutive in RP037-mChe cells grown in minimal medium with acetate, although variation of the red fluorescence intensity was observed among single cells in the population (Fig. 2). The mean red fluorescence over the whole population was lower during exponential phase, reached a maximum at early stationary phase and then remained stable for at least 15 hours in stationary phase (Fig. 2B). We then exposed RP037-mChe cultures growing with acetate to various amounts of NAH and/or PHE, which were dosed by dissolving them in the non-aqueous phase liquid heptamethylnonane (HMN). HMN formed an insoluble and non-degradable second-phase layer on top of the growth medium, from which PAHs would diffuse to the cells within the aqueous phase. Controls with acetate only rapidly became turbid from RP037-mChe growth until all acetate was used and growth ceased (Fig. 3A). Cultures with 50 mg PHE per L of growth medium (concentrations are presented in mg of PAH per liter of minimal medium, even though they are dissolved in HMN) did not visibly grow different from the controls. By contrast, 500 mg PHE per L in addition to acetate was sufficient to promote supplementary growth, which started off after the acetate seemed depleted, as indicated by a second, linear increase of culture turbidity (Fig. 3A). Strangely, the addition of 50 mg NAH per L had an inhibitory effect on the growth rate, although the turbidity finally equalled that of the control at the end of the incubation period. The addition of lower amounts of PHE (5 and 25 mg per L) or naphthalene (5 mg per L) had no effect on growth rate compared to the control, whereas the addition of 25 mg NAH per L produced an intermediate reduction of growth rate (data not shown). After one day of incubation, mCherry expression in single cells showed little variation between the cultures, but eGFP expression was induced dependent on the amount and nature of the offered PAH (Fig. 3B). In general, despite growth inhibition, NAH was a much stronger inducer than PHE, and 5 mg NAH per L produced a higher response than 500 mg PHE per L.

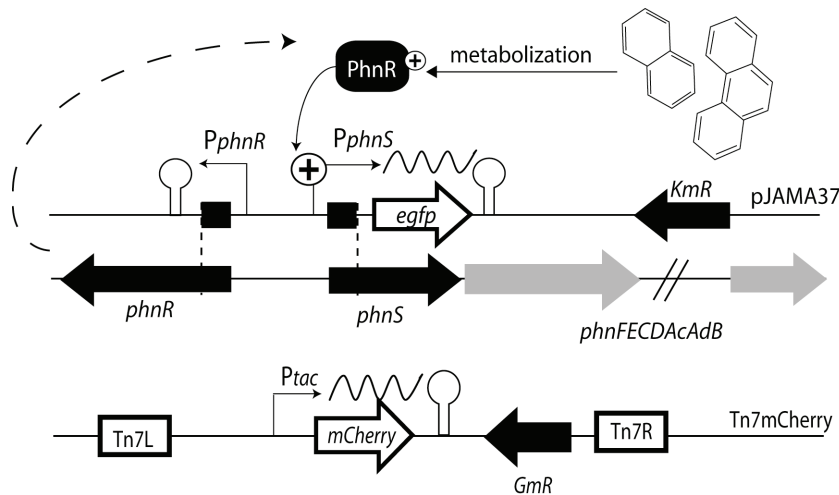


Fig. 1. Genetic constructs introduced in the double-tagged bacterial bioreporter *Burkholderia sartisoli* RP037-mChe. The reporter plasmid pJAMA37 is responsible for naphthalene (NAH) and phenanthrene (PHE) detection via the inducible promoter P_{phnS} and carries *egfp* as reporter gene [58]. Briefly, basal PHE and NAH metabolization lead to production of an (unidentified) metabolite that interacts with the constitutively expressed transcriptional activator PhnR, which triggers the expression of the *egfp* gene from P_{phnS} . The promoter P_{tac} permits the constitutive expression of *mCherry*, which was inserted into the chromosome of *B. sartisoli* via Tn7 transposition. Genetic maps not drawn to scale. *KmR* and *GmR* encode the enzymes responsible for kanamycin and gentamycin resistance, respectively.

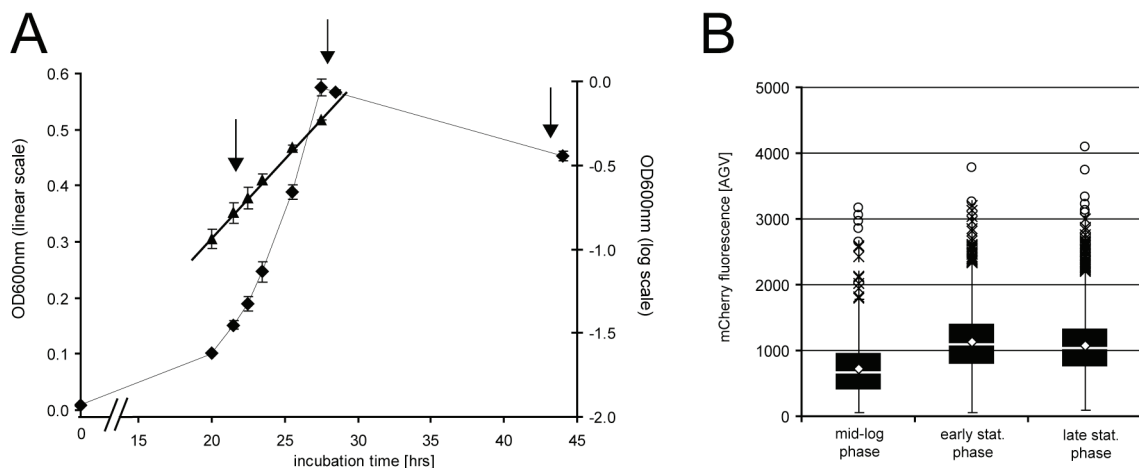


Fig. 2. mCherry expression in *B. sartisoli* RP037-mChe during liquid batch growth in minimal medium with 10 mM acetate. (A). Mean culture turbidity of triplicate measurements at 600 nm (OD600nm) and represented in linear (diamonds) or log scale (triangles). Error bars indicate standard deviations calculated from the mean. Arrows indicate time of sampling for single-cell fluorescence measurements (~mid-log, early and late stationary phase). (B). Boxplots of mCherry fluorescence in individual cells, expressed as average gray value produced by the camera system (AGV). The mean fluorescence is indicated by a white diamond.

eGFP expression was not homogenous among cells of the population, but strongly skewed and with a wide range of intensity values (Fig. 3B). Interestingly, after two days of incubation the eGFP fluorescence had increased in cultures exposed to PHE, but had slightly decreased in those exposed to NAH compared to day one (data not shown). No significant emission of mCherry was detected in the filter range for eGFP, and vice versa, and consequently, green and red fluorescence did not correlate in individual cells. This ensured that the two signals could be discriminated efficiently.

Response of RP037-mChe cultures to PAH contaminated samples

We then asked the question whether RP037-mChe could be used to measure PAH release from contaminated soils and sediments. In order to create similar conditions as in the calibration assays above, soil and sediment samples were mixed in HMN (at 10-20 mg dry weight per ml HMN) prior to be added to RP037-mChe assays. After one day of incubation, the cells exposed to PAH-contaminated sediment from Etang-de-Berre did not show significant eGFP production compared to the non-exposed control or to an assay using non-contaminated forest soil (Fig. 4). This suggested that too little inducible compounds dissolved from the sediment-HMN phase to the cells. Assays with lampblack soil (a high PAH containing material from an ancient gas manufacturing site), however, resulted in strong eGFP production comparable to what was observed with 500 mg PHE and 5 mg NAH per L (Fig. 3B). After two days of incubation, the eGFP fluorescence in the assay with lampblack soil had decreased, which suggests that the cells were actively growing and diluting the otherwise stable eGFP (not shown).

Agarose-embedded bacterial biosensors detect PAH flux from a point source

In order to possibly increase the sensitivity of the bioreporter measurement for PAHs, we developed a new experimental set-up in which a PAH concentration gradient would be created from a point source. Reporter cells close to such a source would possibly be exposed to much higher concentrations than achievable in mixed culture. For this the bacterial bioreporter cells were cultivated in minimal medium with acetate until the cells reached mid-exponential phase, centrifuged and resuspended in fresh medium without acetate at a fixed cell density. The suspension was mixed with medium containing 0.5 % of agarose and 1 mM acetate, and the resulting mixture was used to prepare a 100 μ l 'gel patch' on a glass slide, the dimensions of which were 2 cm \times 0.5 cm \times 1 mm (Fig. 5).

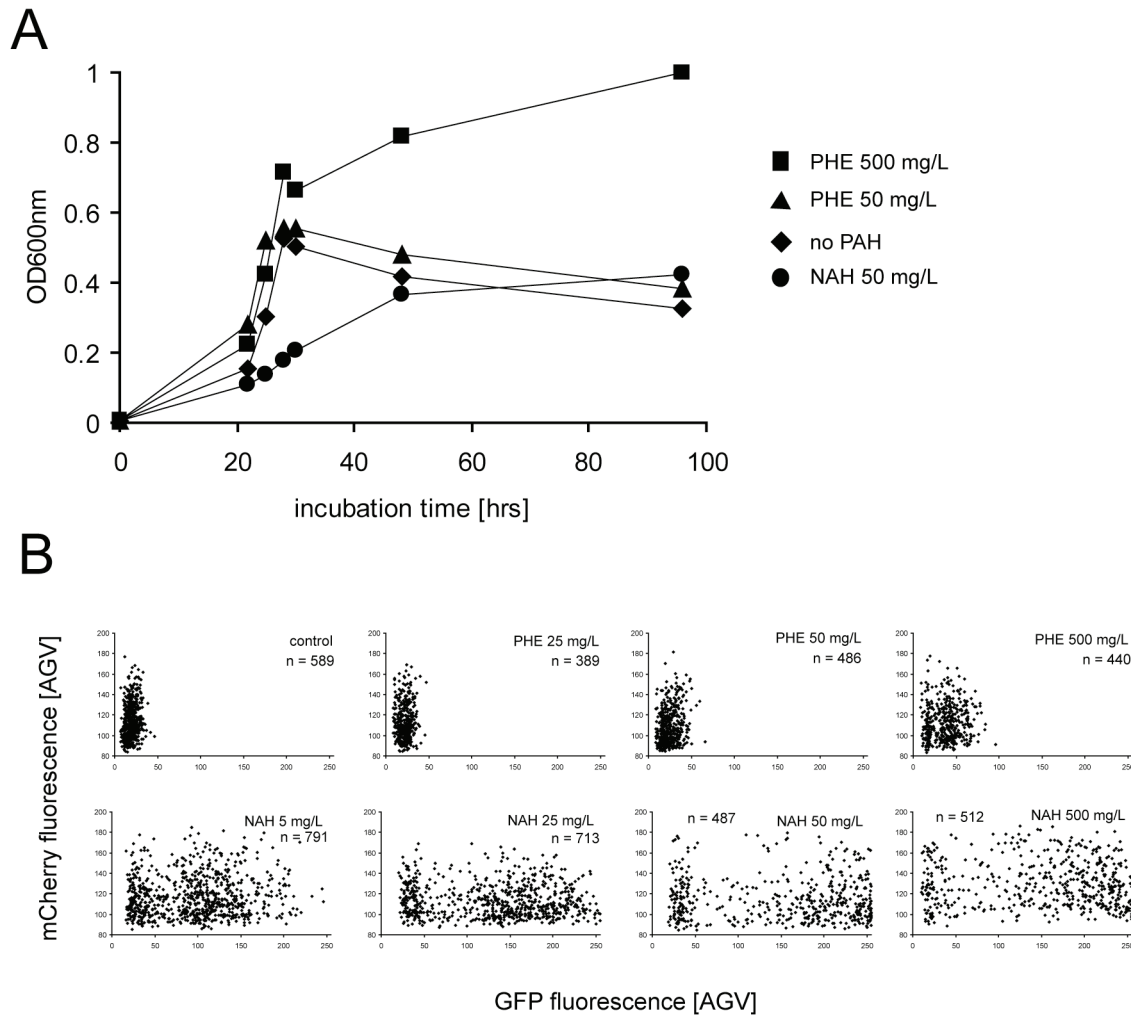


Fig. 3. Dual reporter expression in growing cultures of *B. sartisoli* RP037-mChe with or without PAHs. (A) Culture turbidity as a function of time (OD600nm) in 20 ml of minimal medium supplemented with 10 mM of acetate, with or without different quantities of NAH or PHE predissolved in one ml of heptamethylnonane. Circles, 1 mg NAH (corresponding to 50 mg per L medium); triangles, 1 mg of PHE (50 mg per L); squares, 10 mg of PHE (500 mg per L); diamonds, no PAH. (B) Scatter plots of eGFP and mCherry fluorescence of individual RP037-mChe cells sampled after 22 h incubation time and expressed as average gray value produced by the camera system (AGV). PAH concentrations are indicated in mg per L of medium, although they were predissolved in HMN. Scatter plots show combined data from two images for each sample and culture.

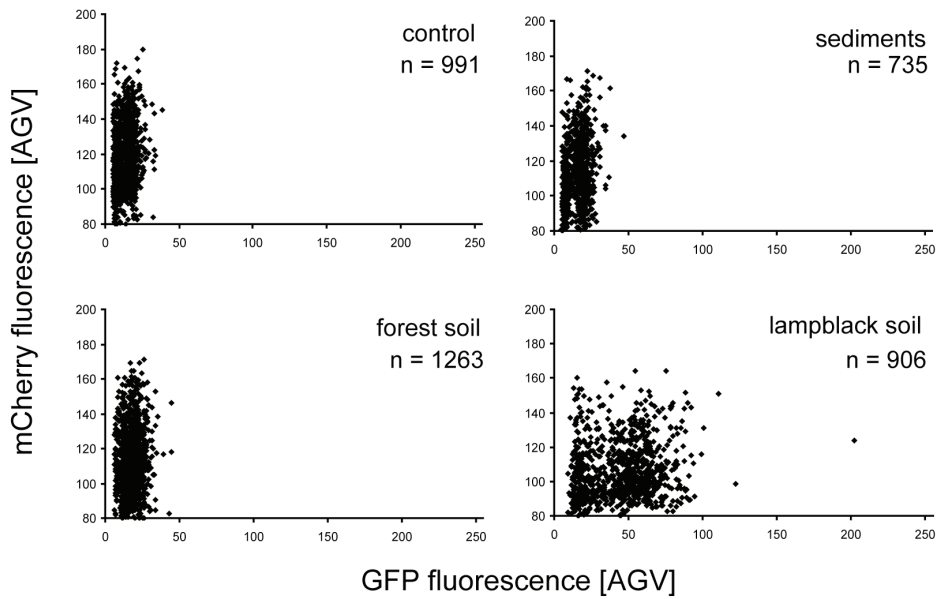


Fig. 4. Scatter plots of eGFP and mCherry fluorescence intensities in individual *B. sartisoli* RP037-mChe cells, measured 22 h after incubation in liquid minimal medium plus 10 mM sodium acetate and with or without PAH contaminated material (mixed in heptamethylnonane). ‘Forest soil’, 10 mg (dry weight) of uncontaminated forest soil, ‘lampblack soil’, 10 mg (dry weight) of PAH-contaminated material; ‘sediments’, 20 mg (dry weight) of PAH-contaminated sediment ‘Etang-de-Berre-1’. Control cells were exposed to heptamethylnonane only. Fluorescence intensities expressed as average gray value produced by the camera system (AGV). Scatter plots show combined data from two different images.

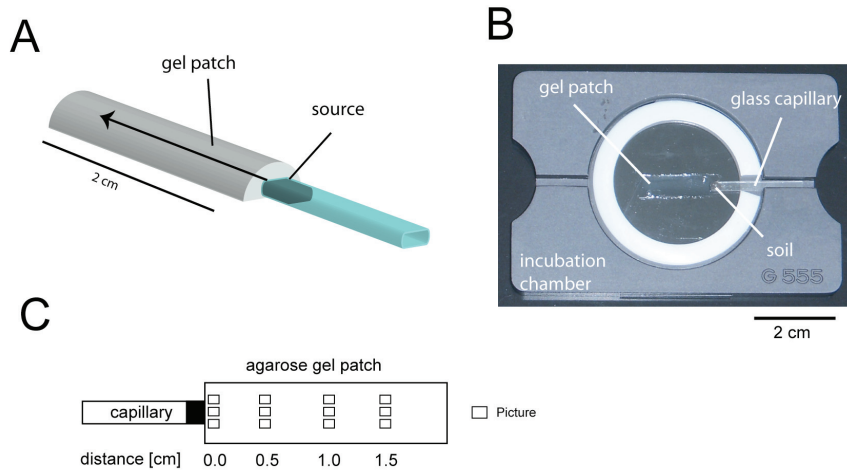


Fig. 5. Experimental set-up deployed for the detection of PAH diffusion. (A) *B. sartisoli* RP037-mChe cells were embedded in an agarose gel patch, the extremity of which was in contact with a glass capillary containing a PAH source. (B) The gel patch was mounted on a glass slide and inserted in an incubation chamber. (C) Schematic view of the positions along the gel patch at which pictures were recorded with epifluorescence microscopy.

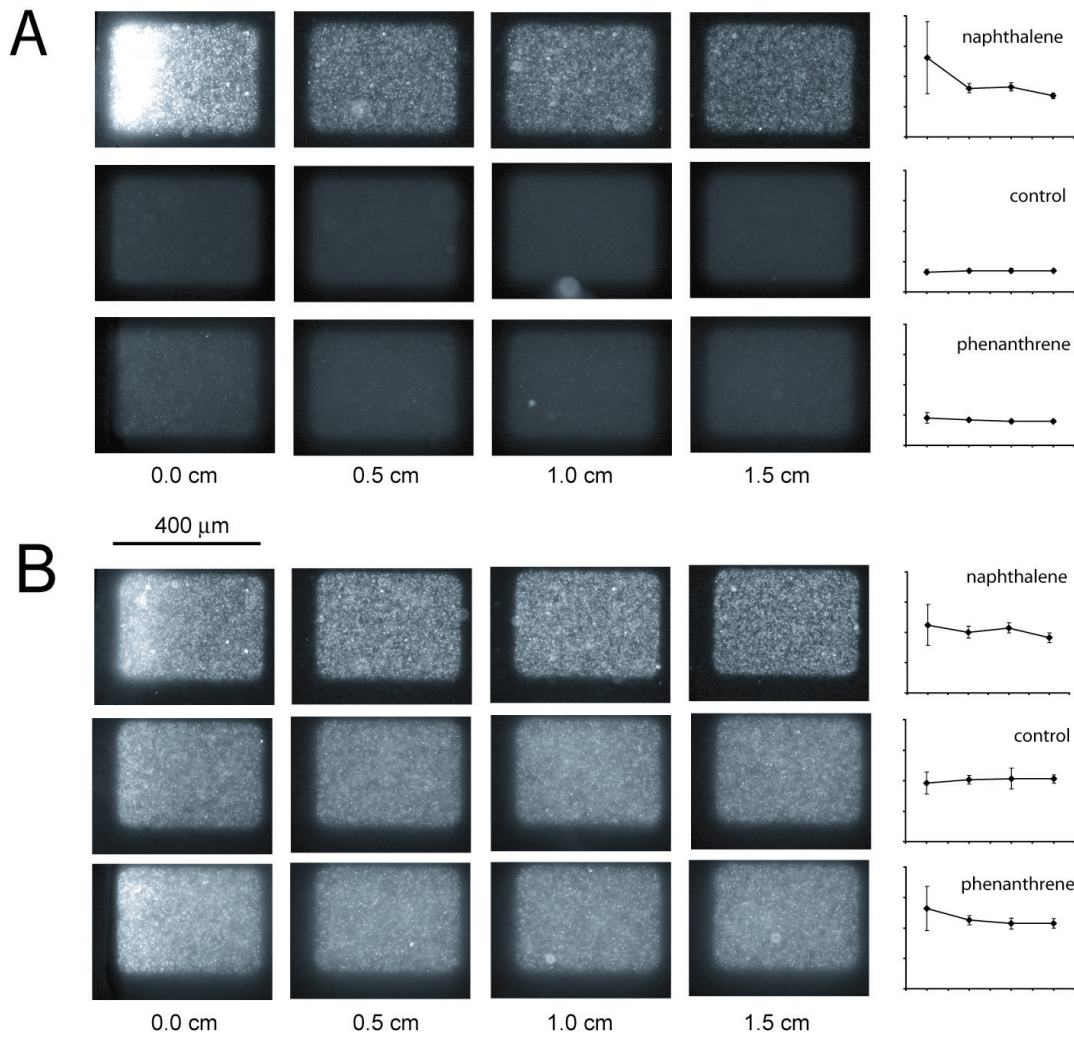


Fig. 6. Image examples of reporter gene induction in *B. sartisoli* RP037-mChe as a function of distance to the source. (A) eGFP fluorescence intensity of cells in the gel patch imaged at 100 \times magnification at four distances (0, 0.5, 1.0 and 1.5 cm) from the source, for 10 μ g of NAH dissolved in 4 μ l heptamethylnonane (HMN, upper row), HMN only (middle) and 10 μ g of PHE dissolved in 4 μ l HMN (lower row). (B) As for (A), but imaged for mCherry fluorescence. Graphs on the side of the images summarize quantified fluorescence intensity (ordinate; scale: 0-200 units) as a function of distance (abcis); error bars indicate standard deviations from the average fluorescence intensity over three images.

The number of cells in the patch equalled approximately 5×10^6 . The glass slide was placed in an incubation chamber and a glass capillary containing the PAH source was introduced in contact with the gel patch (Fig. 5B). Epifluorescence microscopic observations showed that the bioreporter cells embedded in the agarose were immobile but continued to be metabolically active, and several cell doublings could be observed in the gel patch after one day of incubation. The reporter signal could be recorded on single cells at $630\times$ magnification, but we discovered that lower magnification ($100\times$) was easier for detecting the overall 'glow' from the cells as a function of time and distance from the source.

Calibration with $2.5 \mu\text{g}$ NAH per μl of HMN ($10 \mu\text{g}$ NAH in total) after 24 hours of incubation produced a clear distance dependent eGFP induction profile compared to an assay with HMN only (Fig. 6A). Cells closer to the source area produced higher eGFP fluorescence than further away, which suggested they had responded as a function of the amount of NAH diffused through the gel patch until that time. The same amount and concentration of PHE in HMN still induced the reporter cells but to a lower extent than NAH. Images taken close to the source ($0.1\text{-}0.2 \text{ mm}$) showed extremely high fluorescence. In contrast to eGFP, the intensity of mCherry fluorescence was approximately equal over distance of the gel patches and comparable across all treatments (Fig. 6B). This fluorescence, therefore, solely reflected the amount of cells at any particular location in the gel patch but not the local concentration of PAH. mCherry fluorescence intensity was slightly higher in the vicinity of the PAH source, probably reflecting an increase in cell numbers at this position as a consequence of growth on the PAH. For quantitative analysis, three pictures were taken at each position in the gel patch (Fig. 5C). The pictures taken at position 0.0 cm , i.e. very close to the glass capillary, showed higher variation of the fluorescence intensity than the rest (Fig. 6, right outmost panels). In general, the central picture at every location showed higher fluorescence intensity for both eGFP and mCherry, probably because it was slightly closer to the source than the side areas of the gel patch, and, through the curvature of the gel patch towards the sides, may have contained slightly more cells per image volume. NAH induced a detectable eGFP signal in the gel patch as early as four hours after the beginning of incubation, and the signal increased until at least 24 hours of incubation (Fig. 7A). The accumulative eGFP fluorescence integrated over the whole gel patch (see material and methods) increased linearly with time (Fig. 7B).

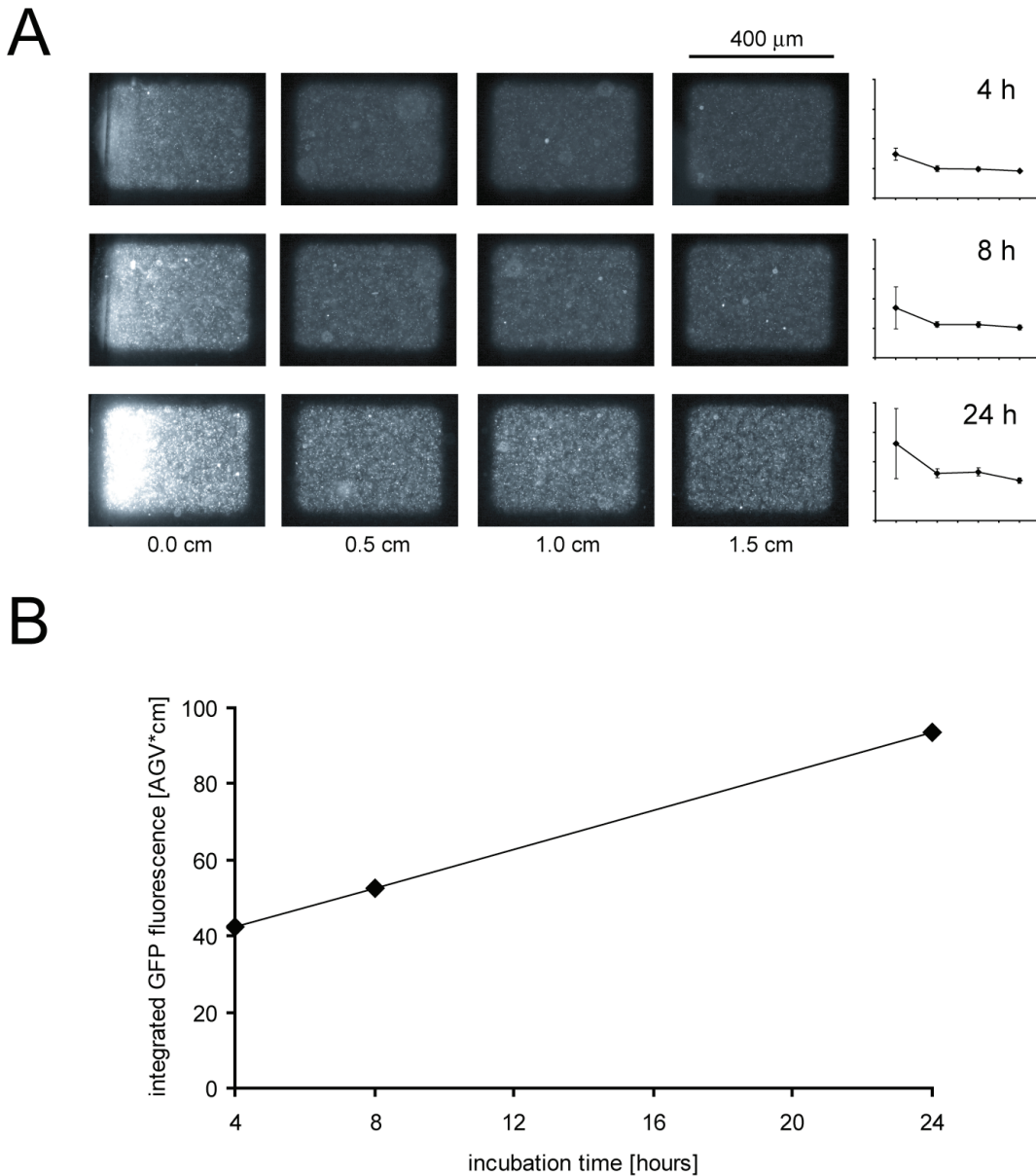


Fig. 7. Integrated eGFP expression as a function of exposure to diffusing NAH by *B. sartisoli* RP037-mChe. (A) Gel patch images at 100 \times magnification across distance from the NAH source (0., 0.5, 1.0 and 1.5 cm), after 4 h incubation time (top row), 8 h (middle row), and 24 h (bottom row). Source is 10 μ g NAH dissolved in 4 μ l of HMN. Panels on the right summarize quantified eGFP fluorescence intensity (ordinate, scale: 0-200 average gray values produced by the camera) as a function of distances (abcis); error bars indicate standard deviations from the average over three images taken along a transect perpendicular to the length of the patch (see, Fig. 5). (B) Integrated GFP fluorescence intensity across the complete gel patch (AGV \times cm) as a function of incubation time. Data points indicate calculated values after 4, 8 and 24 hours of incubation.

Three independent diffusion experiments with each 10 μg of either NAH or PHE showed the same trends for the calculated integrated GFP signals as a function of time, albeit not producing the very same values (Fig. 8A and B). 10 μg of PHE produced an integrated GFP fluorescence signal approximately ten times lower than the same quantity of NAH in the source area (Fig. 8B). Reducing the amount of NAH to 2 μg instead of 10 μg resulted in an approximately five times lower integrated GFP fluorescence after 24 hours (Fig. 8C). For both 2 and 10 μg NAH as sources, the eGFP integrated production did not increase for incubation periods longer than 24 h, suggesting that all NAH was depleted.

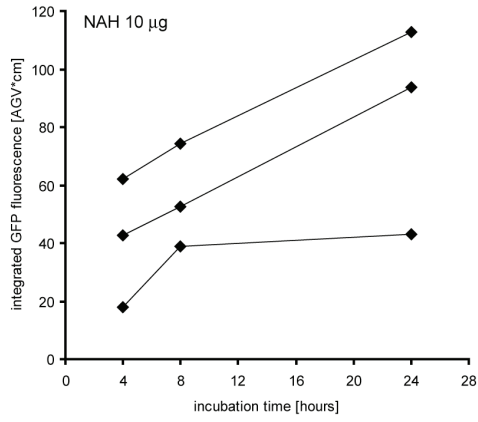
A NAH-source was also able to induce the reporter cells in the agarose patch via the gas phase (Fig. 8C). When a 2 mm gap was introduced between the extremity of the glass capillary and the gel patch, the cells responded but with homogenous fluorescence intensity along the gel patch as would be expected when gas rather than aqueous phase diffusion controlled NAH transport (Fig. 8D). To account for local variations in cell distribution along depth and length of the gel patch, we normalized eGFP fluorescence intensity by that of mCherry. The eGFP/mCherry ratio showed even more clearly than eGFP intensities alone that both 2 and 10 μg NAH produced a gradient of induced cells along the patch compared to the no-PAH control, and that induction via the gas phase resulted in a homogenous fluorescence ratio along the gel patch. eGFP induction in cells after 24 h by 2 μg NAH was mostly limited to the area next to the glass capillary, and rapidly decreased to uninduced levels afterwards.

One mg of PAH contaminated lampblack soil inserted into the capillary was able to induce the production of eGFP to intensities comparable to what was obtained with 10 μg NAH, but with a much less steep gradient. Integrated eGFP intensity showed a strong increase in time between 4 and 24 h (Fig. 8E), suggesting that the PAH-flux from lampblack soil was even more than 10 μg NAH equivalents per 24 h. Lampblack eGFP induction also took place when the material was not in direct contact with the gel, suggesting that volatile PAHs such as naphthalenes evaporated from the material. eGFP/mCherry ratios from lampblack soil incubations were the same along the gel patch in either direct contact or evaporation mode, suggesting that perhaps volatile naphthalenes even evaporated from the gel patch after diffusion into them. Model calculations of NAH diffusion states along the gel patch at three different time points suggested that at 24 h, NAH had diffused as far as the end of the gel patch (Fig. 8F).

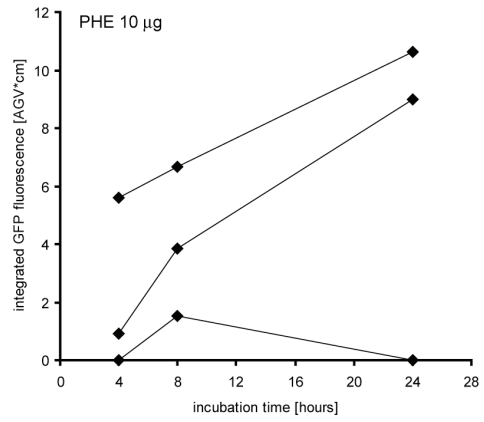
RP037-mChe incubated with PAH-spiked soils

In order to observe possible PAH induction at even smaller diffusion distances than in the gel patches, we mixed and immobilized RP037-mChe bioreporter cells with soil particles that were artificially PHE contaminated, and imaged induction over time as a function of accidental particle distance. Approximately 2.5×10^6 RP037-mChe cells were embedded in the resulting soil-gel, which had a diameter of ~ 1 cm on glass slide and was again mounted in an incubation chamber (Fig. 5). After incubation at room temperature for two days the bacterial bioreporter cells were still metabolically active in the gel, evident from the formation of microcolonies (data not shown). After 16 hours of incubation, a high eGFP fluorescence intensity was observed in cells exposed to lampblack soil, much less among cells exposed to 1 or 10 mg PHE per g soil, and basically none in the control soil without any PAH added (data not shown). The heterogeneity of eGFP expression among individual cells in the population was quite large. mCherry fluorescence was present in most cells irrespective of exposure to PAH-containing material, and was much less variable. Because of the mCherry production in reporter cells, they were easy to identify among soil particles, even if they did not express eGFP. After 42 hours of incubation cells exposed to control amounts of PHE were more clearly induced for eGFP, but lampblack soil caused even higher expression (Fig. 9). Single-cell measurements of both mCherry and eGFP fluorescence intensities again indicated a strong heterogeneity in eGFP expression, and less in terms of mCherry (Fig. 9A). mCherry expression was the same for PAH exposed and non-exposed cells (Fig. 9B). This indicated that PAHs had clearly induced eGFP in the reporter cells. Probably, as a result of heterogenous particle distribution, variability of eGFP expression among individual cells was important. Although this was difficult to quantify, we also observed that cells exposed to PHE spiked-soils had the tendency to form bigger microcolonies than cells incubated with lampblack particles or cells without PAH exposure. This may indicate that reporter cells were growing on PHE, whereas with lampblack they reacted to fortuitous non-metabolizable effectors.

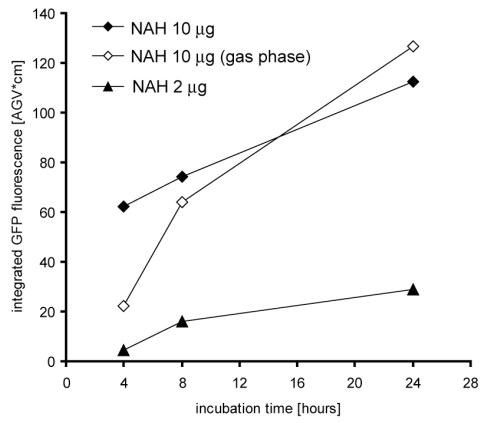
A



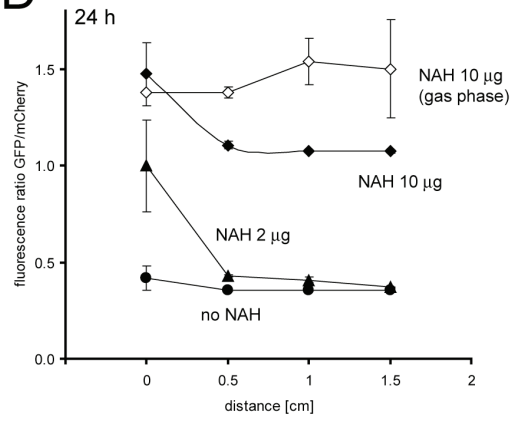
B



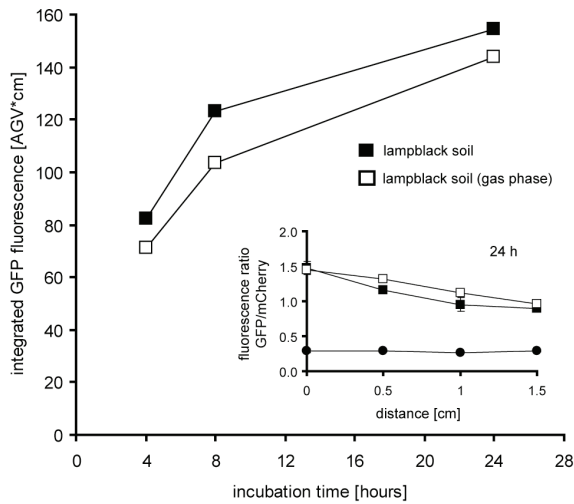
C



D



E



F

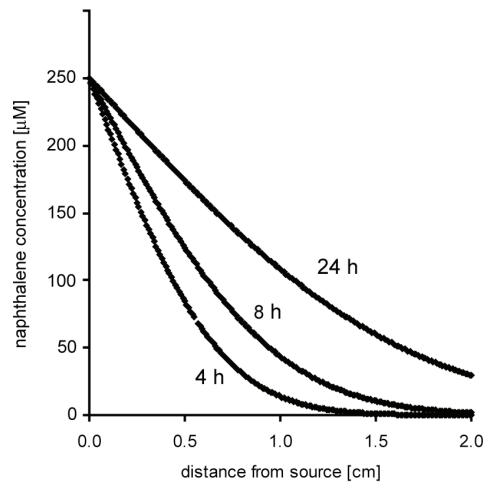
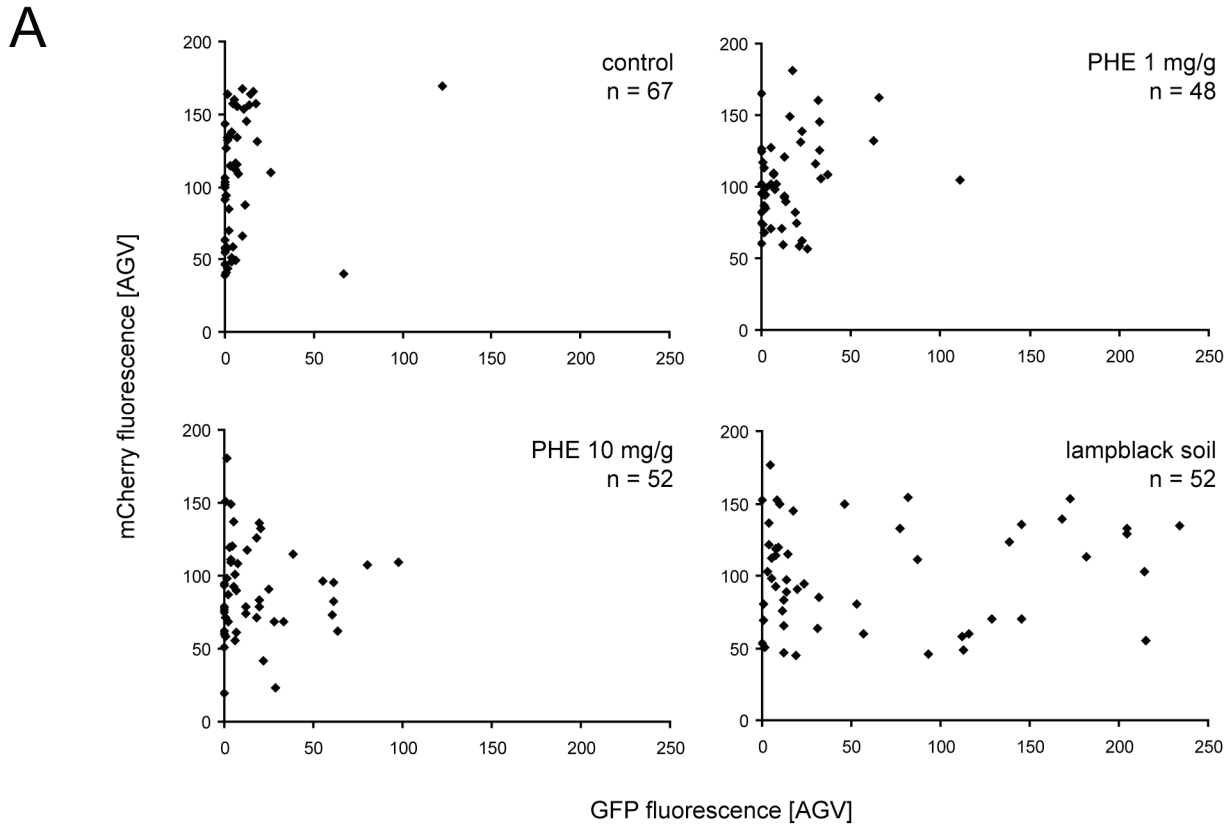


Fig. 8. Integrated eGFP expression by *B. sartisoli* RP037-mChe as a function of incubation time for different source materials. (A) Triplicate independent gel patch assays with 10 µg NAH dissolved in 4 µl HMN as source. (B) As above, but with 10 µg PHE in HMN. (C) Comparison of integrated eGFP expression in gel patches exposed to 2 or 10 µg NAH dissolved in HMN in direct contact, or with 10 µg NAH in HMN at a distance of 2 mm from the gel's extremity. (D) Fluorescence intensity ratios between eGFP and mCherry at different positions along the gel patch at time point 24 h for the experiments shown in C, compared to a non-exposed control. Error bars indicate the standard deviations from the average ratios calculated in three images taken along a perpendicular transect (see Fig. 5). (E) Integrated eGFP fluorescence intensity in gel patches exposed to 1 mg of lampblack soil in direct contact with the patch (black squares) or at a distance of 2 mm from its extremity (white squares). (F) Modelling of the NAH concentration as a function of distance along the gel patch at three different diffusion times, assuming an infinite point source of NAH and a diffusion coefficient similar as in water ($9.4 \times 10^{-6} \text{ cm}^2/\text{s}$)



B

soil type	GFP fluorescence [AGV]		mCherry fluorescence [AGV]
	average	75th percentile	average
control soil	7.9	7.4	103.4
PHE 1 mg/g	15.8	21.9	104.2
PHE 10 mg/g	16.6	20.2	86.6
lampblack soil	63.4	113.4	101.0

Fig. 9. Reporter gene expression in *B. sartisoli* RP037-mChe in gels mixed with or without contaminated soil after 42 h of incubation time. (A) Scatter plots of eGFP versus mCherry fluorescence intensities in individual cells or small cell clusters of *B. sartisoli* RP037-mChe, expressed as average gray value given by the camera (AGV). Top left, reporter cells embedded in 50 μ l minimal medium agarose gel with 2-3 mg forest soil ('control'); top right, forest soil spiked 1 mg PHE per g; lower left, forest soil spiked with 10 mg PHE per g; lower right, PAH-contaminated lampblack soil. *n*, number of cells or cell clusters used for quantification collected from imaging five to ten areas in the gel at 1000 \times magnification. (B) Summary of the average and 75th percentile of eGFP and mCherry fluorescence intensities over the populations of cells shown in (A).

DISCUSSION

Our aim in this work was to deploy new bioreporter assays, which would enable to detect bioavailable and bioaccessible fractions of PAHs from contaminated material. The term *bioavailability* in this sense is defined as the fraction of a chemical that is free to enter a cell at a given moment, whereas *bioaccessibility* represents the fraction of pollutant that could become bioavailable over time [33]. Typically, due to the very low aqueous phase concentration of PAHs and a short (2-3 hours) assay period for bioreporter measurements, the bioavailable fraction is not sufficient to cause significant induction of the promoter driving reporter gene expression. Sole exception to this are naphthalene(s), which are sufficiently soluble (~30 mg per L) to induce detectable reporter protein formation in the cells. This difficulty was again illustrated by some of our experiments, in which we incubated reporter cells with different amounts of NAH or PHE via HMN (Fig. 3), and which showed that the same total quantity of NAH after 24 h induces more than ten times as much eGFP fluorescence as PHE. With poorly soluble PAHs, we thus face the paradox that the reporter cells correctly detect very little immediately available (within a 2-3 hours period) effector compound, but that much more of the material might be accessible in the long run. This bioaccessible fraction cannot be easily detected by biological means except with long term mineralization assays deploying radiolabeled substrates [147]. Possible solutions for this paradox may thus be found in (i) prolonging somehow the time period for the bioreporter assay (capturing more of the bioaccessible fraction), (ii) deploying assays, which can detect higher local bioavailability on a microscale, or (iii) pre-extracting a larger fraction using organic solvents or substances promoting PAH solubilization [35, 150].

As a matter of fact, most reporter assays are done in liquid batch cultures, where the cells are exposed either to PAH-containing material directly, or to some form of extract from the material. A constant shaking of the assays ensures that the dissolved PAH molecules are homogenized in the culture and that all cells have access to the same. This, however, leads to a loss of existing diffusion or dissolution gradients, where concentrations close to a PAH-containing surface might be much higher and potentially lead to better induction in reporter cells than the lower completely mixed concentration. In one type of assay, the gel patch, we thus avoided mixing and tested conditions where the molecules could only reach the bacteria by diffusion in the aqueous phase. To ensure that the reporter cells would detect such a gradient over a much longer period of time (2-3 days), they were immobilized in 0.5 % agarose. Our data showed that the cells remained active and alive under such conditions

without interfering with their functioning and reporter abilities. In order to allow ‘integration’ of the bioavailability response over a period of 2-3 days exposure, we used a stable eGFP as reporter gene. Since this protein will not be degraded in the reporter cells [151], even very small produced quantities within a short induction period (2-3 hours) will accumulate to more detectable amounts over a long exposure period. Indeed our results demonstrated that the accumulation of eGFP was time-dependent (Fig. 7, 8), which indicated that the reporter cells were integrating the PAH bioavailable fraction over the time course of the experiment. We noticed that some growth of reporter cells was occurring. This would in theory dilute the accumulated eGFP signal on a *per cell* basis, but since we measured an integrated eGFP fluorescence over an area covering hundreds of cells, we detect the total amount of eGFP present. More importantly, the results of the patch experiments indicated that one can ‘gain’ inducing power for more poorly water soluble PAHs (like PHE). For example, the eGFP accumulated signal in the patch was equivalent for 10 μg PHE and 1 μg NAH (Fig. 8), whereas in a mixed batch assay not even 10 mg PHE per 20 ml medium produced the same induction as 0.25 mg NAH (Fig. 3B). This suggests that diffusion-type assays and longer incubation periods can help to acquire a reporter signal from contaminated sources with low level of PAH or low PAH availability.

A third point of importance for bioavailability experiments, is that the PAH bioreporter used here can act as a ‘sink’ for NAH and PHE, since it is metabolizing both compounds in order to produce the inducer signal for the *PhnR-PphnS-egfp* reporter circuit. The eGFP fluorescence signal along the gel patch therefore must show the outcome of two effects: first, PAH diffusion from the source material, and, secondly, PAH degradation. A simple model was used to predict the NAH diffusion gradient along the patch at three different time points based on the molecular diffusion coefficient in the aqueous phase (Fig. 8F). Obviously, this model was not taking NAH degradation by the bacterial bioreporter cells into account, possibly therefore overestimating the magnitude of NAH diffusion. Surprisingly, however, the gradient of eGFP fluorescence along gel patches with 10 μg NAH as source was systematically higher than predicted from molecular diffusion at any time point (Fig. 8D and F). The reason for this might be that part of NAH entering the gel is evaporating into the gas phase and diffusing more rapidly to areas downstream in the patch. In this respect, the reporter gene distribution within the first 0.5 cm of the gel patch produced from 2 μg NAH as source were more in agreement with the prediction that both diffusion and degradation would govern the distribution of NAH along distance (Fig. 8C and D).

Because we noticed that it still was very difficult to measure reporter gene expression very close ($< 100 \mu\text{m}$) to the source in the patch set-up, we deployed a system in which soil particles were directly mixed with immobilized reporter cells. This, we hypothesized, would create very short transport distances and possibly higher eGFP induction in cells. The assay was definitively more difficult in terms of cellular imaging and high magnifications were required in order to see the induction of individual reporter cells among soil particles. We noticed that spiked soil-assays with 2 or 20 μg PHE material both produced a threefold induction compared to a non-spiked soil, which was comparable to the induction seen with 1 mg PHE in 1 ml HMN (50 mg PHE per L medium) in batch (Fig. 3B). This may indicate that the 2 and 20 μg PHE had the same surface ratio, as shown previously [58]. Two mg Lampblack soil induced sixteen-fold, which was much more than the five- to sixfold induction seen in batch with 10 mg per 20 ml (Fig. 4). Unfortunately, it was not possible to recognize PAH-sources at the microscale, making it impossible to measure proper diffusion distances to induced cells.

The new fluorescent protein variant mCherry proved to be both stable and well tolerated in *B. sartisoli* strain RP037-mChe. The bacterial cells sustained the presence of both eGFP and mCherry fluorescent proteins even at all expression levels found here. Double-tagging using both green and red fluorescent proteins has been reported before in bacteria with the pair GFP and DsRed [152, 153], but DsRed in many cases was not properly maintained by the bacteria. In eukaryotic cells the pair GFP and mCherry has been co-expressed [154], but to our knowledge, not yet in bacterial cells. Although the *mCherry* gene was inserted as mono-copy in the chromosome, it was well-expressed from *Ptac* in *B. sartisoli*. Even so, there was considerable variation of mCherry fluorescence in individual RP037-mChe cells (standard deviation was equivalent to $\sim 60\%$ of the mean at exponential phase and $\sim 40\%$ at stationary phase). In addition, mCherry expression varied slightly between exponentially growing and stationary phase cells. The main risk of double-tagging is the overlapping of fluorescence excitation and emission spectra, which limits accurate intensity measurements. However, we found that with a relatively far red emission spectrum ($\lambda = 610 \text{ nm}$), there was no crosstalk of high mCherry expression within the eGFP detection wavelength range. The mCherry marker thus aided well to localize cells in mixtures with soil particles. Unfortunately, it was rather the eGFP fluorescence which became too difficult to quantify in the presence of PAH-contaminated soils and sediments at high dosage. Contrary to our expectations (and apart from lampblack material), the Etang-de-Berre sediments and other PAH-contaminated soils produced very high autofluorescence in the patch diffusion and mixed gel assays (not shown),

the exact source of which is unknown but might implicate some PAHs. This autofluorescence interfered with eGFP but not mCherry. As a consequence and in conclusion, we demonstrated the possibility to use diffusion assays to analyze bioaccessible PAHs from contaminated materials, but for more optimal measurement of PAH diffusing from such materials it will be necessary in the future to exchange the labels in the reporter strain to have PAH-inducible mCherry and constitutive eGFP for cell recognition.

ACKNOWLEDGMENTS

The authors greatly thank Maria Péchy and Christoph Keel for the gift of the mini-Tn7Ptac-mCherry construct, and Itzel Ramos and Dianne Newman for their kind gift of the *mcherry* gene. This work was supported by grant 018391 (FACEiT) from the European Community FP6 Framework Program.

MATERIAL AND METHODS

Chemicals and soil samples

Phenanthrene (97% purity) and naphthalene (99% purity) were purchased from Fluka (Buchs, Switzerland). Lampblack soil was taken from a PAH contaminated oil-gas manufacturing site and kindly provided by Upal Ghosh. Its composition is described in Hong *et al.*, in which it is referred to as soil CA-18 [104]. Sample 'Etang-de-Berre 1' is a marine petroleum-oil contaminated sediment with a total PAH load of 80 µg per g dry weight (Robert Duran, pers. communication). The forest soil is known as soil 11661, a reference number given by the Swiss Federal Institute of Technology Lausanne (EPFL). It was sampled in Yvonnand (Switzerland), at a depth of 0 to 10 cm. To 1 g of soil 11661, we added 1 ml or 0.1 ml of dichloromethane in which 10 mg PHE per ml had been dissolved, in order to obtain contaminations of 1 or 10 µg PHE per mg soil. The soil was stirred with a metal bar and kept under the hood for 4 hours until all dichloromethane had evaporated. One g of soil into which 1 ml of pure dichloromethane was mixed and treated in the same manner as above, was used as non-PAH exposed control soil.

Strains and growth conditions

B. sartisoli sp. strain RP037 is a GFP-based biosensor described in a previous work [58]. The strain RP037-mChe is a derivative of RP037, which contains a mini-Tn7 insertion containing the *mCherry* gene (see below). RP037-mChe was routinely grown at 30°C in modified Tryptone Yeast medium (mTY, contains 3 g/l of yeast extract, 5 g/l of Bacto tryptone plus 50 mM NaCl). The strain was grown with the presence of 50 µg/ml of kanamycin to maintain the reporter plasmid pJAMA37. Minimal medium (MM) plus 50 mM sodium chloride was used for defined growth conditions (type 21C mineral medium, [105]). If not specified differently, 10 mM sodium acetate was added as a carbon source.

Construction of RP037-mChe

The plasmid miniTn7Ptac-mChe contains the mini-Tn7 transposon boundaries around a gentamycin resistance cassette and encodes the mCherry fluorescent protein under the control of the constitutive promoter P_{tac} . We used heat shock to transform the strain *E. coli* S17λpir with the plasmid miniTn7Ptac-mChe [155]. We performed a mating with *E. coli* S17λpir (miniTn7PtacmChe) as conjugable donor strain, *E. coli* (pUX-BF13) as helper strain for transposition and *B. sartisoli* RP037 as recipient strain. The transconjugants were selected on mTY agar plates using gentamycin (for selecting the insertion of the mini-Tn7 transposon), kanamycin (selection of pJAMA37) and rifampycin (selection of *B. sartisoli* RP037). Several transconjugants were isolated and examined for the presence of constitutive red fluorescence. The presence of both reporter plasmid pJAMA37 and *phn* genes for PHE metabolism was verified by PCR. One isolate was selected and named *B. sartisoli* RP037-mChe.

Induction assays in liquid batch cultures

B. sartisoli strain RP037-mChe was pre-cultivated overnight in mTY medium, then centrifuged at $1,000 \times g$ for 10 min. Subsequently the supernatant was discarded and the cells were resuspended in an appropriate volume of MM to obtain a culture turbidity of 0.4 at 600 nm. A 50 ml-flask containing 20 ml of MM with 10 mM acetate and 50 µg/ml of kanamycin was inoculated with 2% (400 µl) of resuspended preculture. The flasks were supplemented with 1 ml of 2,2',4,4',6,8,8'-heptamethylnonane (Sigma-Aldrich Chemie, Steinheim, Germany) containing various amounts of dissolved NAH or PHE, or soils. These were either 10 mg forest soil, 10 mg lampblack soil or 20 mg (dry weight) Etang-de-Berre-1. Incubation was performed at 30°C with shaking at 180 rpm. Cultures were sampled at different times and

bacteria were immobilized on a cover slip [58] for further epifluorescence microscopy analysis of the bacterial biosensors.

Gradient induction assays in agarose gel patches

Pre-cultivation and inoculation of fresh MM were deployed as described for the batch flask assays, except that no heptamethylnonane was added. After overnight growth, cells were centrifuged at $2,500 \times g$ for 10 min, prior to be resuspended in MM without acetate in order to obtain a culture turbidity of ~ 0.4 . Fifty μl of this suspension was mixed with an aliquot of 500 μl of MM containing 1 mM acetate into which 0.5 % of standard agarose was dissolved by heating (Eurobio, France), and which was stored at 50°C prior to use. One hundred μl of the gel-bacteria suspension was pipeted immediately with the help of a mask on a round glass cover slip of 25 mm diameter and 0.17 mm thickness (H. Saur, Reutlingen, Germany) to form a gel patch with dimensions of $0.5 \times 2.0 \text{ cm} \times 0.1 \text{ mm}$. The coverslip was mounted on an incubation chamber (POC chamber, H. Saur, Germany). A glass capillary of $0.2 \times 2 \text{ mm}$ (Vitrocom, New Jersey, USA) was filled at one extremity with 4 μl of HMN containing or not various concentrations of either NAH or PHE. The extremity containing HMN was directed towards one extremity of the gel patch (Fig. 5), in order to obtain a direct contact surface between the gel and the HMN. In case of contaminated material, $\sim 1 \text{ mg}$ soil was inserted into the capillary and brought into contact with the agar patch. In several cases we tested induction of the cells in the gel without having contacted the capillary with the patch. Two Teflon rings of 0.5 mm thickness and a second coverslip were placed successively on top of the system. Finally the system was closed with a metal ring and incubated in a closed box containing moisturized paper to prevent water evaporation from the patch. At defined time intervals, the fluorescence intensity in the gel patch was monitored using epifluorescence microscopy, either at $100 \times$ or at $630 \times$ magnification without opening the system.

Direct induction assays in gels

Bacterial reporter cells were prepared as above and directly mixed with 50°C MM plus 0.5% dissolved agarose, but without acetate. Two to three mg of either forest soil, forest soil spiked with 1 or 10 μg PHE per mg soil, or lampblack soil were placed in the centre of a 4.2 cm \varnothing round glass coverslip (H.Saur). Fifty μl of the cell-agarose suspension were mixed with the soil particles on the cover slip to form a circular patch of about 1 cm diameter. The coverslip with the patch was mounted in an incubation chamber similarly as above. Reporter

cells were imaged at 1000 × magnification at random positions in the gel on the basis of their mCherry fluorescence light, after which the corresponding eGFP fluorescence was recorded.

Epifluorescence microscopy and image analysis

GFP and mCherry fluorescence intensities in individual biosensor cells in batch cultures were imaged using a Leica DRI4000 fluorescence microscope (Leica Microsystems, Switzerland) equipped with a 63× objective (PL Fluotar L 63x/0.70 CORR, Leica). Images were recorded with a Leica DFC 350FX monochrome camera (Leica Microsystems, Switzerland) with an exposure time of 450 ms using a GFP filter cube (excitation filter: BP 470/40; dichromatic mirror 500; emission filter: BP525/50) and a Y3 filter cube (excitation filter: BP 545/30; dichromatic mirror 565; emission filter: BP610/75) for the detection of mCherry. Fluorescence Intensity Manager (FIM) was set to 55 % and 100 % for mCherry and eGFP imaging, respectively. Images were recorded sequentially, first for the mCherry signal, after that for the eGFP signal, and analysed in pair with the help of the software Metamorph (Visitron Systems, Germany). Briefly, we used a subroutine that defined a mask based on the mCherry signal image, allowing us to define all cells expressing mCherry. Then, we applied this mask to both mCherry and eGFP images in order to measure red and green fluorescence intensities within the same objects (cells or clusters of cells).

The eGFP and mCherry fluorescence intensities in agarose gel patches were measured using a Leica DRI4000 fluorescence microscope and a 10× objective (N PLAN 10x/0.25, Leica). Images were recorded as described above with an exposure time of 600 ms. Using the software Metamorph, we defined 250 identical circular regions that were distributed over each image area without overlapping. We measured the intensity of eGFP and mCherry fluorescence in each region and calculated from this an average fluorescence intensity per image. Three images were taken at every position in the patch (0, 0.5, 1.0, and 1.5 cm).

For the analysis of embedded cells that were directly mixed with soil particles, we used a Leica DRI4000 fluorescence microscope and a 100× objective (HCX PL Fluotar 100x/1.30, Leica). FIM was set to 17% for both mCherry and GFP, and an exposure time of 450 ms was used. We used the software Metamorph to define individual objects in the mCherry image that corresponded to cells (or clusters of cells), and measured the corresponding intensity of mCherry and eGFP fluorescence in these objects. Local background fluorescence in mCherry- or eGFP light due to autofluorescence from soil particles was defined from circular regions of a constant size in the vicinity of each cellular object, and subtracted from both mCherry and eGFP fluorescence intensities of every cell or cluster of cells.

Calculations and modelling

Integrated eGFP fluorescence along a gel patch containing RP037-mChe was calculated with the following formula:

$$\Delta GFP_{posx} = avgGFP_{posx}^{induced} - avgGFP_{posx}^{control}$$

$$int GFP_1 = ((\Delta GFP_{pos0.0} + \Delta GFP_{pos0.5}) / 2) \times 0.5cm$$

$$int GFP_2 = ((\Delta GFP_{pos0.5} + \Delta GFP_{pos1.0}) / 2) \times 0.5cm$$

$$int GFP_3 = ((\Delta GFP_{pos1.0} + \Delta GFP_{pos1.5}) / 2) \times 0.5cm$$

$$int GFP = \sum int GFP_i$$

with avg = average fluorescence, expressed in average gray value (AGV); int = integrated fluorescence, expressed in AGV×cm.

NAH diffusion modeling along the gel patch was predicted using the solution of Fick's second law of diffusion [40]:

$$C(x, t) = C_0 \times erfc\left(\frac{x}{2(Dt)^{1/2}}\right)$$

with erfc(y) = the complement error function and D = molecular diffusivity of NAH (we used here 9.4×10^{-6} cm²/s) in water, and assuming a constant NAH concentration at the position $x = 0$.

CHAPTER 6

DEVELOPMENT OF A MULTIWELL BACTERIAL BIOSENSOR PLATFORM FOR THE MONITORING OF HYDROCARBON CONTAMINANTS IN AQUEOUS ENVIRONMENTS

Robin Tecon, Siham Beggah, Vladimir Sentchilo, Myrsini Chronopoulou, Terry McGenity

Petroleum hydrocarbons are common contaminants in marine and freshwater aquatic habitats because of intensive ship trafficking. In the case of severe oil spills, substantial (bio)-remediation operations are needed. It is therefore of high interest to develop rapid and reliable analysis tools for the detection and monitoring of the bioavailable hydrocarbon fractions, i.e., those which are most likely to cause toxic effects or are available for biodegradation. Here we examined the suitability of a set of different *luxAB*-based bacterial biosensors on a multiwell platform to measure simultaneously the presence of short-chain linear alkanes, monoaromatic and polyaromatic compounds, biphenyls, or DNA damaging agents in seawater after an induced oil spill at laboratory scale. Hereto 20 ml of crude oil was spilled in 2 L of seawater in an open 5 L glass flask. Five independent spills with two types of seawater (e.g., North Sea, Mediterranean Sea) were carried out. Biosensor cells detected short-chain alkanes and BTEX (i.e., benzene, toluene, ethylbenzene and xylenes) in the seawater within minutes to hours after the spill, increasing to a maximum of up to 100 μM within 6 to 24 h, after which they decreased to low or even undetectable levels. Two and three-ring PAHs appeared in the seawater phase after 24 h up to 1 μM equivalent naphthalene concentration and did not decrease below 0.5 μM afterward. The strong decrease in short-chain alkanes and BTEX may have been due to their volatilization or biodegradation. DNA damage-sensitive biosensors did not produce any signal with the oil-spilled aqueous phase samples, and (hydroxy-)biphenyl biosensors responded occasionally. Interestingly, our results indicated a sequential appearance of the major contaminants, with BTEX and alkanes being predominant at the very beginning of the spill, and then gradually replaced by PAHs. This may reflect the fate of these contaminants in real environments.

INTRODUCTION

In November 2007, at least ten ships sank in the Black Sea as a result of storms, releasing thousands of tons of oil and sulphur. In particular, the oil tanker Volganef-139 ran aground and released half of its 4'800-ton load of heavy fuel oil into the sea [156]. Such pollution disasters occur with a frightening regularity and often lead to unpredictable outcomes on the polluted ecosystems. Besides these dramatic and highly media-related events, it has to be realized that the marine environment is constantly exposed to smaller spill accidents and deliberate releases, which represent the major part of the total petroleum hydrocarbon entering the marine environment [157]. It has been estimated that several millions of tons of petroleum hydrocarbons contaminate marine environments annually, which makes crude oil one of the most important organic pollutant at sea [158].

Effective disaster management, for instance, after an accidental oil spill from a supertanker, necessitates an accurate and rapid estimation of the magnitude of the pollution, of its effects on the ecosystems, and of bioremediation possibilities. At present time, there is an increasing interest in the development of biomonitoring tools that can measure the bioavailability of hydrocarbon contaminants, thereby bringing the biological level into the global risk and disaster management analysis. Besides the evident impact that crude oil exerts on sea fauna and flora (for instance, causing death of birds covered with oil), the pollutant fraction that is dissolved in the water (i.e., bioavailable) may importantly impact the fate of the exposed ecosystem, both in terms of toxicity towards the indigenous organisms and biodegradation potential. A variety of organisms have been employed as biomarkers to investigate oil pollution, ranging from micro-organisms [159-161] to aquatic invertebrates [162, 163] and fish embryos [164]. Traditionally, these methods can be separated between those, which examine indigenous incidentally exposed organisms, and those methods, which use a number of preselected test organisms that are exposed to contaminated samples during a defined period of time and under standardized conditions. Ideally, an integrated biological study of a contaminated ecosystem should rely on a multi-approach strategy, combining information from different biological levels.

Whole cell bacterial biosensors have been presented as a useful tool for the multi-target analysis of environmental contaminants (Chapter 1). Not only can bacterial biosensors be engineered for the detection of a wide variety of chemicals, but they can also be implemented

Bacterial strains and plasmids	chemicals detected	selection ^a	reference
<i>E. coli</i> DH5 α			
pGEc74, pJAMA7	alkanes (C ₆ -C ₁₀)	Ap100 + Tc10	[76]
pPROBE-LuxAB-TbuT	BTEX compounds	Km50	This study
pHYBP109	2-hydroxybiphenyl	Ap100	[11]
pHYBP103M3	2-hydroxybiphenyl, biphenyl	Ap100	[69]
<i>E. coli</i> MG1655			
pJAMA8-cda	DNA-damaging agents	Ap100	This study
<i>B. sartisoli</i> RP007			
pPROBE-phn-luxAB	PAHs (naphthalene, phenanthrene)	Km50	This study

^a Antibiotics used for plasmid selection. Ap: ampicillin. Tc: tetracyclin. Km: kanamycin. Number indicates the required antibiotics concentration in $\mu\text{g/ml}$.

Table 1. Bacterial strains and plasmids that were used in the multiwell bacterial biosensor platform.

in a single analytical device that facilitates the screening for multiple simultaneous contaminants in environmental samples. Bacterial biosensor assays are relatively rapid (hours) and can be performed with simple equipment, which make them a useful analytical tool in a multi-approach investigation of risk assessment and environmental pollution. Here we developed and tested a multiwell bacterial biosensor platform that can be customised with a variety of strains, each of which dedicated to the measurement of a specific pollutant's aqueous concentration. Since crude oil is a very complicated mixture of hundreds to thousands organic compounds [165], it is necessary to focus the analysis on target chemicals that represent major components of crude oil. We selected short-chain alkanes (saturated hydrocarbons), BTEX compounds (i.e., benzene, toluene, ethylbenzene and xylenes) and low-molecular weight Poly Aromatic Hydrocarbons (PAHs) as target components from petroleum oil for our bacterial biosensor platform. In addition to that, we added to the platform a well-defined bacterial biosensor detecting the fungicide 2-hydroxy-biphenyl (2-HBP), and a general toxicity biosensor that responds to any condition leading to DNA damage. Due to the hydrophobic properties of hydrocarbons, and in particular their tendency to sorb to plastics, glass was considered as an optimal material and the platform was based on a microtiter plate composed of individual glass vials. In order to validate our system, we mimicked an oil spill

at sea by contaminating natural sea water with a known amount of crude oil in an open glass bottle, and measured the concentrations of contaminants in the sea water over time using the biosensor platform.

RESULTS

Analysis of oil-spilled sea water with a multiwell bacterial biosensor platform

In order to mimic an oil spill at sea, we poured 20 ml of crude oil on top of 2 L uncontaminated sea water in an open 5 L glass flask (Fig. 1A). After different incubation periods during one week, we sampled the water via a tap located at the bottom of the glass bottle so as to avoid the direct oil phase. The bottle was gently shaken on a rotary platform, while oil remained as an organic layer on top of the sea water. This prevented the formation of an emulsion and guaranteed that our aqueous phase measurements would only consider the truly dissolved oil fraction. The bottle was open and allowed the loss of the volatile compounds from the organic phase, similarly to what would happen at open sea during an oil spill. Our analysis considered both the early stage of the oil contamination, i.e. from minutes to hours after the spill, as well as up to one week. The original set-up of the multiwell bacterial biosensor platform included four different *Escherichia coli* strains (Table 1): DH5 α (pGEc74, pJAMA7) and DH5 α (pPROBE-LuxAB-TbuT) were directed against the common oil components alkanes and BTEX, respectively; MG1655 (pJAMA8-cda) was responding to genotoxic agents, hence acting as a general toxicity sensor; DH5 α (pHYBP109) is a previously reported biosensor whose chemical target was 2-hydroxy-biphenyl, but which might have reacted to hydroxylated compounds in crude oil. In some cases strain DH5 α (pHYBP109) was replaced by strain DH5 α (pHYBP103M3). This strain produces a mutant of the sensor protein HbpR, and shows both hypersensitivity towards 2-HBP and increased sensitivity for biphenyl(s) [69]. The experiment was repeated three times sequentially and with sea water of different origin (e.g., North Sea and Mediterranean). The water samples were either analysed immediately with the bacterial biosensors (Table 2 shows an exemplary layout for the multistrain platform), or in some cases stored at 4°C in a 4-ml glass vial filled to the top with sample. Standard calibrations with pure compounds were included in each platform assay for each bacterial biosensor strain, and used to calculate linear regression (for toluene and 2-HBP calibration) or binomial regression curves (for octane and nalidixic acid).

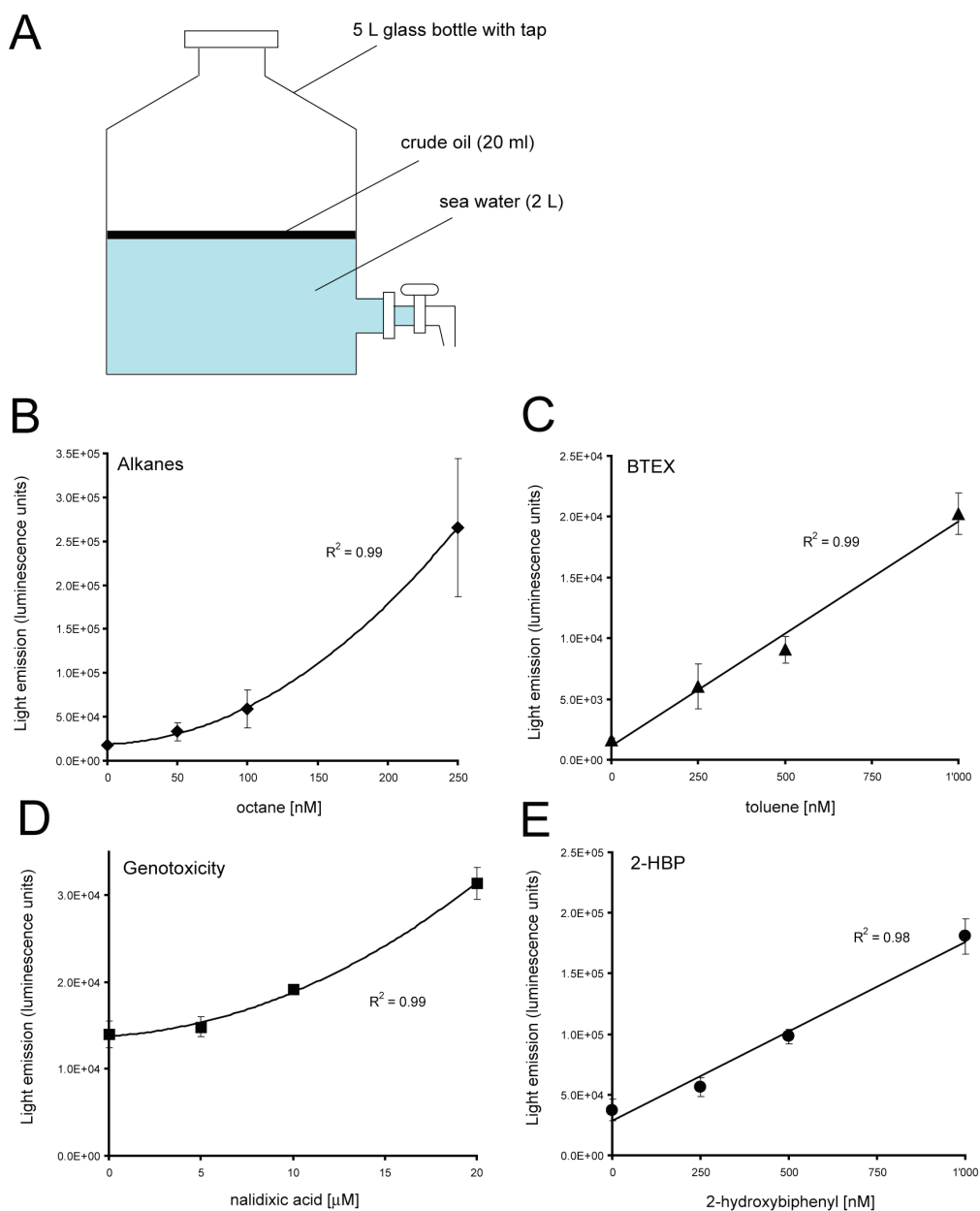


Fig. 1. Experimental set-up and calibration. (A) Two liters of sea water were contaminated with 1% (v/v) of crude oil in a glass flask equipped with a tap. At different time intervals after the addition of oil, water was sampled via the tap and subsequently submitted to multi-target biosensor analysis. Selected bacterial biosensors detected alkanes, BTEX compounds, PAHs, genotoxicity or 2-hydroxybiphenyl (2-HBP) and biphenyls. Panels B, C, D and E show exemplary calibration curves from one biosensor measurement series. Error bars indicate standard deviations from triplicate well measurements. Binomial (B and D) or linear (C and E) regression was used to fit the calibration curve with the data. The regression coefficient (R^2) is indicated.

Although for every platform assay a new calibration curve was produced, they were sufficiently similar across different day-to-day measurements to produce a typical calibration curve such as in Figure 1. The curve equation was then used to transform light emission values measured in the contaminated samples into an equivalent concentration of standard 'target'. For instance, the response of the alkane bacterial biosensor was expressed in 'equivalent octane concentration', although the sample was probably composed of a mixture of many different alkanes. In general, the signal output of the alkane and 2-HBP biosensors DH5 α (pGEc74, pJAMA7) and DH5 α (pHYBP109), respectively, was approximately one order of magnitude higher than that of the BTEX and genotox sensors DH5 α (pPROBE-LuxAB-TbuT) and MG1655 (pJAMA8-cda). This difference in the absolute level of luciferase activity may have been a consequence of the particular inducibility of each reporter construct and of their functioning in *E. coli*, but did not influence the biosensor's sensitivity (i.e., the slope of the induction curve). In addition to a triplicate analysis of every sample, they were all re-analyzed after spiking, i.e. after addition of a known concentration of pure target inducer to the sample. This was done in order to verify if the bacterial biosensor was still able to report faithfully and was not inhibited by the presence of toxic compounds. If necessary, values were corrected for the spiking difference.

The octane and toluene equivalent concentrations reported by the bacterial biosensors in the aqueous phase over time for four replicate oil spill experiments are summarized in Figure 2. The experiment was repeated twice with Mediterranean sea water from two different sites and twice with North sea water. Measurements with the alkane biosensor pointed to a maximum equivalent octane concentrations in the aqueous phase (black squares) two to six hours after the oil spill (Fig. 2A). The maximum occurred in all experiments, and amounted to between 200 and 600 nM equivalent octane. The calculated equivalent octane concentrations were in general in good agreement between spiked and non-spiked samples, suggesting that in these samples the bacterial biosensors were not critically inhibited by other chemicals present in the sample. On the other hand, not for all samples a spiking correction was possible, and therefore, the calculated equivalent octane concentration may be an underestimation. This occurred when light emissions in the spiked and non-spiked samples were very close or even the same. As spiking correction can only be carried out when spiked samples produce an increase in light emission compared to their non-spiked partner, the equivalent octane concentration could not be properly calculated for such samples. In such samples, the equivalent octane concentration was calculated based on the non-spiked sample.

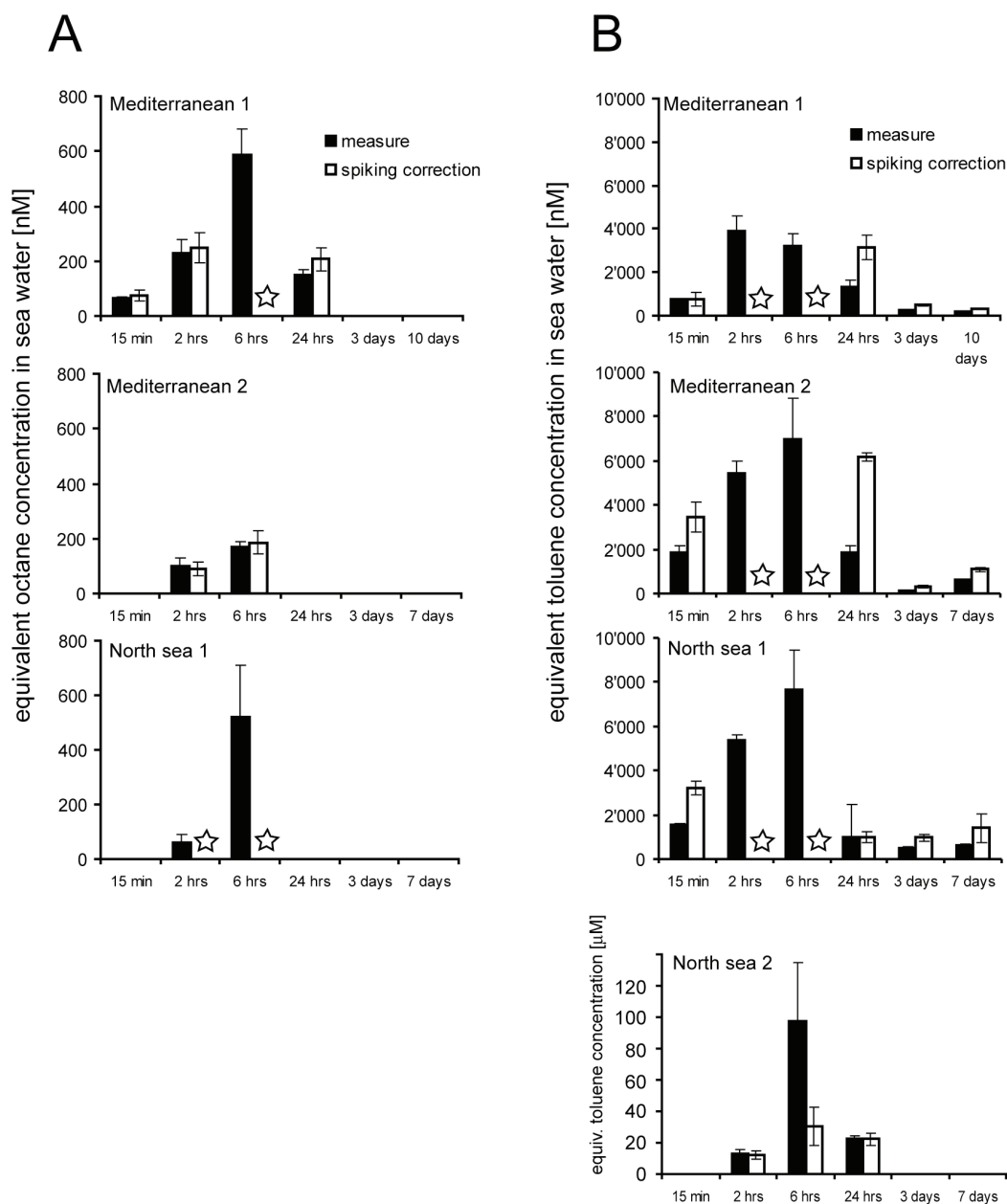


Fig. 2. Evolution of equivalent octane and equivalent toluene concentrations in sea water over time after the artificial oil spill, as measured by two of the biosensors. (A) Measurements of equivalent octane concentration (representative for short-chain alkanes) with the sensor strain DH5 α (pGEc74, pJAMA7) in three independent spills with seawater from the Mediterranean sea (sites 1 and 2) or from the North sea. (B) Measurements of equivalent toluene concentration (representative for BTEX) by strain DH5 α (pPROBE-LuxAB-TbuT). The results from experiment North sea 2 were obtained with samples diluted three times (2 h and 24 h) and ten times (6 h) in non contaminated sea water prior addition in the assay. Black squares indicate the equivalent target concentrations calculated for the non-spiked sample; white squares are those corrected on the basis of measurements in the spiked sample. Error bars point to calculated standard deviations from triplicate assays. The star indicates that no spiked-sample calculation was possible, because the spiked value was equal to the non-spiked value.

Different to alkanes, BTEX could be detected by the biosensor at any time during the spill in replicate experiments Mediterranean 1, 2 and North sea 1 (Fig. 2B). Interestingly, for BTEX also a maximum toluene equivalent concentration was measured two to six hours after the spill. In contrast, the toluene equivalent concentration was much higher than the octane equivalent concentration (between at least 4 and 8 μM for BTEX, compared to 0.2 and 0.6 for alkanes). In fact, the light emission from samples at that time point was outside the toluene calibration range. Hence, the BTEX concentration in those samples was not measured accurately, in particular early after the spill (Fig. 2B), because of the saturation of the bacterial biosensor by the presence of high amounts of BTEX. We conducted a new experiment (North sea 2) with that biosensor, in which several additional dilutions (up to ten times) of the sea water samples were examined (Fig. 2B). Interestingly, measurements now revealed equivalent toluene concentrations of up to 100 μM after 6 h. BTEX concentrations in the samples clearly decreased one day after the spill, but remained detectable for at least seven days (Mediterranean 2 and North sea 1) and ten days (Mediterranean 1). In experiment North sea 2, however, we did not detect any compound eliciting a reaction equivalent to toluene later than 24 h. Light emission from spiked versus non-spiked samples suggested a partial inhibition of the functioning of the BTEX biosensor in some of the contaminated samples.

In none of the spills and for none of the samples, any significant induction of the genotoxicity biosensor MG1655 (pJAMA8-cda) compared to the non-exposed seawater control was detected (data not shown). Spiking of the samples with a known amount of nalidixic acid showed that the genotoxicity biosensors reacted as expected even in contaminated samples, indicating that there was no inhibition of the cells. The 2-HBP biosensor DH5 α (pHYBP109) was used only in the Mediterranean-1 experiment, and produced significant induction ($>$ the method detection limit) on two occasions: after 3 and after 10 days of spill (data not shown). Strangely, no signal was detected with samples taken 7 days after spill. What is more, the spiked samples were 20 to 40 % lower than predicted, suggesting that some inhibition of this biosensor occurred. For the other two oil spills the hypersensitive 2-HBP mutant strain DH5 α (pHYBP103M3) was used. This biosensor detected a small but significant signal in only one sample taken 6 hours after the Mediterranean-2 spill. Unlike DH5 α (pHYBP109), the mutant DH5 α (pHYBP103M3) showed no inhibition of its functioning at any time during the experiment.

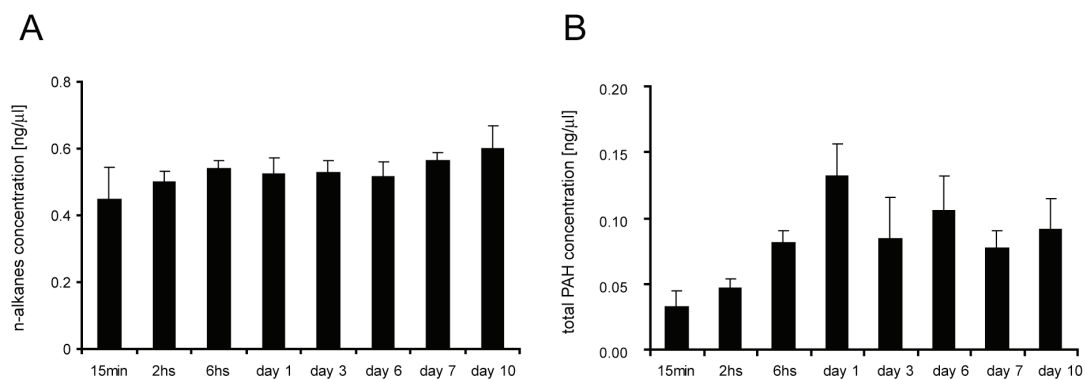


Fig. 3. GC-MS analysis of dissolved hydrocarbons in seawater over time after the oil spill for experiment Mediterranean 1. (A) Total *n*-alkanes (C₁₁-C₄₀). (B) Total PAHs. Error bars indicate standard errors from four replicate samples.

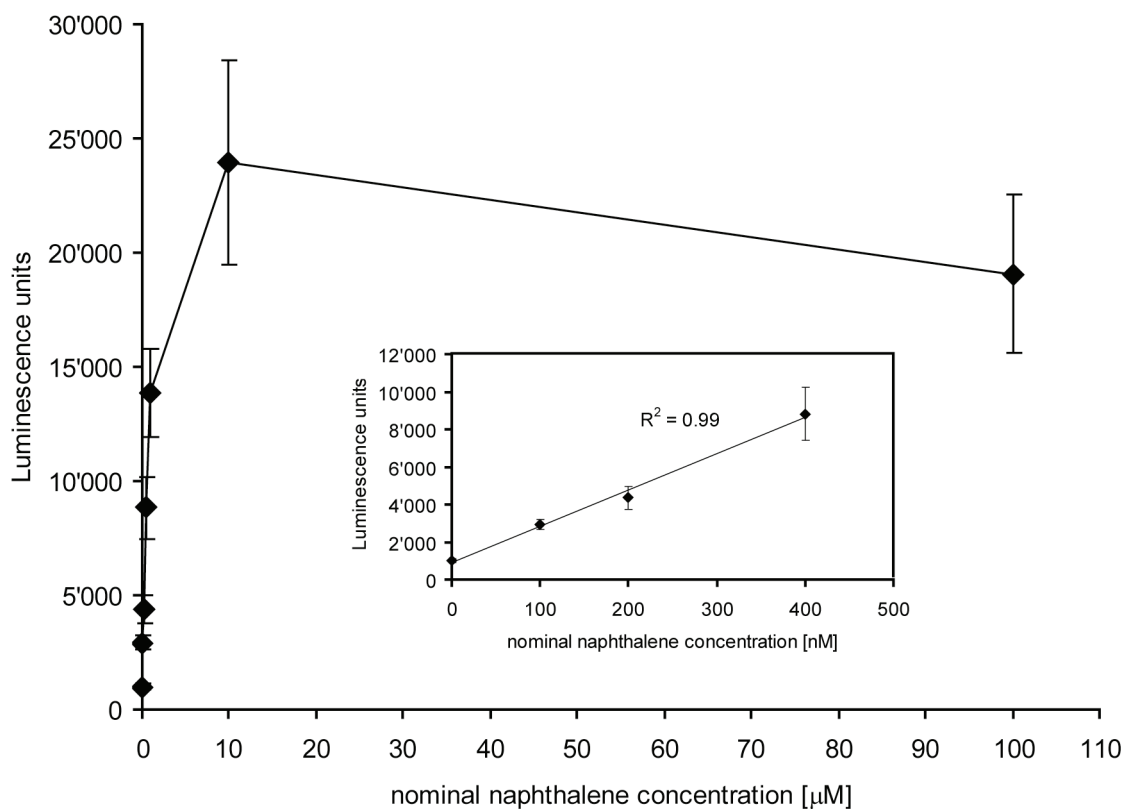


Fig. 4. Light emission as a function of naphthalene concentration in bioassays with *B. sartisoli* RP007 (pPROBE-phn-luxAB). Bioluminescence measurements were recorded after three hours of incubation time, addition of 0.09 mM *n*-decanal, further 5 minutes incubation and integration of light output during 0.1 sec (\pm SD, $n=5$).

Chemical analyses were performed in parallel on samples from the Mediterranean-1 spill and results for n-alkanes and PAHs are presented in Figure 3. Unfortunately, BTEX and hydroxylated compounds could not be measured in the same series. In contrast to the biosensor analysis, chemical methods showed an approximately constant concentration of total n-alkanes (C₁₁-C₄₀) at any time point after oil spill (Fig. 3A). Total PAHs increased and peaked at ~1 day after spill, after which a gradual decrease took place (Fig. 3B). The most abundant n-alkanes were undecane, tetradecane, pentadecane, hexadecane and octadecane. N-alkanes shorter than C₁₁ were not measured in this chemical analysis method. Pristane was also detected in high amounts in the water samples. Assuming a common molecular mass for all alkanes (for instance, the molecular mass of hexadecane), the total n-alkane concentration in the aqueous phase ranged from 2 to 3 μ M.

Implementation of the naphthalene-sensing *Burkholderia sartisoli* RP007 (pPROBE-phn-luxAB) in the multiwell bacterial biosensor platform

At that point, the bacterial biosensor platform was lacking an effective reporter strain for PAHs. We failed to obtain a naphthalene sensor using *E. coli* as a host strain and only had a *Pseudomonas putida* naphthalene sensor at our disposition, which required a totally different induction regime. Therefore, we examined the possibility to use *B. sartisoli* RP007 equipped with the plasmid pPROBE-phn-luxAB, which contains a transcriptional fusion between the operator/promoter region of the *phnSFECDAcAdB* operon from RP007 and the *luxAB* genes encoding the bacterial luciferase (see further [58]). We first determined whether *B. sartisoli* RP007 (pPROBE-phn-luxAB) could be used under the same assay conditions as was developed for *E. coli*. RP007 (pPROBE-phn-luxAB) cultures were hereto deep-frozen as for *E. coli*, thawed directly before assay and diluted in MOPS medium. Biosensor cell suspensions were exposed to increasing naphthalene concentrations in a glass microtiter plate, which resulted in proportionally increasing luciferase activity (data not shown). However, we observed that the addition of n-decanal (used as a substrate for the bacterial luciferase) at the concentration employed for *E. coli* (1.8 mM) strongly inhibited the light emission from *B. sartisoli* RP007. A twenty times dilution of the decanal concentration (0.09 mM) was necessary to prevent inhibition of the luciferase activity. The resulting light emission from *B. sartisoli* cells was low compared to most of the *E. coli* strains, which might be due to different stability of the luciferase in *Burkholderia*. For this reason we increased the incubation time to 3 hours (instead of 2 hours for the *E. coli* strains), which resulted in slightly higher light emission values.

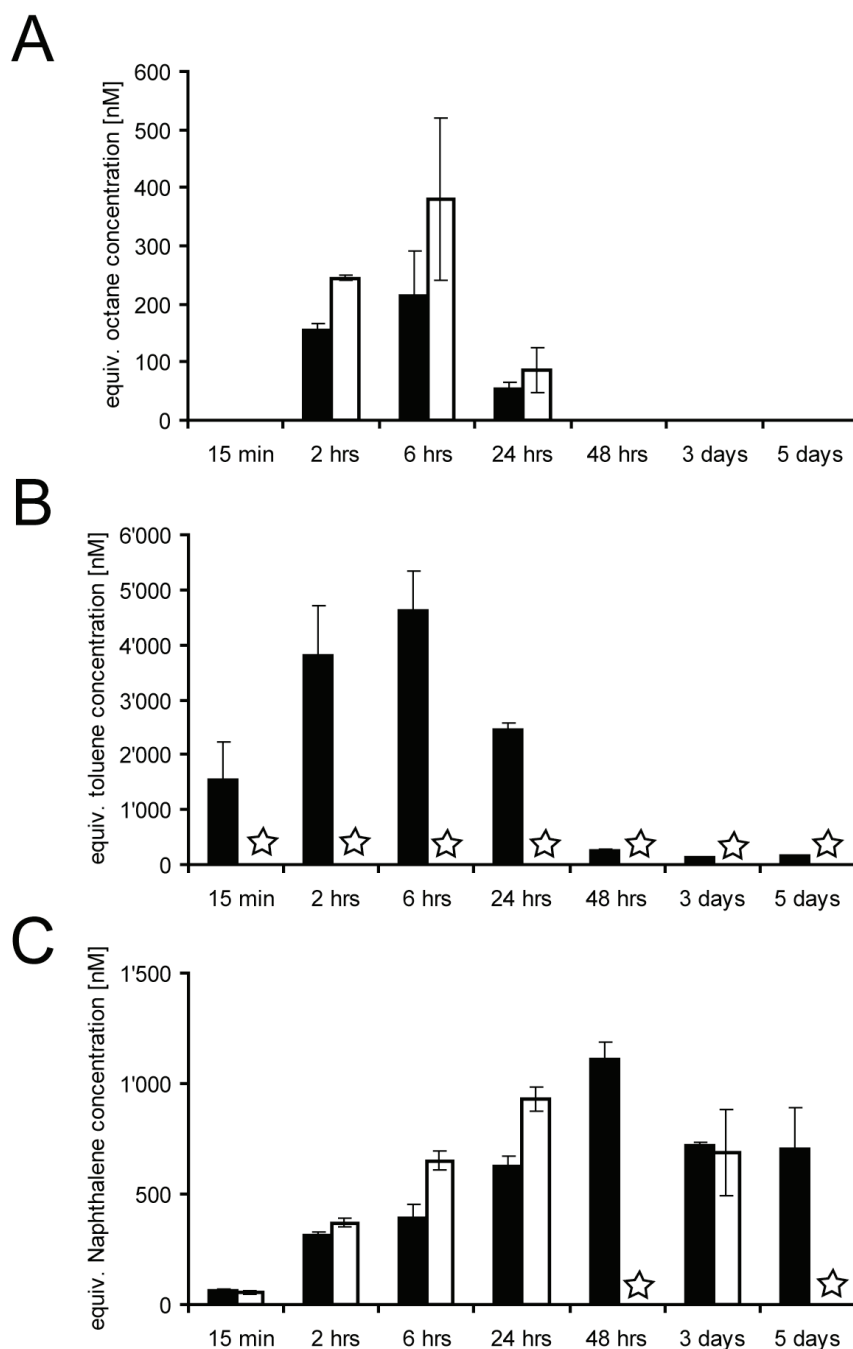


Fig. 5. Evolution of equivalent octane, toluene and naphthalene concentrations over time in seawater after an artificial oil spill to Mediterranean sea water in laboratory scale setting (Experiment *four*). (A) Measurements by sensor strain DH5 α (pGec74, pJAMA7) for alkanes. (B) Measurements with sensor DH5 α (pPROBE-LuxAB-TbuT) for BTEX. (C) Measurements with *B. sartisoli* RP007 (pPROBE-phn-luxAB) for low molecular mass PAHs. Black squares indicate the equivalent inducer concentrations calculated in the non-spiked samples; white squares are those calculated from spiked-samples. Error bars are standard deviations calculated from triplicate assays. The star indicates that no spiked-sample calculation was possible, because the spiked value was equal to the non-spiked value.

Using the adapted assay, we found that the light emission by *B. sartisoli* RP007 (pPROBE-phn-luxAB) was linearly proportional to increasing naphthalene concentrations between ≈ 25 nM and $10 \mu\text{M}$ (Fig. 4). Above that concentration, which is far below the maximal aqueous solubility of naphthalene ($\sim 250 \mu\text{M}$), luciferase activity did not further increase. Relative errors based on standard deviations ranged from 9 to 18 %. We concluded that the RP007 (pPROBE-phn-luxAB) biosensor could be used to measure naphthalene below 1 and up to $10 \mu\text{M}$ without further sample dilution, and that it could be implemented in the multiwell bacterial biosensor platform on condition that n-decanal concentration was reduced.

The naphthalene biosensor was then used on a repeated oil spill ('Mediterranean-3'), in conjunction with the octane [DH5 α (pGEc74, pJAMA7)] and BTEX biosensors [DH5 α (pPROBE-LuxAB-TbuT)]. As expected, the alkane and BTEX profiles were highly similar to what was observed in the previous three experiments (Fig. 2, 5), with maximum compound appearance in the water phase early after the spill and decreasing rapidly after 24 h of incubation. Interestingly, the PAHs (expressed as equivalent naphthalene concentration) had a different time dilution profile, with a maximum appearance 24 to 48 h after spill (Fig. 5C) and much slower disappearance of the compounds in the water phase. PAHs could still be detected at concentrations above $0.5 \mu\text{M}$ equivalent naphthalene after 5 days, at which time point alkanes were below the biosensor detection limits and BTEX decreased to around 200 nM equivalent toluene. Spiked samples for naphthalene produced lower light emission than predicted from the calibration curve, suggested that the *Burkholderia* sensor was partially inhibited by other compounds in the assay. Although the chemical PAHs analyses presented in Figure 3 were performed on water samples from a different experiment (Mediterranean 1), we can assume that they reflect a general dissolution profile of PAHs under those conditions.

The most abundant dissolved PAHs detected by GC-MS were the low molecular mass PAHs naphthalene, methyl-naphthalenes, di-methyl-naphthalenes and phenanthrene. The total PAH concentration estimated by chemistry was maximal in samples taken after one day of incubation with a concentration of $\sim 130 \mu\text{g/L}$. Approximately half of this ($60 \mu\text{g/L}$) was composed of naphthalene, which corresponds to ~ 500 nM. The equivalent naphthalene concentrations measured by the biosensors were thus in the same order of magnitude. *B. sartisoli* RP007 (pPROBE-phn-luxAB) is known to respond to naphthalene and phenanthrene, and to be weakly inducible by di-methyl-naphthalene (data not shown). In the oil spillage samples, the bacterial biosensor therefore likely responded to a mixture of PAHs rather than to naphthalene alone.

96 well	Strain 1			Strain 2			Strain 3			Strain 4		
	1	2	3	4	5	6	7	8	9	10	11	12
A	standard calibration			standard calibration			standard calibration			standard calibration		
B												
C												
D												
E	contaminated sample n°1											
F	contaminated sample n°1 with spiking											
G	contaminated sample n°2											
H	contaminated sample n°2 with spiking											

96 well	Strain 1 Alkanes			Strain 2 BTEX			Strain 3 Genotoxicity			Strain 4 PAHs		
	1	2	3	4	5	6	7	8	9	10	11	12
A	0	0	0	0	0	0	0	0	0	0	0	0
B	50 ^a	50	50	100	100	100	5	5	5	100	100	100
C	100	100	100	200	200	200	10	10	10	200	200	200
D	200	200	200	400	400	400	20	20	20	400	400	400
E	0	0	0	0	0	0	0	0	0	0	0	0
F	100 _a	100	100	200	200	200	10	10	10	200	200	200
G	0	0	0	0	0	0	0	0	0	0	0	0
H	100	100	100	200	200	200	10	10	10	200	200	200

^aExample of inducer concentrations added to each well and to the spiked sample in nM (or μ M for strain 3).

Table 2. Exemplary layout of the multiwell bacterial biosensor platform

DISCUSSION

The microbial world presents an enormous reservoir of transcriptional regulators that in their cognate cell are dedicated to the recognition of specific chemicals. Much of this reservoir has become accessible due to the exponential increase of gene and genome sequences in databases. This expanding knowledge can be effectively mined in order to engineer bacterial biosensors for the detection of a multitude of chemicals, while conserving a core mode of functioning and output signal. These characteristics allow multi-target analysis

with bacterial biosensors, for instance on a sensing array [10]. We tested here the utilization of a multiwell bacterial biosensor platform for the detection of several key hydrocarbons in sea water, in order (i) to verify the capacity of the biosensor platform to detect and measure the concentration of contaminants in sea water and (ii) to study the dynamics of the hydrocarbon dissolution and the fate of the dissolved chemicals after several days of incubation in a model oil spill experiment. We managed to analyse four different bacterial biosensor strains on a single 96-well plate at the same time. Although this seems a small number for a 96-well plate, most of the wells in praxis are needed for triplicate analysis, sample dilution and sample spiking, and simultaneous calibrations, which are absolute necessities for accurate biosensor measurements. The multiwell design, therefore, is a compromise between a parallel target sample analysis and measurement accuracy. Standard calibrations were integrated into every test plate for all biosensor strains. This was a requirement because reporter output values are a function of assay incubation time, biosensor cell density and incubation conditions, which are very difficult to standardize completely. Standard curves with satisfying fitting ($R^2 > 0.9$) could usually be obtained. However, the pipetting of small volumes of octane and toluene solutions was often a bit erratic, and measurement variation between replicates was much higher for volatile (e.g., octane and toluene) than for non-volatile compounds (e.g., 2-HBP). This difficulty could be partially overcome by improving the pipetting material, by using 96-well glass plates that prevented the adsorption of the hydrocarbons to plastic, and by sealing the plate with a foil to reduce the volatilization of compounds.

Three of the oil-targeted bacterial biosensors (i.e., octane, BTEX and naphthalene) detected significant concentrations of 'inducers' in seawater samples over time after a simulated crude oil spill, which is in agreement to what is predicted from known crude oil compositions [165]. The fourth, the 2-HBP and biphenyl directed biosensor(s), only responded to a few samples, whereas the genotoxicity biosensor did not react to anything dissolved or metabolized over time from oil into seawater. Interestingly, measured octane, toluene and naphthalene equivalent concentrations showed a clear trend over time after the crude oil spill, which was similar for alkanes and BTEX, but different to PAHs. For alkanes and BTEX a maximum concentration occurred after a couple of hours after which a gradual decrease took place (Fig. 2, 5). PAHs appeared more slowly and disappeared less drastically. The maximum concentration could represent the time needed to dissolve the maximal amount of the 'inducing compounds' from the crude oil into the seawater phase. If nothing were to happen, this concentration would not further decrease. However, the decrease of alkane and

BTEX concentrations after approximately one day is an indication for volatilization and perhaps metabolism by indigenous micro-organisms in the (non-sterile) seawater. The fact that the naphthalene equivalent concentration decreased much less drastically after its peak, compared to octane and toluene, is a good indication for the correctness of the volatilization hypothesis. Low molecular mass PAHs (the targets for the *Burkholderia* sensor) are much less volatile than short-chain alkanes and BTEX, and would thus remain in the aqueous phase for much longer periods. Volatilization in the experimental system is clearly limited compared to an outside situation, due to the geometry of the flask, which means that the concentration decrease observed in the experimental spills is slower than what might be seen in a completely open situation. We can also conclude that, apparently, the provenance of the sea water had no or little impact on the dissolution profile over time, suggesting that if biodegradation occurred, it might be similar for both types of seawater. Chemical analyses for alkanes was at first sight not in agreement with the biosensor data, however, it should be noted that this chemical analysis only assessed n-alkanes from C₁₁ to C₄₀, whereas the biosensor DH5 α (pGEc74, pJAMA7) responds to C₆ to C₁₀ linear alkanes, and to the branched alkane 3-methylheptane [76]. It is thus possible that short-chain alkanes have a different dissolution profile than long-chain alkanes. In particular, they are more susceptible to loss by volatilization or biodegradation than alkanes with longer chain lengths, meaning that their concentration would decrease faster over time. No chemical data could be produced on the concentration of mono-aromatics in the seawater over time after the spill. However, these light and volatile compounds are known to rapidly disappear from oil spills [166]. Hence, the three biosensors functioned in our system as a potential time indicator for the age of the spill: if alkanes and BTEX are still readily detectable, a spill would be less old than a day. If both are low but PAHs still high, the spill would be older than one to two days. It would be valuable to have had a bacterial strain at our disposal that could detect long-chain alkanes, but as results in Chapter 7 will show the very poor aqueous solubility of long-chain alkanes strongly limits their detection by bacterial biosensors (which traditionally only take up compounds dissolved in the aqueous phase).

When it comes to the toxicity biosensor MG1655 (pJAMA8-cda), we concluded that the contaminated sea water samples did not contain anything sufficient to trigger DNA damage or SOS response in the biosensor, which is somehow surprising given that the other biosensor strains detected all kinds of organic compounds in the contaminated samples. Since we targeted an unspecific process – DNA damage caused by oil or oil derivative compounds –, increased incubation times might be necessary to obtain more consistent results. This,

however, is not really suitable for the multistrain bacterial biosensor platform, which needed a common incubation time for all strains. Other bacterial biosensors for the detection of general toxicity might be envisaged to replace MG1655 (pJAMA8-cda), such as oxidative stress or lipid damage.

B. sartisoli RP007 (pPROBE-phn-luxAB) appeared to be a useful replacement biosensor for naphthalenes. In contrast to the previously described *P. putida* sensor with inducible reporter gene expression from the *nahG* promoter [3, 59], which required continuous culturing for optimal induction in the bioassay, *Burkholderia* could be frozen and used from batch grown precultures directly in the assays. In addition, the *Burkholderia* biosensor has a wider effector range than *P. putida*, comprising phenanthrene and dimethyl naphthalenes, thanks to the indigenous transcriptional activator PhnR and active PAH metabolism. The use of luciferase as reporter instead of *gfp* as used earlier [58] permitted a more easily quantifiable response to naphthalene in a 96-well glass plate (Fig. 4). Only minor adaptations of the assay were required for the effective integration of this new sensor into the multistrain platform. Intriguingly, *B. sartisoli* luciferase activity was inhibited by n-decanal concentrations regularly used for *E. coli* luciferase biosensors. Perhaps as a consequence, the level of light emission by RP007 (pPROBE-phn-luxAB) was relatively low, but the sensitivity and accuracy were satisfying. The reason for this sensitivity to n-decanal is currently not clear.

To date, as many as twenty different luminescent bacterial biosensors have been combined in cell arrays, both on plate and chip [167-169], showing impressive and promising miniaturization efforts. However, these biosensor arrays were limited to the detection of general toxicity, such as oxidative stress and genotoxicity, and did not consider appropriate replicate analysis, internal calibration and multi-sample analysis. We integrated on a single biosensor platform different bacterial strains that detected a battery of specific contaminants, which to our knowledge has not been achieved beforehand. Obviously, our 96-well plate system is still a macroplatform, albeit very handy and suitable for most automated plate readers. The design may be substantially improved in terms of miniaturization and number of strains for further applications [10]. Its relative simplicity, however, makes it a rapid and easy-to-use biomonitoring tool that can help in the diagnostics of contaminated aquatic ecosystems.

ACKNOWLEDGMENTS

This work was carried out under the frame of the project FACEiT, financed by the sixth framework programme of the European Community (project n°018391).

MATERIAL AND METHODS

Chemicals

Octane (99% purity), naphthalene crystals (99% purity) and toluene (99% purity), 2-hydroxy-biphenyl (99% purity) were purchased from Fluka (Buchs, Switzerland). Crude oil NSO1 was obtained from the Norwegian Petroleum Directorate.

Strains and culture conditions

E. coli strains were routinely grown on Luria Bertani (LB) medium at 37°C in the presence of appropriate antibiotics. *B. sartisoli* RP007 was routinely grown at 30°C on Tryptone Yeast (TY, contains 3 g/l of yeast extract and 5 g/l of Bacto tryptone) agar plates or liquid medium amended with 50 mM NaCl and 50 µg/ml of kanamycin. For biosensor assays, *E. coli* and *B. sartisoli* strains were resuspended in MOPS medium (MOPS medium contains 10% (v/v) of MOPS buffer; 2 mM MgCl₂; 0.1 mM CaCl₂; 2 g per L glucose; pH 7.0). MOPS buffer contains, per liter: 5 g NaCl, 10 g NH₄Cl, 98.4 g 3-(*N*-morpholino)propanesulfonic acid, sodium salt), 0.59 g Na₂HPO₄·2H₂O, and 0.45 g KH₂PO₄.

Genetic constructions

A ~1.1 kb-fragment containing the complete operator/promoter region of the operon *phnSFECDAcAdB* from *B. sartisoli* RP007 (flanked with the 5' extremities of *phnR* and *phnS* genes) was cut from plasmid pJAMA37 (see chapter 2) with *Xba*I and *Hind*III and inserted into the reporter plasmid pPROBE-luxAB treated with the same enzymes. After ligation and transformation in *E. coli*, the result was the plasmid pPROBE-phn-luxAB, in which the presumed *phnS*-promoter drives expression of the promoterless *luxAB* genes encoding the bacterial luciferase. The gene coding for neomycine phosphotransferase (*nptII*) on pPROBE-luxAB allowed selection of the plasmid via resistance to kanamycin. Triparental mating was performed with *E. coli* DH5α (pPROBE-phn-luxAB) as donor and *E. coli* HB101 (pRK2013) as helper to conjugate pPROBE-phn-luxAB into *Burkholderia* sp. strain RP007-rif as

recipient. *Burkholderia* transconjugants were selected on TY agar plates with kanamycin and rifampicin to counter select against donor, helper and wild type recipient strains. Potential transconjugants were purified and the reporter plasmid was reisolated to verify its integrity.

Preparation of frozen bacterial biosensor cells

Each bacterial biosensor strain was pre-cultivated overnight in LB (*E. coli*) or TY (*B. sartisoli*) at the appropriate growth temperature and antibiotics selection. Two % (v/v) of preculture was used to inoculate fresh medium and the incubation was continued until the culture reached a turbidity of ~0.6 at 600 nm. The bacterial cultures were subsequently placed on ice for 15 min. After that we mixed 6.5 volumes of bacterial culture with 1.5 volume of ice-cold 80 % glycerol solution in water (final glycerol concentration was 15 %). Bacterial suspensions were aliquoted in 0.5 ml portions that were transferred at -80°C without pre-freezing.

Artificial oil spill

In a 5 L glass flask, 2 L of sea water (coastal Mediterranean or North sea water) were artificially contaminated with 1% (20 ml) of crude oil (NSO1). The flask was open at its top, and gently shaken at 20 rpm on a rotary platform at room temperature. The rotation did not produce a mixing (emulsion) of organic and aqueous phases. A tap located at the bottom of the bottle permitted the sampling of sea water (Fig. 1). Samples were taken 15 minutes, 2 and 6 hours after the spill, and subsequently after one, three, seven or ten days. Four-ml glass vials were filled to the top with sea water sample and stored at 4°C before further analysis with the biosensor platform. However, the vials were not stored longer than one day prior to analysis. Additional sea water samples were kept in filled amber glass vials, which were filled to the top and acidified to pH<2 with two drops of 1 N HCl in order to block any biological activity. They were conserved at 4°C and used for the chemical analysis of hydrocarbon content. After each sampling, the volume of water sampled was replaced in the bottle by uncontaminated sea water, in order to keep the total volume constant.

Bioluminescence assay with the multiwell bacterial biosensor platform

Frozen biosensor cells aliquots were thawed in a water bath at 25°C for 2 min. Then one aliquot (0.5 ml) was diluted in 4.5 ml of MOPS medium (or, according to the required volume of each bacterial biosensor suspension for the total amount of assays, n aliquots were diluted in $n \times 4.5$ ml of MOPS medium). Each bacterial biosensor suspension was used to fill all

wells in three columns of a 96-well Multi-Tier™ glass plate (150 µl bacterial suspension per well, each well consisting of a 0.5 ml glass vial) (Wheaton Science Products, USA). Seventy-five µl of MOPS medium were added to each well. Each well was completed to 300 µl by adding 75 µl of contaminated water sample, or 75 µl of standard solution. Standard solutions were prepared with 75 µl uncontaminated water (same origin as used for the spill), to which three µl of a concentrated chemical stock solution were added. For simplicity, the calibration was performed with a single chemical that was representative of the target components in oil. The alkane responsive strain DH5α (pGEc74, pJAMA7) was calibrated using *n*-octane. DH5α (pPROBE-LuxAB-TbuT) was calibrated with toluene, representative for the BTEX family. DH5α (pHYBP109) was calibrated using 2-hydroxy-biphenyl (2-HBP), whereas *B. sartisoli* was calibrated using naphthalene (NAH). The bacterial biosensor for genotoxicity was calibrated with the antibiotic nalidixic acid, a member of the quinolones antibiotics family which blocks the activity of the bacterial DNA gyrase, thereby inhibiting correct DNA replication in the cell. All chemicals were dissolved in dimethylsulfoxide (DMSO), except nalidixic acid which was dissolved in water. Pure compound concentrations in standard series typically ranged from 0, 50, 100, 250 nM for octane; 0, 250, 500, 1000 and 3000 nM for toluene; 0, 100, 200 and 400 nM for NAH; 0, 5, 10, 20 µM for nalidixic acid; and 0, 250, 500, 1000 nM for 2-HBP. To the blank pure DMSO (for all organic contaminants) or water (for nalidixic acid) was added. Spiking of the contaminated sea water samples was done by adding three µl of inducer stock solution to the assay, to achieve spiking concentrations of 100 nM for octane, 500 nM for toluene, 10 µM for nalidixic acid, 500 nM for 2-HBP, and 100 nM for NAH. If those concentrations resulted in a response of the cells outside the range of the calibration curve, the assay was repeated with half that amount of spiking concentration. The microtiter plate was finally sealed with an adhesive plate seal (Thermo scientific, Epsom, UK) and incubated at 30°C in a Thermostar orbital shaker (BMG Labtechnologies, Germany) at 400 rpm for 2 hours in the case of *E. coli* and 3 hours in case of *B. sartisoli* RP007 sensors. Subsequently, 200 µl of each well were transferred into a white 96-well plate (Cliniplate, Thermo scientific, Finland), and *n*-decanal substrate solution was added and mixed to measure luciferase activity. For *E. coli* sensors we used 20 µl of an 18 mM *n*-decanal solution (1:1 v/v ethanol/water solution), whereas for RP007 this was 1 µl. After 3 min (for *E. coli* sensors) or 5 min (for *Burkholderia*) of incubation at room temperature, the bioluminescence was measured using a microtiter plate luminometer (Centro LB 960 luminometer, Berthold AG, Switzerland) with an integration time of 0.1 sec.

Platform data analysis

Light emission values for the control series with known concentrations of pure target compound were used to calculate a calibration curve for each of the bacterial biosensor strains. We used linear or binomial regression calculated with the program Excel to fit the curve with the light emission values in the control series. The equation of the curve was then used to calculate corresponding ‘equivalent target concentrations’ from the bioluminescence values in the samples or their dilutions (the cutoff value was set as the light emission value in the blanc plus three times the standard deviation of the blanc; all sample values below this threshold were considered as below the detection limit). A similar calculation was done for spiked samples to derive an equivalent target plus spiking concentration. Ideally, the calculated equivalent target concentration in the sample plus the theoretical increase of concentration due to spiking was the same as the equivalent target concentration in the spiked sample. If not, the latter value was used to correct, if possible, the calculated equivalent target concentration in the sample according to the following equation:

$$C_{corr} = (C_{th}^{spiking} / (C_m^{spiking} - C_m^{sample})) \times C_m^{sample} \times 4$$

where $C_{th}^{spiking}$ is the target concentration added to the sample by spiking, C_m^{sample} and $C_m^{spiking}$ the calculated concentrations in the sample and in the spiked sample, respectively. The factor 4 corrects for the dilution of sea water in the assay.

CHAPTER 7

DEVELOPMENT OF NEW BACTERIAL BIOSENSORS FOR THE DETECTION OF ALKANES BASED ON THE TRANSCRIPTIONAL ACTIVATOR ALKS FROM THE MARINE BACTERIUM *ALCANIVORAX BORKUMENSIS* STRAIN SK2

Long-chain alkanes are a major component of crude oil and therefore potentially good indicators of fresh as well as ancient hydrocarbon pollution in aquatic environments. A bacterial biosensor for the detection of alkanes was previously developed based on the transcriptional activator AlkS and the promoter P_{alkB} of *Pseudomonas oleovorans*. However, this bacterial biosensor was not sensitive to n-alkanes with chain lengths higher than C_{10} , hence not suitable for the monitoring of long-chain alkanes. Here we present a set of new bacterial biosensors with green fluorescent protein or bacterial luciferase as reporter, that are based on the regulatory protein AlkS from *Alcanivorax borkumensis*, a widespread alkane degrader in marine habitats. The reporter constructs were inserted into *Escherichia coli* strain DH5 α and *Alcanivorax borkumensis* strain SK2. We calibrated the new bacterial biosensor with different concentrations of octane (C_8) and tetradecane (C_{14}), and compared it with the *E. coli* alkane biosensor based on the *P. oleovorans* system. The new *E. coli* luciferase-producing biosensor with AlkS and the *alkB1*-promoter from *A. borkumensis* was capable of measuring octane at concentrations down to ≈ 10 nM, and with a sensitivity that was comparable to the *P. oleovorans* based system. On the contrary, this sensor did not react to tetradecane at any concentration up to 800 nM nominal concentration. Both *E. coli* and *A. borkumensis* sensors producing GFP from the *alkB1* promoter were inducible to tetradecane, suggesting that the use of a stable reporter protein was necessary to detect the small induction response at such a low water soluble concentration. Surprisingly and in contrast to *E. coli* with the same reporter plasmid, the *A. borkumensis* sensor was not responsive to octane.

INTRODUCTION

Saturated hydrocarbons (alkanes) are a major component of crude oil that can sometimes represent more than 50% of the total oil mass [165]. Therefore, monitoring of alkanes can be used as a reliable indicator for oil pollution. Certain marine environments are, for instance, chronically exposed to oil via accidental spillages, offshore platforms exploitation and shipping activities, and it is thereby relevant to estimate the bioavailability and potential effects of petroleum hydrocarbons on the biota. The bacterial biosensor *Escherichia coli* DH5 α (pGEc74, pJAMA7), which was developed for the detection of alkanes more than ten years ago [76], was based on a transcriptional fusion between the promoter P_{alkB} of *Pseudomonas oleovorans* and the genes encoding bacterial luciferase (*luxAB*). The strain also encoded AlkS, the transcriptional activator of the P_{alkB} promoter which specifically binds to alkanes. DH5 α (pGEc74, pJAMA7) successfully reported the presence of short-chain alkanes (C₆-C₁₀) at concentrations lower than 1 μ M, with maximal sensitivity for the detection of octane (C₈) and nonane (C₉). Long-chain alkanes (>C₁₂), however, proved to be poor inducers of the biosensor system. In oil-contaminated environments, short-chain alkanes volatilize and degrade rather more easily than long-chain alkanes, which makes them less suitable as marker for 'older' contamination. For this reason, a bacterial biosensor with increased sensitivity towards long-chain alkanes would be useful. Not only would such a biosensor be a tool for the detection of oil contamination in environmental samples, but it also might help to better understand the bioavailability of long linear alkanes in various experimental set-ups.

The marine bacterium *Alcanivorax borkumensis* is an ubiquitous γ -*Proteobacterium*, which was isolated for its ability to use alkanes as sole source of carbon and energy [128, 170]. Although usually found in low numbers in pristine environments, *A. borkumensis* rapidly becomes a dominant member of the bacterial community when oil pollution is present [171, 172]. The type strain *A. borkumensis* SK2, whose complete genome sequence was recently published [173], contains the *alkSB₁GHJ* operon, which is involved in the degradation of alkanes (Fig. 1A). The enzymes encoded by this operon are highly similar to those of other alkane degraders including certain *Pseudomonas putida* strains [174].

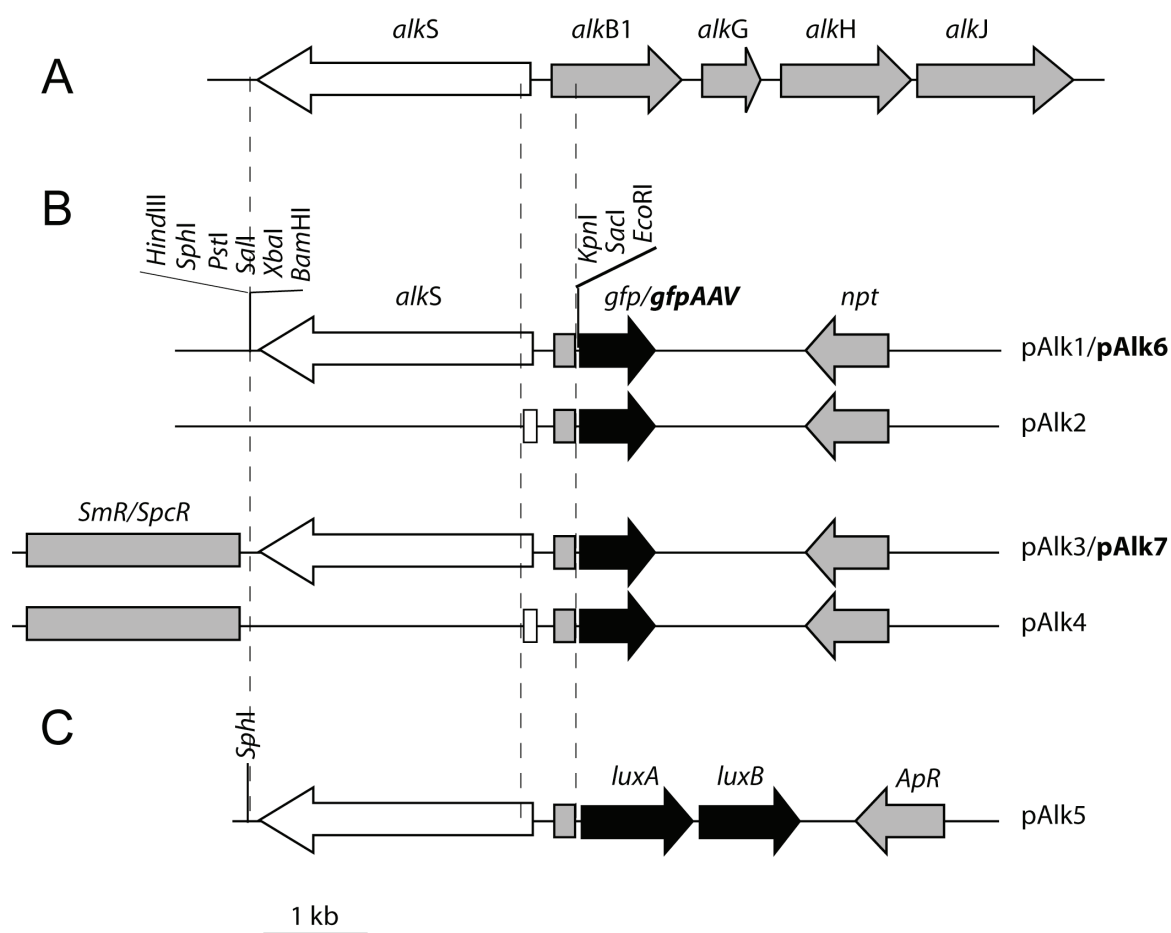


Fig. 1. Genetic constructs for alkane detection. (A) The *alkSB₁GHJ* operon from *A. borkumensis* SK2 (see text for details). (B) A 3-kb fragment (containing the complete operator/promoter region of *alkB₁GHJ* and the full *alkS* gene encoding the regulator AlkS) or a 0.4-kb fragment (containing only the complete operator/promoter region of *alkB₁GHJ*) was inserted upstream of the *gfp* reporter gene in pPROBE-gfp[tagless] (pAlk1, pAlk2) or pPROBE-gfp[AAV] (pAlk6), which encode stable and unstable variants of the green fluorescent protein (GFP), respectively. A Streptomycin/spectinomycin resistance cassette was inserted in pAlk1 and pAlk6, producing the plasmids pAlk3 and pAlk7, respectively. (C) The same 3 kb fragment was inserted upstream of the *luxAB* reporter genes (which encode the bacterial luciferase) in plasmid pJAMA8 to give pAlk5.

In particular, AlkB1 is an alkane hydroxylase that oxidizes alkanes from C₅ to C₁₂ to their corresponding primary alcohols. AlkB1 is strongly expressed when SK2 is grown on long-chain alkanes [173-175]. AlkG, AlkH and AlkJ are, respectively, a rubredoxin, an aldehyde dehydrogenase and an alcohol dehydrogenase, which catalyze further oxidation of the alcohol to a carboxyl group. The transcriptional activator AlkS of SK2, which recruits RNA Polymerase and triggers the expression of the operon *alkSB₁GHI* from the P_{*alkB1*} promoter, shares 27% amino acid similarity with AlkS of *P. oleovorans*.

The goal of the present work was to construct a bioreporter for linear alkanes based on the AlkS- *PalkB1* system from *A. borkumensis* SK2, and to determine whether such a bioreporter would be capable of detecting longer chain linear alkanes (C₁₂-C₁₆). Hereto, a ~3 kb DNA fragment containing the complete operator/promoter region of the *alkSB₁GHI* operon as well as the full *alkS* gene from SK2 was cloned and inserted into reporter plasmids that encoded either the green fluorescent protein (GFP) or the bacterial luciferase as reporter proteins (Fig. 1). As an alternative strategy, a ~0.4 kb fragment containing only the operator/promoter region was fused to the reporter gene *gfp*. All reporter plasmids are represented in Figure 1. These reporter plasmids were used to transform either *E. coli* DH5 α or *A. borkumensis* SK2, and we investigated the response of the new bacterial biosensors towards octane and tetradecane.

RESULTS

Responses of the GFP-based bacterial biosensors to octane and tetradecane

The bacterial biosensors *E. coli* DH5 α (pAlk3), *A. borkumensis* SK2 (pAlk3) and *A. borkumensis* SK2 (pAlk4) (Fig. 1) were exposed to either 2 μ M octane or 100 μ M tetradecane (nominal concentrations) during 4 hours in a microtiter plate assay (Fig. 2). The production of GFP in *E. coli* (pAlk3) exposed to octane was much higher than in non-exposed cultures ($p < 0.01$ with a unilateral Student t-test). Tetradecane also lead to an increased GFP formation by DH5 α (pAlk3) compared to non-exposed cultures ($p < 0.05$), although the GFP intensity with tetradecane was much lower than with octane. *A. borkumensis* SK2 (pAlk3) also induced GFP from the P_{*alkB1*}-promoter both with octane and tetradecane ($p < 0.05$), but GFP fluorescence intensities were rather modestly higher compared to uninduced cells. *A. borkumensis* SK2 with a plasmid without *alkS* but with the P_{*alkB1*}-promoter fused to *gfp* (pAlk4) responded significantly to the presence of tetradecane compared to non-exposed cells

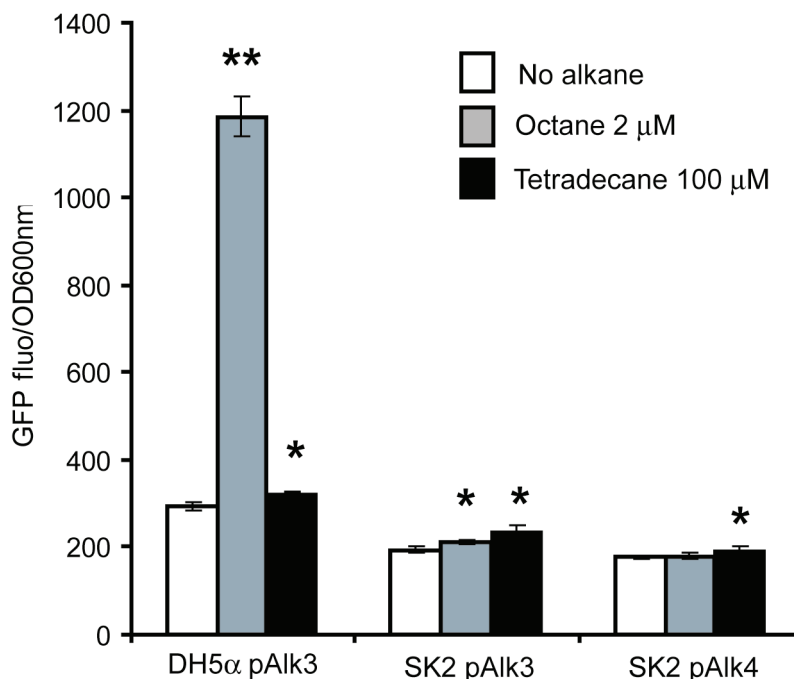


Fig. 2. Alkane induction of green fluorescent protein (GFP) in assays with strains *E. coli* DH5 α (pAlk3), *A. borkumensis* SK2 (pAlk3) and *A. borkumensis* SK2 (pAlk4). All strains were incubated in a 96-well plate and exposed to 2 μ M octane or 100 μ M tetradecane (nominal concentrations) for 4 hours. GFP fluorescence was standardised by the culture turbidity at 600 nm (OD600nm), and error bars indicate standard deviations calculated from triplicate well measurements. Asterixes indicate significant differences in a unilateral Student t-test (* P<0.05, ** P<0.01).

(p<0.05), but GFP intensity was only 1.1-fold higher than the control (Fig. 2). Strangely, this strain was not induced with octane in the same assay.

The GFP fluorescence background in *E. coli* DH5 α (pAlk3) was 1.5 to 2 times higher than in the bacterial biosensor *E. coli* DH5 α (pJAMA30), which was based on the AlkS protein from *P. oleovorans* as regulatory protein for the bioreporter system (data not shown). This suggested that AlkS_{Ab} triggered more unspecific transcription from the P_{alkB1} promoter than AlkS_{Po} from P_{alkB}. However, the fold induction after octane exposure was comparable between the two bacterial biosensors (namely: ~4 at 2 μ M octane). This background fluorescence was also observed in SK2 biosensors at the single cell level using epifluorescence microscopy.

We also incubated cultures of *E. coli* DH5 α (pAlk3) and *A. borkumensis* SK2 (pAlk3) in closed incubation chambers filled with medium and containing tetradecane microdroplets, and could see that GFP became induced over time by using epifluorescence microscopy.

Unfortunately, it was difficult to image the cells near the oil droplets, and the elevated fluorescence background and its high heterogeneity among individual cells rendered quantitative analysis difficult (data not shown). For this reason, we developed a new construct in which we attempted to reduce GFP background. A transcriptional fusion was produced between the fragment containing *alkS* and P_{alkB1} and a reporter gene encoding an unstable version of GFP, whose half-life was reduced to a few hours (compared to >24 hours for the stable GFP) (Fig. 1). The new reporter plasmid was used to transform both *E. coli* DH5 α and *A. borkumensis* SK2, giving DH5 α (pAlk7) and SK2 (pAlk7). We hypothesized that the new bacterial biosensors would benefit from lower fluorescence background without losing their ability to detect alkanes. The results, however, were completely opposite (data not shown). Both biosensors with the unstable GFP did not produce any detectable fluorescence, neither with octane nor with tetradecane, suggesting that the unstable GFP that might have been produced was more rapidly degraded than synthesized from P_{alkB1} .

Calibration of the light emission by the luminescent bacterial biosensor DH5 α (pAlk5) against octane and tetradecane concentration

Figure 3A presents the light emission by *E. coli* DH5 α (pAlk5) as a function of the nominal octane concentration. The bacterial biosensor detected as low as 100 nM octane (with a method detection limit estimated at \sim 10 nM), and showed an approximately linear correlation of the intensity of light emission with the nominal octane concentration up to 1 μ M. Above 1 μ M octane, DH5 α (pAlk5) produced the same bioluminescence signal indicating that the promoter became saturated. Since 1 μ M octane is below its maximal aqueous solubility (\sim 6 μ M), this saturation may reflect the maximal binding and activation ‘velocity’ of AlkS. For comparison, we calibrated the strain DH5 α (pGEc74, pJAMA7), whose construct encodes the AlkS regulator from *P. oleovorans*, under identical assay conditions (Fig. 3B). DH5 α (pGEc74, pJAMA7) showed an approximate similar method detection limit for octane, and similar sensitivity of analysis (i.e., the slope of the linear curve). In contrast, the AlkS- P_{alkB} system of *P. oleovorans* became saturated at lower octane concentrations. In addition, the background luminescence in DH5 α (pGEc74, pJAMA7) was 5 to 10 times lower than in DH5 α (pAlk5), which confirmed what we observed with the GFP-based bacterial biosensors. Finally, we tested the sensitivity of DH5 α (pAlk5) towards tetradecane (Fig. 3C). In contrast to previous GFP measurements, nominal tetradecane

concentrations as high as 800 nM did not trigger any substantial luciferase production compared to non-exposed conditions.

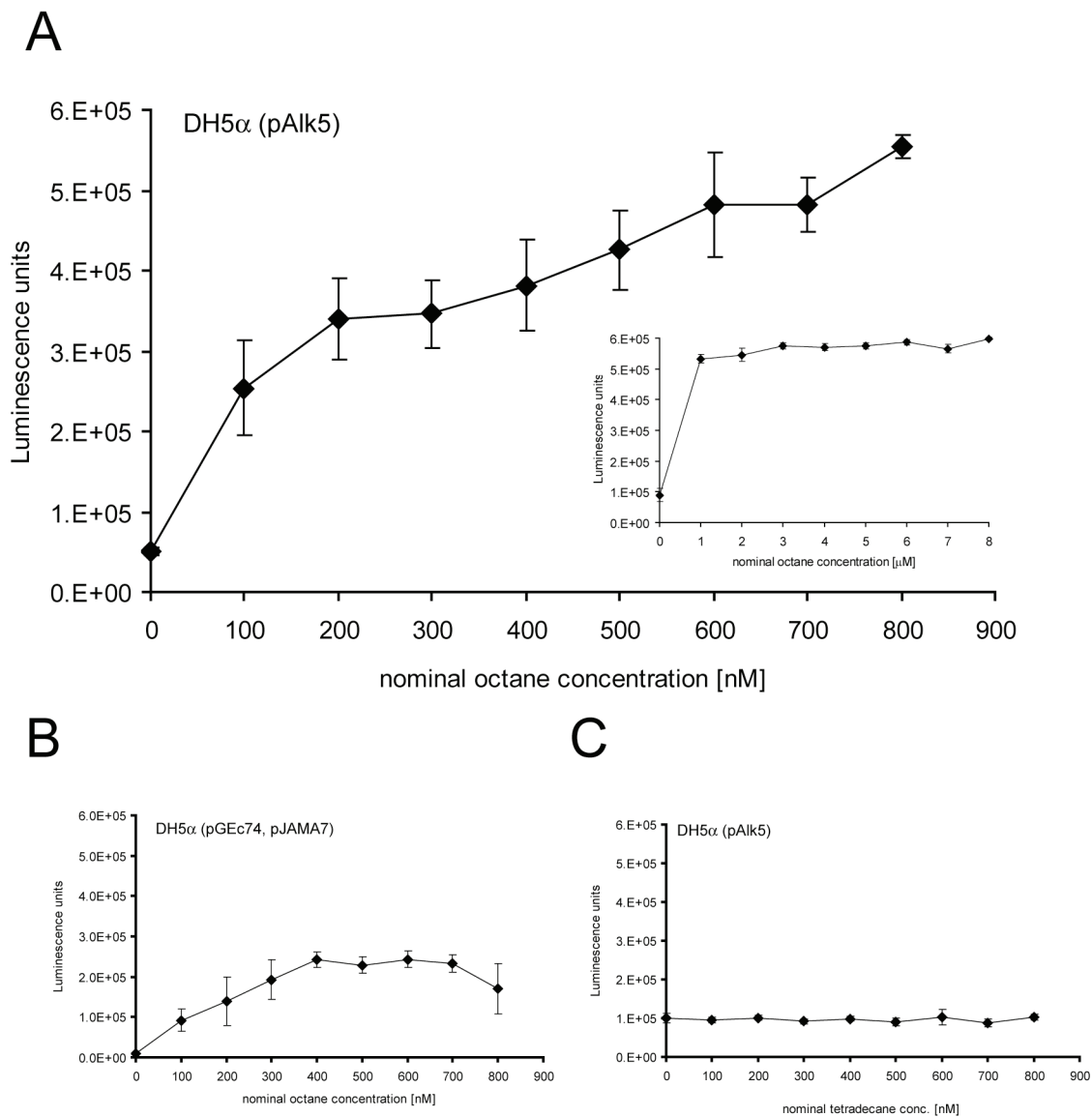


Fig. 3. Induction of light emission by *E. coli* DH5α (pAlk3) (AlkS from *A. borkumensis*, panel A and C) and by *E. coli* DH5α (pGec74, pJAMA7) (AlkS from *P. oleovorans*, panel B) as a function of octane or tetradecane concentrations. The bacterial biosensors were incubated at 30°C with shaking in sealed glass test tubes with increasing nominal concentrations of either octane (A and B) or tetradecane (C). After two hours of incubation, the cells were transferred in a 96-well plate for luminescence measurements (\pm SD, $n=5$).

DISCUSSION

We developed a set of new *E. coli* biosensors for the detection of alkanes based on the AlkS regulator and the operator/promoter region of the *alkB1GHJ* operon from the marine bacterium *A. borkumensis* SK2. Two versions were produced, either with GFP or with bacterial luciferase as a reporter protein. The GFP-based biosensor satisfyingly detected octane (C₈), but responded only weakly to tetradecane (C₁₄). The luminescent-based biosensor, which can be quantified more easily than the GFP-based sensor, was used to calibrate the response as a function of alkane concentration. The results presented in Fig. 3 indicated that the detection of short-chain alkanes by the new bacterial biosensor was similar to what could be achieved with the existing alkane biosensor DH5 α (pGEc74, pJAMA7). Contrary to our expectations, the biosensor DH5 α (pAlk5) did not significantly responded to tetradecane. This is contrast to results in the literature on expression of *alkB1* in *A. borkumensis* strain SK2 grown on tetradecane, which was measured by quantitative real time PCR [173]. In that study *A. borkumensis* was actively metabolising long-chain alkanes, which is not the case for the *E. coli* (pAlk5) biosensor, and which may be of relevance for promoting further induction of P_{*alkB1*}. Another reason for poor performance with tetradecane might have been its lower aqueous phase solubility than octane. Both octane and tetradecane are extremely poorly soluble in water (~6 μ M and ~20 nM, respectively), but the calibration curve with octane suggests that 20 nM is close to the method detection limit (Fig. 3). Therefore, the aqueous solubility of tetradecane might be too close to the lower limit of induction of the system, if we assume that its functioning depends directly on the aqueous concentration of the target compound. In this case, one might still observe a signal with a stable reporter protein that accumulates over time (such as GFP), or apparently the *alkB1* mRNA, whereas bacterial luciferase is not completely stable and its turnover rate may lay in the order of the degradation rate. In addition, *A. borkumensis* may have further strategies to enhance long-chain alkane solubility, such as via biosurfactants [173], which may lead to continued induction of P_{*alkB1*}, whereas this would not be measurable in *E. coli*. From our results, therefore, we cannot conclude if AlkS_{*Ab*} possesses a higher affinity for long-chain alkanes than AlkS_{*Po*}.

Because of the possible bioavailability ‘enhancing’ strategies, we were interested in using *A. borkumensis* SK2 as a host strain rather than *E. coli*. In addition, the strain is actively metabolising alkanes, therefore triggering a higher flux of compounds to the cytoplasm. Apart

from the problems outlined above, also cloning was not completely trivial in *A. borkumensis* SK2. First of all, selection for the presence of the reporter plasmid pPROBE-gfp by resistance to kanamycin was a bit erratic and it seemed that not all cells retained the plasmid after conjugation. For this reason we added a spectinomycin resistance cassette into the reporter plasmid, and further used spectinomycin for selection, which seemed to improve plasmid stability in SK2 (Fig. 1). An important basal GFP production, however, was observed in SK2 (pAlk3), confirming that the *gfp* gene was efficiently expressed and translated. Future work may attempt to change to a different vector to further increase stability of the reporter in SK2, or to design transposon delivery strategies, which up to now were not successful in SK2 as well.

One of the surprising differences between the behaviour of P_{alkB1} in *E. coli* and SK2 was the poor response to octane by SK2 compared to *E. coli*. This was already obvious in strain SK2 (pAlk3), which was far less sensitive to octane than DH5 α (pAlk3), while its sensitivity to tetradecane was conserved (Fig. 2). The difference was even more pronounced for SK2 (pAlk4), which had totally lost its ability to detect octane. The reason for the further loss of octane responsivity in SK2 (pAlk4) can only have to do with the lack of a full copy of the *alkS* gene in the reporter plasmid. However, it is at present unclear why a SK2-based sensor would be less sensitive to octane than *E. coli*, unless octane is so rapidly degraded by SK2 that it cannot effectively induce the promoter. In conclusion, we have shown that despite initial promising results, the application of a long-chain alkane bioreporter is hampered by physical phenomena and lack of knowledge on alkane degradation in *A. borkumensis*.

ACKNOWLEDGMENTS

We thank Terry McGenity from the University of Essex (UK) for the gift of *Alcanivorax borkumensis* strain SK2. This work was carried out under the frame of the project FACEiT, financed by the sixth framework programme of the European Community (project n°018391).

MATERIAL AND METHODS

Chemicals

Octane (99% purity) and tetradecane (99% purity) were purchased from Fluka (Buchs, Switzerland).

Strains and culture conditions

A. borkumensis strain SK2 was grown on ONR7a [176] agar plates or liquid cultures with 10 g pyruvate per L at 30°C. *E. coli* strains were routinely grown on Luria Bertani agar plates or LB liquid medium at 37°C in the presence of appropriate antibiotics. For bioreporter assays, *E. coli* strains were incubated in MOPS medium (MOPS medium contains 10% (v/v) of MOPS buffer; 2 mM MgCl₂; 0.1 mM CaCl₂; 2 g per L glucose; pH 7.0). MOPS buffer contains, per liter: 5 g NaCl, 10 g NH₄Cl, 98.4 g 3-(*N*-morpholino)propanesulfonic acid, sodium salt), 0.59 g Na₂HPO₄·2H₂O, and 0.45 g KH₂PO₄.

Genetic constructions

A 2939-bp fragment containing the complete *alkS* gene, the operator/promoter region of the *alkB₁G_{HJ}* operon and the 5' extremity of the *alkB₁* gene (Fig. 1), was amplified by PCR from genomic DNA of strain SK2 using the primers *alkS*-rev1 (5'-CTCTCGGATCCGCCACTTGCTGCGCACTCGC-3') and *alkB1*-rev (5'-CTCTCGGTACCGCTCGGTTAAAATGTTCTCTG-3') (introduced restriction sites *Bam*HI and *Kpn*I are indicated in bold). In addition, a 399-bp fragment containing solely the operator/promoter region of the *alkB₁G_{HJ}* operon flanked by the 5' extremities of *alkS* and *alkB₁* was amplified by PCR using primers *alkS*-rev2 (5'-CTCTCGGATCCGATTCGGACTCGGCAGAGGC-3') and *alkB1*-rev. These fragments were cloned into pGEM-T Easy (Promega, Switzerland), subsequently re-isolated by enzymatic restriction using *Bam*HI and *Kpn*I, and finally ligated with the vector pPROBE-gfp[tagless] [177] cut with the same enzymes. The resulting plasmids pAlk1 and pAlk2 (Fig. 1) were used to transform *E. coli* DH5α using heat shock and selected via invoked resistance to kanamycin. The long fragment was also ligated with the vector pPROBE-gfp[AAV] in a similar way, resulting in the plasmid pAlk6 (Fig. 1). A streptomycin/spectinomycin resistance cassette from pHP45Ω was inserted into vectors pAlk1, pAlk2 and pAlk6 at the unique *Bam*HI site. The resulting plasmids were pAlk3, pAlk4 and pAlk7, respectively (Fig. 1). In these plasmids, the orientation of the streptomycin/spectinomycin resistance cassette was not defined. To produce a reporter construct with the *luxAB* genes, plasmid pAlk1 was cut with *Eco*RI, then treated with the Klenow fragment of DNA Polymerase, and finally digested with *Sph*I. The ~3 kb fragment containing the gene *alkS* and the *alkB₁* operator/promoter region was isolated and purified. The vector pJAMA8 that carried the promoterless *luxAB* genes [11] was cut with *Xba*I, then treated with the Klenow fragment of DNA Polymerase, and finally

digested with *Sph*I. The *alkS-alkB₁* fragment was ligated with the prepared pJAMA8 vector, which after transformation resulted in plasmid pAlk5.

In order to introduce pPROBE-based plasmids into *A. borkumensis* we used triparental mating. *E. coli* DH5 α with one of the pAlk plasmids was used as donor strain; *E. coli* HB101 (pRK2013) as helper strain and *A. borkumensis* SK2 as recipient strain. Conjugation was allowed to proceed for 16 h at 30°C, after which the mating mixture was resuspended and serially diluted. Dilutions were plated and potential transconjugants were selected on ONR7a pyruvate agar plates with 50 mg per L spectinomycin. Some *E. coli* resistance to spectinomycin occurred, but only formed tiny colonies that were easily distinguishable from *Alcanivorax* colonies. Potential SK2 transconjugants were purified and the presence of the plasmid was verified by PCR as well as by miniprep isolation.

Fluorescence assay

E. coli DH5 α (pAlk3) was cultured in LB, *A. borkumensis* strains SK2 (pAlk3) and SK2 (pAlk4) were cultivated in ONR7a with 1% pyruvate with 50 μ g per ml of spectinomycin until mid-log phase. After centrifugation at 500 \times g for 10 min, the supernatant was removed and the cells were resuspended in MOPS (*E. coli*) or ONR7a pyruvate (*A. borkumensis*) in order to obtain a final culture turbidity at 600 nm (OD_{600nm}) of \sim 0.4. Two hundred μ l of this cell suspension were distributed in triplicate in a black 96-well microtiter plate with flat transparent bottom (Greiner Bio-one, Germany). Two μ l of an alkane stock solution in ethanol was added to each well (while nothing was added to the control wells) in order to obtain final nominal concentrations of 2 μ M for octane and 100 μ M for tetradecane. The plate was incubated at 30°C with orbital shaking (500 rpm) in a ThermoStar incubator (BMG Labtechnologies, Germany). After 4 hours of incubation, the intensity of GFP fluorescence (excitation: 480 nm; emission: 520 nm) and the culture turbidity were measured with a Fluostar fluorescence microtiterplate reader (BMG Labtechnologies, Germany). The intensity of GFP fluorescence in each well was divided by the value of OD_{600nm} in order to normalize the data with the cell density.

Bioluminescence assay

For luciferase measurements the strains *E. coli* DH5 α (pAlk5) and *E. coli* DH5 α (pGEc74, pJAMA7) were pre-cultivated in LB in the presence of the appropriate antibiotics (i.e., ampicillin for pAlk5, chloramphenicol and ampicillin for pGEc74 and pJAMA7). After

overnight growth, 2 % (v/v) of the preculture was used to inoculate 20 ml of fresh LB medium with the respective antibiotics. When the new cultures reached an OD_{600nm} of ~0.6, the cells were put on ice for 15 min. Subsequently, 6.5 volumes of cells were mixed with 1.5 volume of ice cold 80% glycerol solution. Aliquots of 0.5 ml were then distributed in 1.5 ml eppendorf tubes and frozen at -80°C. Prior to a luminescence assay, aliquots of frozen cells were thawed in a water bath at 25°C for 2 min, and immediately diluted 40 times in MOPS medium. Four ml of cell suspension were added to a 8 ml glass test tube which was sealed with a borosilicate glass stopper (Verrerie de Carouge, Geneva). The test tubes were previously washed with acetone, rinsed twice with bidistilled water and dried at 80°C. In the closed test tube, the air/liquid volumetric ratio was approximately 1:1. Alkane stock solutions were prepared in DMSO (octane) or ethanol (tetradecane). Forty µl (1%) of different alkane stock solutions were added to each tube in order to obtain the desired nominal concentrations. Five replicate test tubes were used per concentration. The test tubes were incubated at an inclination of 45°, at 30°C with shaking (180 rpm). After 2 hours of incubation, 200 µl from each tube were transferred in a white 96-well microtiter plate (Cliniplate, ThermoScientific, Finland). Twenty-five µl of an *n*-decanal solution (18 mM in a water/ethanol solution) were added to each well and mixed by pipetting (final *n*-decanal concentration was 2 mM). After 3 min of incubation at room temperature, the bioluminescence was measured using a microtiter plate luminometer (Centro LB 960 luminometer, Berthold AG, Switzerland) with an integration time of 0.1 sec.

CHAPTER 8

GENERAL DISCUSSION

MULTISTRAIN PLATFORMS AND ARRAYS

In the introduction of this work (Chapter 1), we presented the concept of bacterial biosensing and reporting, and its application for the measurement of pollutant bioavailability. We emphasized the following advantages brought about by the use of living organisms as detection tools: 1) an easy and low cost production of the sensors; 2) the integration of biological processes into the measurement; and 3) the possibility to build sensing arrays with multiple target analytes. The last point was well illustrated by the development of a multiwell bacterial biosensor platform for the monitoring of crude oil pollution in aquatic samples (Chapter 6). We managed to screen oil-contaminated water samples for a variety of chemicals, including saturated hydrocarbons and monoaromatics, which could be relevant for risk assessment and ecotoxicology studies. This was done at a relatively modest scale, since four different bacterial biosensor strains were used simultaneously in a regular 96-well platform. Citing the nucleic acid microarrays as an example of revolutionary technique in molecular biology, Elad and co-workers suggested in a recent review that microbial whole-cell arrays potentially represented the next important evolution for both arrays and whole-cell biosensor technologies [10]. The authors listed a number of biological and technical issues that needed to be addressed for a full maturation of bacterial cell arrays, including the preservation of the cells, the choice of a suitable substrate material for the platform, an optimization of the emission signal detection and advances in data analysis. In this study, we showed that it was possible and relatively easy to work with stocks of biosensor cells frozen at -80°C . The working cell suspension could be prepared from frozen stocks within minutes, and the stocks remained active for at least six months of storage at -80°C . This considerably simplified the preparation of the assay, since no preliminary growth of the bacterial biosensor cells was required and provided consistent output from a single batch of cells (thus saving several days of preparation). Research is currently at work in partner laboratories in order to produce freeze-dried bacterial biosensors. Promising results have been obtained, and the protocols already allow us to store freeze-dried cells in a normal freezer and simply rehydrate them prior to use. This might represent the best solution for bacterial biosensor storage. We utilized a 96-well glass microtiter plate in our assay, which prevented the sorption of hydrocarbon contaminants on the surface of the wells. In that respect, glass is a more suitable material than plastic, and should be preferentially employed while measuring crude oil components. Bacterial luciferase was selected as reporter protein due to its non-cognate origin

and its high sensitivity, and proved to be suitable for the simultaneous measurement of emission signals with light intensities showing variation of up to two orders of magnitude.

To date, whole-cell arrays that were developed for the analysis of environmental samples have essentially been used for the monitoring of toxicity [167-169]. We demonstrated in this work that there is an important potential for the development of bacterial cell arrays or platforms which target specific chemicals (or a family of chemicals) and allow their quantification even at the nanomolar range. The construction of bacterial biosensors based on the marine bacterium *Alcanivorax borkumensis* (Chapter 7) illustrated the constant search for new promoter-reporter fusions with ameliorated specificities. In fact, the impressive increase of the DNA databases suggests that many new sequences of bacterial origin encoding regulatory elements of interest may be cloned and used in the near future.

UNDERSTANDING THE BIOAVAILABILITY PROCESSES

The measurement of the aqueous concentration of organic contaminants represent one major application of bacterial biosensors. It relies on the rapid and reliable screening of aquatic samples for classes of contaminants that have an environmental relevance, and in that respect it is closely related to risk assessment and ecotoxicology. On the other hand, another important purpose of using bacterial biosensors is to gain better understanding of the parameters that influence the pollutants' availability and accessibility to microorganisms in natural habitats. It is acknowledged that the microbial biodegradation of hydrophobic organic contaminants (HOCs) is governed by their mass transfer from the matrix to the cell [6, 83], and today increasing attention is given to bioavailability in management issues dealing with contaminated soils and sediments [178]. The mass transfer (or flux) of a HOC depends on a variety of physico-chemical parameters including its aqueous solubility, the contact surface between HOCs and the aqueous phase, and its sequestration in a non aqueous phase liquid (NAPL) phase. We illustrated this by using *Burkholderia sartisoli* strain RP037, a GFP-based bacterial biosensor which detected fluxes of the poly aromatic hydrocarbon (PAH) phenanthrene, a model HOC (Chapter 2). Unlike the majority of bacterial biosensors, *B. sartisoli* RP037 was not able to directly detect differences in the aqueous concentration of phenanthrene. On the other hand, long-time exposure and biodegradation of phenanthrene significantly induced the expression of GFP. From this we proposed the concept of 'sink' biosensing, which was opposed to 'equilibrium' biosensing in the introductory chapter

(Chapter 1). Although it showed reduced efficiency in terms of assay speed, the ‘sink’ bacterial biosensor assay allowed us to investigate the bioavailability and bioaccessibility of low molecular weight PAHs under various experimental conditions. Figure 1 sums up the differences between the two types of bacterial biosensors. By degrading the target compound, the ‘sink’ bacterial biosensors increase the flux of PAHs, because they locally reduce the PAH dissolved concentration. Despite its importance for the biodegradation of HOCs, the concept of flux is not extensively employed in bacterial biosensor studies. However, we believe that the discipline would benefit from a closer look at the dynamic of pollutants’ availability.

In Chapter 2, our experimental set-up consisted of a pollutant compartment (a NAPL phase, polymer beads, or simply PAH crystals), a biological compartment (the bacterial biosensors) and an aqueous phase which conditioned the exchanges between the two compartments. This represented the simplest situation that can be modelled in the laboratory. Of course, many other elements can be introduced in such experimental system. Since *B. sartisoli* strain RP037 responded to changes in the phenanthrene flux, we investigated how this flux to the bacterial cell would vary in the presence of additional elements – which were selected for their environmental relevance. Dissolved organic matter (DOM), which is a ubiquitous element in both aquatic and terrestrial habitats, can potentially interact with HOCs and modify their bioavailability/bioaccessibility [111]. Chapter 3 investigated the influence of humic acids (a model DOM) on the phenanthrene flux to RP037 in liquid cultures and on naphthalene volatilization in the gas phase (which was also sensed and reported by RP037). In the experimental conditions that were used, no influence was observed on the phenanthrene flux to the cell, and only limited effect was observed on naphthalene volatilization. This is in contrast to certain literature data [114] and suggests that the interactions between bacteria, HOCs and DOM may be species- or even strain-specific. A variety of microbial strategies may exist in order to take advantage of the presence of DOM for the uptake of HOCs (e.g., the degradation of DOM-sorbed PAHs [115]), and it would be worth studying that issue on a basis that is not limited to a single bacterial species. Chapter 4 then dealt with two additional complications of our core experimental set-up. Firstly, this consisted of the presence of another bacterial species in the biological compartment (the co-cultivation of *Burkholderia sartisoli* with *Pseudomonas putida*), and secondly the presence of a biological surface active agent (or biosurfactant) that was either produced by *P. putida* or added in a purified form in the culture. Interestingly, our results suggested that both the type of biosurfactant and the type of bacterial strain may influence the surfactant’s effects on the availability of HOCs.

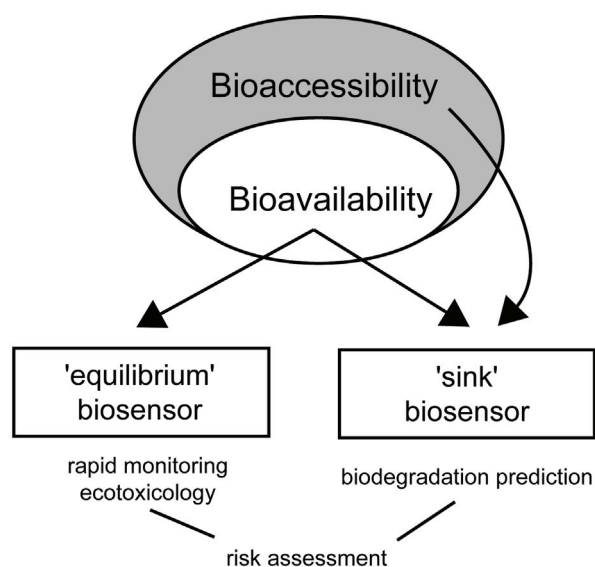


Fig. 1. The bioavailable fraction can be measured by both types of biosensors, whereas the bioaccessible fraction can only be investigated with 'sink' biosensors, which trigger a flux of compound to the cell via active degradation. When using short incubation periods, 'sink' biosensors can function as 'equilibrium' sensors and rapidly quantify a certain pollutant.

SINGLE CELL MICROBIOLOGY AND IN SITU MEASUREMENT

In the last decade, technical innovations have paved the way for the study of environmental microbiology at the single cell level [179]. The on-going improvement of FISH methodologies [180] and their combination with new techniques such as the isotopic measurement using high-resolution ion microprobe (NanoSIMS) [181-183], stable isotope Raman spectroscopy [184], or flow cytometry [161, 185], brought substantial advances for the study of physiology and ecology of individual microbes. In addition, microfluidics and molecular techniques are now available that permit the whole-genome amplification of individual microbes [186, 187], hence complementing the phenotypic observation with the genotypic information. Beyond the study of physiological phenomena, however, there is a real interest in working with individual bacteria because they can serve to investigate natural habitats at the microscale [15, 16]. Most terrestrial environments possess high heterogeneity in terms of nutrients, water saturation, oxygen, etc., that is only apparent at the micrometer scale. Due to their size, bacteria are perfect agents for the study of microheterogeneity and can be applied directly to a wide variety of environmental samples. Monitoring can be performed *in situ* by means of the expression of autofluorescent proteins in the bacterial cells, which

combines valuable properties such as an absence of toxicity in most bacteria, reduced requirements for functioning (only oxygen is needed) and the possibility to detect the fluorescence signal without disturbing the system. Bacterial luciferase and beta-galactosidase have also been employed [188-190], yet at a much lesser extent due to the difficulty of measuring a signal from these reporter proteins at the single-cell level. A vast number of studies have realised the *in situ* observation of individual cells in natural habitats using fluorescent proteins. To our point of view, at present time the challenge is the precise quantification of a reporter signal in a population of bacterial biosensor cells. Due to the complexity of such measurement, only few studies have addressed this question [51, 52]. Background fluorescence, photobleaching, cellular movement are typical aspects that complicate *in situ* quantification [16]. Furthermore, the intrinsic variability of the reporter expression in bacteria necessitates to apply probabilistic considerations to the individual cell measurements (Fig. 2). Another crucial element is to ensure that active but non-induced cells are not excluded from the analysis, which might overestimate the signal intensity in the whole bacterial population. This happens when cells showing no or low reporter fluorescence are indistinguishable from the background fluorescence. In our case, we achieved that by inserting a second fluorescent reporter (mCherry) that would constitutively tag the GFP-based bacterial biosensor *B. sartisoli* strain RP037 (Chapter 5). This work was a follow-up on preliminary trials with the Cyan Fluorescent Protein (CFP) and the DsRed fluorescent protein, which, however, were not very good to combine with GFP. The protein mCherry showed an efficient maturation and stability, was not toxic to the cells and did not cross fluoresce with GFP in the chosen wavelengths of emission. We proved that it is possible to immobilize the double-tagged bacterial biosensors via a simple embedding in culture medium solidified by 0.5% agarose without reducing their reporting abilities. This realisation is an important step in the direction of studying microheterogeneity *in situ*, and we already showed that it was possible to detect a flux of phenanthrene from an artificially contaminated soil to individual bacterial biosensors within a gel matrix.

CONCLUSIONS

Looking at the recent past, it appears that concepts such as bioavailability and bioaccessibility are gaining in consideration and acknowledgment in the field of bioremediation and risk assessment [30]. In that respect, bacterial biosensors have a number

of advantages to become priority tools for the monitoring of contaminated environments. By selecting a variety of either ‘equilibrium’ or ‘sink’ biosensors, it is possible to address specific questions such as the nature of the contaminants, their bioavailability or their bioaccessibility to micro-organisms.

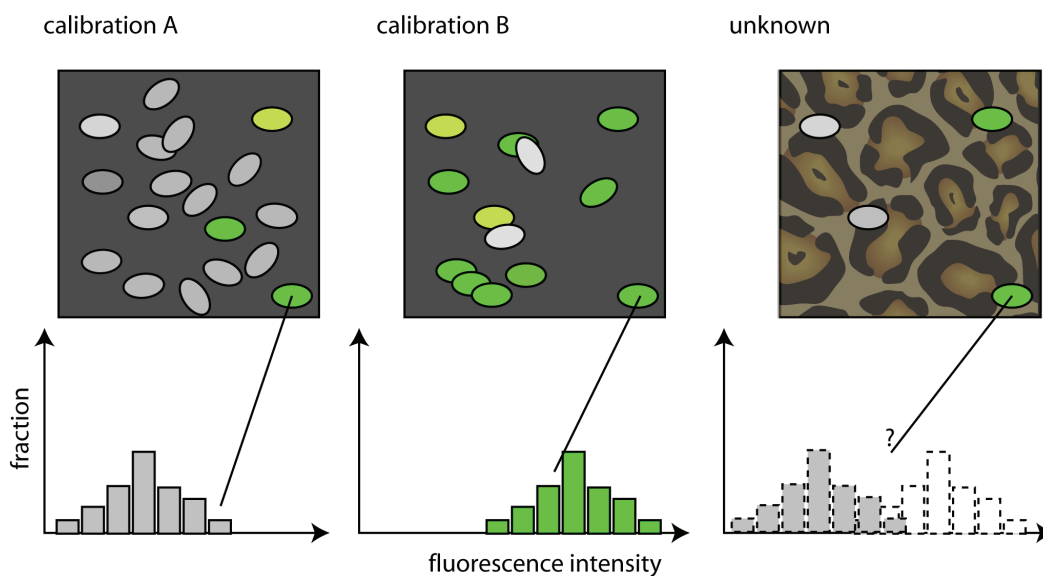


Fig. 2. Illustration of the problem associated with interpreting the reporter intensity of single cells due to variability throughout a population. As a result of physiological, phenotypic and genetic variability, and superimposed by transcriptional noise, the reporter output from a genetic construct introduced in the cell to measure a specific chemical signal or condition, will vary per individual (here shown as histogram for the population of cells from the imaginative micrograph above). Different conditions can be used to calibrate the reporter response, e.g., different analyte concentrations (*calibration A*: low analyte concentration, *B*: higher analyte concentration, therefore, overall higher fluorescence levels than *A*). However, for a single cell in an unknown sample (panel outmost to the right), one cannot per se decide to which of the population distributions its reporter intensity should belong (and, hence, to which past analyte exposure history). We can only ascribe a probability for the reporter intensity to belong to one or the other distribution. (Obviously, in this illustration, two extreme cases are drawn.)

REFERENCES

1. Heitzer A, Malachowsky K, Thonnard JE, Bienkowski PR, White DC, Saylor GS: **Optical biosensor for environmental on-line monitoring of naphthalene and salicylate bioavailability with an immobilized bioluminescent catabolic reporter bacterium.** *Applied and Environmental Microbiology* 1994, **60**(5):1487-1494.
2. Dorn JG, Frye RJ, Maier RM: **Effect of temperature, pH, and initial cell number on luxCDABE and nah gene expression during naphthalene and salicylate catabolism in the bioreporter organism *Pseudomonas putida* RB1353.** *Applied and Environmental Microbiology* 2003, **69**(4):2209-2216.
3. Werlen C, Jaspers MCM, van der Meer JR: **Measurement of biologically available naphthalene in gas and aqueous phases by use of a *Pseudomonas putida* biosensor.** *Applied and Environmental Microbiology* 2004, **70**(1):43-51.
4. Bastiaens L, Springael D, Dejonghe W, Wattiau P, Verachtert H, Diels L: **A transcriptional luxAB reporter fusion responding to fluorene in *Sphingomonas* sp. LB126 and its initial characterisation for whole-cell bioreporter purposes.** *Research in Microbiology* 2001, **152**(10):849-859.
5. Laurie AD, Lloyd-Jones G: **The phn genes of *Burkholderia* sp. strain RP007 constitute a divergent gene cluster for polycyclic aromatic hydrocarbon catabolism.** *Journal of Bacteriology* 1999, **181**(2):531-540.
6. Harms H, Bosma TNP: **Mass transfer limitation of microbial growth and pollutant degradation.** *Journal of Industrial Microbiology & Biotechnology* 1997, **18**(2-3):97-105.
7. King JMH, DiGrazia PM, Applegate B, Burlage R, Sanseverino J, Dunbar P, Larimer F, Saylor GS: **Rapid, sensitive bioluminescent reporter technology for naphthalene exposure and biodegradation.** *Science* 1990, **249**(4970):778-781.
8. Burlage RS: **Emerging technologies: bioreporters, biosensors, and microprobes.** In: *Manual of environmental microbiology.* Edited by Hurst CJ, Knudsen GR, McInerney MJ, Stetzenbach LD, Walter MV. Washington, D. C.: ASM Press; 1997: 115-123.
9. Daunert S, Barrett G, Feliciano JS, Shetty RS, Shrestha S, Smith-Spencer W: **Genetically engineered whole-cell sensing systems: coupling biological recognition with reporter genes.** *Chemical Reviews* 2000, **100**(7):2705-2738.
10. Elad T, Lee JH, Belkin S, Gu MB: **Microbial whole-cell arrays.** *Microbial Biotechnology* 2008, **1**(2):137-148.
11. Jaspers MCM, Suske WA, Schmid A, Goslings DAM, Kohler H-PE, van der Meer JR: **HbpR, a new member of the XylR/DmpR subclass within the NtrC family of bacterial transcriptional activators, regulates expression of 2-hydroxybiphenyl metabolism in *Pseudomonas azelaica* HBP1.** *Journal of Bacteriology* 2000, **182**(2):405-417.
12. Belkin S: **Microbial whole-cell sensing systems of environmental pollutants.** *Current Opinion in Microbiology* 2003, **6**(3):206-212.
13. Suar M, van der Meer JR, Lawlor K, Holliger C, Lal R: **Dynamics of multiple lin gene expression in *Sphingomonas paucimobilis* B90A in response to different**

- hexachlorocyclohexane isomers. *Applied and Environmental Microbiology* 2004, **70**(11):6650-6656.**
14. Harms H, Wells M, van der Meer J: **Whole-cell living biosensors: are they ready for environmental application?** *Applied Microbiology and Biotechnology* 2006, **70**(3):273-280.
 15. Leveau JHJ, Lindow SE: **Bioreporters in microbial ecology.** *Current Opinion in Microbiology* 2002, **5**(3):259-265.
 16. Tecon R, van der Meer JR: **Information from single-cell bacterial biosensors: what is it good for?** *Current Opinion in Biotechnology* 2006, **17**(1):4-10.
 17. Shaner NC, Lin MZ, McKeown MR, Steinbach PA, Hazelwood KL, Davidson MW, Tsien RY: **Improving the photostability of bright monomeric orange and red fluorescent proteins.** *Nature Methods* 2008, **5**(6):545-551.
 18. Shaner NC, Steinbach PA, Tsien RY: **A guide to choosing fluorescent proteins.** *Nature Methods* 2005, **2**(12):905-909.
 19. Drepper T, Eggert T, Circolone F, Heck A, Krauss U, Guterl JK, Wendorff M, Losi A, Gartner W, Jaeger KE: **Reporter proteins for in vivo fluorescence without oxygen.** *Nature Biotechnology* 2007, **25**(4):443-445.
 20. Magrisso S, Erel Y, Belkin S: **Microbial reporters of metal bioavailability.** *Microbial Biotechnology* 2008, **1**(4):320-330.
 21. van der Meer JR, Tropel D, Jaspers M: **Illuminating the detection chain of bacterial bioreporters.** *Environmental Microbiology* 2004, **6**(10):1005-1020.
 22. Loening AM, Wu AM, Gambhir SS: **Red-shifted *Renilla reniformis* luciferase variants for imaging in living subjects.** *Nature Methods* 2007, **4**(8):641-643.
 23. Shapiro E, Lu C, Baneyx F: **A set of multicolored *Photinus pyralis* luciferase mutants for in vivo bioluminescence applications.** *Protein Engineering, Design and Selection* 2005, **18**(12):581-587.
 24. Heitzer A, Applegate B, Kehrmeier S, Pinkart H, Webb OF, Phelps TJ, White DC, Saylor GS: **Physiological considerations of environmental applications of lux reporter fusions.** *Journal of Microbiological Methods* 1998, **33**(1):45-57.
 25. Looger LL, Dwyer MA, Smith JJ, Hellinga HW: **Computational design of receptor and sensor proteins with novel functions.** *Nature* 2003, **423**(6936):185-190.
 26. Marques S, Aranda-Medo I, Ramos JL: **Controlling bacterial physiology for optimal expression of gene reporter constructs.** *Current Opinion in Biotechnology* 2006, **17**(1):50-56.
 27. Legler J, Dennekamp M, Vethaak AD, Brouwer A, Koeman JH, van der Burg B, Murk AJ: **Detection of estrogenic activity in sediment-associated compounds using in vitro reporter gene assays.** *Science of the Total Environment* 2002, **293**(1-3):69-83.
 28. Meerts I, Letcher RJ, Hoving S, Marsh G, Bergman A, Lemmen JG, van der Burg B, Brouwer A: **In vitro estrogenicity of polybrominated diphenyl ethers, hydroxylated PBDEs, and polybrominated bisphenol A compounds.** *Environmental Health Perspectives* 2001, **109**(4):399-407.
 29. Hammer B, Wenger C: **Contaminated sites: register, evaluate, remediate.** Swiss Agency for the Environment, Forests and Landscape (SAEFL); In: revue Environnement 2001: 5-7.
 30. Harmsen J: **Measuring bioavailability: from a scientific approach to standard methods.** *Journal of Environmental Quality* 2007, **36**(5):1420-1428.
 31. **Bioavailability of contaminants in soils and sediments: processes, tools, and applications.** National Research Council; National Academies Press; The National Academic Press Location; 2003.

32. Patterson CJ, Semple KT, Paton GI: **Non-exhaustive extraction techniques (NEETs) for the prediction of naphthalene mineralisation in soil.** *FEMS Microbiology Letters* 2004, **241**(2):215-220.
33. Semple KT, Doick KJ, Wick LY, Harms H: **Microbial interactions with organic contaminants in soil: Definitions, processes and measurement.** *Environmental Pollution* 2007, **150**(1):166-176.
34. Cases I, de Lorenzo V: **The black cat/white cat principle of signal integration in bacterial promoters.** *Embo Journal* 2001, **20**(1-2):1-11.
35. Doick KJ, Clasper PJ, Urmann K, Semple KT: **Further validation of the HPCD-technique for the evaluation of PAH microbial availability in soil.** *Environmental Pollution* 2006, **144**(1):345-354.
36. Fries MR, Zhou J, Chee-Sanford J, Tiedje JM: **Isolation, characterization, and distribution of denitrifying toluene degraders from a variety of habitats.** *Applied and Environmental Microbiology* 1994, **60**(8):2802-2810.
37. Harwood C, Gibson J: **Shedding light on anaerobic benzene ring degradation: a process unique to prokaryotes?** *Journal of Bacteriology* 1997, **179**(2):301-309.
38. Agency for Toxic Substances and Disease Registry (ATSDR). U. S. Department of Health and Human Services PHS: **Interaction profile for benzene, toluene, ethylbenzene, and xylenes (BTEX).** 2004.
39. Agency for Toxic Substances and Disease Registry (ATSDR). U. S. Department of Health and Human Services PHS: **Toxicological profile for benzene.** 2007.
40. Schwarzenbach RP, Gschwend PM, Imboden DM: **Environmental organic chemistry.** Second edition; John Wiley & Sons, Inc.; 2003.
41. Greated A, Lambertsen L, Williams PA, Thomas CM: **Complete sequence of the IncP-9 TOL plasmid pWW0 from *Pseudomonas putida*.** *Environmental Microbiology* 2002, **4**(12):856-871.
42. Garmendia J, Devos D, Valencia A, de Lorenzo V: **A la carte transcriptional regulators: unlocking responses of the prokaryotic enhancer-binding protein XylR to non-natural effectors.** *Molecular Microbiology* 2001, **42**(1):47-59.
43. Willardson BM, Wilkins JF, Rand TA, Schupp JM, Hill KK, Keim P, Jackson PJ: **Development and testing of a bacterial biosensor for toluene-based environmental contaminants.** *Applied and Environmental Microbiology* 1998, **64**(3):1006-1012.
44. Applegate B, Kelly C, Lackey L, McPherson J, Kehrmeyer S, Menn F-M, Bienkowski P, Sayler G: ***Pseudomonas putida* B2: a tod-lux bioluminescent reporter for toluene and trichloroethylene co-metabolism.** *Journal of Industrial Microbiology and Biotechnology* 1997, **18**(1):4-9.
45. Applegate BM, Kehrmeyer SR, Sayler GS: **A chromosomally based tod-luxCDABE whole-cell reporter for benzene, toluene, ethylbenzene, and xylene (BTEX) sensing.** *Applied and Environmental Microbiology* 1998, **64**(7):2730-2735.
46. Lovanh N, Alvarez PJJ: **Effect of ethanol, acetate, and phenol on toluene degradation activity and tod-lux expression in *Pseudomonas putida* TOD102: evaluation of the metabolic flux dilution model.** *Biotechnology and Bioengineering* 2004, **86**(7):801-808.
47. Stiner L, Halverson LJ: **Development and characterization of a green fluorescent protein-based bacterial biosensor for bioavailable toluene and related compounds.** *Applied and Environmental Microbiology* 2002, **68**:1962-1971.
48. Van Dien SJ, de Lorenzo V: **Deciphering environmental signal integration in sigma54-dependent promoters with a simple mathematical model.** *Journal of Theoretical Biology* 2003, **224**(4):437-449.

49. Dawson JJC, Iroegbu CO, Maciel H, Paton GI: **Application of luminescent biosensors for monitoring the degradation and toxicity of BTEX compounds in soils.** *Journal of Applied Microbiology* 2008, **104**(1):141-151.
50. Li Y-F, Li F-Y, Ho C-L, Liao VH-C: **Construction and comparison of fluorescence and bioluminescence bacterial biosensors for the detection of bioavailable toluene and related compounds.** *Environmental Pollution* 2008, **152**(1):123-129.
51. Leveau JHJ, Lindow SE: **Appetite of an epiphyte: quantitative monitoring of bacterial sugar consumption in the phyllosphere.** *PNAS* 2001, **98**(6):3446-3453.
52. Casavant NC, Thompson D, Beattie GA, Phillips GJ, Halverson LJ: **Use of a site-specific recombination-based biosensor for detecting bioavailable toluene and related compounds on roots.** *Environmental Microbiology* 2003, **5**(4):238-249.
53. Agency for Toxic Substances and Disease Registry (ATSDR). U. S. Department of Health and Human Services PHS: **Toxicological profile for polycyclic aromatic hydrocarbons.** 1995.
54. Doick KJ, Lee PH, Semple KT: **Assessment of spiking procedures for the introduction of a phenanthrene-LNAPL mixture into field-wet soil.** *Environmental Pollution* 2003, **126**(3):399-406.
55. Burlage RS, Palumbo AV, Heitzer A, Sayler G: **Bioluminescent reporter bacteria detect contaminants in soil samples.** *Applied Biochemistry and Biotechnology* 1994, **45-6**:731-740.
56. Schell MA: **Regulation of naphthalene degradation genes of plasmid NAH7: example of a generalized positive control system in *Pseudomonas* and related bacteria.** In: *Pseudomonas: biotransformations, pathogenesis and evolving biotechnology.* Edited by Silver S, Chakrabarty AM, Iglewski B, Kaplan S. Washington: American Society for Microbiology; 1990.
57. Burlage RS, Sayler GS, Larimer F: **Monitoring of naphthalene catabolism by bioluminescence with *nah-lux* transcriptional fusions.** *Journal of Bacteriology* 1990, **172**(9):4749-4757.
58. Tecon R, Wells M, van der Meer JR: **A new green fluorescent protein-based bacterial biosensor for analysing phenanthrene fluxes.** *Environmental Microbiology* 2006, **8**(4):697-708.
59. Kohlmeier S, Mancuso M, Tecon R, Harms H, van der Meer JR, Wells M: **Bioreporters: *gfp* versus *lux* revisited and single-cell response.** *Biosensors and Bioelectronics* 2007, **22**(8):1578-1585.
60. Agency for Toxic Substances and Disease Registry (ATSDR). U. S. Department of Health and Human Services PHS: **Draft toxicological profile for phenol.** 2006.
61. Hay AG, Rice JF, Applegate BM, Bright NG, Sayler GS: **A bioluminescent whole-cell reporter for detection of 2,4-dichlorophenoxyacetic acid and 2,4-dichlorophenol in soil.** *Applied and Environmental Microbiology* 2000, **66**(10):4589-4594.
62. Shingler V, Moore T: **Sensing of aromatic compounds by the DmpR transcriptional activator of phenol-catabolizing *Pseudomonas* sp. strain CF600.** *Journal of Bacteriology* 1994, **176**(6):1555-1560.
63. Park J, Malinverni J, Adriaens P, Kukor JJ: **Quantitative structure-activity relationship (QSAR) analysis of aromatic effector specificity in NtrC-like transcriptional activators from aromatic oxidizing bacteria.** *FEMS Microbiology Letters* 2003, **224**(1):45-52.
64. Abd-El-Haleem D, Ripp S, Scott C, Sayler GS: **A *luxCDABE* -based bioluminescent bioreporter for the detection of phenol.** *Journal of Industrial Microbiology and Biotechnology* 2002, **29**(5):233-237.

65. Wise AA, Kuske CR: **Generation of novel bacterial regulatory proteins that detect priority pollutant phenols.** *Applied and Environmental Microbiology* 2000, **66**(1):163-169.
66. Leedjarv A, Ivask A, Virta M, Kahru A: **Analysis of bioavailable phenols from natural samples by recombinant luminescent bacterial sensors.** *Chemosphere* 2006, **64**(11):1910-1919.
67. Sandhu A, Halverson LJ, Beattie GA: **Bacterial degradation of airborne phenol in the phyllosphere.** *Environmental Microbiology* 2007, **9**(2):383-392.
68. Jaspers MCM, Schmid A, Sturme MHJ, Goslings DAM, Kohler H-PE, van der Meer JR: **Transcriptional organization and dynamic expression of the *hbpCAD* genes, which encode the first three enzymes for 2-hydroxybiphenyl degradation in *Pseudomonas azelaica* HBP1.** *Journal of Bacteriology* 2001, **183**(1):270-279.
69. Beggah S, Vogne C, Zenaro E, van der Meer JR: **Mutant HbpR transcription activator isolation for 2-chlorobiphenyl via green fluorescent protein-based flow cytometry and cell sorting.** *Microbial Biotechnology* 2008, **1**(1):68-78.
70. Toba FA, Hay AG: **A simple solid phase assay for the detection of 2,4-D in soil.** *Journal of Microbiological Methods* 2005, **62**(2):135-143.
71. Agency for Toxic Substances and Disease Registry (ATSDR). U. S. Department of Health and Human Services PHS: **Toxicological profile for polychlorinated biphenyls (PCBs).** 2000.
72. Layton AC, Muccini M, Ghosh MM, Sayler GS: **Construction of a bioluminescent reporter strain to detect polychlorinated biphenyls.** *Applied and Environmental Microbiology* 1998, **64**(12):5023-5026.
73. Boldt TS, Sorensen J, Karlson U, Molin S, Ramos C: **Combined use of different Gfp reporters for monitoring single-cell activities of a genetically modified PCB degrader in the rhizosphere of alfalfa.** *FEMS Microbiology Ecology* 2004, **48**(2):139-148.
74. Feliciano J, Xu S, Guan X, Lehmler H-J, Bachas L, Daunert S: **ClcR-based biosensing system in the detection of cis-dihydroxylated (chloro-)biphenyls.** *Analytical and Bioanalytical Chemistry* 2006, **385**(5):807-813.
75. Turner K, Xu S, Pasini P, Deo S, Bachas L, Daunert S: **Hydroxylated polychlorinated biphenyl detection based on a genetically engineered bioluminescent whole-cell sensing system.** *Analytical Chemistry* 2007, **79**(15):5740-5745.
76. Sticher P, Jaspers MCM, Stemmler K, Harms H, Zehnder AJB, vanderMeer JR: **Development and characterization of a whole-cell bioluminescent sensor for bioavailable middle-chain alkanes in contaminated groundwater samples.** *Applied and Environmental Microbiology* 1997, **63**(10):4053-4060.
77. Jaspers MCM, Meier C, Zehnder AJB, Harms H, van der Meer JR: **Measuring mass transfer processes of octane with the help of an *alkS-alkB::gfp*-tagged *Escherichia coli*.** *Environmental Microbiology* 2001, **3**(8):512-524.
78. Yang G, Ran Y, Yalkowsky SH: **Prediction of the aqueous solubility: comparison of the general solubility equation and the method using an amended solvation energy relationship.** *Journal of Pharmaceutical Sciences* 2001, **91**:517-533.
79. Trang PTK, Berg M, Viet PH, Mui NV, van der Meer JR: **Bacterial bioassay for rapid and accurate analysis of arsenic in highly variable groundwater samples.** *Environmental Science and Technology* 2005, **39**(19):7625-7630.
80. Baumann B, van der Meer JR: **Analysis of bioavailable arsenic in rice with whole cell living bioreporter bacteria.** *Journal of Agricultural and Food Chemistry* 2007, **55**(6):2115-2120.

81. Habe H, Omori T: **Genetics of polycyclic aromatic hydrocarbon metabolism in diverse aerobic bacteria.** *Bioscience, Biotechnology, and Biochemistry* 2003, **67**(2):225-243.
82. Bosma TNP, Middeldorp PJM, Schraa G, Zehnder AJB: **Mass transfer limitation of biotransformation: quantifying bioavailability.** *Environmental Science and Technology* 1997, **31**(1):248-252.
83. Semple KT, Morriss AWJ, Paton GI: **Bioavailability of hydrophobic organic contaminants in soils: fundamental concepts and techniques for analysis.** *European Journal of Soil Science* 2003, **54**:809-818.
84. Semple KT, Doick KJ, Jones KC, Burauel P, Craven A, Harms H: **Defining bioavailability and bioaccessibility of contaminated soil and sediment is complicated.** *Environmental Science and Technology* 2004, **38**(12):228A-231A.
85. Johnsen AR, Wick LY, Harms H: **Principles of microbial PAH-degradation in soil.** *Environmental Pollution* 2005, **133**(1):71-84.
86. Wick LY, Colangelo T, Harms H: **Kinetics of mass transfer-limited bacterial growth on solid PAHs.** *Environmental Science and Technology* 2001, **35**(2):354-361.
87. Hatzinger PB, Alexander M: **Effect of aging of chemicals in soil on their biodegradability and extractability.** *Environmental Science and Technology* 1995, **29**(2):537-545.
88. Eriksson M, Swartling A, Dalhammar G: **Biological degradation of diesel fuel in water and soil monitored with solid-phase micro-extraction and GC-MS.** *Applied Microbiology and Biotechnology* 1998, **50**(1):129-134.
89. Cuypers C, Grotenhuis T, Joziassse J, Rulkens W: **Rapid persulfate oxidation predicts PAH bioavailability in soils and sediments.** *Environmental Science and Technology* 2000, **34**:2057-2063.
90. Reid BJ, Stokes JD, Jones KC, Semple KT: **A non-exhaustive cyclodextrin based extraction technique for the evaluation of PAH bioavailability.** *Environmental Science and Technology* 2000, **34**:3174-3179.
91. Reid BJ, MacLeod CJA, Lee PH, Morriss AWJ, Stokes JD, Semple KT: **A simple ¹⁴C-respirometric method for assessing microbial catabolic potential and contaminant bioavailability.** *FEMS Microbiology Letters* 2001, **196**(2):141-146.
92. Ahn Y, Sanseverino J, Saylor GS: **Analyses of polycyclic aromatic hydrocarbon-degrading bacteria isolated from contaminated soils.** *Biodegradation* 1999, **10**(2):149-157.
93. Moser R, Stahl U: **Insights into the genetic diversity of initial dioxygenases from PAH-degrading bacteria.** *Applied and Environmental Microbiology* 2001, **55**:609-618.
94. Hall K, Miller CD, Sorensen DL, Anderson AJ, Sims RC: **Development of a catabolically significant genetic probe for polycyclic aromatic hydrocarbon-degrading *Mycobacteria* in soil.** *Biodegradation* 2005, **16**(5):475-484.
95. Lee HJ, Villaume J, Cullen DC, Kim BC, Gu MB: **Monitoring and classification of PAH toxicity using an immobilized bioluminescent bacteria.** *Biosensors and Bioelectronics* 2003, **18**:571-577.
96. Vanlaere E, van der Meer JR, Falsen E, Salles JF, de Brandt E, Vandamme P: ***Burkholderia sartisoli* sp. nov., isolated from a polycyclic aromatic hydrocarbon-contaminated soil.** *International Journal of Systematic and Evolutionary Microbiology* 2008, **58**(2):420-423.
97. DeLong EF, Wickham GS, Pace NR: **Phylogenetic stains: ribosomal RNA-based probes for the identification of single cells.** *Science* 1989, **243**(4896):1360-1363.

98. Stocker J, Balluch D, Gsell M, Harms H, Feliciano J, Daunert S, Malik KA, van der Meer JR: **Development of a set of simple bacterial biosensors for quantitative and rapid measurements of arsenite and arsenate in potable water.** *Environmental Science and Technology* 2003, **37**(20):4743-4750.
99. Wells M, Wick LY, Harms H: **A model polymer release system study of PAH bioaccessibility: the relationship between rapid release and bioaccessibility.** *Environmental Science and Technology* 2005, **39**(4):1055-1063.
100. Wells M, Wick LY, Harms H: **Perspectives on modeling the release of hydrophobic organic contaminants drawn from model polymer release systems.** *Journal of Materials Chemistry* 2004, **14**:2461-2472.
101. Mulder H, Breure AM, Rulkens WH: **Prediction of complete bioremediation periods for PAH soil pollutants in different physical states by mechanistic models.** *Chemosphere* 2001, **43**(8):1085-1094.
102. Sikkema J, de Bont JAM, Poolman B: **Mechanisms of membrane toxicity of hydrocarbons.** *Microbiology Reviews* 1995, **59**(2):201-222.
103. Ghosh U, Talley JW, Luthy RG: **Particle-scale investigation of PAH desorption kinetics and thermodynamics from sediment.** *Environmental Science and Technology* 2001, **35**:3468-3475.
104. Hong L, Ghosh U, Mahajan T, Zare RN, Luthy RG: **PAH sorption mechanism and partitioning behavior in lampblack-impacted soils from former oil-gas plant sites.** *Environmental Science and Technology* 2003, **37**(16):3625-3634.
105. Gerhardt P, Murray RGE, Costilow RN, Nester EW, Wood WA, Krieg NR, Briggs Philipps G: **Manual of methods for general bacteriology.** *American society for microbiology, Washington, D C* 1981.
106. Miller WG, Lindow SE: **An improved GFP cloning cassette designed for prokaryotic transcriptional fusions.** *Gene* 1997, **191**(2):149-153.
107. Ihaka R, Gentleman R: **R: a language for data analysis and graphics.** *Journal of Computational and Graphical Statistics* 1996, **5**:299-314.
108. Amann RI, Krumholz L, Stahl DA: **Fluorescent-oligonucleotide probing of whole cells for determinative, phylogenetic, and environmental studies in microbiology.** *Journal of Bacteriology* 1990, **172**(2):762-770.
109. Wu SC, Gschwend PM: **Sorption kinetics of hydrophobic organic compounds to natural sediments and soils.** *Environmental Science & Technology* 1986, **20**(7):717-725.
110. Shor LM, Rockne KJ, Taghon GL, Young LY, Kosson DS: **Desorption Kinetics for Field-Aged Polycyclic Aromatic Hydrocarbons from Sediments.** *Environmental Science & Technology* 2003, **37**(8):1535-1544.
111. Haitzer M, Hoss S, Traunspurger W, Steinberg C: **Effects of dissolved organic matter (DOM) on the bioconcentration of organic chemicals in aquatic organisms -- a review --.** *Chemosphere* 1998, **37**(7):1335-1362.
112. Ogawa H, Tanoue E: **Dissolved organic matter in oceanic waters.** *Journal of Oceanography* 2003, **59**:129-147.
113. Gourlay C, Mouchel J-M, Tusseau-Vuillemin M-H, Garric J: **Influence of algal and bacterial particulate organic matter on benzo[a]pyrene bioaccumulation in *Daphnia magna*.** *Science of The Total Environment* 2005, **346**(1-3):220-230.
114. Ortega-Calvo J-J, Saiz-Jimenez C: **Effect of humic fractions and clay on biodegradation of phenanthrene by a *Pseudomonas fluorescens* strain isolated from soil.** *Applied and Environmental Microbiology* 1998, **64**(8):3123-3126.

115. Vacca DJ, Bleam WF, Hickey WJ: **Isolation of soil bacteria adapted to degrade humic acid-sorbed phenanthrene.** *Applied and Environmental Microbiology* 2005, **71**(7):3797-3805.
116. Kohlmeier S, Mancuso M, Deepthike U, Tecon R, van der Meer JR, Harms H, Wells M: **Comparison of naphthalene bioavailability determined by whole-cell biosensing and availability determined by extraction with Tenax.** *Environmental Pollution* 2008, **156**(3):803-808.
117. Leveau JH, Zehnder AJB, van der Meer JR: **The *tfdK* gene product facilitates uptake of 2,4-dichlorophenoxyacetate by *Ralstonia eutropha* JMP134(pJP4).** *Journal of Bacteriology* 1998, **180**(8):2237-2243.
118. Akkanen J, Tuikka A, Kukkonen JVK: **Comparative sorption and desorption of benzo[a]pyrene and 3,4,3',4'-tetrachlorobiphenyl in natural lake water containing dissolved organic matter.** *Environmental Science and Technology* 2005, **39**(19):7529-7534.
119. Poerschmann J, Zhang Z, Kopinke F-D, Pawliszyn J: **Solid phase microextraction for determining the distribution of chemicals in aqueous matrices.** *Analytical Chemistry* 1997, **69**(4):597-600.
120. Van Dyke MI, Lee H, Trevors JT: **Applications of microbial surfactants.** *Biotechnology Advances* 1991, **9**(2):241-252.
121. Zhang Y, Miller RM: **Enhanced octadecane dispersion and biodegradation by a *Pseudomonas* rhamnolipid surfactant (biosurfactant).** *Applied and Environmental Microbiology* 1992, **58**(10):3276-3282.
122. Bertrand J-C, Bonin P, Goutx M, Gauthier M, Mille G: **The potential application of biosurfactants in combatting hydrocarbon pollution in marine environments.** *Research in Microbiology* 1994, **145**(1):53-56.
123. Desai J, Banat I: **Microbial production of surfactants and their commercial potential.** *Microbiology and Molecular Biology Reviews* 1997, **61**(1):47-64.
124. Garcia-Junco M, De Olmedo E, Ortega-Calvo J-J: **Bioavailability of solid and non-aqueous phase liquid (NAPL)-dissolved phenanthrene to the biosurfactant-producing bacterium *Pseudomonas aeruginosa* 19SJ.** *Environmental Microbiology* 2001, **3**(9):561-569.
125. Mulligan CN: **Environmental applications for biosurfactants.** *Environmental Pollution* 2005, **133**(2):183-198.
126. Urum K, Grigson S, Pekdemir T, McMenamy S: **A comparison of the efficiency of different surfactants for removal of crude oil from contaminated soils.** *Chemosphere* 2006, **62**(9):1403-1410.
127. Soberón-Chávez G, Lépine F, Déziel E: **Production of rhamnolipids by *Pseudomonas aeruginosa*.** *Applied Microbiology and Biotechnology* 2005, **68**(6):718-725.
128. Yakimov M, Golyshin P, Lang S, Moore E, Abraham W, Lunsdorf H, Timmis K: ***Alcanivorax borkumensis* gen. nov., sp. nov., a new, hydrocarbon- degrading and surfactant-producing marine bacterium.** *International Journal of Systematic Bacteriology* 1998, **48**(2):339-348.
129. Noordman WH, Janssen DB: **Rhamnolipid stimulates uptake of hydrophobic compounds by *Pseudomonas aeruginosa*.** *Applied and Environmental Microbiology* 2002, **68**(9):4502-4508.
130. Olivera NL, Nievas ML, Lozada M, del Prado G, Dionisi HM, Siñeriz F: **Isolation and characterization of biosurfactant-producing *Alcanivorax* strains: hydrocarbon accession strategies and alkane hydroxylase gene analysis.** *Research in Microbiology* 2009, **160**(1):19-26.

131. Garcia-Junco M, Gomez-Lahoz C, Niqui-Arroyo J-L, Ortega-Calvo J-J: **Biosurfactant- and biodegradation-enhanced partitioning of polycyclic aromatic hydrocarbons from nonaqueous-phase liquids.** *Environmental Science and Technology* 2003, **37**(13):2988-2996.
132. Shin K-H, Kim K-W, Seagren EA: **Combined effects of pH and biosurfactant addition on solubilization and biodegradation of phenanthrene.** *Applied Microbiology and Biotechnology* 2004, **65**(3):336-343.
133. Volkering F, Breure AM, Rulkens WH: **Microbiological aspects of surfactant use for biological soil remediation.** *Biodegradation* 1997, **8**(6):401-417.
134. Kuiper I, Lagendijk EL, Pickford R, Derrick JP, Lamers GEM, Thomas-Oates JE, Lugtenberg BJJ, Bloemberg GV: **Characterization of two *Pseudomonas putida* lipopeptide biosurfactants, putisolvin I and II, which inhibit biofilm formation and break down existing biofilms.** *Molecular Microbiology* 2004, **51**(1):97-113.
135. Dubern J-F, Lagendijk EL, Lugtenberg BJJ, Bloemberg GV: **The heat shock genes *dnaK*, *dnaJ*, and *grpE* are involved in regulation of putisolvin biosynthesis in *Pseudomonas putida* PCL1445.** *Journal of Bacteriology* 2005, **187**(17):5967-5976.
136. Dubern J-F, Guido V. Bloemberg: **Influence of environmental conditions on putisolvins I and II production in *Pseudomonas putida* strain PCL1445.** *FEMS Microbiology Letters* 2006, **263**(2):169-175.
137. Dubern J-F, Lugtenberg BJJ, Bloemberg GV: **The *ppuI-rsaL-ppuR* quorum-sensing system regulates biofilm formation of *Pseudomonas putida* PCL1445 by controlling biosynthesis of the cyclic lipopeptides putisolvins I and II.** *Journal of Bacteriology* 2006, **188**(8):2898-2906.
138. Dean SM, Jin Y, Cha DK, Wilson SV, Radosevich M: **Phenanthrene degradation in soils co-inoculated with phenanthrene-degrading and biosurfactant-producing bacteria.** *Journal of Environmental Quality* 2001, **30**(4):1126-1133.
139. Straube WL, Nestler CC, Hansen LD, Ringleberg D, Pritchard PH, Jones-Meehan J: **Remediation of polyaromatic hydrocarbons (PAHs) through landfarming with biostimulation and bioaugmentation.** *Acta Biotechnologica* 2003, **23**(2-3):179-196.
140. An D, Danhorn T, Fuqua C, Parsek MR: **Quorum sensing and motility mediate interactions between *Pseudomonas aeruginosa* and *Agrobacterium tumefaciens* in biofilm cocultures.** *PNAS* 2006, **103**(10):3828-3833.
141. Mellefont LA, McMeekin TA, Ross T: **Effect of relative inoculum concentration on *Listeria monocytogenes* growth in co-culture.** *International Journal of Food Microbiology* 2008, **121**(2):157-168.
142. Hickey A, Gordon L, Dobson A, Kelly C, Doyle E: **Effect of surfactants on fluoranthene degradation by *Pseudomonas alcaligenes* PA-10.** *Applied Microbiology and Biotechnology* 2007, **74**(4):851-856.
143. Gu MB, Chang ST: **Soil biosensor for the detection of PAH toxicity using an immobilized recombinant bacterium and a biosurfactant.** *Biosensors and Bioelectronics* 2001, **16**(9-12):667-674.
144. **Persistent organic pollutants: a global issue, a global response.** U.S. Environmental Protection Agency 2002.
145. Maier RM, Pepper IL, Gerba CP: **Environmental microbiology.** London: Academic Press; 2000.
146. Efrogmson RA, Alexander M: **Reduced mineralization of low concentrations of phenanthrene because of sequestering in nonaqueous-phase liquids.** *Environmental Science and Technology* 1995, **29**(2):515-521.

147. Semple KT, Dew NM, Doick KJ, Rhodes AH: **Can microbial mineralization be used to estimate microbial availability of organic contaminants in soil?** *Environmental Pollution* 2006, **140**(1):164-172.
148. Uyttebroek M, Ortega-Calvo J-J, Breugelmans P, Springael D: **Comparison of mineralization of solid-sorbed phenanthrene by polycyclic aromatic hydrocarbon (PAH)-degrading *Mycobacterium* spp. and *Sphingomonas* spp.** *Applied Microbiology and Biotechnology* 2006:1-8.
149. Shaner NC, Campbell RE, Steinbach PA, Giepmans BNG, Palmer AE, Tsien RY: **Improved monomeric red, orange and yellow fluorescent proteins derived from *Discosoma* sp. red fluorescent protein.** *Nature Biotechnology* 2004, **22**(12):1567-1572.
150. Trott D, Dawson JJC, Killham KS, Miah MRU, Wilson MJ, Paton GI: **Comparative evaluation of a bioluminescent bacterial assay in terrestrial ecotoxicity testing.** *Journal of Environmental Monitoring* 2007, **9**(1):44-50.
151. Leveau JHJ, Lindow SE: **Predictive and interpretive simulation of green fluorescent protein expression in reporter bacteria.** *Journal of Bacteriology* 2001, **183**(23):6752-6762.
152. Hakkila K, Maksimow M, Rosengren A, Karp M, Virta M: **Monitoring promoter activity in a single bacterial cell by using green and red fluorescent proteins.** *Journal of Microbiological Methods* 2003, **54**(1):75-79.
153. Nancharaiah YV, Wattiau P, Wuertz S, Bathe S, Mohan SV, Wilderer PA, Hausner M: **Dual labeling of *Pseudomonas putida* with fluorescent proteins for in situ monitoring of conjugal transfer of the TOL plasmid.** *Applied and Environmental Microbiology* 2003, **69**(8):4846-4852.
154. Anderson KI, Jeremy Sanderson SG, Jan Peychl.: **A new configuration of the Zeiss LSM 510 for simultaneous optical separation of green and red fluorescent protein pairs.** *Cytometry Part A* 2006, **69A**(8):920-929.
155. Sambrook J, Russel DW: **Molecular Cloning, A Laboratory Manual**, 3rd edition edn: Cold Spring harbor, New York; 2001.
156. **Black Sea faces environmental disaster.** *New Scientist* 2007, **2630**: 6.
157. de Lorenzo V: **Blueprint of an oil-eating bacterium.** *Nature Biotechnology* 2006, **24**(8):952-953.
158. Head IM, Swannell RP: **Bioremediation of petroleum hydrocarbon contaminants in marine habitats.** *Current Opinion in Biotechnology* 1999, **10**(3):234-239.
159. Oberholster PJ, Botha A-M, Cloete TE: **Using a battery of bioassays, benthic phytoplankton and the AUSRIVAS method to monitor long-term coal tar contaminated sediment in the Cache la Poudre River, Colorado.** *Water Research* 2005, **39**(20):4913-4924.
160. Varela M, Bode A, Lorenzo J, Álvarez-Ossorio MT, Miranda A, Patrocinio T, Anadón R, Viesca L, Rodríguez N, Valdés L *et al*: **The effect of the "Prestige" oil spill on the plankton of the N-NW Spanish coast.** *Marine Pollution Bulletin* 2006, **53**(5-7):272-286.
161. Czechowska K, Johnson DR, van der Meer JR: **Use of flow cytometric methods for single-cell analysis in environmental microbiology.** *Current Opinion in Microbiology* 2008, **11**(3):205-212.
162. Dissanayake A, Galloway TS, Jones MB: **Physiological responses of juvenile and adult shore crabs *Carcinus maenas* (Crustacea: Decapoda) to pyrene exposure.** *Marine Environmental Research* 2008, **66**(4):445-450.

163. Lewis C, Pook C, Galloway T: **Reproductive toxicity of the water accommodated fraction (WAF) of crude oil in the polychaetes *Arenicola marina* (L.) and *Nereis virens* (Sars).** *Aquatic Toxicology* 2008, **90**(1):73-81.
164. Carls MG, Holland L, Larsen M, Collier TK, Scholz NL, Incardona JP: **Fish embryos are damaged by dissolved PAHs, not oil particles.** *Aquatic Toxicology* 2008, **88**(2):121-127.
165. Head IM, Jones DM, Roling WFM: **Marine microorganisms make a meal of oil.** *Nature Reviews Microbiology* 2006, **4**(3):173-182.
166. Wang Z, Fingas M, Blenkinsopp S, Sergy G, Landriault M, Sigouin L, Foght J, Semple K, Westlake DWS: **Comparison of oil composition changes due to biodegradation and physical weathering in different oils.** *Journal of Chromatography A* 1998, **809**(1-2):89-107.
167. Lee JH, Mitchell RJ, Kim BC, Cullen DC, Gu MB: **A cell array biosensor for environmental toxicity analysis.** *Biosensors and Bioelectronics* 2005, **21**(3):500-507.
168. Lee JH, Youn CH, Kim BC, Gu MB: **An oxidative stress-specific bacterial cell array chip for toxicity analysis.** *Biosensors and Bioelectronics* 2007, **22**(9-10):2223-2229.
169. Tani H, Maehana K, Kamidate T: **On-chip bioassay using immobilized sensing bacteria in three-dimensional microfluidic network.** *Methods in Molecular Biology* 2007, **385**: 37-52.
170. Sabirova JS, Ferrer M, Regenhardt D, Timmis KN, Golyshin PN: **Proteomic insights into metabolic adaptations in *Alcanivorax borkumensis* induced by alkane utilization.** *Journal of Bacteriology* 2006, **188**(11):3763-3773.
171. Hara A, Syutsubo K, Harayama S: ***Alcanivorax* which prevails in oil-contaminated seawater exhibits broad substrate specificity for alkane degradation.** *Environmental Microbiology* 2003, **5**(9):746-753.
172. Kasai Y, Kishira H, Sasaki T, Syutsubo K, Watanabe K, Harayama S: **Predominant growth of *Alcanivorax* strains in oil-contaminated and nutrient-supplemented sea water.** *Environmental Microbiology* 2002, **4**(3):141-147.
173. Schneiker S, dos Santos VAM, Bartels D, Bekel T, Brecht M, Buhrmester J, Chernikova TN, Denaro R, Ferrer M, Gertler C *et al*: **Genome sequence of the ubiquitous hydrocarbon-degrading marine bacterium *Alcanivorax borkumensis*.** *Nature Biotechnology* 2006, **24**(8):997-1004.
174. van Beilen JB, Marín MM, Smits THM, Röthlisberger M, Franchini AG, Witholt B, Rojo F: **Characterization of two alkane hydroxylase genes from the marine hydrocarbonoclastic bacterium *Alcanivorax borkumensis*.** *Environmental Microbiology* 2004, **6**(3):264-273.
175. Hara A, Baik S, Syutsubo K, Misawa N, Smits THM, van Beilen JB, Harayama S: **Cloning and functional analysis of *alkB* genes in *Alcanivorax borkumensis* SK2.** *Environmental Microbiology* 2004, **6**(3):191-197.
176. Dyksterhouse S, Gray J, Herwig R, Lara J, Staley J: ***Cycloclasticus pugetii* gen. nov., sp. nov., an aromatic hydrocarbon- degrading bacterium from marine sediments.** *International Journal of Systematic Bacteriology* 1995, **45**(1):116-123.
177. Miller WG, Leveau JHJ, Lindow SE: **Improved *gfp* and *inaZ* broad-host range promoter-probe vectors.** *Molecular Plant-Microbe Interactions* 2000, **13**(11):1243-1250.
178. Ehlers LJ, Luthy RG: **Peer reviewed: contaminant bioavailability in soil and sediment.** *Environmental Science & Technology* 2003, **37**(15):295A-302A.
179. Brehm-Stecher BF, Johnson EA: **Single-cell microbiology: tools, technologies, and applications.** *Microbiology and Molecular Biology Reviews* 2004, **68**(3):538-559.

180. Amann R, Fuchs BM: **Single-cell identification in microbial communities by improved fluorescence in situ hybridization techniques.** *Nature Reviews Microbiology* 2008, **6**(5):339-348.
181. Popa R, Weber PK, Pett-Ridge J, Finzi JA, Fallon SJ, Hutcheon ID, Nealson KH, Capone DG: **Carbon and nitrogen fixation and metabolite exchange in and between individual cells of *Anabaena oscillarioides*.** *The ISME Journal* 2007, **1**(4):354-360.
182. Behrens S, Losekann T, Pett-Ridge J, Weber PK, Ng W-O, Stevenson BS, Hutcheon ID, Relman DA, Spormann AM: **Linking microbial phylogeny to metabolic activity at the single-cell level by using enhanced element labeling-catalyzed reporter deposition fluorescence in situ hybridization (EL-FISH) and NanoSIMS.** *Applied and Environmental Microbiology* 2008, **74**(10):3143-3150.
183. Li T, Wu TD, Mazéas L, Toffin L, Guerquin-Kern J-L, Leblon G, Bouchez T: **Simultaneous analysis of microbial identity and function using NanoSIMS.** *Environmental Microbiology* 2008, **10**(3):580-588.
184. Huang WE, Stoecker K, Griffiths R, Newbold L, Daims H, Whiteley AS, Wagner M: **Raman-FISH: combining stable-isotope Raman spectroscopy and fluorescence *in situ* hybridization for the single cell analysis of identity and function.** *Environmental Microbiology* 2007, **9**(8):1878-1889.
185. Kalyuzhnaya MG, Lidstrom ME, Chistoserdova L: **Real-time detection of actively metabolizing microbes by redox sensing as applied to methylotroph populations in Lake Washington.** *The ISME Journal* 2008, **2**(7):696-706.
186. Marcy Y, Ishoey T, Lasken RS, Stockwell TB, Walenz BP, Halpern AL, Beeson KY, Goldberg SMD, Quake SR: **Nanoliter reactors improve multiple displacement amplification of genomes from single cells.** *PLoS Genetics* 2007, **3**(9):e155.
187. Binga EK, Lasken RS, Neufeld JD: **Something from (almost) nothing: the impact of multiple displacement amplification on microbial ecology.** *The ISME Journal* 2008, **2**(3):233-241.
188. Koch B, Worm J, Jensen LE, Hojberg O, Nybroe O: **Carbon limitation induces sigmaS-dependent gene expression in *Pseudomonas fluorescens* in soil.** *Applied and Environmental Microbiology* 2001, **67**(8):3363-3370.
189. Sternberg C, Christensen BB, Johansen T, Toftgaard Nielsen A, Andersen JB, Givskov M, Molin S: **Distribution of bacterial growth activity in flow-chamber biofilms.** *Applied and Environmental Microbiology* 1999, **65**(9):4108-4117.
190. Sternberg C, Eberl L, Poulsen LK, Molin S: **Detection of bioluminescence from individual bacterial cells: a comparison of two different low-light imaging systems.** *Journal of Bioluminescence and Chemiluminescence* 1997, **12**:7-13.

CURRICULUM VITAE

Robin Tecon

Born in Morges, Switzerland, November 22nd 1979

nationality : Swiss

- 1995-1998:** Gymnase de Nyon (Nyon High School)
Swiss Federal Maturity in mathematics-sciences (1998).
- 1998-2003:** Undergraduate student at the University of Lausanne
Diploma in Biology (September 2003).

diploma thesis
‘Isolation of naphthalene-degrading bacteria: a comparison between culture-based and molecular methods’.
Laboratory of Soil Science, Swiss Institute of Technology Lausanne (EPFL). Director: Prof. Hauke Harms.
- 2004-2009:** PhD student, Department of Fundamental Microbiology, Faculty of Biology and Medicine, University of Lausanne.
Director: Prof. Jan Roelof van der Meer.

LIST OF PUBLICATIONS

Tecon R. and J. R. van der Meer. Information from single-cell bacterial biosensors: what is it good for? *Current Opinion in Biotechnology*. 2006 Feb; 17(1):4-10.

Tecon R., Wells M. and J. R. van der Meer. A new green fluorescent protein-based bacterial biosensor for analysing phenanthrene fluxes. *Environmental Microbiology*. 2006 Apr; 8(4):697-708.

Kohlmeier S., Mancuso M., Tecon R., Harms H., van der Meer J. R. and M. Wells. Bioreporters: gfp versus lux revisited and single-cell response. *Biosensors and Bioelectronics*. 2007 Mar; 22(8):1578-85.

Tecon R. and J. R. van der Meer. Bacterial biosensors for measuring availability of environmental pollutants. *Sensors*. 2008 Jul; 8, 4062-4080.

Kohlmeier S., Mancuso M., Deepthike U., Tecon R., van der Meer J.R., Harms H. and M. Wells. Comparison of naphthalene bioavailability determined by whole-cell biosensing and availability determined by extraction with Tenax. *Environmental Pollution*. 2008 Dec; 156(3):803-8.